wge

Working Group on Effects
of the
Convention on Long-range Transboundary Air Pollution

Report 259101016/2005
ISBN: 9069601281

European Critical loads and Dynamic Modelling: CCE Status Report 2005

M. Posch, J. Slootweg, J.-P. Hettelingh (eds.)

Contact:
M. Posch
European Air Quality & Sustainability
max.posch@mnp.nl



ICP M&M Coordination Center for Effects

This investigation has been performed by order and for the account of the Directorate for Climate Change and Industry of the Dutch Ministry of Housing, Spatial Planning and the Environment within the framework of RIVM-project M259101, 'UNECE-LRTAP'; and for the account of (the Working Group on Effects within) the trustfund for the partial funding of effect oriented activities under the Convention. Part of this work is supported by the European Commission under Service Contract 070501/2004/380217/MAR/C1.

Netherlands Environmental Assessment Agency
(MNP associated with the RIVM), P.O. Box 303,
3720 AH Bilthoven, telephone: +31–30–274 2745,
website: www.mnp.nl

Contents

Acknowledgements 4
Abstract 5
Rapport in het kort 6
Preface 7

PART I Status of Maps and Methods

1. Status of European Critical Loads and Dynamic Modelling 9
2. Summary of National Data 27
3. Harmonizing European land cover maps 47
4. The European Background Database 63
5. Use of Critical Loads in Integrated Assessment Modelling 71
6. Dynamic Modelling of Lakes in Eastern Canada 77

PART II National Focal Centre Reports 85

AUSTRIA 86
BELARUS 89
BELGIUM 95
BULGARIA 96
CZECH REPUBLIC 100
GERMANY 105
FRANCE 109
HUNGARY 116
IRELAND 121
ITALY 125
NETHERLANDS 129
NORWAY 132
POLEN 135
SLOVAKIA 141
SWEDEN 142
SWITZERLAND 148
UNITED KINGDOM 158

Appendix A. Instructions for the Call for Data 161

Acknowledgements

The methods and resulting maps contained in this report are the product of collaboration within the Effects Programme of the UNECE Convention on Long-range Transboundary Air Pollution, involving many institutions and individuals throughout Europe. National Focal Centres, whose reports regarding modelling and mapping activities appear in Part II are gratefully acknowledged for their contribution.

In addition the Coordination Center for Effects of the Netherlands Environmental Assessment Agency (MNP) associated with RIVM thanks the following:

- The Directorate for Climate Change and Industry of the Dutch Ministry of Housing, Spatial Planning and the Environment and Mr. J. Sliggers in particular for their continued support,
- The Working Group on Effects, the Task Force of the International Co-operative Programme on the Modelling and Mapping of Critical Levels and Loads and Air Pollution Effects, Risks and Trends for their collaboration and assistance,
- The EMEP Steering Body for its collaboration,
- The UNECE secretariat of the Convention on Long-range Transboundary Air Pollution for its valuable support, including the preparation of official documentations,

Abstract

European Critical Loads and Dynamic Modelling

The analysis of air pollution impacts on environment and health becomes ever more important for the support of air pollution policies also because the health risk op particulate matter has recently become more recognised . A number of air pollution abatement agreements will be reviewed and possibly revised in the near future. These include the UNECE Protocol to Abate Acidification, Eutrophication and Ground Level Ozone, the EC's National Emissions Ceiling Directive and the UNECE Protocol on Heavy Metals. In support of the review of the first two agreements the report provides updated European maps of critical loads for acidification and eutrophication as well as novel results regarding the temporal delay of damage or recovery of acidification. While decreasing since the 1980s, the exceedance of critical loads for acidification remains a European-wide issue. 'Acid rain' may seem yesterday's problem, but the risk of acidification of ecosystems continues to demand attention. Based on data provided by 14 countries, 95% of the European forest soils are estimated to recover by 2030 provided depositions of sulphur and nitrogen are sufficiently reduced below critical loads. It is noted that the exceedance of critical loads for eutrophication, and allied risks for biodiversity, remain high and widespread. Finally, regarding the Heavy Metals Protocol, the report summarizes recent CCE work on heavy metals. Perhaps unexpectedly, it turns out that critical loads of lead continue to be widely exceeded on a European scale. Part I of this report describes recent European work addressing both temporal and spatial environmental impacts of transboundary air pollution. Part II provides detailed national reports justifying methods and data applied by National Focal Centres to enable the CCE compilation of European maps of critical loads.

Keywords: acidification, atmospheric deposition, CCE background database, critical loads, eutrophication, exceedances, heavy metals, National Focal Centres

Rapport in het kort

Europese Kritische Drempels en Dynamische Modellering

De analyse van effecten van luchtverontreiniging op mens en milieu wordt belangrijker ondermeer omdat de risico's van fijn stof voor de menselijke gezondheid recentelijk meer worden onderkend. In de komende jaren worden verschillende Europese overeenkomsten over de luchtkwaliteit geëvalueerd en mogelijk herzien. Het betreft ondermeer het UNECE protocol voor de bestrijding van verzuring, vermesting en ozon op leefniveau, de Europese Commissie richtlijn inzake Nationale Emissie Plafonds en het protocol voor zware metalen. Voor de evaluatie van de eerste twee overeenkomsten beschrijft dit rapport de vernieuwde Europese kaarten van kritische drempels voor verzuring en vermesting en nieuwe resultaten van de analyse van tijdsvertragingen van herstel van - en schade door verzuring. Resultaten laten zien dat de overschrijding van kritische drempels voor verzuring weliswaar afnemen sinds 1980, maar dat de spreiding van de risico's nog altijd grootschalig is. In zijn letterlijke betekenis schijnt 'zure regen' een probleem van gisteren te zijn, maar de risico's van verzuring van ecosystemen blijven om aandacht vragen. Op basis van gegevens van 14 landen is berekend dat herstel van circa 95% van de voornamelijk bosbodems in deze landen in 2030 kunnen herstellen bij vermindering van zure depositie tot de kritische drempels. Met betrekking tot de overschrijding van kritische drempels voor vermesting, en daarmee samenhangende risico's voor de biodiversiteit, wordt geconstateerd dat deze vrijwel overal in Europa bijna onverminderd hoog blijven. Tenslotte blijken de huidige emissies van lood, cadmium en kwik te hoog. De intuïtie weersprekend worden de kritische drempels van looddepositie grootschalig in Europa overschreden. Deel I van dit rapport beschrijft het Europese werk om de milieueffecten van grensoverschrijdende luchtverontreiniging in ruimte en tijd uit te drukken. Deel II bestaat uit nationale rapportages die de bijdragen onderbouwen van National Focal Centres aan de Europese kaarten van kritische drempels.

Trefwoorden: atmosferische depositie, kritische drempels, luchtkwaliteit, overschrijdingen.

Preface

This report describes the results of the call for data on critical loads on acidification and eutrophication and novel outcomes with European applications of dynamic models addressing time delays of recovery from acidification or damage caused by the latter.

In its 17th session in December 1999, the Executive Body of the Convention '... underlined the importance of ... dynamic modelling of recovery' (ECE/EB.AIR/68 p. 14, para. 51. b) to enable the assessment of time delays of recovery in regions where critical loads stop being exceeded and time delays of damage in regions where critical loads continue to be exceeded.

The Working Group on Effects (WGE), at its 23rd session (Geneva, 1-3 September 2004), approved the proposal made at the 20th Task Force meeting of the ICP-M&M (Laxenburg, 27-28 May 2004) to issue a call for data on critical loads for acidification and eutrophication, and for data on dynamic modelling of acidification (EB.AIR/WG.1/2004/2 para. 57c).

The Commission of the European Communities emphasized the importance of the response to the call for data, in particular by the EU Member States. The outcomes of the call are not only used for the support of policy processes under the Convention (possible revision process of the Gothenburg Protocol), but also have the potential to support the Clean Air for Europe (CAFE) programme under the European Commission (preparation of the revision of the National Emission Ceilings directive).

The CCE issued the call on 24 November 2004, setting the deadline to 28 February 2005. In addition to information provided in the Mapping Manual (www.icpmapping.org), also a detailed instruction document had been compiled by the CCE and distributed to the National Focal Centres and also made available on the CCE website (before 1 May 2005 www.mnp.nl/cce).

The objective of the call, in accordance to the medium-term work plan of the WGE, was to produce an updated database on critical loads and dynamic modelling results which could be made available for use in integrated assessment modelling to support European air pollution abatement policies.

Chapter 1 serves as an executive summary including critical loads for acidification, eutrophication and of heavy metals (latest updates), exceedance maps and dynamic modelling of time delays of acidification impact changes. Chapter 2 analyses the data on critical loads and dynamic modelling submitted by National Focal Centres including an inter-country comparison of data statistics. Chapter 3 addresses the information on land cover and ecosystems that are used under the LRTAP Convention. Chapter 4 describes the latest CCE background database for calculating critical loads for forest soils in Europe. This database could is used to provide critical loads in countries that did not submit any data. Chapter 5 summarizes recent CCE work to identify so-called impact factors that describe the relationship between marginal emission changes and changes in the area exceeded. This chapter particularly addresses the application in the optimization model of the RAINS model. Finally, chapter 6 describes a first tentative Canadian map of critical loads for acidification and eutrophication developed at the Trent University (Peterborough, Ontario).

Part II provides national reports justifying methods and data applied by National Focal Centres to enable the CCE compilation of European maps of critical loads.

The report is completed with Appendix A, which is a reprint of the 'instructions' provided to the NFCs to assist in their response to the call for data.

1. Status of European Critical Loads and Dynamic Modelling[1]

Jean-Paul Hettelingh, Maximilian Posch, Jaap Slootweg

1.1 Acidification and eutrophication: background

The Working Group on Effects, at its 23rd session (Geneva, 1-3 September 2004), approved the proposal made at the 20th Task Force meeting of the ICP-M&M (Laxenburg, 27-28 May 2004) to issue a call for data on critical loads for acidification and eutrophication, and for data on dynamic modelling of acidification (EB.AIR/WG.1/2004/2 para. 57c).

The objective of the call, in accordance to the medium-term work plan of the WGE was to produce an updated database on critical loads and dynamic modelling results which could be submitted to Task Force on Integrated Assessment Modelling (TFIAM).

At the meeting of the Working Group on Effects the representative of the Commission of the European Communities emphasized the importance of the response to the call for data, in particular by the EU member states. The outcomes of the call are not only used for the support of policy processes under the Convention (possible revision process of the Gothenburg Protocol), but also have the potential to support the Clean Air for Europe (CAFE) programme under the European Commission (preparation of the revision of the National Emission Ceilings directive).

The CCE issued the call on 24 November 2004, setting the deadline to 28 February 2005. In addition to information provided in the Mapping Manual (www.icpmapping.org), also detailed instructions had been compiled by the CCE and distributed to the National Focal Centres. It was also made available on the CCE website (www.mnp.nl/cce) and can be found in Appendix A.

The following sections provide a summary of the results of the call for data on critical loads for acidification and eutrophication and dynamic modelling variables, including exceedance maps. A more detailed overview and analysis of national data submissions regarding critical loads and dynamic modelling variables is presented in Chapter 2, whereas country reports can be found in Part II of this report.

1.2 Response to the call for data

In 2005 fourteen parties under the Convention submitted updated data on critical loads of acidity and of nutrient-N, while 13 countries provided dynamic modelling data. Considering earlier submissions of Parties Table 1-1 gives an overview of the year in which the latest update by a NFC was recorded.

The critical loads consist of four basic variables which were asked to be submitted and which were used to support the Gothenburg Protocol. These variables are the basis for the maps used in the effect modules of the European integrated assessment modelling effort: (a) the maximum allowable deposition of S, $CL_{max}(S)$, i.e. the highest deposition of S which does not lead to 'harmful effects' in the case of zero nitrogen deposition, (b) the minimum critical load of nitrogen, $CL_{min}(N)$ to ensure sufficient nitrogen for plant uptake including nitrogen immobilisation (c) the maximum 'harmless' acidifying deposition of N, $CL_{max}(N)$, in the case of zero sulphur deposition, and (d) the critical load of nutrient N, $CL_{nut}(N)$, preventing eutrophication of ecosystems.

[1] Note that this chapter also includes an update on critical loads of Cd, Pb and Hg in section 1.7 including latest results following the CCE workshop and meeting of the Task Force of the ICP M&M (Berlin, 25-29 April 2005).

Table 1-1. Overview of the year in which a Party submitted the latest update on critical loads for acidification, eutrophication and dynamic modelling data.

	Critical loads for Acidification based on data of:		Critical loads for eutrophication based on data of:		Dynamic Modelling data based on data of:	
Austria (AT)		2005		2005		2005
Belgium (BE)[1]	2003[1]		2003[1]		-	
Bulgaria (BG)		2005		2005		2005
Belarus (BY)		2005		2005	-	
Switzerland (CH)		2005		2005		2005
Cyprus (CY)	2004		2004		-	
Czech Rep. (CZ)		2005		2005		2005
Germany (DE)		2005		2005		2005
Denmark (DK)	2004		2004		-	
Estonia (EE)	2001		2001		-	
Spain (ES)	1997		1997		-	
Finland (FI)	2004		2004		-	
France (FR)		2005		2005		2005
United Kingd. (GB)		2005	2004			2005
Croatia (HR)	2003		2003		-	
Hungary (HU)	2004		2004		2004	
Ireland (IE)		2005		2005		2005
Italy (IT)		2005		2005		2005
Moldava (MD)	1998		1998		-	
Netherlands (NL)		2005		2005		2005
Norway (NO)		2005		2005		2005
Poland (PL)		2005		2005		2005
Russia (RU)	1998		1998		-	
Sweden (SE)		2005		2005		2005
Slovakia (SK)	2003		2003		-	
Total # parties	11	14	11	14	1	13

[1]The last update of data from Wallonia is of 2001

Dynamic modelling results submitted in 2005 may be different to the results of 2004 also because depositions of acidifying compounds had to be used which were now computed with the Unified Model on an EMEP50 grid (see Simpson et al., 2003).

1.3 Critical load maps

This section contains maps of critical loads for ecosystems within 50×50 km^2 EMEP (EMEP50) grid cells. The maps are based on updated national contributions from 14 countries. For other countries the most recent data submission was used as listed in Table 1-1. For countries that never submitted critical loads data the European background database (see Chapter 4) has been used.

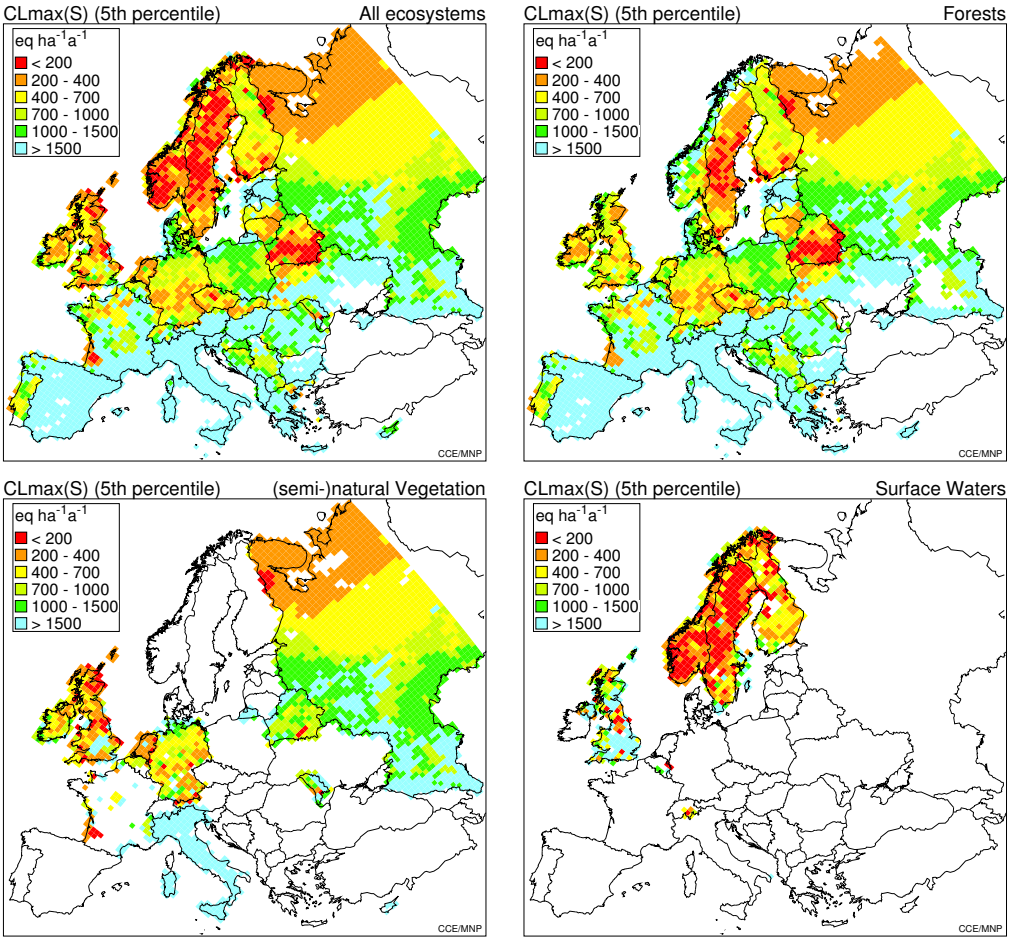


Figure 1-1. The 5th percentiles of the critical loads for acidity for all ecosystems (top left), forests (top right), semi-natural vegetation (bottom left) and surface waters. The maps present these quantities on the EMEP50 grid.

Figure 1-1 shows 5th percentile maps of $CL_{max}(S)$ for all ecosystems combined (top-left), forest ecosystems (top-right), semi-natural vegetation (bottom-left) and aquatic ecosystems. Low critical loads below 200 eq ha^{-1}a^{-1} (red shaded) show up north of 50^{o} latitude. In Sweden low critical loads reflect highly sensitive forest and aquatic ecosystems. In Belarus low deposition values are needed to protect forests and natural vegetation. In south-western France low critical loads exist for semi-natural vegetation.

Figure 1-2 shows analogous maps for $CL_{nut}(N)$. Low values of the 5th percentile (below 400 eq ha^{-1}a^{-1}) occur particularly for forest soils in most of Europe.

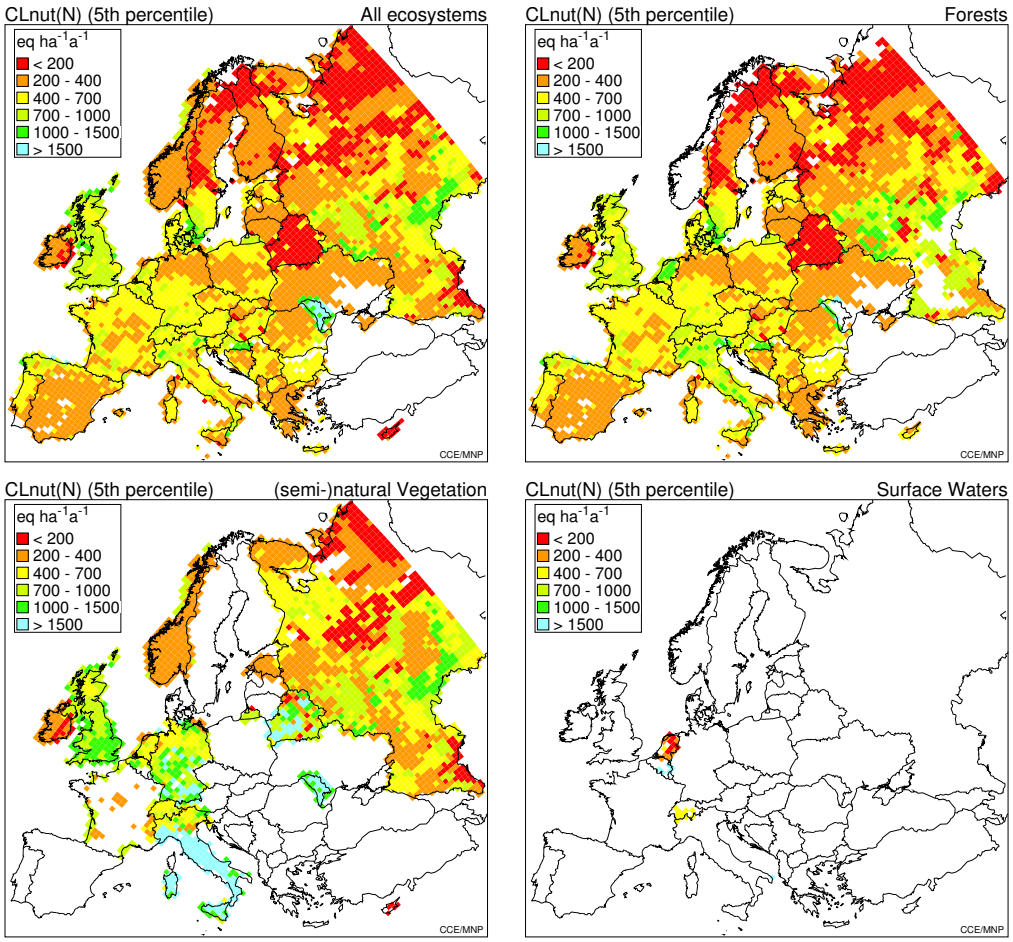


Figure 1-2. The 5th percentiles of the critical loads of nutrient nitrogen for all ecosystems (top left), forests (top right), semi-natural vegetation (bottom left) and surface waters. The maps present these quantities on the EMEP50 grid.

1.4 Robustness of critical load submissions

Figure 1-3 provides a comparison of the statistics of the national focal centre submissions since 1998 until the year in which the NFC made its last update. The minimum, 5th, 25th (lower quartile), 50th, 75th (upper quartile), 95th percentiles and the maximum of the critical loads of each country that submitted data are shown in an analogy to the well known 'Box and Whisker plot', i.e. a 'diamond plot'. A diamond plot offers some visual advantages, e.g. when diamonds are overlaid.

Statistics of $CL_{max}(S)$ are on the left ranging over an interval of 0 to 4000 eq $ha^{-1}a^{-1}$, while $CL_{nut}(N)$ (right) ranges from 0 to 2000 eq $ha^{-1}a^{-1}$. If we focus on the submission of this year and 2004 the following can be said. Compared to 2004 the median values (shown as vertical line dividing a 'diamond') of $CL_{max}(S)$ in 2005 increased in Austria, Switzerland, the Czech Republic, France, Norway and Poland, while decreasing in Belarus, Germany, the Netherlands and Sweden. The median value of data for $CL_{nut}(N)$ in 2005 revealed an increase for submissions from Austria, Bulgaria, Belarus, Germany, France, Italy, Poland and Sweden while the median decreased in the Czech Republic, Ireland and the Netherlands.

The striking increase of Austrian critical loads submitted in 2005 in comparison to earlier submissions is the result of replacing the entire database by another one due to improved knowledge on base cation weathering.

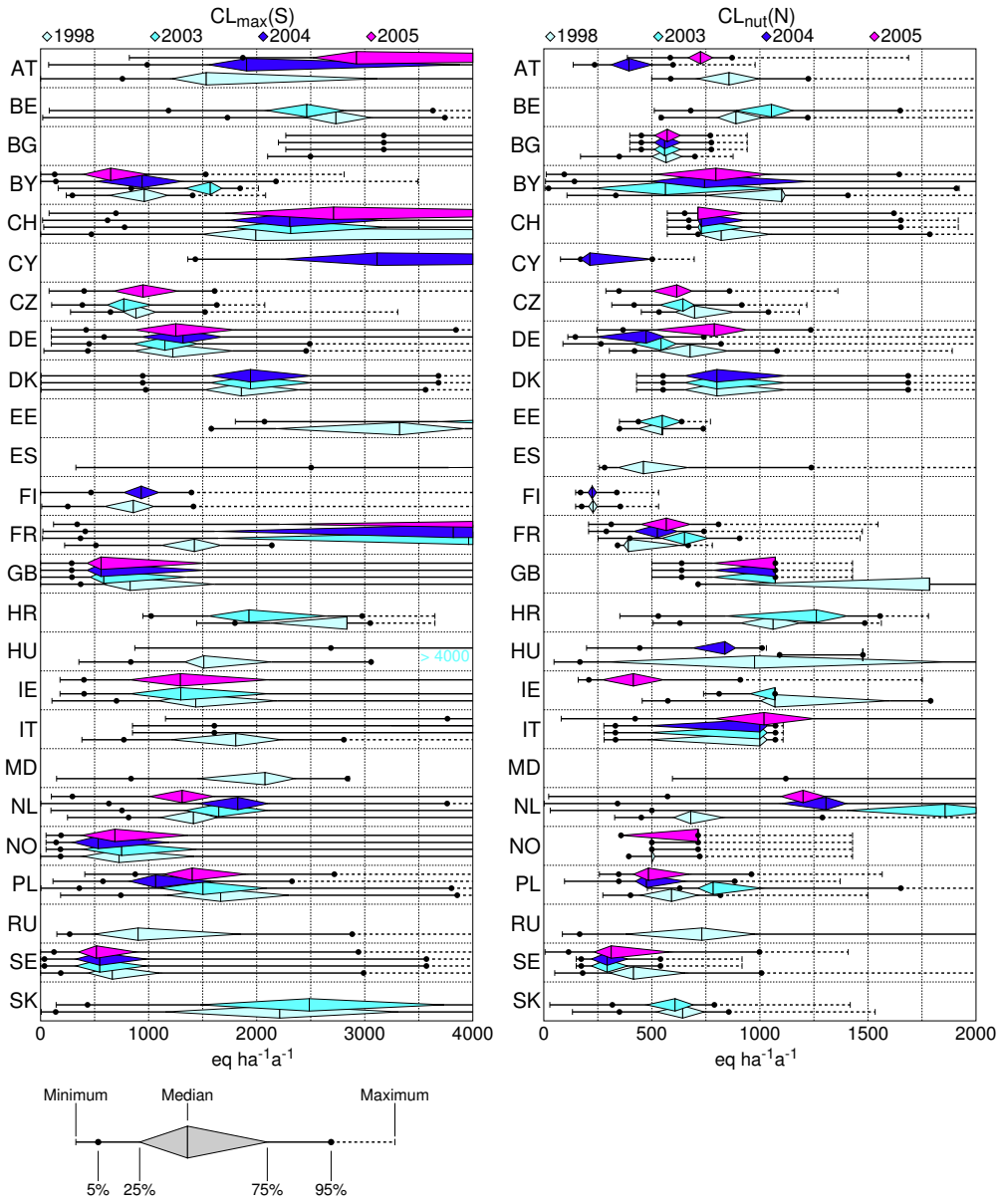


Figure 1-3. Diamond plot of the minimum (left extreme), 5th (left dot), 25th (left corner of diamond), 50th (vertical line in the diamond), 75th (right corner), 95th (right dot) percentiles and maximum (right extreme) critical loads of $CL_{max}(S)$ (left) and $CL_{nut}(N)$ (right) for the national data of (or before) 1998 (light blue), 2003 (turquoise), 2004 (dark blue) and 2005 (purple), respectively.

Inspecting the range of critical loads submitted since 1998 (which have been used for the support of the Gothenburg protocol) we can see that the last recorded NFC submission of the 5th percentile $CL_{max}(S)$ was markedly lower than in 1998 for Belgium, Belarus, the Czech Republic, France, Croatia, Ireland, United Kingdom, the Netherlands and Sweden while the median shifted downwards since 1998 in Belgium, Belarus, United Kingdom, Croatia, Ireland, the Netherlands, Poland and Sweden. Finally, it can be concluded that the $CL_{max}(S)$ values between the 25th and 75th percentile ('the diamond') generally show a cluster between 1998 and the last recorded submission. This is most striking in most of the country data of which the median in 2005 has shifted within a range of about 500 eq $ha^{-1}a^{-1}$ from the median in 1998. With respect to $CL_{nut}(N)$ the 5th percentile of the last recorded submission decreased with respect to the 1998 data in Belarus, Switzerland, the Czech Republic, Germany, France, Croatia, Ireland, Norway, Sweden and Slovakia. Also for $CL_{nut}(N)$ submissions of data in the range between the 25th and 75th percentile a clustering tendency can be remarked between 1998 and the latest recorded year for most of the countries. This tendency does not contradict the preliminary assertion that critical loads data have been robust over time.

1.5 Critical load exceedances and robustness

The term exceedance in this section refers to the 'average accumulated exceedance' (AAE). The AAE is the area-weighted average of exceedances (accumulated over all ecosystem points) in a grid cell, and not only the exceedance of the most sensitive ecosystem. An AAE may be computed for all ecosystem categories within a grid cell, but also for one single ecosystem category (such as a forest) in a grid cell for which data points are submitted by an NFC. The European database of critical loads (both submitted and from the back ground database) covers 5,918,115 km^2 of ecosystem area (see Table 1-2) part of which is covered by ecosystems of 25 Parties under the LRTAP Convention that have submitted data over the past 15 years (1,654,876 km^2 is covered by critical loads data from the EU25 of which 18 Member States submitted data).

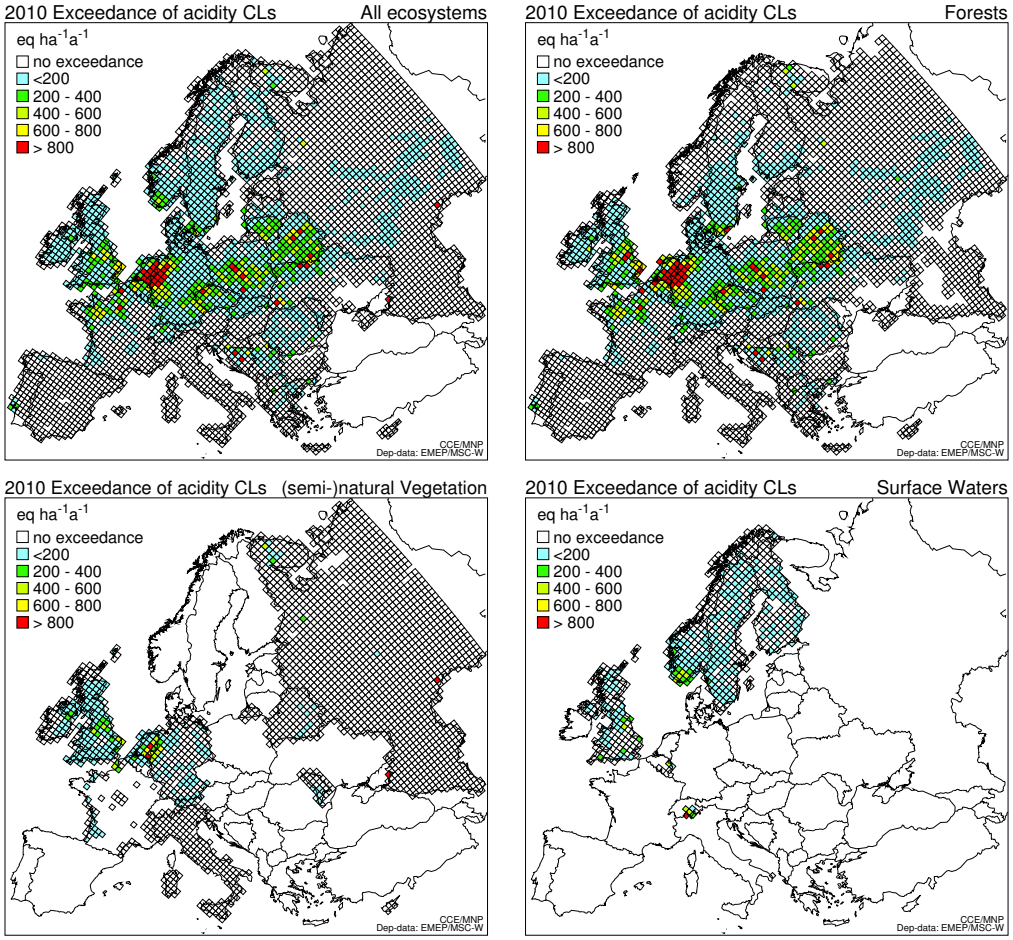


Figure 1-4. Average Accumulated Exceedance for acidity for all ecosystems (top left), forests (top right), vegetation (bottom left) and surface water using acid deposition computed by the EMEP Unified Model for 2010.

Figure 1-4 shows the AAE of acidity with the highest values occurring for exceedances in forest soils mostly north of 50^o latitude and for vegetation on the border of the Netherlands and Germany and in the east of the United Kingdom.

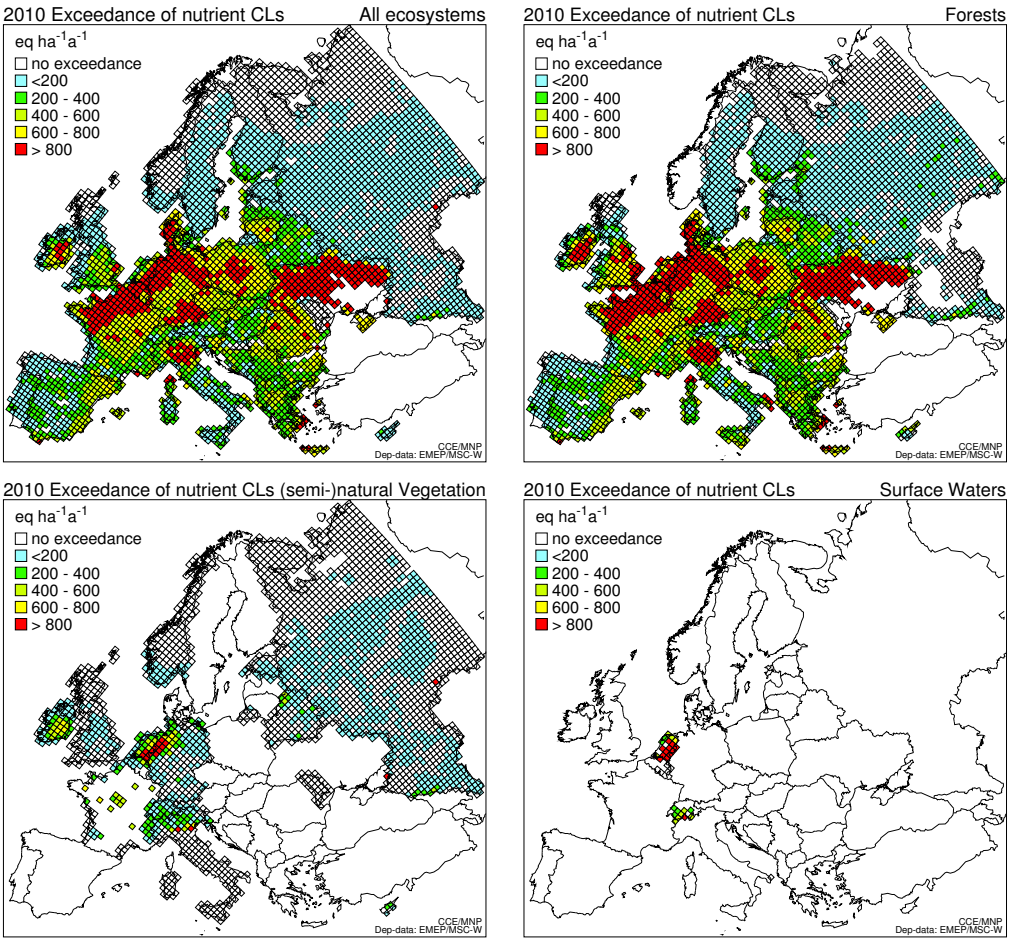


Figure 1-5. Average Accumulated Exceedance for eutrophication for all ecosystems (top left), forests (top right), vegetation (bottom left) and surface water using deposition of oxidized and reduced nitrogen computed by the EMEP Unified Model for 2010.

Figure 1-5 shows the AAE of critical loads of nutrient nitrogen. It reveals that submitted data on the critical load of nutrient nitrogen focuses on forest soils (top right). The highest exceedances are south of 58^{o} latitude with peaks in a broad coastal area between northern France and Denmark as well as in the north of Italy. Semi natural vegetation at risk occurs mostly in the border area between the Netherlands and Germany.

Figures 1-4 and 1-5 illustrate the spatial variation of the AAE. The cross border variation of exceedances was shown in Hettelingh et al. (2004) to change in particular due to the application of the EMEP Unified Model which replaced the lagrangian model results. We will not repeat the comparison here between the exceedances computed with the lagrangian and Unified Model. Suffices to say that it was shown that the spatial distribution of exceedances computed with the Unified Model was robust (areas with high exceedances under the lagrangian remained high under the Unified Model) but that the magnitude of the exceedances increased.

In Figure 1-6 we focus on the influence of the change of acidity critical load since 1998 on the national distribution of exceedances with particular attention on the occurrence of high national exceedances (the median and 95th percentile of the exceedance distribution in each country).

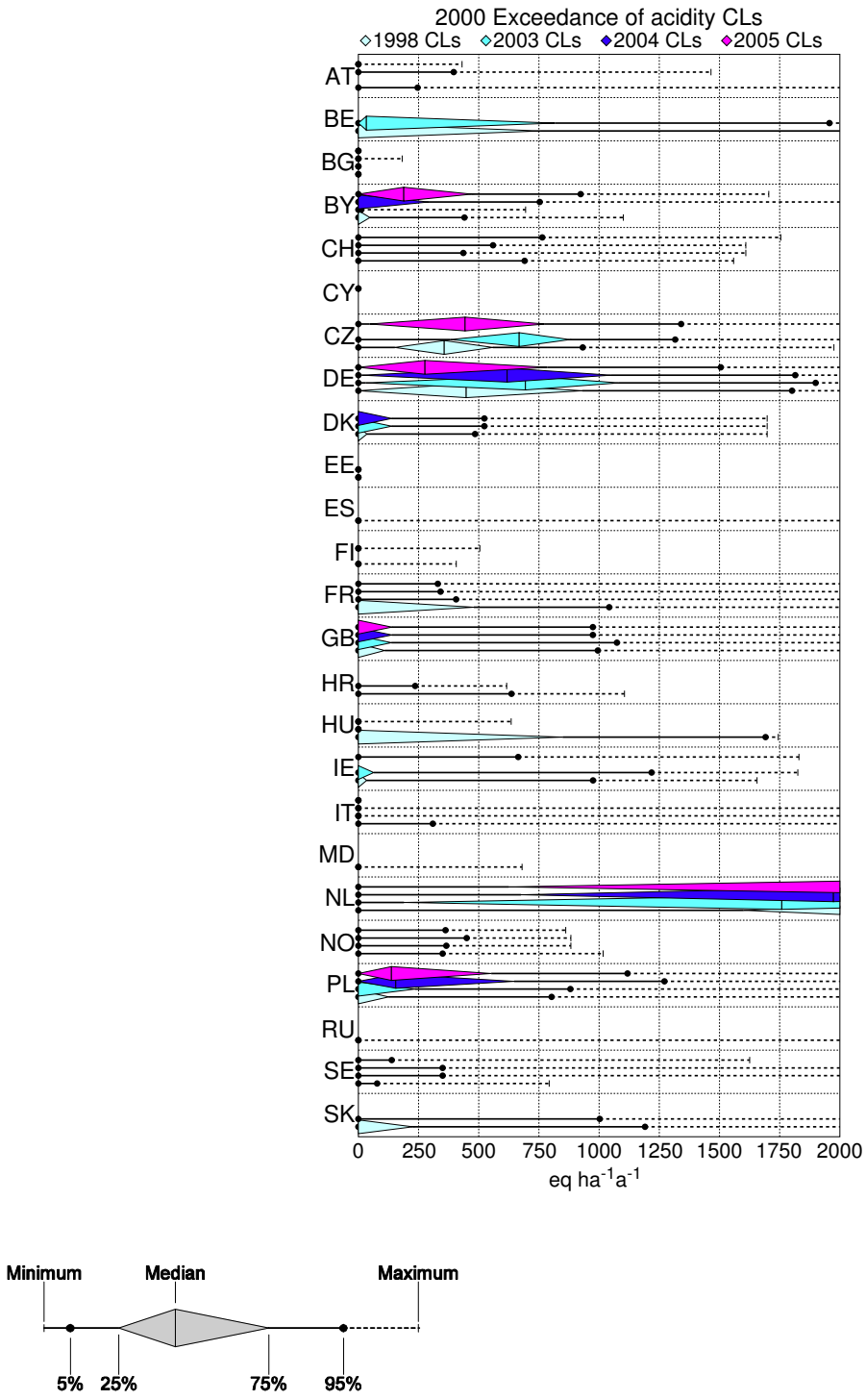


Figure 1-6. Diamond plot of national exceedances for acidity computed with critical load databases from 1998 until 2005, or the latest recorded submission of a National Focal Centre using depositions computed with the EMEP Unified Model and acidifying emissions of 2000.

Figure 1-6 shows that the median of the exceedances with recent critical loads (purple diamonds) compared to the median using 1998 critical loads (light blue) increased in Belarus, the Czech Republic, the Netherlands and in Poland. In the other countries the median exceedance is zero or decreased somewhat in comparison to the distribution of exceedances in 1998 as can be seen for Germany. Since the 1998 submission, the 95th percentile

(the right dot) of the distribution of exceedances increased in Belarus (about +483 eq ha^{-1} a^{-1}), the Czech Republic (about +409 eq ha^{-1} a^{-1}), Poland (about +316 eq ha^{-1} a^{-1}), Sweden (about +61 eq ha^{-1} a^{-1}) and the Netherlands (about +255 eq ha^{-1} a^{-1}). Exceedances in the Netherlands are the highest in comparison to other countries that submitted critical load data. A decrease between 1998 and 2005 of the 95th percentile exceedance is seen in Austria (about -246 eq ha^{-1} a^{-1}), Switzerland (about -73), Germany (about -296 eq ha^{-1} a^{-1}) and France (about -711 eq ha^{-1} a^{-1}).

Finally, Figure 1-7 displays the temporal development since 1940 of the Average Accumulated Exceedance of critical loads for acidity on all European ecosystems (top left) and of the ecosystem area percentage that is unprotected by acid deposition (top right). The development of the AAE illustrates the marked decrease of AAE especially on forest soils (brown graph). In 1985 about 60% of the forest soils (broadly distributed in Europe) and more than 40% of the surface waters (in northern Europe in particular) are unprotected. In 2010 these percentages become reduced below 20%. From Figure 1-4 it can be seen that the exceeded forest ecosystems in 2010 are located in about one third of the EMEP grid cells covering pan-Europe.

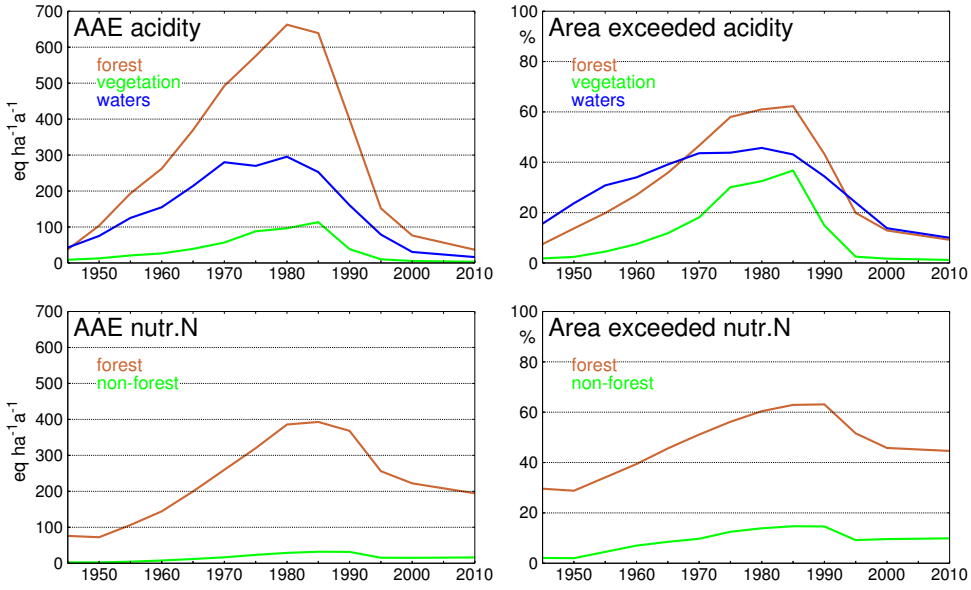


Figure 1-7. The Temporal development between 1945 and 2010 of the Average Accumulated Exceedance (AAE) of critical loads for acidity on all European ecosystems (top left), of the ecosystem area percentage that is exceeded by acid deposition (top right), of the AAE for eutrophication (bottom left) and % of areas unprotected from eutrophication (bottom right).

Figure 1-7 also shows that natural vegetation continues to be at risk of acid deposition after 1995 mostly in Germany, the Netherlands and in the United Kingdom (see Figure 1-4).

With respect to European forest ecosystems at risk of eutrophication, Figure 1-7 (bottom graphs) illustrates that the European AAE has decreased from about 400 to 200 eq ha^{-1} a^{-1} between 1985 and 2010 (bottom left graph). In terms of areas this implies (bottom right map) a reduction of unprotected areas from more than 60% in 1985 to about 45% in 2010. Note that about 10% of natural vegetation remains at risk of nutrient nitrogen as of about 1995. The latter also holds for surface waters, data for which are too limited to produce a meaningful plot from a European point of view.

1.6 Dynamic modelling[2]

Dynamic modelling and terminology

Important dynamic modelling results for possible use by the TFIAM are so-called target loads. A target load is the deposition (path) which ensures recovery by having the prescribed chemical (or, ideally, biological) criterion (e.g., the Al:Bc ratio) be met in a given year and maintained thereafter. The variety of deposition paths to reach a target load is numerous. We restrict to deposition pathways that are characterised by three numbers (years): (i) the protocol year, (ii) the implementation year, and (iii) the target year (see Figure 1-8). The protocol year for dynamic modelling is the year up to which the deposition path is assumed to be known and cannot be changed any more. This can be the present year or a year in the (near) future, for which emission reductions are already agreed. As *protocol year* countries were requested to use 2010, the year for which the Gothenburg Protocol and the EU NEC Directive are expected to be in place. The *implementation year* for dynamic modelling is the year in which all reduction measures to reach the final deposition (the target load) are assumed to be implemented *relative to a new protocol or directive.*

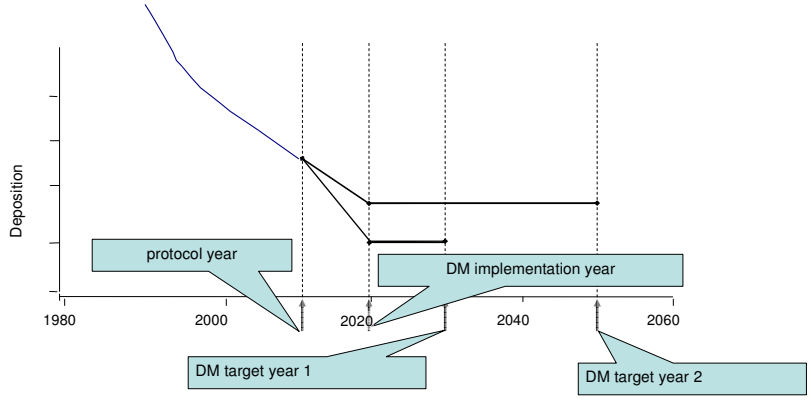


*Figure 1-8. Schematic representation of deposition paths leading to target loads by dynamic modelling (DM), characterised by three key years. (i) The year up to which the (historic) deposition is fixed (**protocol year**); (ii) the year in which the emission reductions leading to a target load are implemented (**DM implementation year**); and (iii) the years in which the chemical criterion is to be achieved (**DM target years**) (Source: Posch et al., 2003).*

Between the protocol year and the implementation year deposition is assumed to change linearly. After consultation with the chairmen of the ICP M&M, the WGE, the Working Group on Strategies and Review (WGSR) and other Convention representatives, 2020 was chosen as a preliminary implementation year and 2030 and 2050 as *target year.* A target year for dynamic modelling is the year in which the chemical criterion (e.g., the Al:Bc ratio) is met (for the first time). For scientific and technical purposes countries were also requested to submit a target load for 2100.

In addition to information on target loads and target years, National Focal Centres (NFCs) were also requested to ensure consistency between critical loads and dynamic modelling. This implies that each ecosystem-record in the critical load database should contain data that can be used to compute critical loads and to run the dynamic model. However, to maintain important statistical information on the (distribution of) sensitivity of ecosystems within an EMEP grid cell, NFCs were requested not to leave out records for which only critical loads and no dynamic modelling data are available. Deposition data are based on the Unified Model of EMEP (Simpson et al., 2003). However, no historical data based on the Unified Model of EMEP is yet available. Therefore, the ratio in 2000 of the magnitude of depositions generated by the lagrangian model (on 150×150 km^2; Schöpp et al., 2003; EMEP, 1998) to those from the new EMEP Unified Model (on 50×50 km^2) were used as a basis to scale the historical lagrangian deposition trends between 1880 and 2000.

[2] Part of this work is supported by the European Commission under Service Contract 070501/2004/380217/MAR/C1

Dynamic modelling results

A geographical representation of the areas for which we received target loads to ensure recovery in 2030, 2050 and 2100 is shown in Figure 1-9. Target loads have been set equal to critical loads in areas which are 'safe', i.e. where critical loads are not exceeded or critical limits niot violated (see Table 2-2 columns 7, 11, 15) and in areas where target loads have not been computed. A map showing grid cells in which target loads have been computed is given in Chapter 2 (see Fig 2-2). Target loads are set to 0 in areas where they are infeasible.

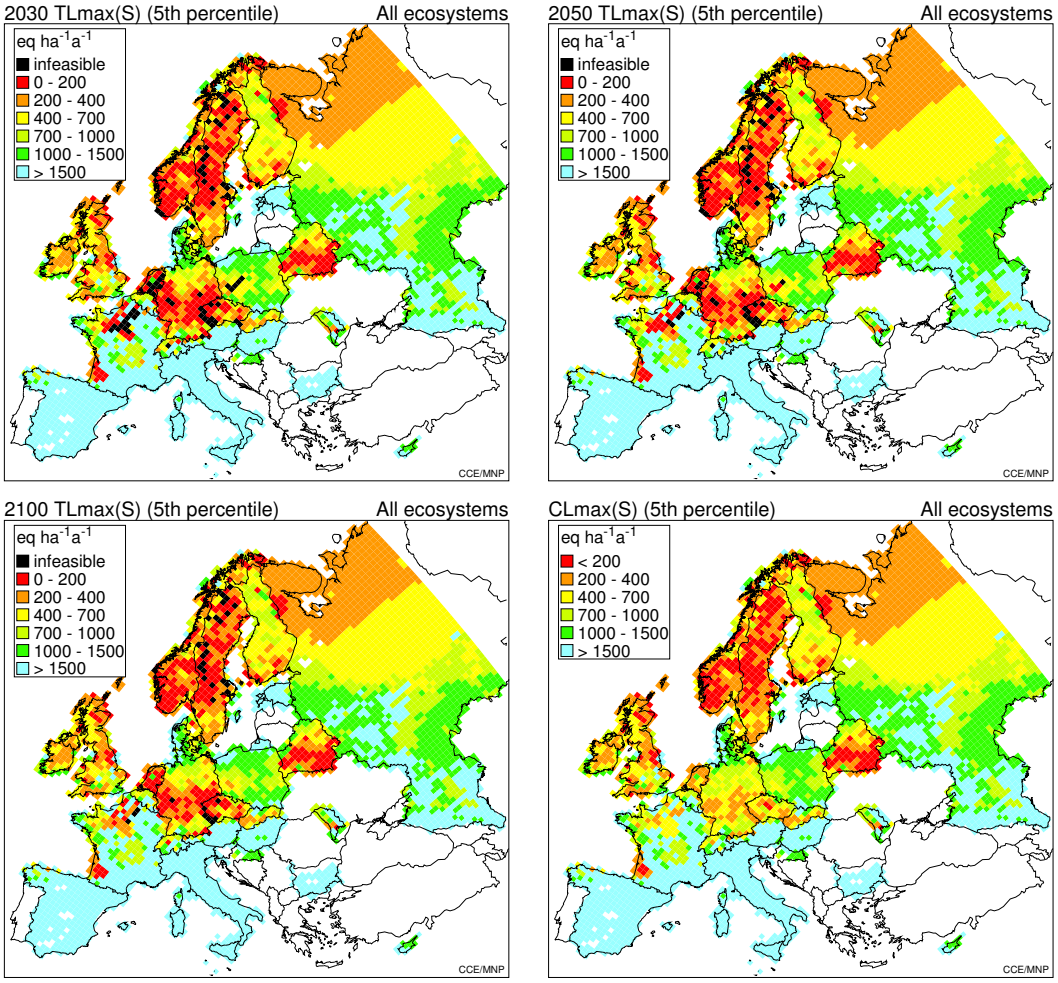


Figure 1-9. Location and magnitude of target loads that lead to recovery of 95% of the ecosystem area in 2030 (upper left), 2050 (upper right) and 2100 (lower left). For comparison the 5% map of CLmax(S) is shown as well.

Comparison of target load maps to the critical load map in Figure 1-9 shows grid cells where the 5th percentile target load values are lower than critical loads values (lower-right map) e.g. in the Czech Republic, France, Germany, the Netherlands, Poland and Sweden. Grid cells where target loads are equal to critical loads do include areas for which dynamic modelling was not performed .

We were able to compute Recovery Delay Times (RDT) under the Base Line Current Legislation (BL-CLE) scenario. It turned out in the CLRTAP-domain that 29.2% (25.7% in EU25) of the area which is not safe now could recover in the future, i.e. 20.2% (21.9%) before 2030, 20.7% (22.5%) before 2050 and 22.3% (24.2) before 2100. We conclude that another 6.9% (1.5 %) of the area which is not safe at present would recover after 2100. Deposition levels would need to be reduced further to either increase the area that recovers before 2100, or to bring closer the year of recovery. How much depositions should be reduced below BL-CLE deposition patterns depends on the year in which recovery is aimed to occur, i.e. on the target load required to obtain recovery in that year. In doing this we found that about 95% of the ecosystems which is not safe now could recover already in 2030 if acid deposition is sufficiently reduced in 2020 (implementation year). This does include ecosystems for

which acid deposition needs to be reduced below critical loads. In chapter 2 a more detailed analysis of dynamic modelling elements is provided.

Figure 1-10 shows a comparison on a country scale between target loads and critical loads in the form of diamond-graphs.

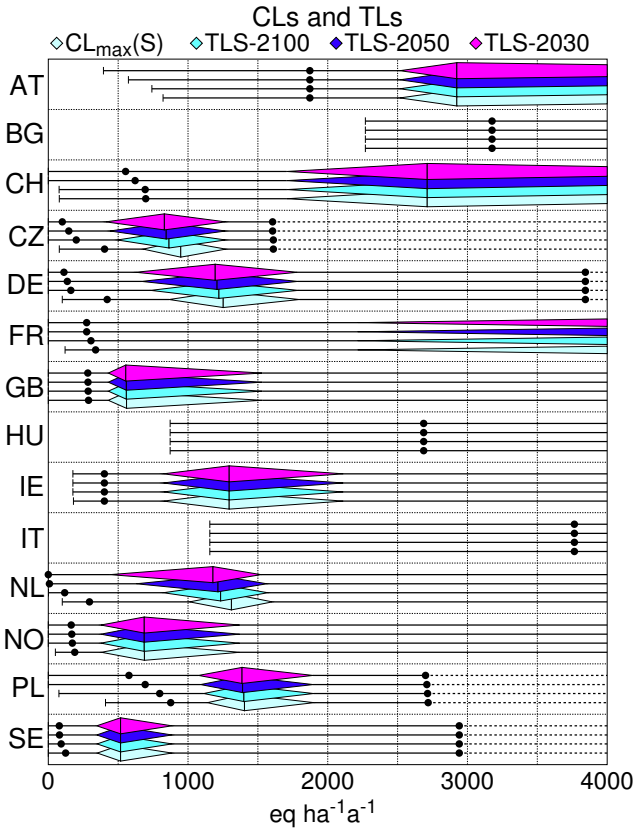


Figure 1-10. Diamond plot of the distribution of critical loads (light blue) and target load distributions in 2100 (turquoise), 2050 (dark blue) and 2030 (purple).

Figure 1-10 confirms that a marked differentiation between the 5th percentile values (left dot) of target loads and critical loads are in Switzerland, the Czech Republic, Germany, France, the Netherlands, Poland and Sweden. A decrease of the median values can be seen in the Czech Republic, Germany and the Netherlands in particular.

Finally, Table 1-2 provides an overview of trends from 1980 to 2010 of non-protected area in each country, including critical loads from the CCE European background database (EU-DB) for countries that did not ever submit data.

Deposition fields for 1980-2010 were provided by EMEP/MSC-W. The ecosystem area in the CLRTAP domain which is at risk from acidification (left part of Table 1-2) reduces from about 48% (48.6% in the EU25) in 1980 to about 6% (11% in the EU25) in 2010. For the risk of eutrophication (right part of Table 1-2) the percentages go from about 38% (80.5% in the EU25) to 28% (60% in the EU25). The persisting broad European areas that are unprotected from eutrophication point to the requirement of using dynamic models to improve knowledge of the delays by which damage from excessive nitrogen could occur.

Table 1-2. Exceedances of the critical load for acidification (left) and for eutrophication (right) as % of the European ecosystem area for which critical loads are available (including the CCE back ground database), using depositions computed with the EMEP-Unified Model (Simpson et al., 2003) from 1980 to 2010 on the basis of the BL_CLE scenario (totals include Andorra, Liechtenstein and San Marino).

country	$CL_{max}(S)$ Ecoarea	Area NOT protected from acidification (%)				country	$CL_{nut}(N)$ Ecoarea	Area NOT protected from eutrophication (%)			
-	(km^2)	1980	1990	2000	2010	-	(km^2)	1980	1990	2000	2010
AL	6,334	0.9	0.9	0.0	0.0	AL	6,334	100.0	100.0	100.0	99.9
AT	35,745	35.2	16.7	1.0	0.3	AT	35,745	99.8	99.8	97.2	87.8
BA	10,241	70.4	65.3	52.7	45.2	BA	10,241	99.9	99.9	99.7	99.6
BE	7,282	99.2	96.3	51.3	24.8	BE	7,282	97.5	97.1	95.1	93.8
BG	52,032	0.0	2.7	0.0	0.0	BG	52,032	100.0	100.0	99.0	99.3
BY	107,841	96.0	91.1	63.7	58.4	BY	107,841	75.8	76.0	58.6	59.9
CH	11,792	59.4	38.7	19.2	13.2	CH	22,790	91.4	90.9	81.6	71.8
CY	4,434	-	-	0.0	0.0	CY	4,434	-	-	89.1	89.0
CZ	11,178	99.4	99.3	78.6	47.1	CZ	11,178	100.0	100.0	99.5	98.6
DE	104,186	94.6	93.3	61.7	41.5	DE	104,186	99.0	98.7	97.6	96.8
DK	3,136	98.4	94.8	31.6	8.2	DK	3,136	100.0	100.0	93.8	85.4
EE	21,416	0.0	0.0	0.0	0.0	EE	22,377	99.9	99.8	45.2	34.0
ES	85,175	4.3	2.9	1.0	0.1	ES	85,175	72.2	82.3	87.9	81.6
FI	265,919	39.0	15.6	1.5	1.0	FI	239,507	77.1	74.7	36.0	28.3
FR	180,102	24.5	21.3	14.7	7.9	FR	180,102	98.4	98.6	97.9	97.2
GB	77,129	75.4	67.1	33.9	16.5	GB	73,649	40.9	35.9	28.5	24.0
GR	9,288	11.3	15.2	10.5	6.8	GR	9,288	100.0	100.0	100.0	100.0
HR	6,931	96.7	80.7	10.7	1.2	HR	7,009	75.3	68.8	52.5	44.0
HU	10,448	10.0	5.3	0.2	0.0	HU	10,448	100.0	100.0	98.5	87.5
IE	8,933	41.0	33.6	24.6	12.9	IE	8,933	86.7	86.1	88.3	85.1
IT	125,477	1.2	0.0	0.0	0.0	IT	125,477	76.9	78.1	71.3	65.1
LT	17,651	92.5	89.7	76.6	68.1	LT	17,651	100.0	100.0	100.0	100.0
LU	821	99.9	78.7	33.2	22.2	LU	821	100.0	100.0	100.0	100.0
LV	27,321	56.3	46.8	24.7	14.8	LV	27,321	100.0	100.0	97.9	96.4
MD	11,985	37.5	22.7	2.7	2.7	MD	11,985	0.2	0.2	0.1	0.1
MK	5,068	47.4	47.4	42.9	17.3	MK	5,068	100.0	100.0	100.0	100.0
NL	7,295	87.6	86.7	84.7	81.7	NL	4,334	98.1	98.1	94.3	90.5
NO	386,692	42.4	33.8	15.5	11.3	NO	317,025	10.5	9.7	3.1	1.5
PL	88,383	99.9	97.3	57.5	38.8	PL	88,383	99.5	99.3	97.8	97.0
PT	21,221	10.0	12.4	10.8	4.6	PT	21,221	81.9	92.4	94.4	92.1
RO	62,807	67.7	49.5	7.2	5.8	RO	62,807	100.0	100.0	99.1	99.5
RU	3,516,432	46.4	24.3	1.1	1.1	RU	3,516,432	19.0	21.7	11.2	12.4
SE	517,818	58.7	45.3	13.7	7.8	SE	223,771	56.6	55.1	17.6	10.3
SI	5,264	70.1	51.2	2.2	0.0	SI	5,264	100.0	100.0	100.0	100.0
SK	19,253	80.1	71.5	24.4	13.5	SK	19,253	100.0	100.0	100.0	99.6
UA	63,600	93.1	82.1	27.8	22.7	UA	63,600	100.0	100.0	100.0	100.0
YU	21,307	53.6	52.8	42.8	30.5	YU	21,307	100.0	100.0	100.0	100.0
EU25	1,654,876	48.6	38.7	17.8	11.0	EU25	1,328,936	80.5	80.4	65.2	60.5
CLRTAP	5,918,115	48.1	31.2	8.5	6.1	CLRTAP	5,533,584	38.2	39.9	28.5	28.0

1.7 Update of European critical loads of heavy metals[3]

A detailed description of the response by the National Focal Centres, of European maps on critical loads of cadmium, lead, and mercury as well as of preliminary exceedance maps can be found in a collaborative report between CCE and MSCE (Slootweg et al., 2005). The deadline of the call for data on critical loads of heavy metals was 31 December 2004. However, results were sent to the CCE until a few weeks before the CCE workshop and meeting of the Task Force of the ICP M&M (Berlin, 25-29 April 2005). Updates that were made following that meeting could not be incorporated in Slootweg et al. (2005). Therefore this section addresses issues and summarizes recent results that were compiled following these ICP meetings.

Table 1-3. Overview of the country response on the call for critical loads of cadmium, lead and mercury and the 5 effects.

Country	Country code	Effect number*									
		Cd				**Pb**			**Hg**		
		1	2	3	4	1	3	4	1	3	5
Austria	AT	x	x	x		x	x		x	x	
Belarus	BY			x			x				
Belgium	BE	x		x	x	x	x	x	x	x	x
Bulgaria	BG	x				x					
Cyprus	CY	x	x	x		x	x		x		
Czech Republic	CZ	x				x			x		
Finland	FI										x
France	FR			x			x				
Germany	DE	x	x	x		x	x		x	x	
Italy	IT			x			x				
Netherlands	NL	x	x	x		x	x				
Poland	PL			x			x			x	
Russia	RU	x		x		x	x				
Slovakia	SK			x			x			x	
Sweden	SE		x	x			x			x	x
Switzerland	CH	x		x		x	x			x	
Ukraine	UA	x				x					
United Kingdom	GB			x			x				
Total	18	10	5	14	1	10	14	1	5	7	3

*1 = protect ground water (human health); 2 = limit content in food (human health); 3 = protect micro-organism (terrestrial ecosystem health); 4 = protect algae (aquatic ecosystem health); 5 = content in fish (human health). See UBA (2004) and Slootweg *et al.* (2004) for details.

Belgium, the Czech Republic, Germany, Poland, Slovakia, Sweden and the Ukraine sent updated data to the CCE between 29 April 2005 and 15 May 2005. A summary of the final country participation is given in Table 1-3.

Following a recommendation of the 21st Task Force meeting on Modelling and Mapping (Berlin, 28-29 April 2005) maps of critical loads should separate the protection against adverse health effects (effects 1, 2) from the protection against adverse ecosystem effects (effects 3 and 4). The result is shown in Figure 1-11 that gives the maps of critical loads of cadmium (top), lead (middle) and mercury (bottom) that will protect 95% of the ecosystems against adverse effects on human health (left) and on ecosystems (right). Figure 1-11 shows that ecosystem effects prevail as endpoint for critical loads that have been submitted.

[3] Part of this work has benefited from help in kind from Germany in 2005 under MNP-CCE project M259101/02/ entitled “Support of reporting obligations regarding the modelling and mapping of European critical loads of heavy metals”.

Furthermore, the meeting reviewed the use of the CCE background database (see Slootweg et al., 2005; chapter 3). In order to provide reliable effect-based information on the risk of air pollution impacts (exceedances) on a pan-European scale the need for a representative cover of Europe with critical loads for acidity, nutrient nitrogen and more recently heavy metals is considered a necessity.

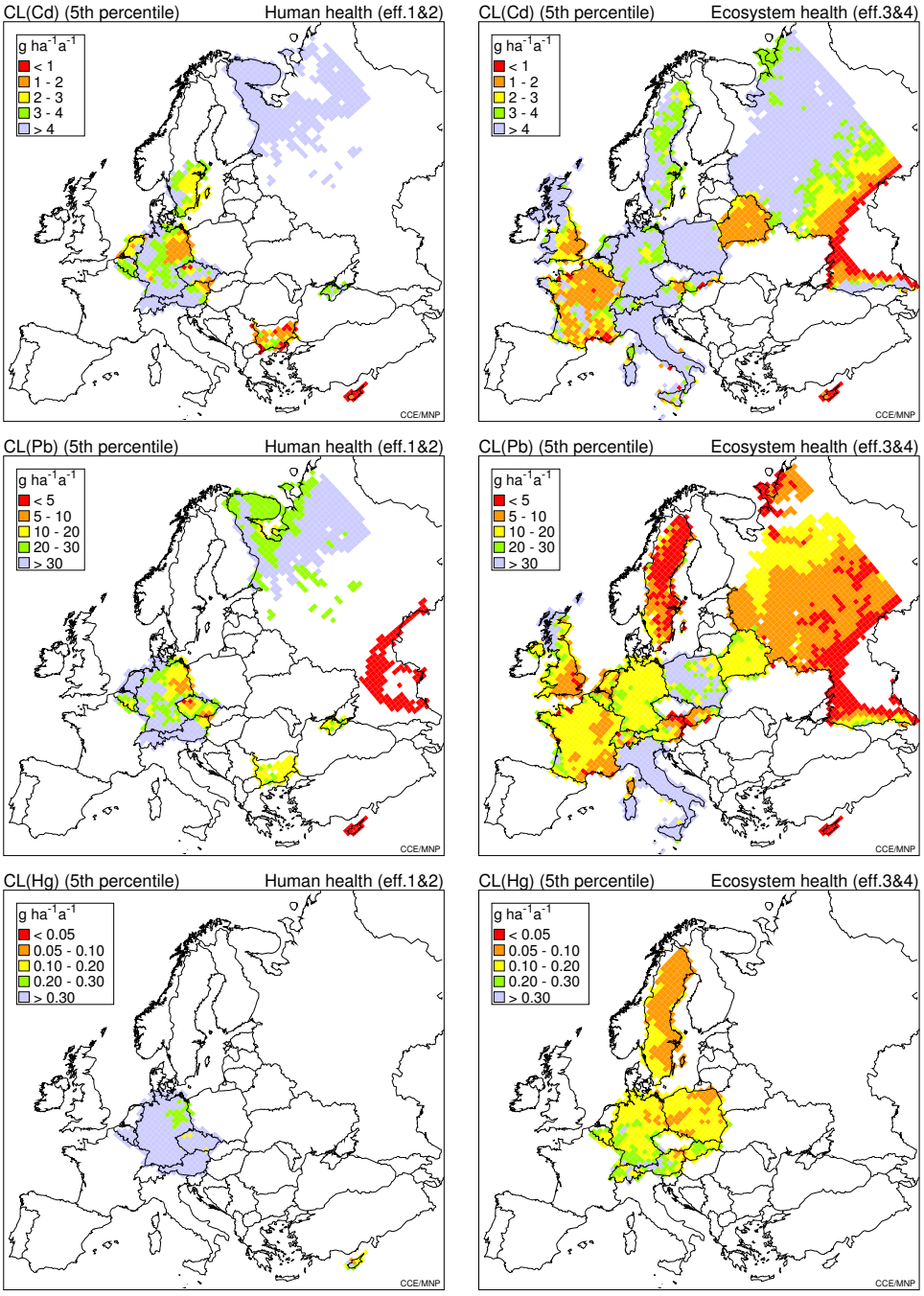


Figure 1-11. Maps of critical loads of cadmium (top), lead (middle) and mercury (bottom) that will protect 95% of the ecosystems against adverse effects on human health (left) and on ecosystems (right). Dark shaded areas indicate the occurrence of sensitive ecosystems.

Table 1-4 gives an overview of the percentage of national ecosystem areas that are at risk of health effects (effects 1 and 2) in countries that submitted critical loads of cadmium, lead and/or mercury. Table 1-5 gives an overview of the percentage of national ecosystem areas that are at risk of ecosystem effects (effects 3 and 4) in countries that submitted critical loads of cadmium, lead and/or mercury.

*Table 1-4. Percentages of national ecosystem areas that are at risk of **health effects** in countries that submitted critical loads of cadmium, lead and/or mercury.*

	Cadmium (Cd)			Lead (Pb)			Mercury (Hg)		
Country	Eco area (km^2)	1990 at risk (%)	2000 at risk (%)	Eco area (km^2)	1990 at risk (%)	2000 at risk (%)	Eco area (km^2)	1990 at risk (%)	2000 at risk (%)
AT	61,371	0.0	0.0	61,371	24.0	0.0	61,371	0.0	0.0
BE	5,228	0.0	0.0	5,228	62.3	18.2	5,228	22.7	6.1
BG	48,330	42.0	14.8	48,330	99.9	77.2	-	-	-
CH	2,200	0.0	0.0	2,218	72.0	2.3	-	-	-
CY	7,973	1.3	0.8	7,973	74.1	70.4	7,973	4.2	4.1
CZ	25,136	1.1	0.5	25,136	93.1	19.9	25,136	7.4	1.9
DE	290,003	1.4	0.1	290,003	79.0	7.4	290,003	17.9	4.8
NL	19,471	0.1	0.0	19,471	89.2	0.1	-	-	-
RU	425,425	0.0	0.0	650,575	3.3	2.5	-	-	-
SE	22,050	0.0	0.0	-	-	-	-	-	-
UA	18,002	0.0	0.0	18,002	91.6	41.4	-	-	-
EU25	431,232	1.1	0.1	409,182	71.8	8.1	389,711	14.2	3.9
Europe	925,190	2.7	0.8	1,128,308	33.8	8.3	389,711	14.2	3.9

*Table 1-5. Percentages of national ecosystem areas that are at risk of **ecosystem effects** in countries that submitted critical loads of cadmium, lead and/or mercury.*

	Cadmium (Cd)			Lead (Pb)			Mercury (Hg)		
Country	Eco area (km^2)	1990 at risk (%)	2000 at risk (%)	Eco area (km^2)	1990 at risk (%)	2000 at risk (%)	Eco area (km^2)	1990 at risk (%)	2000 at risk (%)
AT	61,371	0.0	0.0	61,371	48.7	11.1	32,601	39.2	11.7
BE	5,237	0.0	0.0	5,237	63.0	12.8	5,228	100.0	83.5
BY	121,128	9.1	0.1	121,128	100.0	10.2	-	-	-
CH	9,411	0.0	0.0	9,393	99.0	24.1	11,611	80.2	44.4
CY	7,973	0.0	0.0	7,973	80.9	78.4	-	-	-
DE	290,003	0.1	0.0	290,003	83.8	9.0	99,866	97.0	59.8
FR	170,638	0.1	0.0	170,638	93.7	9.8	-	-	-
GB	50,075	0.5	0.0	50,075	25.9	6.0	-	-	-
IT	278,128	0.0	0.0	278,128	0.3	0.0	-	-	-
NL	22,314	0.0	0.0	22,314	98.4	21.5	-	-	-
PL	88,383	0.5	0.0	88,383	73.5	14.7	88,383	100.0	99.9
RU	1,393,300	1.1	0.2	1,194,125	70.8	51.0	-	-	-
SE	151,432	0.0	0.0	151,432	60.5	1.9	152,074	56.0	22.9
SK	19,253	2.6	1.1	19,253	52.3	22.6	19,253	99.0	65.3
EU25	1,144,807	0.1	0.0	1,144,807	56.3	7.4	397,405	77.4	51.2
Europe	2,668,646	1.0	0.1	2,469,453	65.7	28.7	409,016	77.4	51.0

Tables 1-4 and 1-5 show that the risks of effects of lead are more widespread than those of cadmium. Comparison of Tables 1-4 and 1-5 also reveals that the area of excess deposition of Pb in 2000 is strongly reduced in comparison to 1990. In Europe 33.8 % of the ecosystem area in 1990 is subjected to excess deposition of Pb for human health effects, which is reduced to 8.3% in 2000 (see Table 1-4). The risk for ecosystem effects of Pb in 1990 and 2000 is 65.7% and 28.7%, respectively (see Table 1-5).

To ensure this, the use of a European background database containing relevant European forest soil information was used in the past for countries that never submitted critical loads data on acidity and nutrient nitrogen. In the nineties critical loads for other air pollution compounds were not computed yet. The use of these background data, noted by the Task Force on Mapping already in 1993 (EB.Air/WG.1/R.85 paragraphs 5 and 26) has led to European maps of critical loads that were approved by the WGE since 1994. Critical load maps, based on national contributions and background data when national data were not available, have then been used in the support of

the assessment of areas at risk during negotiations of the 1994 Oslo protocol (only sulphur) and the 1999 Gothenburg protocol.

This historic practice regarding the use of the European background database has also been the guiding principle for the CCE to compile a European background data base of critical loads of heavy metals. The result is shown in Figure 1-12. Areas that are sensitive for cadmium (top left) are generally located in the south of Europe. Areas that are most sensitive to lead (top right) are in the north, while the risk of mercury (bottom left) turns out to be widespread with particularly sensitive areas in the north of Europe. The Task Force recommended using the European Background database for the assessment of exceedances in countries that did not submit data and do not object to this. In this section, the risk of heavy metal deposition is only computed for countries that submitted data. This is reflected in Tables 1-4 and 1-5.

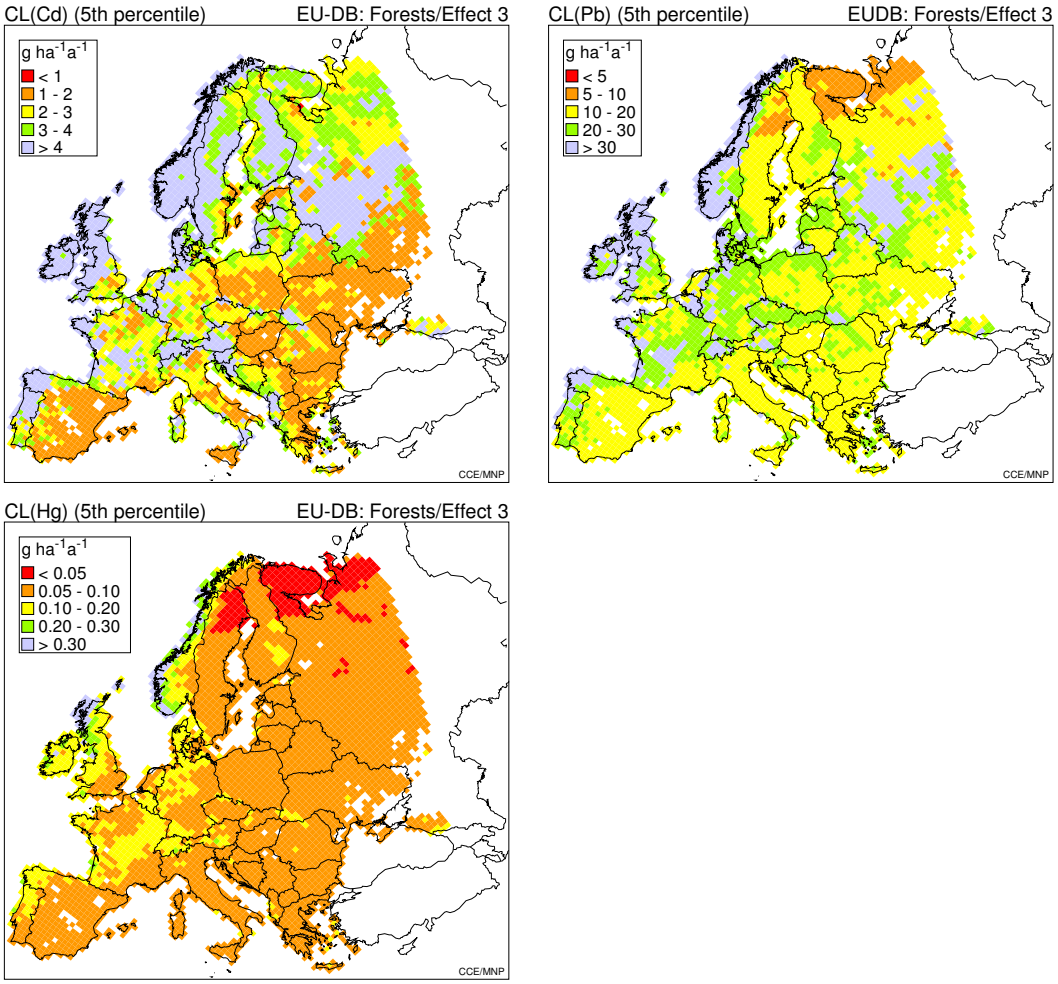


Figure 1-12. The 5th percentile map of critical loads for forest soils of cadmium (top left), lead (top right) and mercury based on the CCE European background database (see Slootweg et al., 2005, chapter 3).

1.8 Conclusions

In 2005 fourteen parties under the LRTAP Convention submitted updated data on critical loads of acidity and of nutrient-N, while 13 countries (10 EU countries) provided dynamic modelling data for acidification. Including results of 2004 dynamic modelling data are available for 14 parties under the Convention (11 EU Member States). Critical load exceedances were computed with depositions computed with the EMEP Unified Model. Results reveal that still 8.5% of the ecosystem area in pan-Europe and 17.8% in the EU25 are still at risk of acidification in 2000. For eutrophication the risk stretches over an even larger area covering 28.5% and 65.2%, respectively. Dynamic modelling of the risk for acidification indicates that about 95% of the ecosystems concerned could

recover already in 2030 if acid deposition is sufficiently reduced in 2020. This does include ecosystems for which acid deposition needs to be reduced below critical loads. It is recommended that dynamic modelling should be carried out for the remaining unprotected pan-European area for which results are not yet available to identify areas that can become protected in one of the target years. The persisting high exceedances of critical loads for eutrophication point to the requirements of using dynamic models to improve knowledge on time delays of damage and recovery.

Critical loads for cadmium, lead and mercury were successfully computed and mapped by 18 Parties of the LRTAP Convention. Critical loads for cadmium, lead and mercury were computed by 17, 17 and 10 countries, respectively. The methodology that was recommended in the call for data was carefully reviewed and documented in the Mapping Manual of the ICP on Modelling and Mapping (UBA, 2004). The methodology enabled the assessment of ecosystem specific critical loads to protect human or environmental health. These critical loads were compared to preliminary computations of ecosystem specific deposition of the respective metals in 1990 and 2000. The robustness of deposition results can not yet well be established due to the uncertainty of reported emissions. Bearing these uncertainties in mind, it is shown that atmospheric deposition of cadmium does not cause widespread risk in 2000, that the risk of lead deposition decreases since 1990 but is still widespread in 2000 and, finally, that the risk caused by mercury remains important without much change throughout the years in most of the countries that provided data on mercury.

References

EMEP (1998) Transboundary acidifying air pollution in Europe, MSC-W Status Report 1998 – Parts 1 and 2. EMEP/MSC-W Report 1/98, Norwegian Meteorological Institute, Oslo, Norway

Hettelingh J-P, Posch M, Slootweg J (2004) Status of European critical loads and dynamic modelling, in: Hettelingh JP, Posch M, Slootweg J (eds.), Critical loads and dynamic modelling results, CCE Progress Report, 2004. RIVM Report 259101014, Bilthoven, The Netherlands, pp .9-20, www.mnp.nl/cce

Posch M, Hettelingh J-P, Slootweg J (eds) (2003) Manual for dynamic modelling of soil response to atmospheric deposition. Coordination Center for Effects, RIVM Report 259101012, Bilthoven, Netherlands, pp.71 www.mnp.nl/cce

Posch M, Hettelingh J-P, De Smet PAM (2001) Characterization of critical load exceedances in Europe. Water Air Soil Pollut. 130: 1139-1144.

Schöpp W, Posch M, Mylona S, Johansson M (2003) Long-term development of acid deposition (1880–2030) in sensitive freshwater regions in Europe. Hydrol Earth Syst Sci 7: 436–446

Simpson D, Fagerli H, Jonson JE, Tsyro S, Wind P, Tuovinen, JP (2003) Transboundary Acidification Eutrophicationand Ground Level Ozone in Europe, Part 1 Unified EMEP Model Description, EMEP Status Report 2003, EMEP-Report 1/2003-PART I, Norwegian Meteorological Institute, Oslo, Norway

Slootweg J, Hettelingh JP, Posch M, Dutchak SV, Ilyin I (eds.) (2005) Critical loads of cadmium, lead and mercury in Europe. MNP-Report 259101015, RIVM, Bilthoven, The Netherlands, www.mnp.nl/cce

Tarrasón L, Jonson JE, Fagerli H, Benedictow A, Wind P, Simpson D, Klein H (2003) Transboundary Acidification Eutrophication and Ground Level Ozone in Europe, Part III: Source-receptor relationships. EMEP Report 1/2003-PART III, Norwegian Meteorological Institute, Oslo, Norway

UBA (2004) Manual on methodologies and criteria for modelling and mapping critical loads & levels and air pollution effects, risks and trends. UNECE Convention on Long-range Transboundary Air Pollution, Federal Environmental Agency (Umweltbundesamt), Berlin www.icpmapping.org

2. Summary of National Data

Jaap Slootweg, Maximilian Posch, Maarten van 't Zelfde*

*Institute of Environmental Sciences (CML), Leiden, the Netherlands

2.1 Introduction

The Working Group on Effects (WGE) '… approved calls for data for … critical loads of acidification and eutrophication and target loads (in early 2005)' (EB.AIR.WG.1.2004.2.e). In this call, with a deadline of 28 February 2005, the Coordination Center for Effects (CCE) requested National Focal Centres (NFCs) to submit data with only a few changes/additions since the previous call (compare with Hettelingh et al., 2004); *inter alia*:

- The implementation year changed from 2015 to 2020;
- The values of several output variables from dynamic modelling for 5 key years and 2 different scenarios ('Gothenburg' and 'Background') were requested;
- The computation of Damage Delay Times (DDT) and Recovery Delay Times (RDT) was requested;
- Updated software provided by the CCE enabled NFCs to perform consistency checks on their data before submission.

The full text of the 'Instructions for Submitting Critical Loads and Dynamic Modelling Data', which was sent to the NFCs with the call for data, is reproduced in Appendix A.

This Chapter reports on the results of the call for data (critical loads and dynamic modelling results) and shows statistical analyses of some of the most interesting variables.

2.2 National responses

A total of 14 countries updated their critical loads (CLs), and all except one also updated and extended their dynamic modelling (DM) results. Of these, the Czech Republic, Ireland and Switzerland submitted DM data for the first time. Altogether, critical load data are now available from 25 NFCs, and from these 14 have provided dynamic modelling results. Table 1-1 in Chapter 1 shows the most recent submission date for each NFC. Table 2-1 shows details about the 14 submissions following this call for data. The table lists the number of records and the total area covered for each ecosystem type. The EUNIS ecosystem classification system was applied by all countries, and for this overview the numbers are aggregated to EUNIS level 1.

Table 2-1. Type and number of ecosystem records for which data were provided in this call for data.

Country	Country Area (km^2)	EUNIS level 1	Acidity CLs		Nutrient N CLs		Dynamic Modelling	
			# ecosyst	Area (km^2)	# ecosyst	Area (km^2)	# ecosyst	Area (km^2)
Austria	83,858	Forest	496	35,745	496	35,745	496	35,745
Belarus	207,595	Forest	8,631	93,305	8,631	93,305		
		Grassland	1,779	15,257	1,779	15,257		
		Wetlands	100	773	100	773		
		total	10,510	109,334	10,510	109,334		
Bulgaria	110,994	Forest	87	52,032	87	52,032	83	47,887
Czech Republic	78,866	Forest	2,257	11,178	2,257	11,178	2,257	11,178
France	543,965	Forest	3,840	170,657	3,840	170,657	3,840	170,657
		Grassland	81	1,580	81	1,580	80	1,553
		Wetlands	67	5,123	67	5,123	67	5,123
		Other	156	2,741	156	2,741	156	2,741
		total	4,144	180,102	4,144	180,102	4,143	180,074
Germany	357,022	Forest	100,954	100,954	100,954	100,954	100,954	100,954
		Grassland	1,520	1,520	1,520	1,520	1,520	1,520
		Shrub	310	310	310	310	310	310

Country	Country Area (km²)	EUNIS level 1	Acidity CLs		Nutrient N CLs		Dynamic Modelling	
			# ecosyst	Area (km²)	# ecosyst	Area (km²)	# ecosyst	Area (km²)
		Wetlands	1,195	1,195	1,195	1,195	1,195	1,195
		Other	2,16	216	216	216	216	216
		total	104,195	104,195	104,195	104,195	104,195	104,195
Ireland	70,273	Forest	17,242	4,254	17,242	4,254	17,242	4,254
		Grassland	6,895	2,050	6,895	2,050	6,895	2,050
		Shrub	6,847	2,631	6,847	2,631	6,847	2,631
		total	30,984	8,936	30,984	8,936	30,984	8,936
Italy	301,336	Forest	714	89,560	714	89,560	714	89,560
		Grassland	185	23,027	185	23,027	185	23,027
		Shrub	210	12,822	210	12,822	210	12,822
		Water	1	6	1	6	1	6
		Other	19	463	19	463	19	463
		total	1,129	125,878	1,129	125,878	1,129	125,878
Netherlands	41,526	Forest	90,155	5,635	42,686	2,668	76,222	4,764
		Grassland	14,112	880	14,112	880	10,135	633
		Shrub	5,675	355	5,675	355	5,540	346
		Wetlands	1,637	104	1,637	104	1,101	69
		Water			417	5		
		Other	5,148	322	5,148	322	3,839	240
		total	116,727	7,295	69,675	4,334	96,837	6,052
Norway	323,759	Forest	662	67,011				
		Water	2,324	322,150			131	20,535
		Other			35,418	318,762		
		total	2,986	389,161	35,418	318,762	131	20,535
Poland	312,685	Forest	88,383	88,383	88,383	88,383	88,383	88,383
United Kingdom	243,307	Forest	150,208	19,748	151,815	19,896		
		Grassland	99,451	20,010	119,062	21,897		
		Shrub	78,550	24,669	78,985	24,785		
		Wetlands	18,682	5,455	19,079	5,506		
		Water	1,717	7,790			320	1,190
		Other			10,299	2,119		
Switzerland	41,285	Forest	260	11,612	9,886	9,886	260	11,612
		Grassland			9,488	9,488		
		Shrub			1,640	1,640		
		Wetlands			1,727	1,727		
		Water	100	180	49	49		
		total	360	11,792	22,790	22,790	260	11,612
Sweden	449,964	Forest	25,442	225,264	25,442	225,264	542	24,400
		Water	3,084	284,819			234	6,724
		total	28,526	510,084	25,442	225,264	776	31,124
Grand Total	3,166,435		739,392	1,711,786	774,750	1,361,137	329,994	672,790

Figure 2-1 shows the same information in the form of bar charts, with the coverage of the different ecosystems relative to the total country area. The figure clearly shows that forests are the most widely used ecosystem, and that dynamic modelling is sometimes applied to a subset only, for which enough input data are available at a national scale.

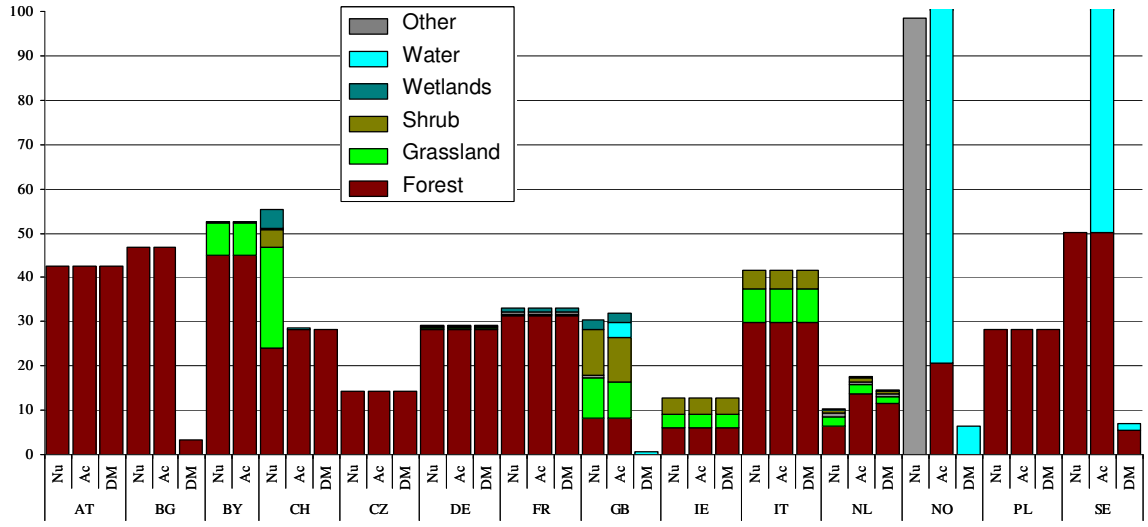


Figure 2-1. National distributions of ecosystem types for which data have been submitted for acidification (Ac), eutrophication (Nu) and dynamic modelling (DM).

The spatial coverage of Europe with critical load and dynamic model calculations can be seen in Figure 2-2 for all 25 NFCs. It shows that the dynamic modelling effort is concentrated in areas with the highest CL exceedances (mainly central and north-western Europe).

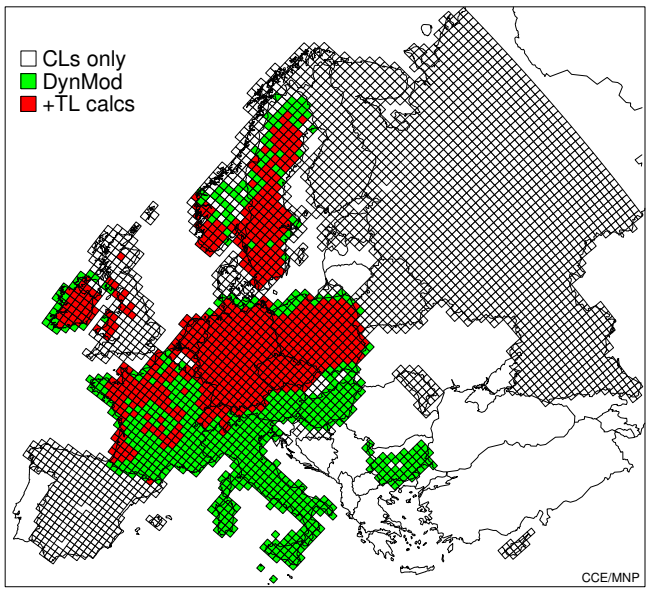


Figure 2-2. Map displaying the EMEP50 grid cells for which critical loads have are available from national submissions (25 NFCs). Coloured (green and red) cells indicate that also dynamic modelling has been performed (for at least one ecosystem); red cells that also target loads have been calculated.

A key quantity in determining a critical load is the chemical criterion linking soil (water) chemistry to the 'harmful effects on specified sensitive elements of the environment'. Figure 2-3 summarizes the critical values that NFCs selected in their critical load calculation. The area plotted is relative to the total area of all submitted ecosystems with a maximum critical load for sulphur. Not plotted are the following criteria:

- [ANC], which has been used for all aquatic ecosystems;
- Base saturation, used for the remaining 29% of Cypriot forest, and shrubs (57 %).

'Other' or 'missing' criteria. An increasing number of ecosystems is considered to be limited by different, or a combination of two or more criteria.

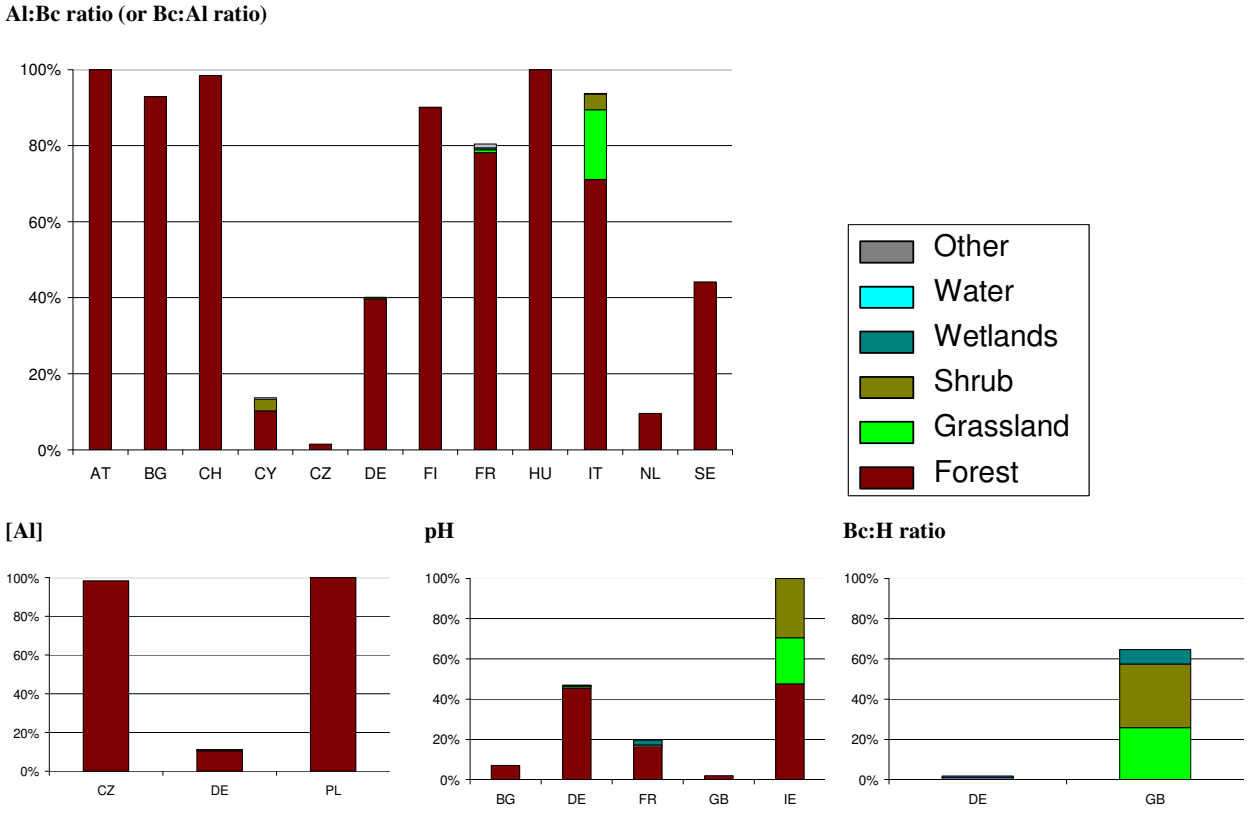


Figure 2-3. Area, relative to the total area of submitted ecosystems for acidity, for a selection of chemical criteria, broken down by ecosystem types.

2.3 Critical load maps and distributions

All 2005 national submissions contained critical loads for nutrient nitrogen, $CL_{nut}(N)$. Figure 2-4 shows the critical load in two ways. On the left are maps of CLnut(N) for the 5th, 25th, and 50th percentile in the 50×50 km EMEP grid cells, and on the right the cumulative distribution functions for each country, separately for 3 ecosystem classes, are plotted. The black dashed line, with the legend 'EU-DB', gives the distribution of CLnut(N) as computed with the European background database held at the CCE. This dataset is described in Chapter 4. EU-DB contains only data on forests, and thus only the national contribution for forest (the brown line) should be compared with it. The numbers at the right of the CDFs is the number of ecosystem records for the indicated ecosystem type.

Most of the sensitive areas in the 5th percentile also show sensitive in the 25th and even in the map showing the median values. The CDFs show relatively steep functions, also demonstrating this phenomenon. This means that reductions in these areas, if exceeded, are likely to be efficient. The 5th percentile is also shown in Figure 1-3 (Chapter 1), where it is mapped next to the 5th percentile for subsets of ecosystem types: forests, (semi-) natural vegetation and surface waters.

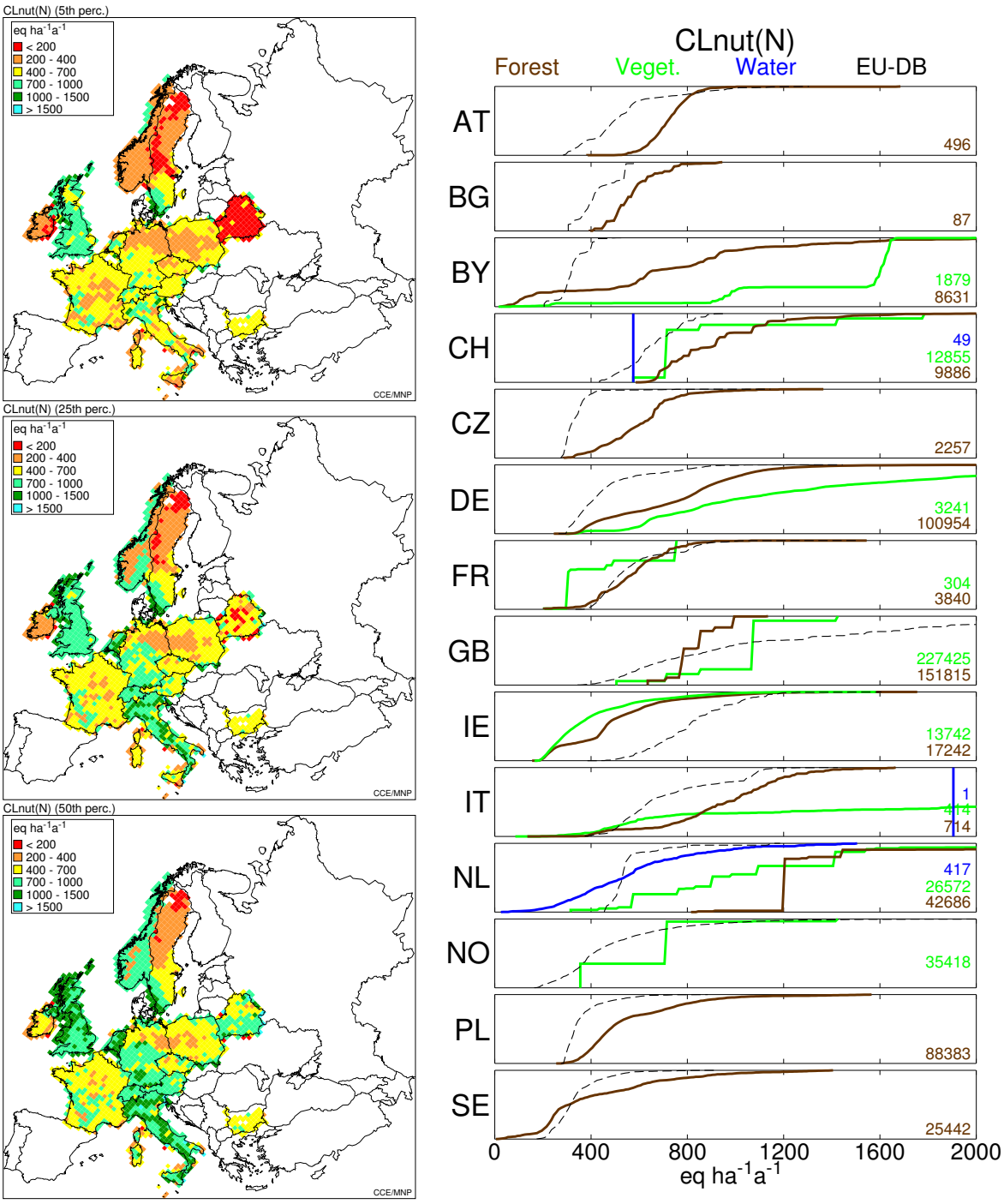


Figure 2-4. Critical loads of nutrient nitrogen from the 14 NFCs which responded to the last call The EMEP50 maps of the 5th, 25th and 50th percentile on the left and the cumulative distributions for 3 ecosystem classes on the right (EU-DB=European background data base).

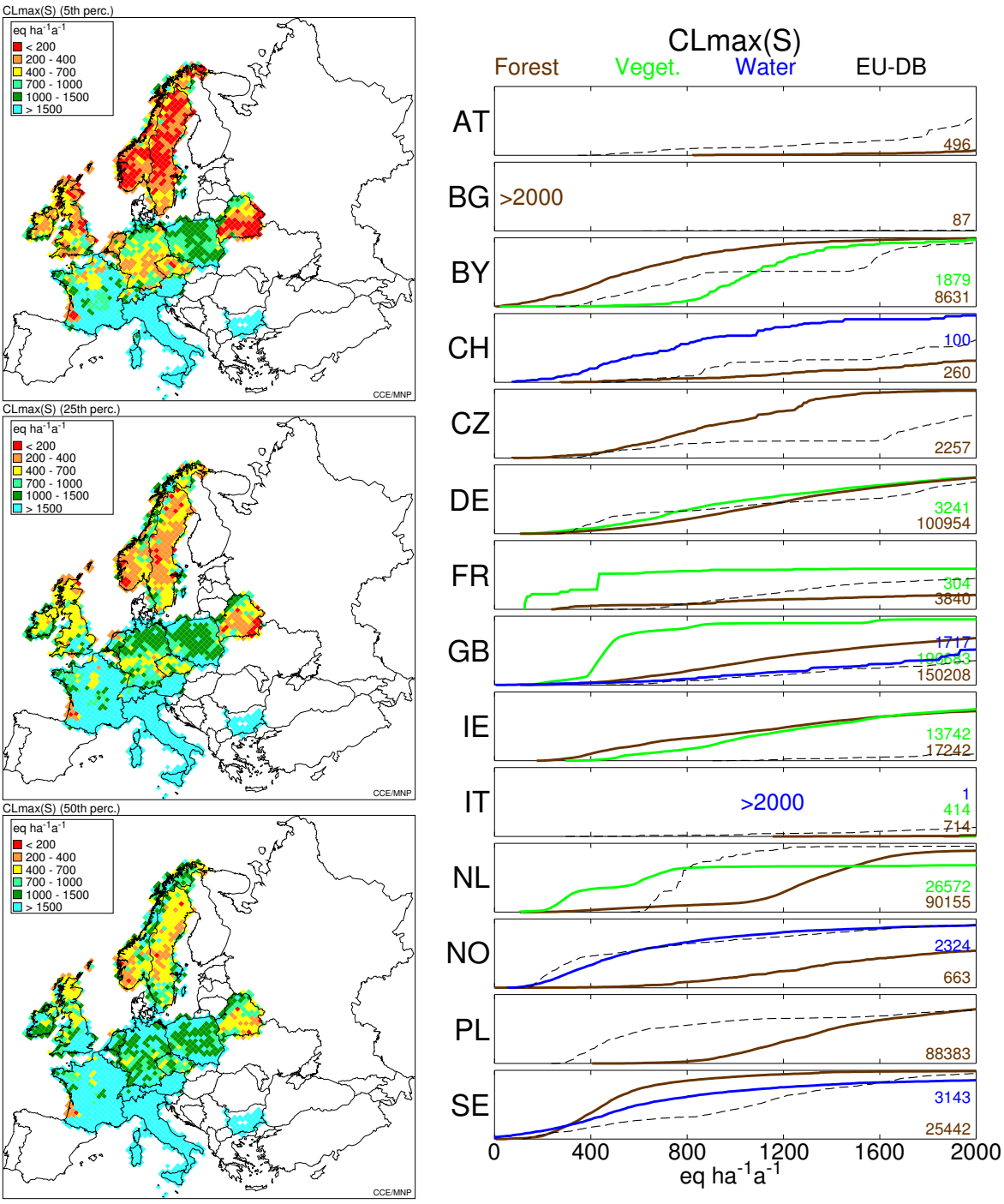


Figure 2-5. Maximum critical loads of sulphur from the 14 NFCs which responded to the last call The EMEP50 maps of the 5th, 25th and 50th percentile on the left and the cumulative distributions for 3 ecosystem classes on the right (EU-DB=European background data base).

In Figure 2-5 the same maps and functions are displayed for the maximum critical load of sulphur, $CL_{max}(S)$, chosen as a representative quantity for the acidity critical load function. The Figure shows that the ecosystems most sensitive to acidification are mostly located in the Nordic countries and Scotland.

Finally, in Figure 2-6 these maps and functions are shown for the minimum critical load of N, $CL_{min}(N)$. This quantity, which also is part of the critical load function of acidity, is (in most cases) the sum of net N uptake by vegetation and the long-term immobilisation of N. The maps and graphs show that this quantity has a much more narrow distribution than $CL_{max}(S)$.

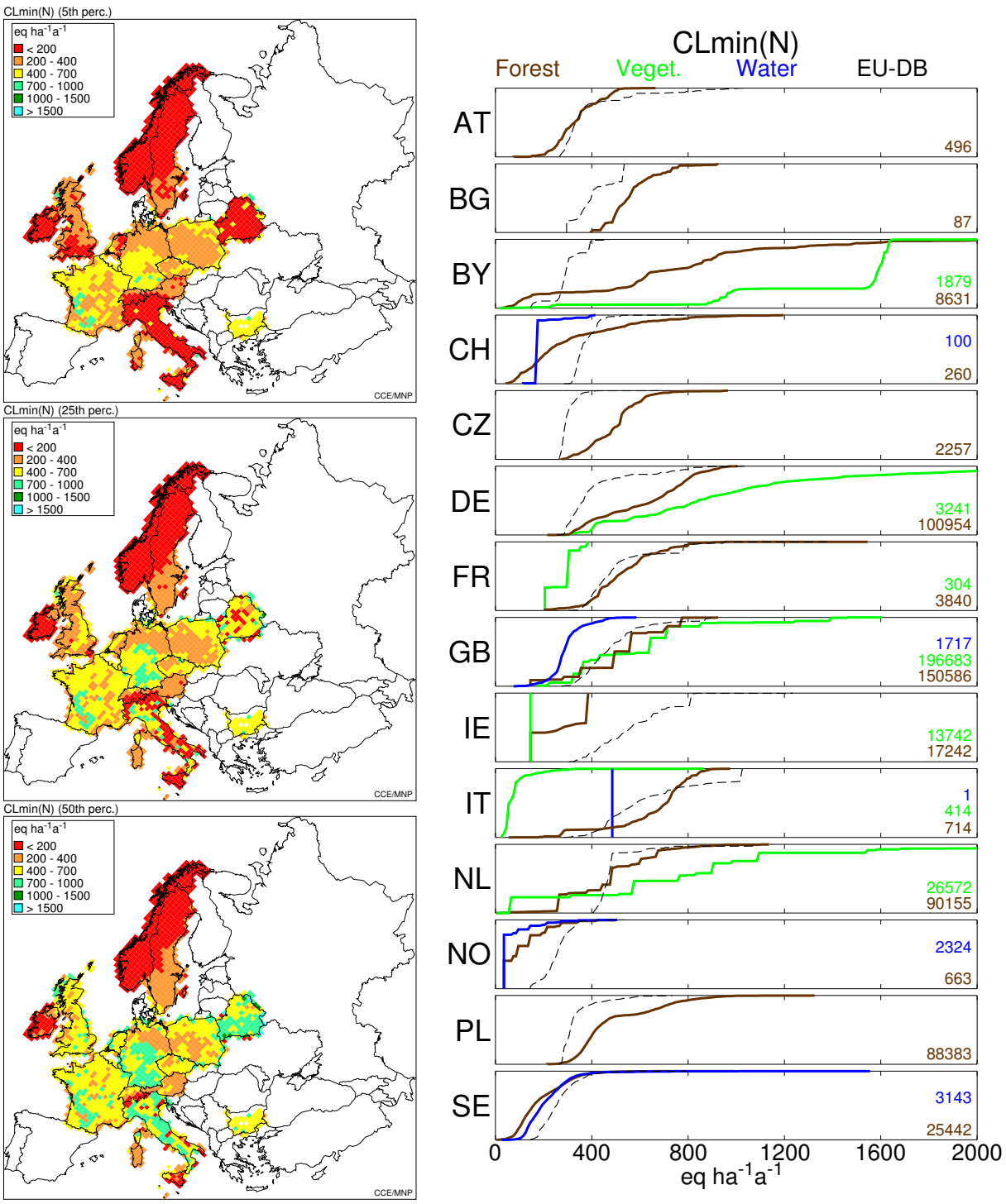


Figure 2-6. Minimum critical load of nitrogen from the 14 NFCs which responded to the last call The EMEP50 maps of the 5th, 25th and 50th percentile on the left and the cumulative distributions for 3 ecosystem classes on the right (EU-DB=European background data base).

2.4 Input variables for critical loads and dynamic modelling

The soil and other site specific parameters, which are used in critical load and dynamic model calculations, have been asked in the call for data to enable consistency checks and inter-country comparisons. In most cases the differences between counties can easily be explained, and it is the hope of the CCE that some differences or peculiarities in distributions shown in this section may lead to improvements in future data submissions. Important element fluxes in the Simple Mass Balance (SMB) model are weathering, leaching, uptake and N

immobilisation. A basic variable is the amount of water percolating through the root zone, Q_{le}. Its CDFs are shown for the countries that submitted data, separately for forests, semi-natural vegetation and surface waters. All CDFs shown in this section also display as a thin black dashed line the respective variable of the European background data base (see Chapter 4).

As can be seen in Figure 2-7, some countries show quite high values for Q_{le}, close to the annual precipitation, which could hint to at inconsistencies in the evapotranspiration calculations. Not all countries modelled denitrification, f_{de}, as a fraction of the net N input, but used an absolute amount of N denitrified N_{de}; thus no respective CDFs are shown for those countries (e.g. the United Kingdom

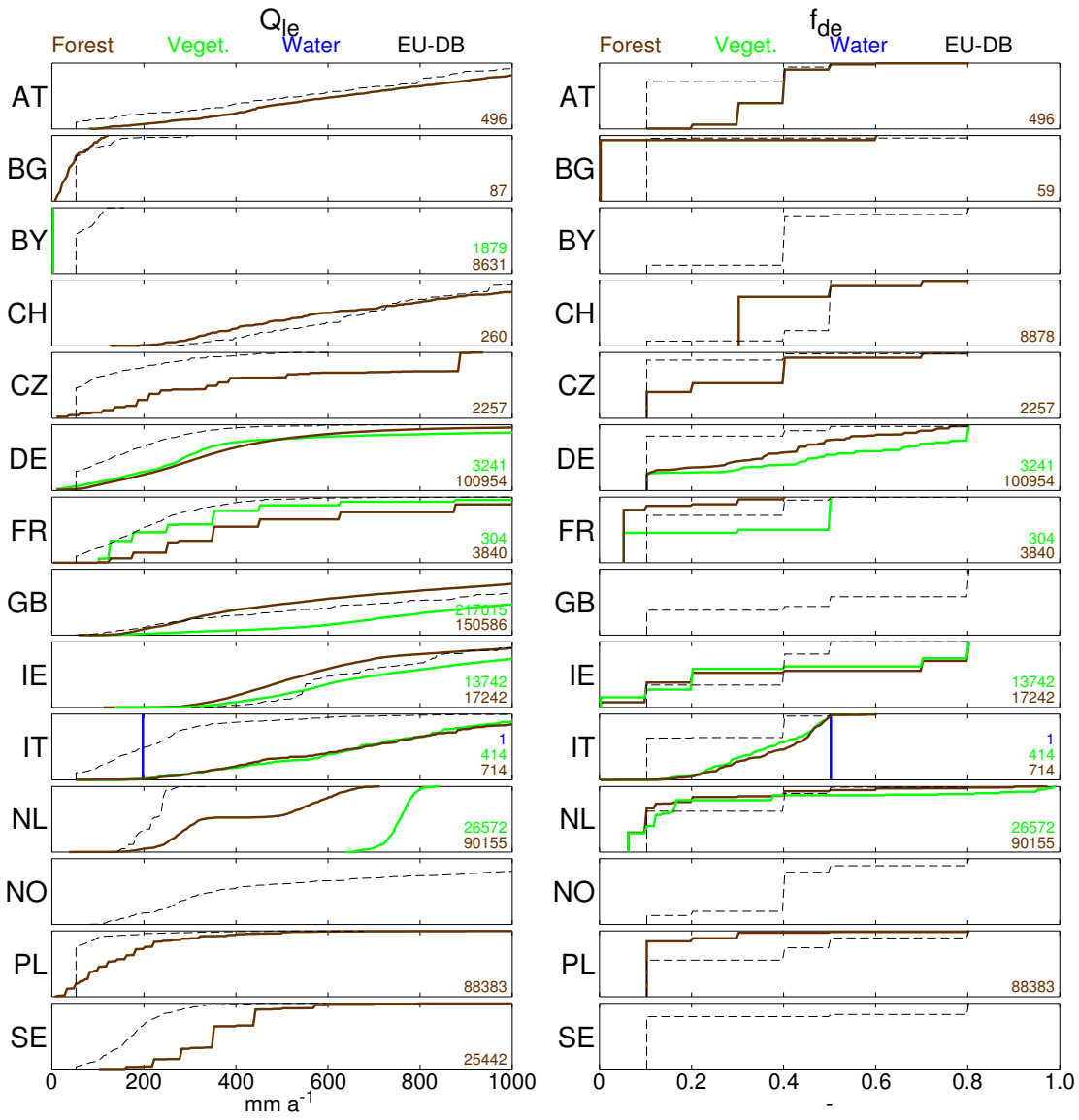


Figure 2-7. The CDFs of the amount of water percolating through the root zone, (Q_{le}, left) and the fraction of nitrogen denitrified in the soil (f_{de}, right) (EU-DB=European background data base).

Figure 2-8 shows the national CDFs of the acceptable leaching fluxes (left) and the N immobilisation fluxes. Whereas in the European background data base a constant value of 1 kg N $ha^{-1}a^{-1}$ (about 71.43 eq $ha^{-1}a^{-1}$); the upper limit suggested in the Mapping Manual) is used for the whole of Europe, NFCs have chosen very different – and in general larger – amounts on a national scale.

.

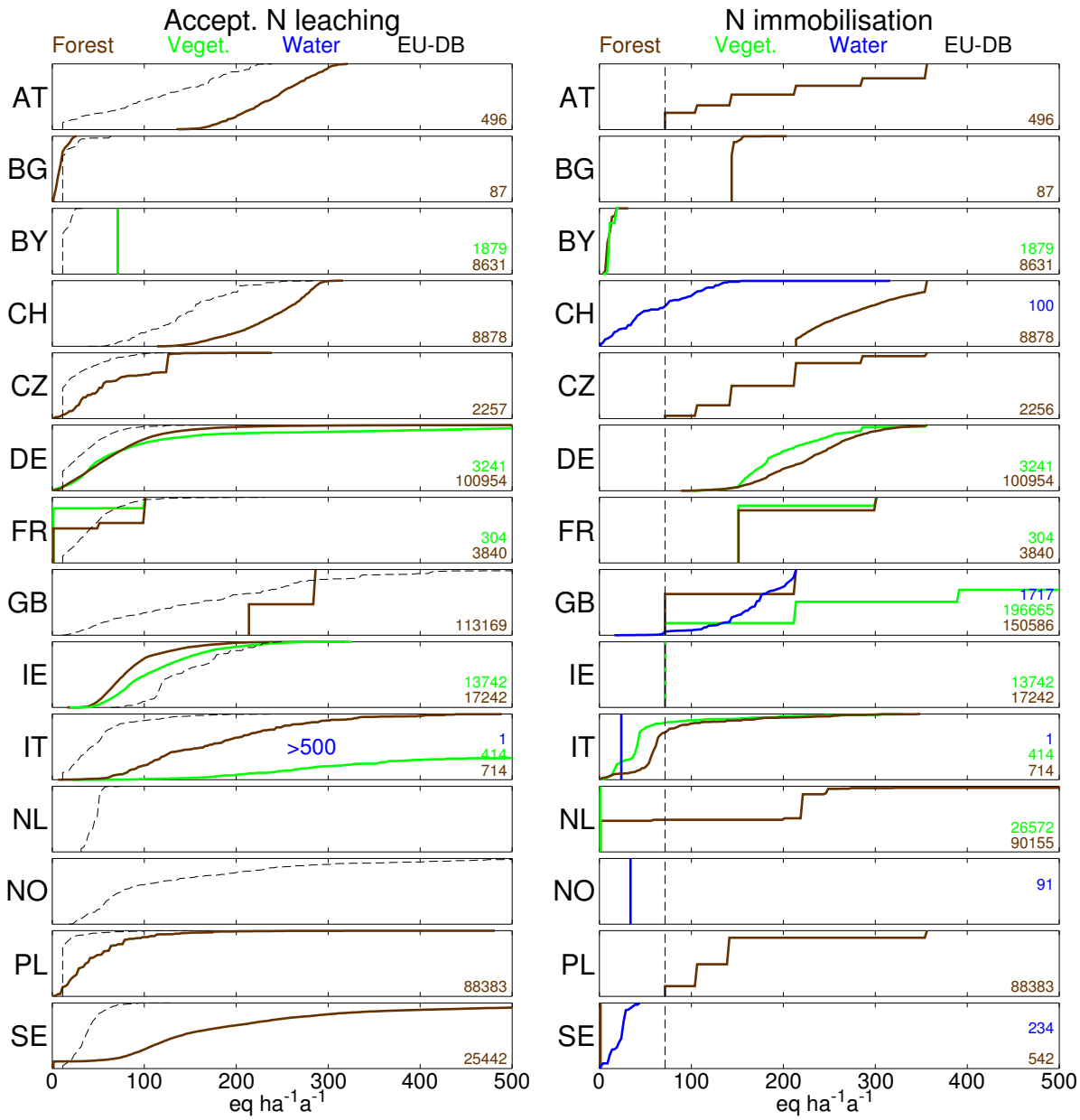


Figure 2-8. The CDFs of the acceptable amount of nitrogen leached per year from the soil ($N_{le(acc)}$, left), and the N immobilisation fluxes (right) (EU-DB=European background data base).

Figure 2-9 shows the correlation between nitrogen and base cation uptake for forests, vegetation, and waters (catchments). Plant and tree species have quite characteristic contents for nitrogen and the base cations in stem, branches, leaves and roots (Jacobsen et al., 2002). The amount of matter removed from the area can vary due to species and harvesting practises, but the ratio between nitrogen and the sum of base cations should reflect the mentioned specific contents. The grey lines in Figure 2-9 show the upper and lower limit of this ratio, using the numbers from Table 5.8 of the Mapping Manual (UBA, 2004). The top line is represents the content-ratio for oak, including branches, and the lower is for beech, stems only. It is remarkable that so many plots are outside of these lines, up to a few hundreds of equivalents. For areas, in which nitrogen uptake exceeds base cation uptake, the removal (harvest) of biomass would help combat acidification, a notion not everyone would agree with.

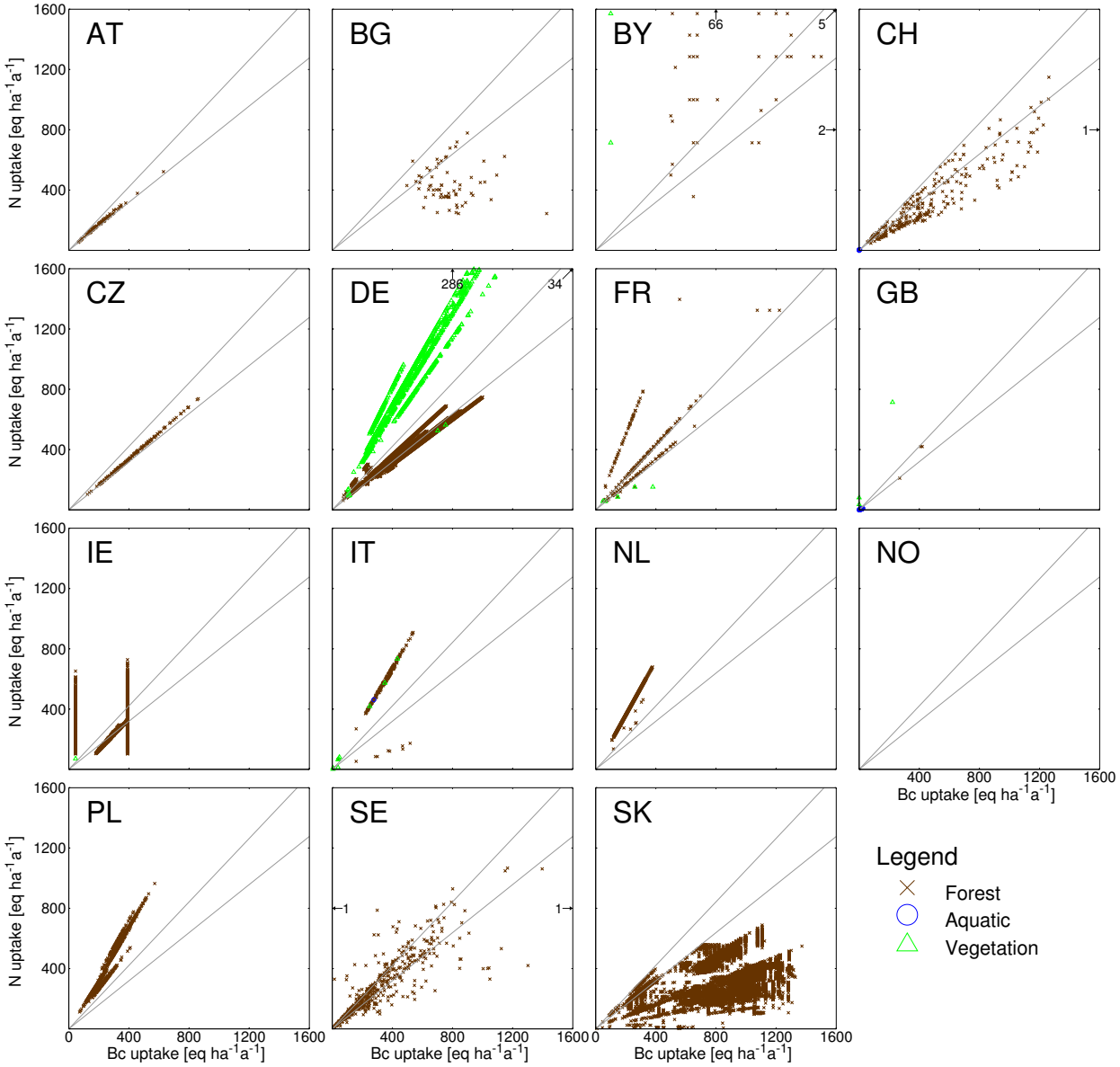


Figure 2-9. Net base cation uptake versus nitrogen uptake. The grey lines indicate the range given in the Mapping Manual.

The cumulative distributions of the total base cation weathering fluxes are shown for all submitting countries in Figure 2-10. Compared to last year's submission (see Hettelingh et al., 2004) Austria, Belarus and Switzerland have updated their values for weathering.

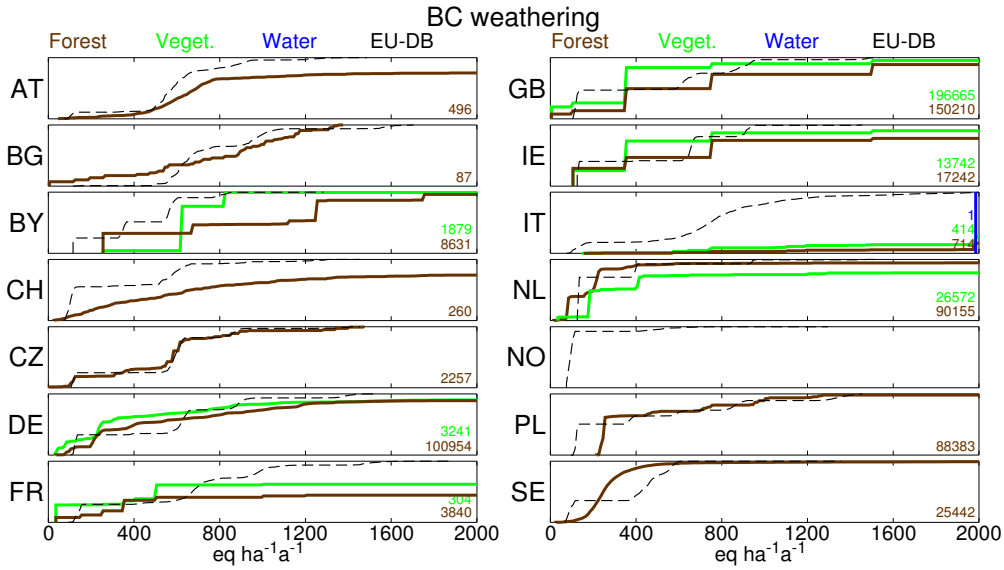


Figure 2-10. The CDFs of base cation weathering (BC= Ca+Mg+K+Na; EU-DB=European background data base).

Several countries have made use of the base cation deposition data that was made available by EMEP (Van Loon et al., 2005). Figure 2-11 shows of a map of the EMEP data on the left, and to the right a map of the average base cation deposition of the most recent submission of all NFCs. EMEP made also data available for deposition on forests. This explains why the maps differ, even for the countries that used the EMEP data. Both maps show sea salt corrected base cation depositions. For the national submissions that contained the individual ions, chloride is used as a tracer. Since the EMEP dataset does not contain chloride, it was assumed to have the same ratio to Na as in sea water. This might be the reason for the striking difference between the maps.

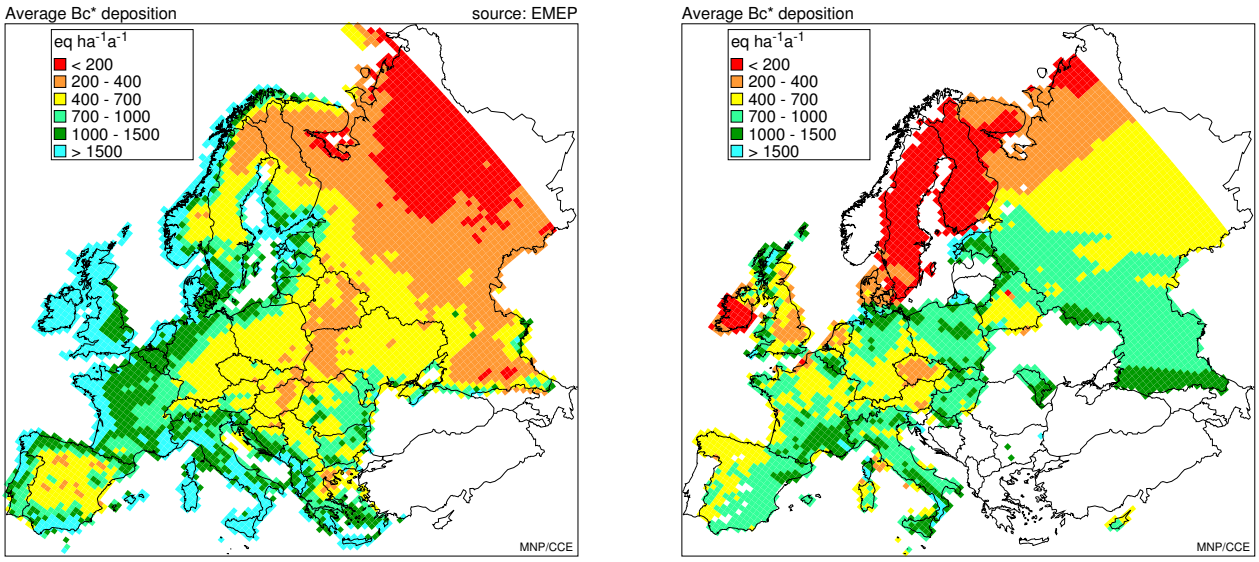


Figure 2-11. Sea salt corrected base cation deposition derived from EMEP data (left) and sea salt corrected base cation deposition submitted by NFCs, averaged over the EMEP50 grid (right).

In addition to variables used in critical load calculations, also variables only needed for dynamic modelling have been asked from the NFCs. In Figure 2-12 the cumulative distributions of the soil bulk density (left) and the cation exchange capacity (CEC) are displayed for each country that submitted new data. Bulk densities are quite low in some countries, hinting at a large proportion of organic soils. CEC values are in expected an expected range for all countries; and the rough estimates of the background database (dashes line) do not always agree with national estimates/measurements.

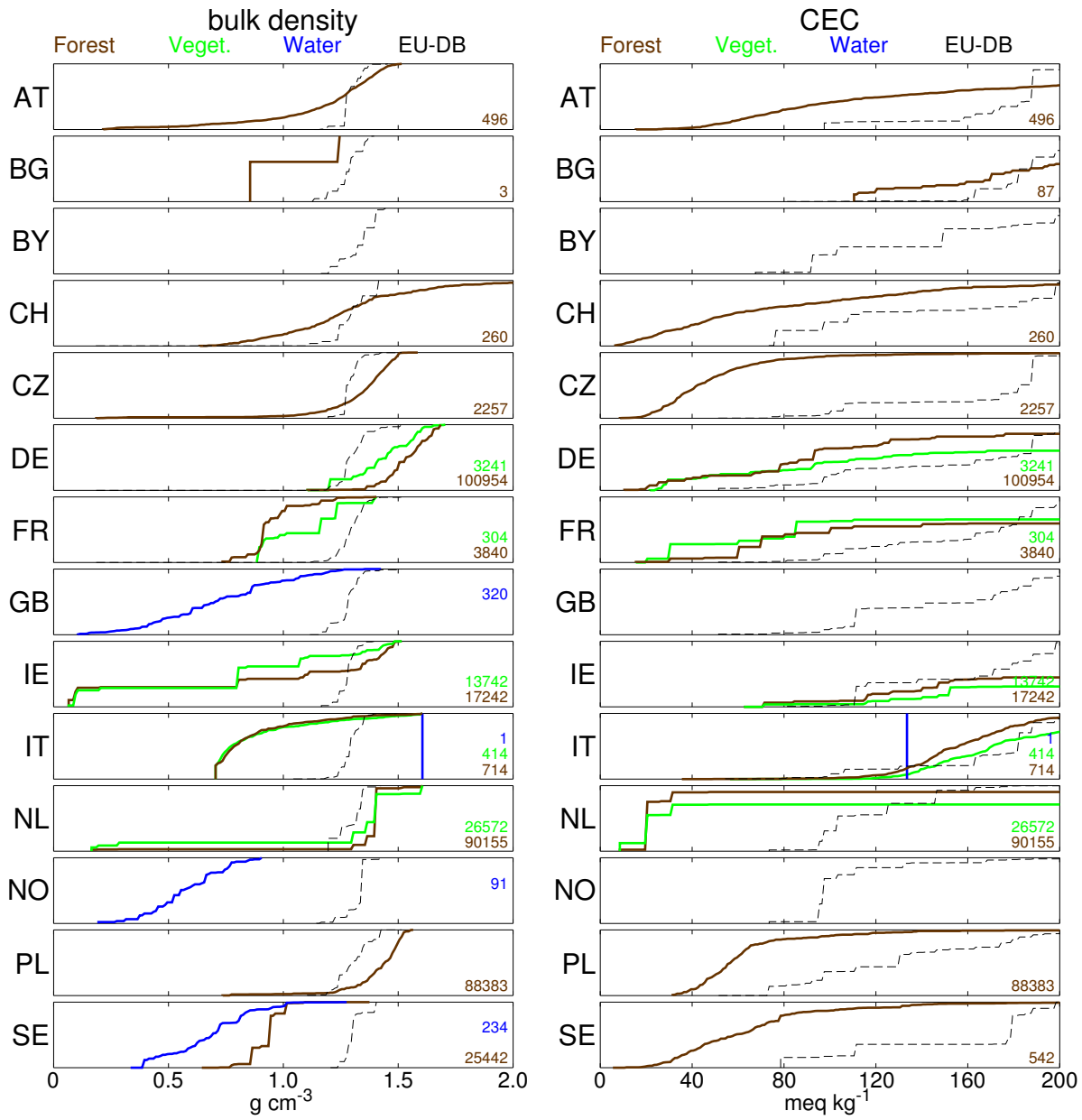


Figure 2-12. Cumulative distributions of bulk density (left) and cation exchange capacity (right) (EU-DB=European background data base).

Not only *input* variables used in critical load calculations and dynamic modelling, but also dynamic modelling *output* was asked for some key variables in a few years (1990, 2010, 2030, 2050 and 2100). Figure 2-13 shows national cumulative distribution functions of the molar [Al]:[Bc] ratio in the soil solution or surface water for the years 1990, 2010, 2030 and 2050 for two scenarios: (a) keeping the Gothenburg Protocol deposition constant after 2010 (right) and reducing deposition linearly to background values between 2010 and 2020 (right graphs in Figure 2-13). Obviously, the CDFs are identical for 1990 and 2010 in both sets of graphs; after that, however, a much faster and more widespread recovery, i.e. lower values, can be observed for the 'background scenario'. But even under this extreme scenario not all ecosystems recover, i.e. reach a value below one, before 2050. The figure also shows that in many countries the values for 2050 are (very) close to those for 2030. This reaching of a steady state is due to the fact depositions do not change after 2010 (for 'Gothenburg') or 2020 (for 'Background').

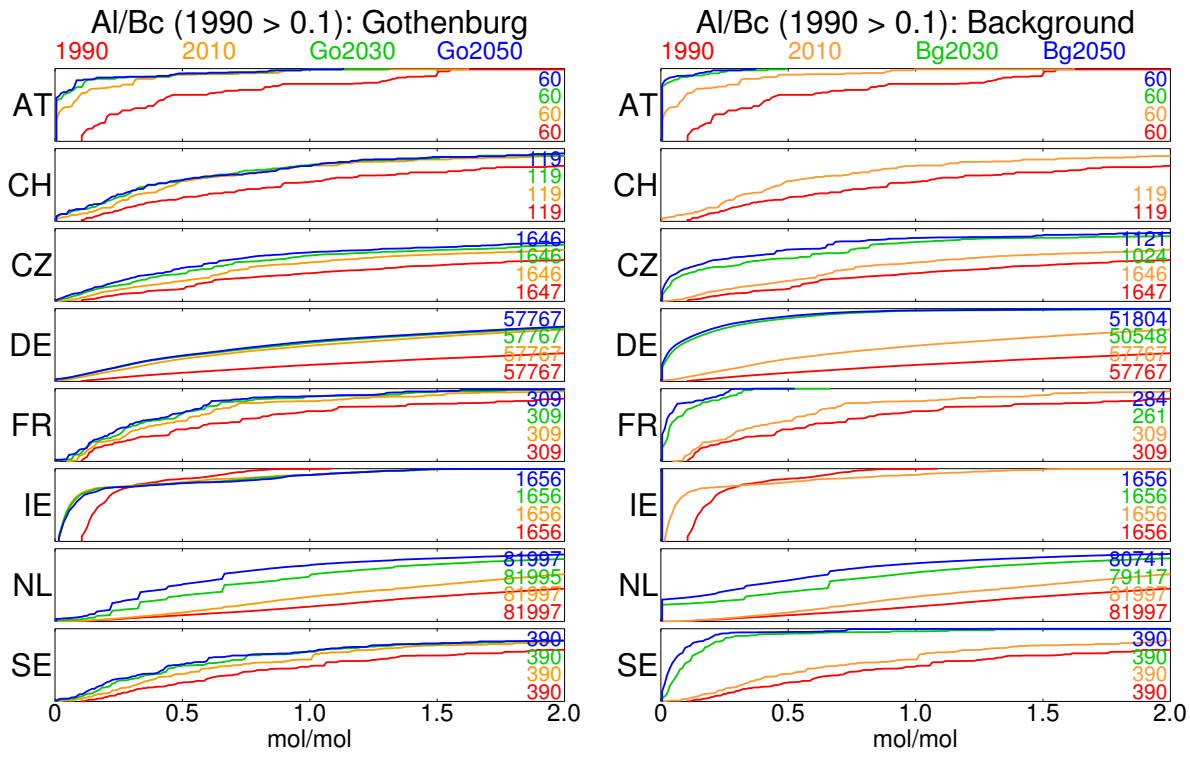


Figure 2-13. Molar Al:Bc ratio for 1990, 2010 (assuming the Gothenburg Protocol implementation) and for 2030 and 2050 with (a) deposition kept constant after 2010 (left) and (b) reducing deposition to background level into 2020 and keeping it constant thereafter (right) (only the sites with an Al:Bc ratio greater than 0.1 are plotted).

In Figure 2-14 the C:N ratio in the topsoil in the year 2010 is plotted versus the N concentration in the soil solution in the same year. The C:N ratio in the VSD model (and other dynamic models) controls the immobilisation of N in the soil (above the constant value used in CL calculations) and decreases over time. Thus one could expect an increase in N leaching for lower C:N ratios; but this seems not to be the case for the Dutch data.

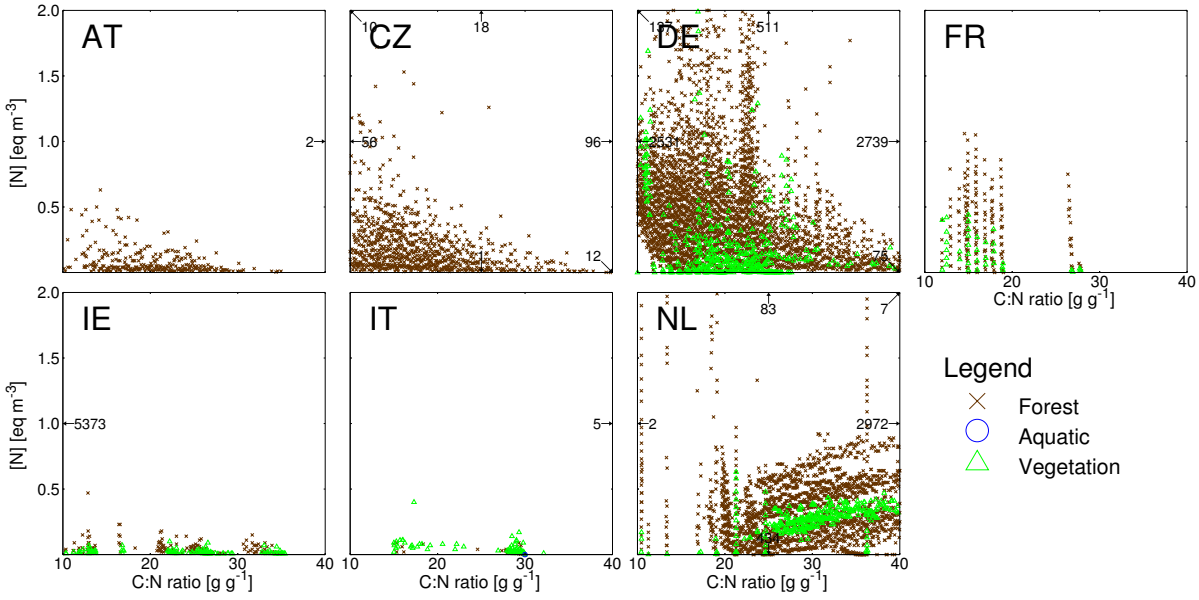


Figure 2-14. C:N ratio versus nitrogen concentration in the soil solution for 2010 (assuming the implementation of the Gothenburg Protocol).

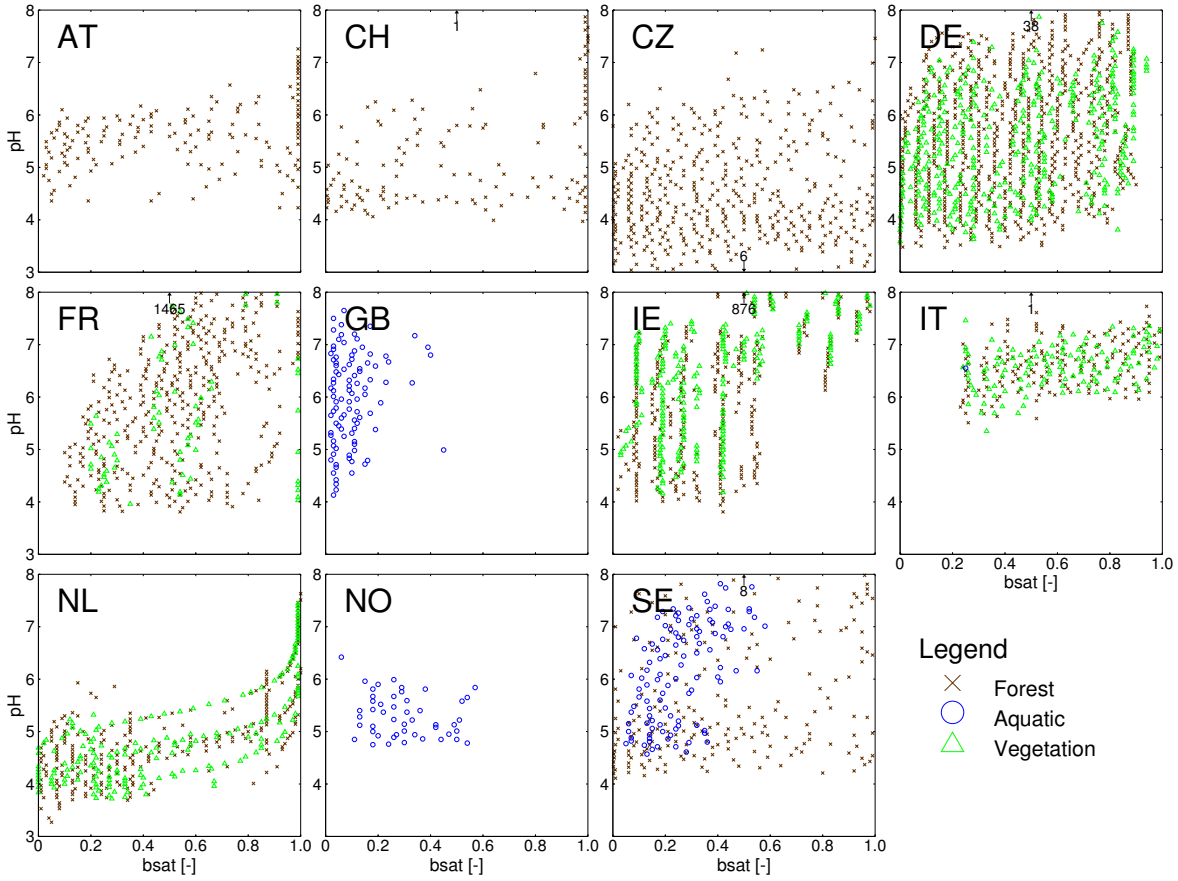


Figure 2-15. pH versus base saturation in 2050 with depositions kept constant after 2010 (Gothenburg).

In Figure 2-15, two other variables, i.e. pH and base saturation are plotted against each other for the year 2050 (with constant Gothenburg deposition after 2010). Except for the Netherlands, in none of the shown countries can one discern the S-shaped pattern, which has been documented in simple dynamic models (see, e.g. Reuss, 1983; De Vries et al., 1989). However, one has to bear in mind that Figure 2-15 shows the pH-base saturation relationship for many different sites at one given point in time, whereas in those references, this pattern is documented for single sites over time.

2.5 Damage delay and recovery times

Comparing critical loads to depositions, i.e. computing exceedances, can tell whether an ecosystem will be at risk or will be safe at some point in time, but it does not provide any insight *when* this will happen. To this end, dynamic models have to be applied. To get insight into, e.g., the length of the period between the occurrence of exceedance and the violation of the chemical criterion (the risk of damage), NFCs were also requested to compute these so-called damage delay times (DDT) and their counterpart in case of no-longer-being-exceeded, the recovery delay times (RDT), both when keeping the deposition after 2010 at the 2010 level (BL-CLE scenario reflecting the implementation of the Gothenburg Protocol and the EC NEC Directive). In Appendix A these quantities are explained in more detail, and in Figure 2-16 the possible cases are summarised in which an DDT or RDT exists as well as their relationship to target loads (TLs). In summary, it has to be noted that: (a) a *damage delay* exists only if there is exceedance of critical loads in the specified year, but non-violation of the chemical criterion; and (b) *recovery* can only occur if there is non-exceedance of critical loads in the specified year, but the criterion is still violated. In the other two possible cases – (c) exceedance and violation of the criterion, and (d) non-exceedance and non-violation – the system is ‘damaged’ or ‘safe’, respectively.

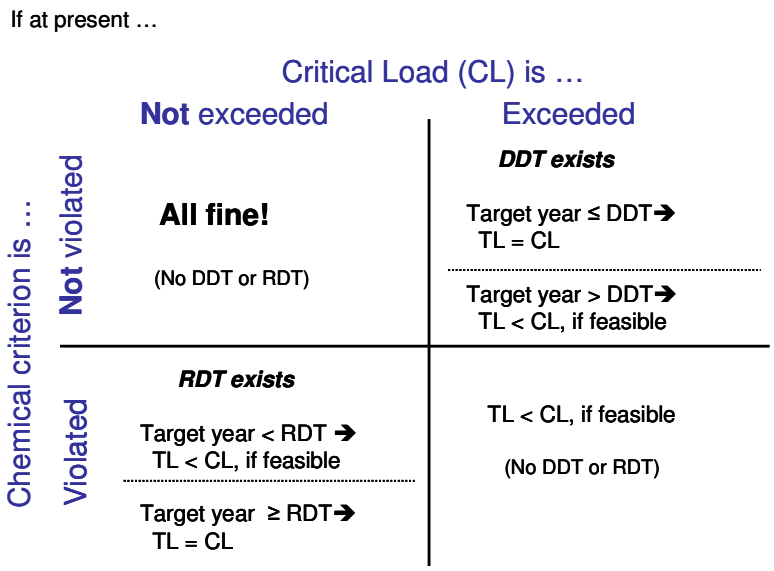


Figure 2-16. Summary of the cases in which damage or recovery delay can occur for all possible combinations of critical load (non-)exceedance and criterion (non-)violation. Also the connections with the existence of a target load are shown.

The cumulative distributions (CDFs) of the recovery and damage delay times between 2010 and 2100, as submitted by the NFCs, are shown in Figure 2-17. It is important to note that 100% in these distributions does not mean 100% of the ecosystems, but 100% of the cases for which the respective quantity exists; and the number of ecosystem to which this applies are also shown in Figure 2-17. From Table 2-1 the reader can infer how this numbers relate to the total number of ecosystems; and columns 5 and 6 in Table 2-2 below show for each country the percentage of ecosystem area for which a RDT or DDT, respectively exists. These percentages refer to the ecosystem area in a country, which is 'not safe' (column 4), i.e. the area of those ecosystems for which the critical load is exceeded or the criterion is (still) violated, or both.

The majority of the CDFs in Figure 2-17 are quite flat between 2010 and 2100, implying that most of the recovery/damage happens before 2010 and/or after 2100. This rather unexpected bimodality of the ecosystems involved, i.e. either recovering/deteriorating very fast or very slowly, certainly merits further investigations.

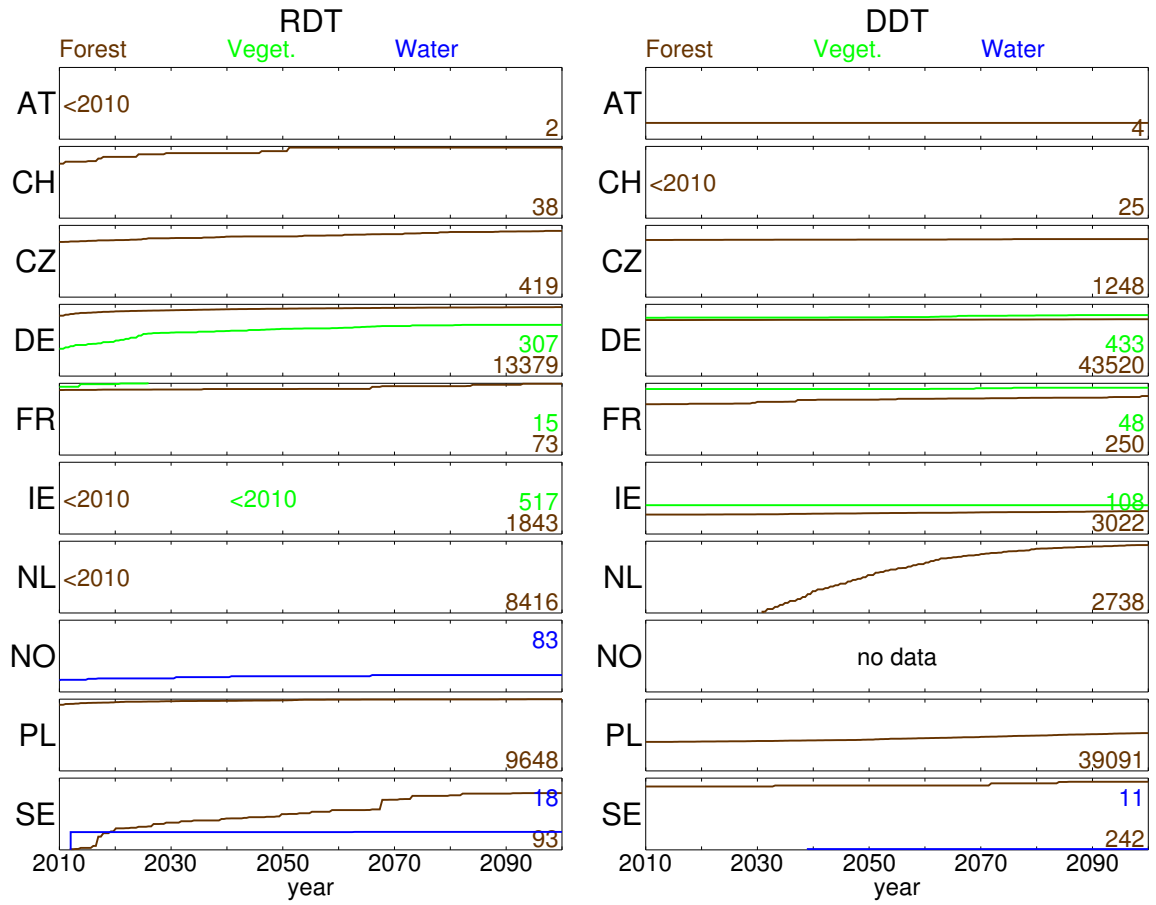


Figure 2-17. Cumulative distributions of recovery (RDT) and damage (DDT) delay times between 2010 and 2100 and three ecosystem classes, as computed by 10 NFCs.

2.6 Target loads for acidification

The emphasis of the last call for data with respect to dynamic modelling was on the calculation of target loads of acidity (sulphur and acidifying nitrogen). A target load (TL) for an ecosystem is a future deposition (path) which, when met, guarantees that the ecosystem is 'safe' – i.e. non-exceeded and chemical criterion met – from a pre-specified year, the target year, onwards. In contrast to the critical load, a target load is not unique – it depends on the target year – and it is not an ecosystem property, but, of course, depends on them. As with critical loads, since both sulphur and nitrogen contribute to acidity, there exists, for a given target year, not a single target load, but a *target load function* (TLF). Since, for a given target year, there are potentially infinite many possible deposition paths to reach the target, for the work under the LRTAP Convention, the deposition path leading to the target load has been uniquely defined by the Protocol year, the implementation year and the target year – see Chapter one (especially Figure 1-1) for details. Fore general overview over dynamic modelling and further details see also chapter 6 of the Mapping Manual (UBA, 2004).

Target load functions of acidity are not available for all ecosystems for which there are critical load functions in the data base. The reasons are either that a country has not carried out dynamic modelling at all, or within a country target load calculations are performed only for a subset of the ecosystems, often due to the lack of the additional information needed to carry out dynamic modelling. To make the target load data set completely compatible with the critical load data set, the following steps have been taken:

(a) If no target loads have been calculated for an ecosystem, the target load function has been set equal to the critical load function.

(b) If the target load computed is greater than the critical load, the critical load is taken (minimum of TLF and CLF). This guarantees that an ecosystem remains safe also after the target year.

(c) If a target load is not feasible for a given target year, i.e. even reducing N and S deposition to zero does not make the ecosystem 'safe' in that year, the target load is set to zero; TLF =(0,0).

To map the full information contained in the target load functions on a European scale is virtually impossible. Therefore, as is routinely done with critical load functions, we look at the maximum S target load, $TL_{max}(S)$, which is the pendant to the maximum critical load of sulphur, $CL_{max}(S)$. In Figure 1-9 of Chapter 1 the 5^{th} percentile in every EMEP50 grid cell of $TL_{max}(S)$ for the three target years 2030, 2050 and 2100 is mapped together with a map showing $CL_{max}(S)$. A comparison of the maps shows that (a) there are grids were more than 5% of the ecosystem area have a non-feasible target load (black grid cells), and (b) on a European scale the magnitude of the target loads does not change significantly as a function of the target year. Furthermore, since we set the target loads equal to critical loads and since the majority of ecosystems is not (or no longer) exceeded by the BL-CLE scenario, the target load maps are close to the critical load map for large areas. The similarity of the overall TLF set and the CLF set can also be seen from Figure 1-10 (Chapter 1), which shows these data per country as so-called diamond plots, a simplified form of displaying and comparing cumulative distributions (CDFs).

Further information on the dynamic modelling results on a country basis is summarised in Table 2-2. The Table is organized as follows. A country's ecosystem area (km^2), for which critical loads of acidity have been computed, is provided in column 2. In column 3 the ecosystem area is given for which dynamic modelling was performed. The last two rows of the table give the results for the EU25 (of which 12 NFCs have provided dynamic modelling data) and all NFCs ('LRTAP'; 14 countries with DM data).

Most relevant for the work under the LRTAP Convention is the area where critical loads are exceeded. This area turns out to include most of the countries that submitted dynamic modelling data. The area at risk of acidification in 2000 within the geographic domain of the Convention and of the EU25 covers 579,975 km^2 and 345,869 km^2, respectively. For part of that area dynamic models were applied. Of that area 168,661 km^2 and 153,828 km^2 turned out *not to be safe* in the LRTAP and EU25 domain, respectively (Table 2-2, column 4), meaning that the critical loads are exceeded *or* that the critical limit is violated (or both).

In the following results for the LRTAP-domain will be used as a reading guide of Table 2-2, with results applying to the EU25-domain given in brackets. Column 5 shows the percentage of the non-safe ecosystem area (given in column 4) for which a Recovery Delay Time (RDT) can be computed under the BL-CLE (Gothenburg) scenario. This is the case in areas where the critical load is at present no longer exceeded, but the critical limit is still violated (see also Figure 2-16). Column 5 tells us that in the LRTAP-domain 29.2% (25.7% in EU25) of the area, which is not safe at present, would recover in the future without further measures. In fact, BL-CLE depositions cause 20.2% (21.9%) to recover already before 2030 (see column 7), while 20.7% (22.5%) recover before 2050 (column 11), and finally by 2100 BL-CLE depositions will lead to a recovery of 22.3% in the LRTAP-domain and 24.2 in the EU25 domain (column 15). Comparing column 15 (2100) to column 5 we conclude that 6.9% (1.5 %) of the area which is not safe now would recover only after 2100. Deposition levels would need to be reduced to either increase the area that recovers before 2100, or to bring closer the year of recovery. How much depositions should be reduced in comparison to BL-CLE deposition patterns depends on the year in which recovery is aimed to occur, i.e. on the target load required to obtain recovery in that year. The percentage of the European area for which target loads for recovery can be identified in 2030, 2050 and 2100 are provided in columns 9, 13 and 17, respectively.

Table 2-2. Country statistics on delay times and dynamic modelling submissions for all 25 NFCs.

1	2	3	4	5	6	7	8	9	10	11	12	13	14	15	16	17	18
Country	CLaci	DynMod	NOT safe	RDT	DDT		**2030**				**2050**				**2100**		
-	km^2	km^2	km^2	%	%	safe	TL=CL	TLFs	n.f.	safe	TL=CL	TLFs	n.f.	safe	TL=CL	TLFs	n.f.
AT	35,745	35,745	334	31.0	53.4	31	36.4	32.6	0	31	36.4	32.6	0	31	36.4	32.6	0
BE	7,282	-	-	-	-	-	-	-	-	-	-	-	-	-	-	-	-
BG	52,032	4,7887	0	0	0	0	0	0	0	0	0	0	0	0	0	0	0
BY	107,843	-	-	-	-	-	-	-	-	-	-	-	-	-	-	-	-
CH	11,792	11,612	2,650	14.8	0	9	24.5	63.8	2.7	10.7	24.5	62.1	2.7	13.7	26.3	59.9	0
CY	4,534	-	-	-	-	-	-	-	-	-	-	-	-	-	-	-	-
CZ	11,178	11,178	8,004	27.1	14.9	22.2	13.6	59.2	4.9	22.9	13.6	60.9	2.6	25	13.6	60.7	0.7
DE	104,195	104,195	57,639	23.7	16.7	21.6	17.2	58.7	2.5	22.2	16.7	59	2.1	22.7	16.5	59.4	1.5
DK	3,149	-	-	-	-	-	-	-	-	-	-	-	-	-	-	-	-
EE	21,450	-	-	-	-	-	-	-	-	-	-	-	-	-	-	-	-
ES	85,225	-	-	-	-	-	-	-	-	-	-	-	-	-	-	-	-
FI	266,830	-	-	-	-	-	-	-	-	-	-	-	-	-	-	-	-
FR	180,102	180,074	21,510	38.9	15.3	35.8	16	43.5	4.7	36	16	46	2	38.6	16	44.1	1.3
GB	77,673	1,190	401	83.8	0	16.2	7	59.2	17.6	16.2	11.2	58	14.6	16.2	16.4	53.9	13.6
HR	6,931	-	-	-	-	-	-	-	-	-	-	-	-	-	-	-	-
HU	10,448	10,448	0	0	0	0	0	0	0	0	0	0	0	0	0	0	0
IE	8,936	8,936	1,542	42.3	41.7	42.3	44.3	13.4	0	42.3	44.3	13.4	0	42.3	44.5	13.1	0
IT	125,878	125,878	0	0	0	0	0	0	0	0	0	0	0	0	0	0	0
MD	11,985	-	-	-	-	-	-	-	-	-	-	-	-	-	-	-	-
NL	7,295	6,052	3,984	1.3	4.3	0	14.2	71.7	14.2	0.2	14.7	77	8.1	1.3	14.3	84.4	0
NO	389,161	20,535	12,183	76.5	0	0	7.5	87.6	4.9	0	11.3	84.9	3.8	0	13	86.4	0.7
PL	88,383	88,383	48,739	19.8	47.8	19.2	47.5	32	1.2	19.5	47.5	32.9	0.2	19.8	46.7	33.5	0
RU	3,517,134	-	-	-	-	-	-	-	-	-	-	-	-	-	-	-	-
SE	519,341	31,124	11,676	38.5	8.8	13.9	2.4	52.3	31.4	17.1	2.4	49.4	31.1	29.1	2.2	41	27.8
SK	19,227	-	-	-	-	-	-	-	-	-	-	-	-	-	-	-	-
EU25	1,576,871	603,204	153,828	25.7	25.6	21.9	25.5	47.5	5	22.5	25.4	48.2	3.9	24.2	25	47.8	2.9
CLRTAP	5,673,748	683,237	168,661	29.2	23.4	20.2	24.2	50.7	5	20.7	24.3	51.1	3.9	22.3	24.2	50.8	2.7

Column 6 gives the percentage of the area for which a Damage Delay Time (DDT) can be computed. This is the case in areas where the critical load is already exceeded but the critical limit is not yet violated (see also Figure 2-16). In Europe 23.4% (25.6%) of the non-safe ecosystem area (column 4) will be damaged in the future at deposition levels under the BL-CLE scenario.

Column 7 gives the percentage of the area that will be safe (critical limit not violated and deposition not exceeding critical loads) in 2030 under the BL-CLE scenario, i.e. 20.2% (21.9%). Column 8 lists the percentages of areas at risk (not safe) where target loads for recovery in 2030 equals the critical loads, i.e. 24.2% in the LRTAP domain and 25.5% in the EU25 domain. Target loads lower than critical loads (column 9) are found for 50.7% (47.5%) of the ecosystem area which is not safe in 2000 (column 4). The European area for which no target loads can be found, i.e. for which even zero deposition would not lead to recovery in 2030, cover 5% (5%) (column 10). We conclude that the area which is – and would become – safe in 2030 (columns 7+8+9) is about 95% (95%) of the areas which are not safe now (column 4).

Finally, columns11–14 and 15–18 provide the analogous information for 2050 and 2100, respectively. It can be seen that the European area for which target loads can be identified in 2050 (column 12) is 24.3% (25.4%). In comparison to 2030 this implies an increment of 0.1% (0.1%). The area for which target loads can be identified need not necessarily be larger than a previous year. This can be seen when we compare column 17 to column 13. The difference of about 0.4% depicts the area for which a target load was required to establish recovery in 2030, but which can recover in 2100 under BL-CLE depositions. This can be seen from the fact that the areas defined as 'safe' (columns 7, 11 and 15) increase from 2030 to 2100, whereas the area for which target loads are non feasible (columns 10, 14 and 18) go down in the same period.

It is difficult to compare a large number of critical load and target load functions in a single plot. Therefore we restrict such a comparison to the maximum critical load of sulphur, $CL_{max}(S)$, and the corresponding quantity for target loads, $TL_{max}(S)$. Figure 2-18 shows for each of the 11 countries, for which TLFs have been calculated, in a so-called 'windmill plot' four correlations, namely between $TL_{max}(S)$ for the target years 2030 and 2050 (top right quadrants), between $TL_{max}(S)$ for 2050 and 2100 (bottom right), $TL_{max}(S)$ for 2100 and $CL_{max}(S)$ (botton left), and $CL_{max}(S)$ and $TL_{max}(S)$ for 2030 (top left quadrants). The different symbols refer to three ecosystem classes (forests, semi-natural vegetation and surface waters). The axes extend to 2000 eq/ha/a in all four directions, and the small numbered arrows indicate the number of ecosystems above this value in the respective direction(s).

A look at Figure 2-18 confirms that target loads for the different target years are fairly close to each other in many countries and for a majority of the ecosystems, and close to the critical loads as well. An extreme case is Ireland (IE) in which target loads for all years and critical loads hardly differ. An interesting case is Sweden (SE) where surface water target and critical loads are very close to each other, whereas the forest TLs, which are similar for the different target years, differ vastly from critical loads. The earlier a target year, the more stringent the target load (if it exists at all!); therefore the data points in Figure 2-18 should all lie on one side of the respective 1:1-line (diagonal), and deviations from this rule should be carefully looked into. This type of figure allows a quick assessment both of the correctness and difference in target loads and their relationship to critical loads.

References

De Vries W, Posch M, Kämäri J (1989) Simulation of the long-term soil response to acid deposition in various buffer ranges. Water, Air and Soil Pollution 48: 349-390

Hettelingh J-P, Posch M, Slootweg J (eds) (2004) Critical loads and dynamic modelling results. CCE Progress Report 2004, Coordination Center for Effects, RIVM Report 259101014, Bilthoven, Netherlands, 134 pp www.mnp.nl/cce

Jacobsen C, Rademacher P, Meesenburg H, Meiwes KJ (2002) Element contents in tree compartments – Literature study and data collection (in German). Report, Niedersächsische Forstliche Versuchsanstalt, Göttingen, Germany, 80 pp.

Reuss JO (1983) Implications of the calcium-aluminum exchange system for the effect of acid precipitation on soils. Journal of Environmental Quality 12(4): 591-595

UBA (2004) Manual on methodologies and criteria for modelling and mapping critical loads & levels and air pollution effects, risks and trends. Umweltbundesamt Texte 52/04, Berlin. www.icpmapping.org

Van Loon M, Tarrasón L, Posch M (2005) Modelling base cations in Europe. EMEP/MSC-W & CCE Note 2/05, Norwegian Meteorological Institute, Oslo, 58 pp

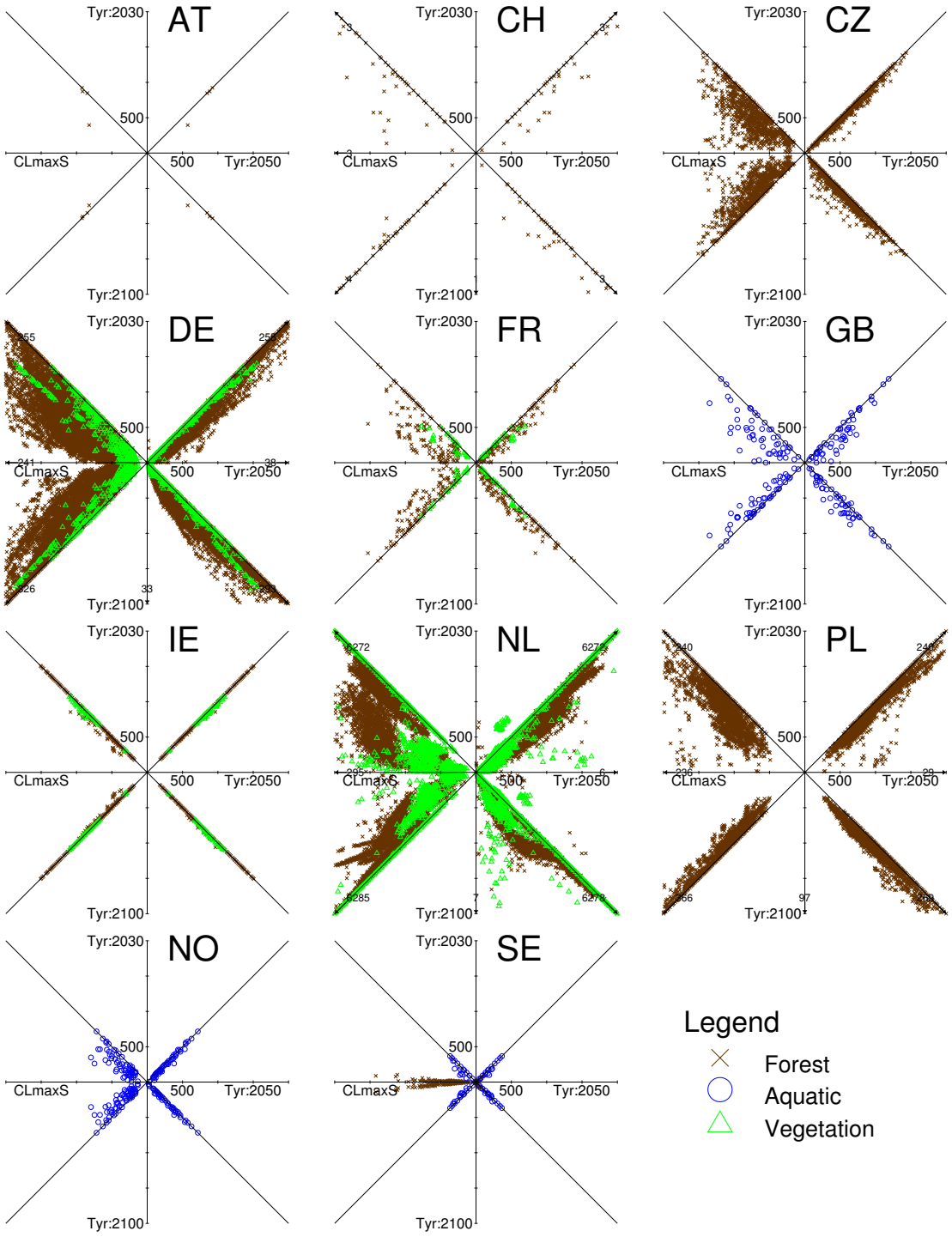


Figure 2-18. Correlations ('windmill plots') between the $TL_{max}(S)$ for the target years 2030, 2050 and 2100 and $CL_{max}(S)$ for 3 ecosystem classes and 11 countries for which TLFs have been computed.

3. Harmonizing European land cover maps

Jaap Slootweg, Jean-Paul Hettelingh, Wil Tamis*, Maarten van 't Zelfde*

*Institute of Environmental Sciences (CML), Leiden, the Netherlands

3.1 Introduction

Several bodies under the Convention have addressed the issue of defining a common land cover dataset during 2003, inter alia the TFIAM (EB.AIR.GE.1/2003/4), the EB and the ICP M&M (Final draft minutes of the taskforce meeting 2003). It was stressed that the land cover data should be the same for all steps in air pollution assessment work and working bodies under the Convention and that it should be freely and easily available. In order to harmonize the land cover maps, the currently used European maps are made compatible with regard to land cover classes and coordinate system, and then compared to each other. Results of the comparison have been presented to an ad-hoc expert meeting on harmonization of land cover information for applications under the Convention on LRTAP by CCE, CIAM, MSC-W and SEI. This meeting recommended a new dataset which merges CORINE data and SEI data to be produced.

This chapter introduces the currently used land cover maps and describes how their classifications are harmonized into the EUNIS classification system. The theoretical background and results of a comparison are presented, including maps that show the largest local differences between the maps, the distinction maps. Finally this chapter documents the creation of a land cover map than can be used for all European applications under the LRTAP Convention.

3.2 Description of relevant maps

An earlier study into existing land cover databases (De Smet and Hettelingh, 2001) narrowed the comparison to three relevant sources:

- the CORINE land cover database (Version 12/2000 extended coverage),
- the Pan-European Land Cover Monitoring (PELCOM) and
- the Land Cover Map of Europe of the Stockholm Environmental Institute (SEI).

All three have been updated since, making an update of the comparison of the three sources useful.

CORINE

The CORINE land cover database is the result of the ongoing CORINE Land Cover project of the European Environment Agency (EEA). Version 12/2000, used in this comparison, covers the EU-25 countries (with the exception of Cyprus and Malta), as well as Albania, Andorra, Bosnia and Herzegovina, Macedonia and the coastal zone of Tunisia and Northern Morocco (see Figure 3-1).

The map consists of national contributions, most of which used Landsat and/or SPOT satellite images, aerial photographs and other data sources to distinguish 44 land cover categories. The 100 meter grid has been made available for the work under the convention. This map is by far the most elaborate and accurate of the three maps, and is used as reference map, the 'truth' for the comparison. (http://dataservice.eea.eu.int/dataservice/)

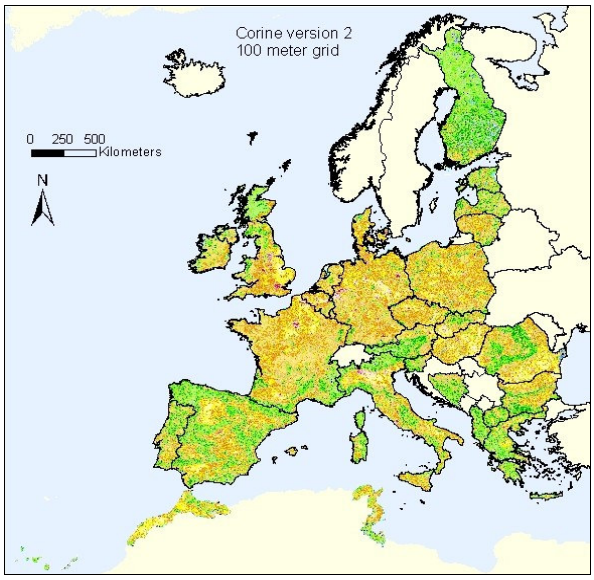


Figure 3-1 CORINE – 100 meter grid

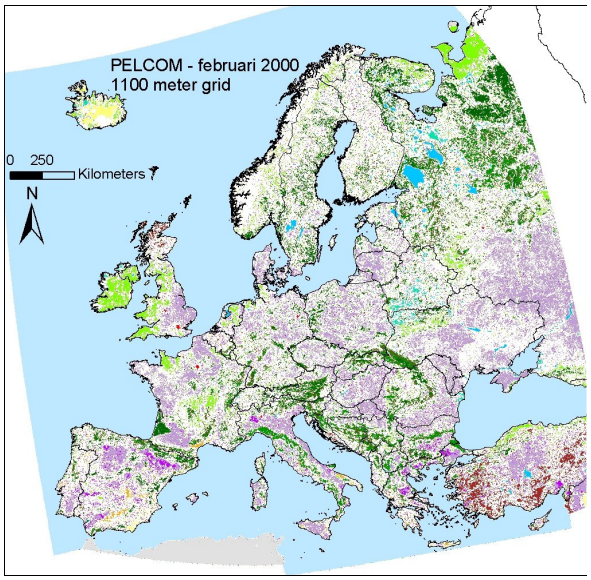


Figure 3-2 PELCOM 1100-grid (February 2000).

PELCOM

The 1-km pan-European land cover database is based on the integrative use of multi-spectral and multi-temporal 1-km resolution NOAA-AVHRR satellite data and ancillary data. PELCOM was a three years project under the Environment & Climate section of the European Union's 4th framework RTD programme. The methodology developed in the PELCOM project is based on combining both unsupervised and supervised classification approaches. The training samples are derived from selected homogeneous areas of the CORINE land cover database. The spectral characteristics of each training sample are used to determine class boundaries and pixel assignments in the supervised classification into the 15 categories used.

The version 02/2000, used in the comparison, covers Europe (http://www.gis.wageningen-ur.nl/cgi)

SEI

The SEI land cover database was originally developed for use in modelling of the impacts of various air pollutants at a continental scale. Its classification reflexes the attempts to identify an ecologically meaningful cover type and/or dominant species across Europe. Several datasets are utilized, among which PELCOM, various soil maps and other maps from international organisations related to agriculture.

The version 07/2003, used in the comparison, covers Europe including the European part of Russia, Turkey, Kazakhstan, Armenia and Azerbaijan (see Figure 3-3) (http://www.york.ac.ul/inst/sei/APS/projects.html)

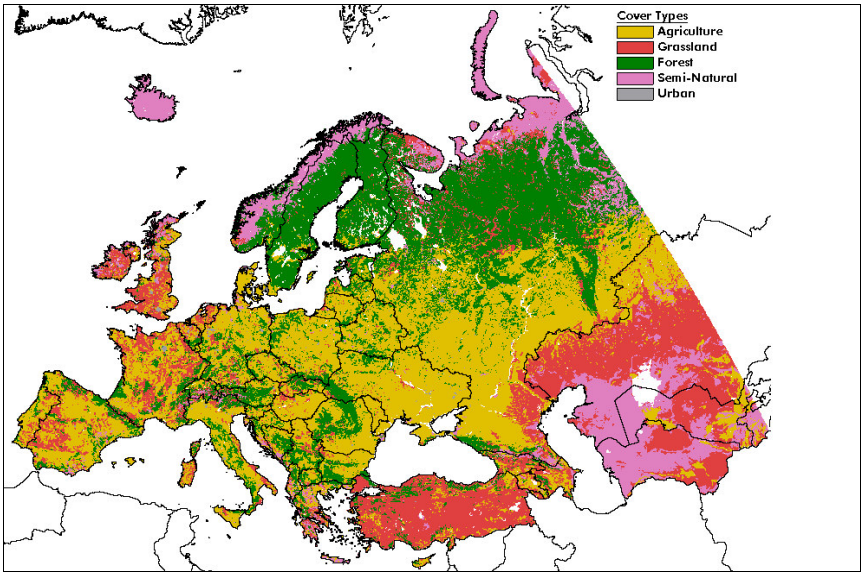


Figure 3-3. SEI coverage version 2003.

In order to identify a common land cover data set the available maps were compared. All of the maps have been created with different objectives and using different sources leading to different classification systems and different resolution and coordination systems. Therefore the next step is the reclassification of the land cover maps to one classification system. (EUNIS)

3.3 Reclassification to the EUNIS classification system

To improve on the uniformity of the ecosystem definitions for the work under the Convention a study was conducted to used classifications (Hall, 2001). The EUNIS (European Nature Information System) Habitat classification (Davies and Moss, 1999) was considered as the best 'target' classification scheme for the harmonization of the three above mentioned maps.

EUNIS is a hierarchic habitat classification system developed by the European Topic Centre for Nature Conservation (http://eunis.eea.eu.int) that uses a common framework with links to other classifications. The EUNIS system aims at defining ecological habitats, taking into account what species are present, but also incorporates features of the landscape.

Method:

The following steps in the cross-classification can be discerned:

1. An aggregated EUNIS-scheme for calculations and map presentations was derived, based on the inventory of relevant ecosystems for critical load calculations (Hall, 2001).This scheme will be referred to as EUNIS-LRTAP.
2. Two new classes were added to the EUNIS-scheme within class I (Regularly or recently agricultural, horticultural and domestic habitats):
   a. II (irrigated arable land)
   b. IN (non-irrigated arable land)
3. Inventory of existing cross-classification schemes (or schemes in development)
4. For those land use/ land cover maps for which cross-classification schemes to EUNIS do not exist yet or do exist partly, additional cross-classification was carried out. This was carried out in two steps
   a. CORINE, SEI and PELCOM were cross-classified to the second level of EUNIS
   b. These 'basic' cross-classifications were further aggregated and simplified, using a number of rules of thumb
5. For CORINE a complete cross-classification scheme was already available (Moss and Davies, 2002), but for SEI and PELCOM this was not the case.

a. For SEI a partial cross-classification scheme was available. It concerned the cross-classification of the second level of the SEI-grasslands to the second level of EUNIS (SEI, 2003). The remaining SEI-classes on the second level were cross-classified to the second level of EUNIS (with exception of the SEI classes for dominant tree species).
b. For PELCOM no cross-classification scheme was available and all 14 relevant classes were cross-classified to the second level of EUNIS.

6. As a consequence of this first cross-classification step quite often a single class within CORINE, SEI or PELCOM was cross-classified to several classes in EUNIS-level 2 (one-to-many relationship). The following rules of thumb were used in the second step to minimize the number of one-to-many relationships.
   a. Cross-classifications were as much as possible aggregated according to the EUNIS-LRTAP scheme. (For example, within CORINE several classes could be cross-classified to several different secondary levels within the EUNIS-category J (Constructed, industrial and other artificial habitats). However, within the EUNIS-LRTAP-scheme no distinction is made on the second level within this category.)
   b. When a source class was cross-classified to all EUNIS level 2 classes within a EUNIS level 1 class (because the source class contained no information, which made it possible to distinguish between level 2 classes within EUNIS); then only the cross-classification to the higher EUNIS level 1 was used.
   c. The different cross-classifications for one source class were evaluated by their importance. Less important cross-classifications were omitted; their weight was set to zero (0).
   d. EUNIS has several classification characteristics which might not be present in CORINE, SEI or PELCOM. Cross-classifications between source classes and EUNIS-classes based on features not present in the source classification were omitted; their weight was set to zero (0). N.B. This must not be misinterpreted as the absence of these EUNIS-classes!
7. The one-to-many relationships that remained after these aggregations were treated as combinations of two (or exceptionally three) EUNIS classes. Each class within the combination has the same proportional weight. Combinations are characterized with a starting X, so the combination of dry (E1) and mesic (E2) grasslands, becomes XE1E2. The combinations are only important for the GIS-manipulations of the maps. In the final use of these combinations, the information of the individual classes of the combinations will be used.

Results:

The aggregated EUNIS-LRTAP-scheme

In Table 3-1 the aggregated EUNIS-LRTAP-scheme is presented of the most relevant ecosystems for the work under the Convention, supplemented with all other ecosystems in order to cover all land use types. On the second level of EUNIS non-relevant classes have been combined, and they are marked with an X.

Table 3-1. Aggregated EUNIS-LRTAP-scheme of all relevant ecosystems marked with a 1 (level 1) or 2 (level 2) in the column L (LRTAP relevant), supplemented with other ecosystems in order to cover all land use/cover types.

Code	EUNIS-description	L
A	Marine habitats	-
B	Coastal habitats	-
C	Inland surface waters habitats	1
C1	Standing waters	2
C2	Running waters	2
C3	Littoral zone of inland surface waterbodies	2
D	Mire, bog and fen habitats	1
D1	Raised & blanket bog	2
D2	Valley mires, poor fens, transition mires	2
DX	Other mire, bog and fen habitats	-
E	Grassland and tall forb habitats	1
E1	Dry grasslands	2
E2	Mesic grasslands	2
E3	Seasonally wet & wet grasslands	2
E4	Alpine & sub-alpine grasslands	2
EX	Other grassland and tall forb habitats	-
F	Heathland, scrub and tundra habitats	1
F2	Arctic, alpine &sub-alpine scrub	2
F3	Temperate & Mediterranean montane scrub	2
F4	Temperate scrub heathland	2
FX	Other heathland, scrub and tundra	-

Code	EUNIS-description	L
	habitats	
G	Woodland and forest habitats and other wooded land	1
G1	Broadleaved deciduous woodland	2
G2	Broadleaved evergreen woodland	2
G3	Coniferous woodland	2
G4	Mixed deciduous and coniferous woodland	2
G5	Lines of trees, small anthropogenic woodlands, recently felled woodland, early-stage woodland	-
	and coppice	
H	Inland unvegetated or sparsely vegetated habitats	-
I	Regularly or recently cultivated agricultural, horticultural and domestic habitats	-
II	Irrigated arable land	-
IN	Non-irrigated arable land	-
J	Constructed, industrial and other artificial habitats	-

The total number of EUNIS-LRTAP map classes is 10 (level 1) or 32 (level 1 + level 2).

Cross-classification

PELCOM-EUNIS cross-classification

As an example a part of the cross-classification table for PELCOM to EUNIS is presented in Table 3-2 (The complete cross-classification table is stored in Annex 3A. In the third column (EUNIS L2) the results of the first step of the cross-classification are presented: classification to the second level of EUNIS. In the fourth column the aggregation/ simplification of the one-to-may cross-classifications and the conversion to the EUNIS-LRTAP-scheme is presented.

Some comments on the cross-classification table PELCOM-EUNIS to illustrate this procedure:

- For the first PELCOM-class, 11 (Coniferous forest), we see that it could be cross-classified to four level 2 classes within EUNIS: B1, B2, G3 and G5. Classes B1 and B2 are coastal areas on different types of soils. Because these class characteristics are not available in PELCOM, these cross-classifications were omitted (0 in fourth column). The same holds for G5: lines of trees etc.

- For the second PELCOM-class, 12 (Deciduous forest), we see in the eighth row that deciduous forest is also cross classified to EUNIS-G2 level: (broad leaved evergreen forest). This is of course contradictory (deciduous and evergreen), but this is the best cross-classification that could be made for this EUNIS-class. Finally this cross-classification is omitted, because PELCOM do not contain information on deciduousness. So in the final cross-classification between PELCOM and EUNIS, class G2 is not present. This must not be misinterpreted that broad-leaved evergreen forests are not present. They are included probably within the category G1, broad leaved deciduous forest.

Table 3-2. Cross-classification table for PELCOM translated to the second level of EUNIS and subsequently to the EUNIS-LRTAP classes; 0 = cross-classification omitted.

code	PELCOM name	EUNIS L2	EUNIS LRTAP
11	Coniferous forest	B1	0
11	Coniferous forest	B2	0
11	Coniferous forest	G3	G3
11	Coniferous forest	G5	0
12	Deciduous forest	B1	0
12	Deciduous forest	B2	0
12	Deciduous forest	G1	G1
12	Deciduous forest	G2	0
12	Deciduous forest	G5	0
13	Mixed forest	B1	0
13	Mixed forest	B2	0
13	Mixed forest	G4	G4
13	Mixed forest	G5	0
20	Grassland	B1	0
20	Grassland	B2	0
20	Grassland	B3	0
20	Grassland	E1	E
20	Grassland	E2	E
20	Grassland	E3	E
20	Grassland	E4	E
20	Grassland	E5	E
20	Grassland	E6	E
20	Grassland	E7	E

CORINE-EUNIS cross-classification

CORINE has three hierarchical levels, already cross-classified to all levels of EUNIS. The existing cross-classification contains many one-to-many relationships and these relationships often contain many relations (on average 3-4 for each CORINE 3 level class). Many of these relationships had been evaluated as less important. The whole cross-classification table (330 lines) is listed in Annex 3A

SEI-EUNIS cross-classification

SEI has up to four levels (for grasslands and semi-natural areas). A part of the grassland and semi-natural areas already had been cross-classified to the second level of EUNIS by SEI itself. A definitive description of the different levels and classes had not been available for the most recent version of the SEI map. This hampered the cross classification of the SEI-classes in some cases. The following choices have been made in order to produce a SEI-EUNIS cross classification:

SEI dominant crops in general and SEI dominant crops irrigated have been cross classified to EUNIS non-irrigated and irrigated agriculture. SEI dominant crops in general which were present twice or even three times with the same name or meaning (e.g. grapes and vineyard) but with different codes in the SEI classification have been cross classified to one dominant EUNIS-crop code.

There are several inconsistencies (as of November 2003) in the SEI-classification (e.g. presence of type 'dry marsh') and in the partial SEI-EUNIS cross classification produced by SEI (e.g. SEI - Wet improved tall grassland -> EUNIS - Dry grassland etc.), which have to be improved in future (cross) classifications.

The whole cross-classification table (525 lines) is listed in Annex 3A

3.4 Comparing maps using contingency matrix and kappa statistics

Comparing maps is often done by creating a contingency matrix or by Kappa statistics. Each cell of a contingency matrix gives the fraction of raster cells classified in a particular category in one map and another category in the other map. Given k categories, i and j the indexes of the categories in the maps, a contingency table looks like:

		map J (j=columns)				Total
		1	2	…	k	
map I (i=row)	1	p_{11}	p_{12}	…	p_{1k}	p_{1+}
	2	p_{21}	p_{22}	…	p_{2k}	p_{2+}
	…	…	…	…	…	…
	k	p_{k1}	p_{k2}	…	p_{kk}	p_{k+}
Total		p_{+1}	p_{+2}	…	p_{+k}	1

With $p_{+j} = \sum_{i=1}^{k} p_{ij}$ and $p_{i+} = \sum_{j=1}^{k} p_{ij}$.

Kappa gives the similarity of the maps and adjusts for the probability, p_e, that cells are equal by chance a priori to the comparison (pe). $kappa = \frac{sim - p_e}{1 - p_e}$ with $sim = \sum_{i=1}^{k} p_{ii}$

If we neglect the auto-correlation of the maps this probability p_e can be calculated from the histograms of the maps as $P_e = \sum_{i=1}^{n} p_{+i} p_{i+}$. *Kappa* equals 1 with perfect agreement and nears zero when the agreement is random.

More can be found in Cohen (1960) and in Monserud and Leemans (1992).

The land cover maps in this comparison are compiled with different objectives, resulting in different classifications. The harmonisation of the classifications will most likely result in category definitions that do not match perfectly. Also the co-ordinate system and resolution of the maps differ, leading to dislocations between the maps. To allow further analysis of the most important differences between the maps two methods have been applied. The first is to split kappa into a measure for the differences in histograms, and a measure for differences in the location of similar categories, respectively $Kappa_{Histo}$ and $Kappa_{Location}$. These quantities are defined by

$$Kappa_{Histo} = \frac{p_{\max} - p_e}{1 - p_e} \quad \text{and} \quad Kappa_{Location} = \frac{sim - p_e}{p_{\max} - p_e}$$ where $p_{\max}$ holds the maximum possible similarity, given the histograms of the distribution: $p_{\max} = \sum_{i=1}^{k} \min(p_{i+}, p_{+i})$. The second method to distinguish small from important differences in the maps is the introduction of fuzziness in category as well as in location. To compare the maps in a fuzzy way the grade of applicability of the category of the other map counts. This grade gives a fuzzy value between 0 for not applicable to 1 for completely equal. Categories of neighbouring cells as well as similarities between categories contribute to this fuzzy value. The fuzzy similarity of two corresponding raster cells is the minimum of the fuzzy value of one map compared to the other, and the value for the comparison the other way around. The fuzzy similarity between the two maps is the average of the similarities of all the corresponding rasters-cells. From this it is possible to calculate a '$Kappa_{Fuzzy}$' that is less sensitive for small differences then the classical *Kappa*.

$$Kappa_{fuzzy} = \frac{sim_{fuzzy} - p_{e,\,fuzzy}}{1 - p_{e,\,fuzzy}}$$

By applying fuzzy set theory the similarity increases in most cases, but also the probability that cells are more or less equal has increased. A way to describe the additional change is described in Hagen (2002). That article describes also the complete method in more detail. Another, but elaborate way of calculating the a priori probability of similarity is by Monte Carlo analysis. If the randomly generated maps would simulate the spatial auto-correlation this way could also adjust for this phenomena.

3.5 Results of the comparison

The histogram's of the maps, as far as they overlap spatially, is given in Table 3-3. From this, the calculated $Kappa_{Histo}$ is calculated as 0.959 between SEI and Corine, and 0.954 for PELCOM and Corine. This indicated a very high similarity for the overal contributions of the land use classes.

Table 3-3. Histograms of the maps for the overlapping area in promilles.

	CORINE	SEI	PELCOM
Water	16	18	15
Vegetation	229	268	197
Broadleaved	117	116	124
Coniferious	175	164	212
Barren	22	1	14
Agricultural	415	413	417
Urban	26	20	21

Table 3-4 and 3-5 show the contingency tables for both comparisons. The resulting Kappa's are 0.275 for CORINE vs. SEI and 0.376 for CORINE vs. PELCOM. There is a large misfit for 'Vegetation'. In the part of the SEI map that overlaps with CORINE a total of 268‰ of the raster cells is classified as such. This includes 101‰ cells that are classified as 'Agricultural' in CORINE, and only 95‰ is also classified as 'Vegetation' in CORINE. Also a large part of the agricultural areas in SEI are classified as vegetation in CORINE.

Table 3-4. Contingency table for the comparison of the CORINE map versus the SEI map. All numbers are in promilles, blank = 0 values.

SEI CORINE	Water	Vegetat.	Broadl.	Conif.	Barren	Agricult.	Urban	Sum
Water	9	2	1	2		2		16
Vegetation	2	95	24	33		73	2	229
Broadleaved	1	28	34	13		40	1	117
Coniferous	4	27	16	88		40	1	175
Barren		9	2	2		6	2	22
Agricultural	3	101	38	24		242	7	415
Urban		5	2	1		11	7	26
Sum	18	268	116	164	1	413	20	1000

Table 3-5. Contingency table for the comparison of the CORINE map versus the PELCOM map. All numbers are in promilles, blank = 0 values.

PELCOM CORINE	Water	Vegetat.	Broadl.	Conif.	Barren	Agricult.	Urban	Sum
Water	7	2	0	3	0	3	0	16
Vegetation	2	97	24	46	3	55	2	229
Broadleaved	1	18	47	19	1	30	1	117
Coniferous	3	24	19	99	2	29	1	176
Barren	0	4	1	5	4	5	2	22
Agricultural	2	50	31	37	4	284	7	415
Urban	0	3	2	2	0	12	7	26
Sum	15	197	124	212	14	417	21	1000

The differences between the maps are not uniformly distributed over Europe. For integrated assessments on a European scale, and mapping ecosystem dependant exceedences a map containing a distribution of ecosystems for each EMEP-50km. grid cell is needed. To compare the maps on this scale the Kappa-Histo's were calculated for each 50km. EMEP grid, see Figure 3-4.

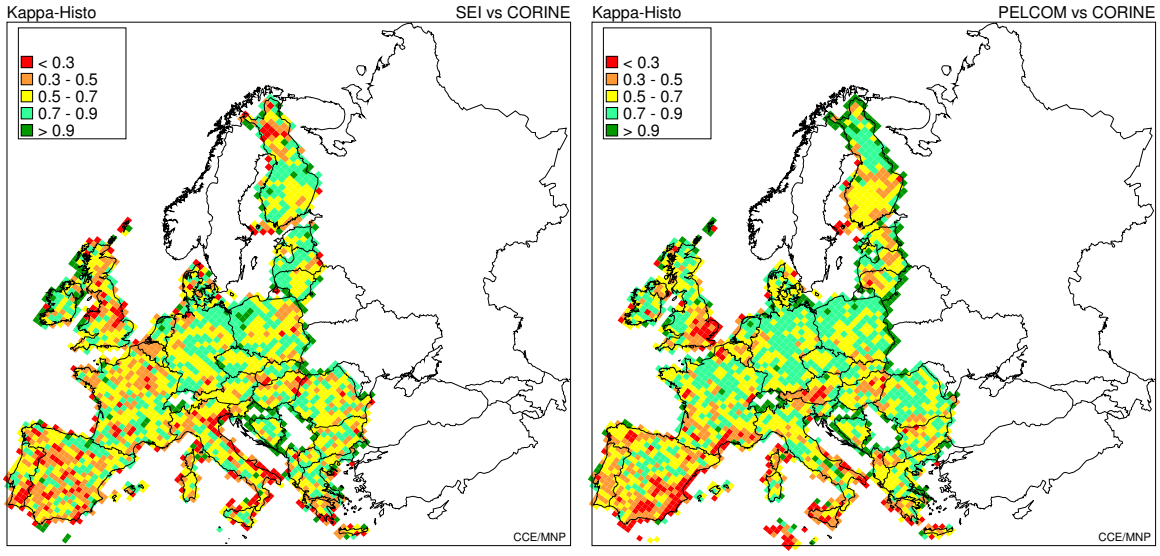


Figure 3-4. Kappa-Histo calculated for each EMEP 50km. grid. CORINE is compared to SEI (left) and PELCOM (right).

The results show a good match for most of Europe, but some areas, like for instance the Mediterranian differ considerably. On this scale PELCOM and SEI resemble CORINE to the same degree.

To investigate the differences between the maps further, the can be plotted next to each other, but only showing the areas in which they differ.

3.6 Distinction maps

Given the fact that the maps differ, it is interesting to search for the areas with the most systematic differences. In order to find those differences, the area with little or no differences needs to be obscured. This has for instance been done for Spain, Portugal and Corse by (1) resampling to a 2.5 km grid, (2) applying a fuzziness in categories according to the cross classification, (3) applying a fuzziness for small dis-locations between the maps. Application of the software made by RIKS (Research Institute for Knowledge Systems) provided a grid-map with $Kappa_{fuzzy}$ values. This map was used as a mask, to show only areas with kappa-fuzzy equal to 0. Figure 3-5 shows the masked SEI map next to the CORINE map with the same masking applied. Both maps only show original, but clustered classes to enable recognition of the colors used in the legend.

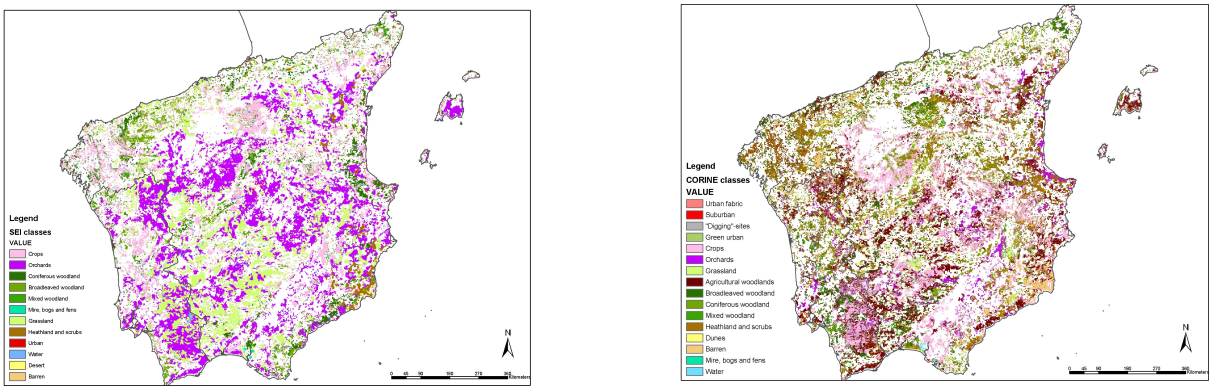


Figure 3-5. Differences between SEI (left) and CORINE (right) for Spain, Portugal and Corse.

Now it is easy to pick an area of interest and investigate the reason for differences. For instance the 'Agricultural Woodlands' in Corse on the CORINE map (in detail 'Annual crops associated with permanent crops' translated to the Agriculture in EUNIS) are in fact classified as 'Fruit' in SEI, and translated to the EUNIS class 'Broadleaved deciduous woodland.' These classes are not as contradicting as the cross classifications suggest. The same is true for an area in the south of Spain which has the classes 'Wet Neutral Unimproved Grassland' (SEI) and 'Water bodies' (CORINE) given the seasonal influences. These samples (and others) suggest that the SEI and CORINE map are more similar than the kappa statistics reveal. A detailed class to class comparison between SEI and CORINE can provide information about the actual land cover.

3.7 Conclusions and recommandations

The overall histograms of the CORINE, PELCOM and SEI maps are very much alike. For integrated studies on a European scale and for coarser resolutions like the EMEP 50km grid the maps are quite similar. For most parts of Europe the distribution of ecosystems within 50 km. EMEP grids give a good match between SEI and CORINE, as well as PELCOM and CORINE. The distributions of critical loads in the European background database are not likely to vary much by the use of either of the three land cover maps.

The contingency tables from the comparisons between SEI and CORINE, and for PELCOM and CORINE on a 250m resolution (Table 3-4 and 3-5) show relatively low similarities and low values for Kappa. Clear quality checks for the land cover category of every ecosystem that is submitted by a NFC will not be possible, but a comparison of the submitted data with a common land cover map can contribute to a consistent critical loads database.

Better results, more in line with earlier reports, are achieved if the maps are aggregated to a resolution similar to the coarser maps, PELCOM and SEI, using the majority of the 250m map. Including fuzziness in location, allowing land cover to be shifted a little between the maps, does generally not raise values for Kappa. Given the fact that 50 km. EMEP grids have relatively high values for KappaHisto, the occurrence of similar land cover in different maps are likely within the region, but not necessary in the close vicinity.

Figure 3-4 shows that the maps differ mostly in the Mediterranean area. The maps showing the differences between the maps clearly show many regions with consistent deviations. This might give clues for improving the compilation process of the maps. More investigations of these areas might also expose the different interpretations of the used categories in all of the maps used to compile CORINE, SEI and PELCOM.

PELCOM is more similar to CORINE then SEI, but this can be expected, because both maps share partly the same data sources. The slightly higher similariry of PELCOM does not nessicarily mean it is closer to the actual land cover, because also CORINE deviates from the 'thruth.'

It is possible to convert the CORINE, PELCOM and SEI maps to the EUNIS classification system. Some subjective choices/weighing had to be made in order to achieve a practical classification. To differentiate between irrigated and non-irrigated land, two EUNIS catagories were added.

The problem of one-to-many relationships has been solved by omitting the less relevant cross-classifications and also cross-classifications to EUNIS-classes for which the source classes actually do no not contain enough information. The last point relates to the problem of classification characteristics used in EUNIS but not in CORINE, SEI and/or PELCOM, see e.g. Table 3-2, PELCOM to EUNIS level 1 B Coastal habitats. There is a risk of misinterpretation that these omitted classes are absent.

Each class in a combination gets a proportional share; e.g. in case of two classes 50%. A more realistic distribution of the shares is possible on basis of map comparisons, in combination with regional differentiation

The development of EUNIS is a large step forwards in the harmonisation of ecosystem description.

Nevertheless EUNIS has some major flaws:

- it is not systematically hierarchical
- landscape and site factor properties are mixed, producing a not completely consistent classification (see e.g. coastal habitats).

A better approach would be to recognize that the classification factors are indeed strict hierarchical.

For the Netherlands a hierarchical system have been developed using factors as salinity, vegetation structure, moisture availability, nutrient availability and acidity (Tamis et al., 2005)

3.8 A harmonised land cover map of Europe

Generally the CORINE map is considered the best available land cover data, but only part of the spatial EMEP modelling domain is available. The best available map, at the time of writing this report, is a combination of CORINE, where available, and SEI data where CORINE is missing. This map has been created by the CCE as a grid map, in the EMEP coordination system. The gridsize is 250*250 meters. Also on the bases of this combination of maps, EMEP compiled a dataset of the distribution of land cover classes for each EMEP grid containing terrestrial area, focussing on dispersion of airborne pollutants. The classes used for this map are listed in Table 3-5.

Land cover classes
Temperate coniferous forest
Temperate deciduous forest
Mediterranean needleleaf forest
Mediterranean broadleaf forest
Wheat (artificial)
Temperate crops
Mediterranean crops
Root crops
Grassland
Semi-natural
Mediterranean scrub
Wetland
Tundra
Desert/Barren
Water
Ice
Urban

Table 3-5. Land cover classes used by EMEP for their dispersion modelling

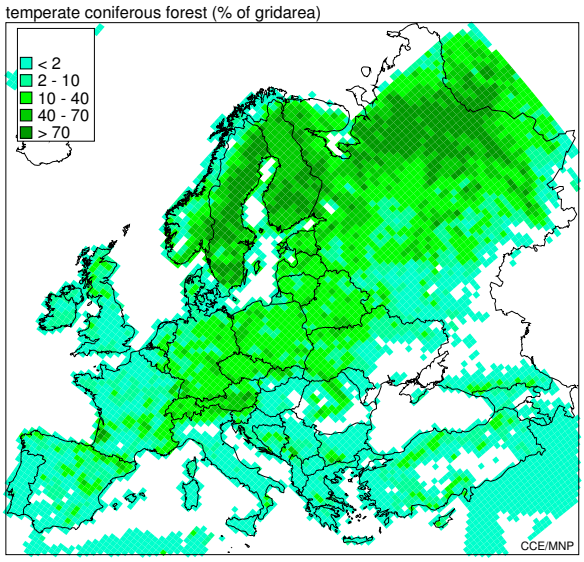


Figure 3-6. Spatial distribution of temperate coniferous forest in the EMEP compilation of the CORINE and SEI land cover data

The disadvange of this merging is the limitations in the classification of CORINE, especially after translation into the EUNIS classification system. It is possible to use the information from SEI to define the actual land cover more precisely. If an area is classified in CORINE as 'Natural grasslands', it will be listed as 'E - Grassland and tall forb habitats' in the general map used for the convention. But if the same area is indicated as being 'Dry Alpine Meadow' in SEI, it can be classified in the EUNIS system as 'E4 - Alpine & sub-alpine grasslands.' If the CORINE and SEI land cover class are not contradicting then the use of the SEI information is straight forward. But also the presents of a compatible SEI land cover class in the vicinity of the CORINE class could be used to improve on the level of the EUNIS classification used in the next version of a general land cover map.

References

Cinderby S (2002) Description of 2002 revised SEI Land-cover map, http://www.york.ac.uk/inst/sei/APS/projects.html

Davies CE, Moss D (1999) EUNIS Habitat Classification, Final Report to the European Environmental Agency

De Smet PAM, Hettelingh J-P (2001) Intercomparison of Current European Land Use/Land Cover Databases, Status Report 2001 Coordination Center for Effects RIVM Report 259101010, Bilthoven, Netherlands, pp. 41-52

Hagen A (2002) Fuzzy set approach to assessing similarity of categorical maps, Int. J. Geographical Information Science 17.3 235-249

Hall, J (2001) Harmonisation of Ecosystem Definitions, Status Report 2001 Coordination Center for Effects pp. 63-66

Monserud R, Leemans R (1992) Comparing global vegetation maps with kappa statistic, Ecological Modelling, 62 275-293

Mücher CA, Champeaux J-L, Steinnocher KT, Griguolo S, Wester K, Heunks C, Winiwarter W, Kressler FP, Goutorbe JP, Ten Brink B, Van Katwijk VF, Furberg O, Perdigao V, Nieuwenhuis GJA (2001) Development of a consistent methodology to derive land cover information on a European scale from remote sensing for environmental monitoring: the PELCOM report, Alterra Report 178, http://cgi.girs.wageningen-ur.nl/cgi/projects/eu/pelcom/public/index.htm

Tamis WLM, Van 't Zelfde M, Van der Meijden R, Groen CLG, Udo de Haes HA (2005) Ecological interpretation of changes in the Dutch flora in the 20th century. Biological Conservation 125: 211-224

Annex 3A Cross-classification to EUNIS

Table 3A-1 Conversion table of CORINE to EUNIS. The descriptions of the EUNIS codes are listed in table 3-1 of the main text. CE are combined EUNIS-classes which are described in Table 3A-4*

CORINE code	CORINE name	EUNIS code
1.1.1	Continuous urban fabric	CE1
1.1.2	Discontinuous urban fabric	CE1
1.2.1	Industrial or commercial units	J
1.2.2	Road and rail networks and associated land	J
1.2.3	Port areas	J
1.2.4	Airports	J
1.3.1	Mineral extraction sites	CE4
1.3.2	Dump sites	CE4
1.3.3	Construction sites	CE4
1.4.1	Green urban areas	CE2
1.4.2	Sport and leisure facilities	CE2
2.1.1	Non-irrigated arable land	IN
2.1.2	Permanently irrigated land	II
2.1.3	Rice fields	II
2.2.1	Vineyards	FX
2.2.2	Fruit trees and berry plantations	G1
2.2.3	Olive groves	G2
2.3.1	Pastures	E2
2.4.1	Annual crops associated with permanent crops	I
2.4.2	Complex cultivation patterns	I
2.4.3	Land principally occupied by agriculture, with significant areas of natural vegetation	I
2.4.4	Agro-forestry areas	I
3.1.1	Broad-leaved forest	G1
3.1.2	Coniferous forest	G3
3.1.3	Mixed forest	G4
3.2.1	Natural grasslands	E
3.2.2	Moors and heathland	F
3.2.3	Sclerophyllous vegetation	CE3
3.2.4	Transitional woodland-shrub	F
3.3.1	Beaches, dunes, sands	B
3.3.2	Bare rocks	H
3.3.3	Sparsely vegetated areas	H
3.3.4	Burnt areas	H
3.3.5	Glaciers and perpetual snow	H
4.1.1	Inland marshes	D
4.1.2	Peat bogs	D
4.2.1	Salt marshes	A
4.2.2	Salines	A
4.2.3	Intertidal flats	A
5.1.1	Water courses	C
5.1.2	Water bodies	C
5.2.1	Coastal lagoons	A
5.2.2	Estuaries	A
5.2.3	Sea and ocean	A

Table 3A-2 Conversion table of PELCOM to EUNIS. The descriptions of the EUNIS codes are listed in table 3-1 of the main text. PE are combined EUNIS-classes which are described in Table 3A-4*

PELCOM code	PELCOM name	EUNIS code
11	Coniferous forest	G3
12	Deciduous forest	G1
13	Mixed forest	G4
20	Grassland	E
31	Rainfed arable land	IN
32	Irrigated arable land	II
40	Permanent crops	PE1
50	Shrub land	F
60	Barren land	H
80	Wetlands	D
91	Inland waters	C
92	Sea	A
100	Urban areas	J

Table 3A-3 Conversion table of SEI to EUNIS. The descriptions of the EUNIS codes are listed in table 3-1 of the main text. SE are combined EUNIS-classes which are described in Annex Table 3A-4*

SEI code	SEI name	EUNIS code
1.1.1	Wheat	I
1.1.11	Sugar Beet	I
1.1.12	Potatoes	I
1.1.15	Cotton	I
1.1.16	Olives	G2
1.1.18	Grapes	FX
1.1.19	Fruit	G1
1.1.2	Barley	I
1.1.24	Vineyards	FX
1.1.25	Orchards	G1
1.1.27	Wheat & Barley	I
1.1.28	Wheat & Barley & Orchards	I
1.1.3	Rye	II
1.1.30	Nuts	G1
1.1.31	Flowers	I
1.1.32	Berries	I
1.1.6	Maize	I
1.1.7	Rice	I
1.1.8	Soya	I
1.2.101	Wheat	I
1.2.102	Barley	I
1.2.103	Rye	II
1.2.106	Maize	I
1.2.107	Rice	I
1.2.108	Soya	I
1.2.111	Sugar Beet	I
1.2.112	Potatoes	I
1.2.115	Cotton	I
1.2.116	Olives	G2
1.2.118	Grapes	FX
1.2.119	Fruit	G1
1.2.124	Vineyards	FX
1.2.125	Orchards	G1
1.2.127	Wheat & Barley	I
1.2.128	Wheat & Barley & Orchards	I
1.2.130	Nuts	G1
1.2.131	Flowers	I
1.2.132	Berries	I
1.3.1	Wheat	II
1.3.11	Sugar Beet	II
1.3.12	Potatoes	II
1.3.13	Cotton	II
1.3.18	Grape	FX
1.3.19	Fruit	G1
1.3.2	Barley	II
1.3.24	Unaccounted	II
1.3.6	Maize	II
1.3.7	Rice	II
2.1.1	Needle Leaf	G3
2.1.2	Needle Leaf - Restricted Lumbering	G3
2.1.3	Broad Leaf	G1
2.1.3	Broad Leaf	G2
2.1.4	Broad Leaf - Restricted Lumbering	G1
2.1.4	Broad Leaf - Restricted Lumbering	G2
2.1.5	Mixed	G4
2.1.6	Mixed - Restricted Lumbering	G4
3.1.1.0	Dry Alpine Meadow	E4
3.1.1.1	Dry Acid Alpine Meadow	E4
3.1.1.2	Dry Neutral Alpine Meadow	E4
3.1.1.3	Dry Alkali Alpine Meadow	E4
3.1.2.0	Wet Alpine Meadow	E4
3.1.2.1	Wet Acid Alpine Meadow	E4
3.1.2.2	Wet Neutral Alpine Meadow	E4
3.1.2.3	Wet Alkali Alpine Meadow	E4
3.100.1.0	Dry Acid Arctic Heath	F2
3.100.2.0	Wet Acid Arctic Heath	F2
3.1000.1.0	Dry Acid Peat Bog	SE01
3.1000.2.0	Wet Acid Peat Bog	SE01
3.11.1.0	Dry Alpine Steppe Meadow	E4
3.11.1.1	Dry Acid Alpine Steppe Meadow	E4
3.11.1.2	Dry Neutral Alpine Steppe Meadow	E4
3.11.1.3	Dry Alkali Alpine Steppe Meadow	E4
3.11.2.1	Wet Acid Alpine Steppe Meadow	E4
3.11.2.2	Wet Neutral Alpine Steppe Meadow	E4
3.11.2.3	Wet Alkali Alpine Steppe Meadow	E4
3.1100.1.0	Dry Alkali Scrub	F4
3.1100.2.0	Wet Acid Scrub	F4
3.1200.1.0	Dry Snow & Ice	H
3.1200.2.0	Wet Snow & Ice	H
3.13.1.2	Dry Neutral Alpine Tugai Meadow	E4
3.13.1.3	Dry Alkali Alpine Tugai Meadow	E4
3.14.1.3	Dry Alkali Alpine Tundra Meadow	E4
3.1400.1.0	Dry Neutral Solonchak & Heath Tundra	SE02
3.1500.1.0	Dry Neutral Solnchak & Marsh	SE03
3.1700.1.0	Dry Alkali Solnchak & Tundra	SE02
3.18.1.3	Dry Alkali Creeper Pasture	SE04
3.1800.1.0	Dry Alkali Sparse Vegetation	H
3.1800.2.0	Wet Sparse Vegetation	H
3.19.1.3	Dry Alkali Creeper Short Grass Pasture	SE04
3.1900.1.0	Dry Alkali Tugai	SE05
3.200.2.0	Wet Acid Arctic Heath & Peat Bog	SE06
3.2000.1.0	Dry Neutral Tundra	FX
3.2000.2.0	Wet Acid Tundra	FX
3.2100.1.0	Dry Acid Tundra with Marsh	SE07
3.2100.2.0	Wet Acid Tundra with Marsh	SE07
3.2200.2.0	Wet Acid Tundra with Peat Bog	SE08
3.2300.1.0	Dry Acid Tundra with Wetland	SE07
3.2300.2.0	Wet Acid Tundra with Wetland	SE07
3.24.1.0	Dry Desert Grassland	E1
3.24.1.2	Dry Neutral Desert Grassland	E1
3.24.1.3	Dry Alkali Desert Grassland	E1
3.2400.1.0	Dry Acid Wetland	DX
3.2400.2.0	Wet Acid Wetland	DX
3.26.1.0	Dry Desert Steppe Pasture	E1
3.26.1.3	Dry Alkali Desert Steppe Pasture	E1
3.28.1.0	Dry Desert Tundra Pasture	E1
3.28.1.3	Dry Alkali Desert Tundra Pasture	E1
3.300.1.0	Dry Bare Stone	H
3.300.2.0	Wet Alkali Bare Stone	H
3.31.1.0	Dry Forest Pasture	EX
3.31.1.1	Dry Acid Forest Pasture	EX
3.31.1.2	Dry Neutral Forest Pasture	EX
3.31.1.3	Dry Alkali Forest Pasture	EX
3.31.2.0	Wet Forest Pasture	EX
3.31.2.1	Wet Acid Forest Pasture	EX
3.31.2.2	Wet Neutral Forest Pasture	EX
3.31.2.3	Wet Alkali Forest Pasture	EX
3.32.1.0	Dry Forest Short Grass Pasture	EX
3.32.1.1	Dry Acid Forest Short Grass Pasture	EX
3.32.1.2	Dry Neutral Forest Short Grass Pasture	EX

SEI code	SEI name	EUNIS code
3.32.1.3	Dry Alkali Forest Short Grass Pasture	EX
3.32.2.0	Wet Forest Short Grass Pasture	EX
3.32.2.1	Wet Acid Forest Short Grass Pasture	EX
3.32.2.3	Wet Alkali Forest Short Grass Pasture	EX
3.33.1.1	Dry Acid Forest Short Montane Grass Pasture	EX
3.33.1.2	Dry Neutral Forest Short Montane Grass Pasture	EX
3.33.1.3	Dry Alkali Forest Short Montane Grass Pasture	EX
3.34.1.0	Dry Forest Tall Grass Pasture	EX
3.34.1.1	Dry Acid Forest Tall Grass Pasture	EX
3.34.1.2	Dry Neutral Forest Tall Grass Pasture	EX
3.34.1.3	Dry Alkali Forest Tall Grass Pasture	EX
3.34.2.1	Wet Acid Forest Tall Grass Pasture	EX
3.36.1.0	Dry Grassland	SE09
3.36.1.1	Dry Acid Grassland	SE09
3.36.1.2	Dry Neutral Grassland	SE09
3.36.1.3	Dry Alkali Grassland	SE09
3.36.2.0	Wet Grassland	SE04
3.36.2.1	Wet Acid Grassland	SE04
3.36.2.2	Wet Neutral Grassland	SE04
3.36.2.3	Wet Alkali Grassland	SE04
3.37.1.0	Dry Grassland/Meadow/Hay	E2
3.37.1.1	Dry Acid Grassland/Meadow/Hay	E2
3.37.1.2	Dry Neutral Grassland/Meadow/Hay	E2
3.37.1.3	Dry Alkali Grassland/Meadow/Hay	E2
3.37.2.0	Wet Grassland/Meadow/Hay	SE04
3.37.2.1	Wet Acid Grassland/Meadow/Hay	SE04
3.37.2.2	Wet Neutral Grassland/Meadow/Hay	SE04
3.37.2.3	Wet Alkali Grassland/Meadow/Hay	SE04
3.38.1.1	Dry Acid Hay Meadow	E2
3.38.1.2	Dry Neutral Hay Meadow	E2
3.38.1.3	Dry Alkali Hay Meadow	E2
3.38.2.1	Wet Acid Hay Meadow	SE04
3.38.2.2	Wet Neutral Hay Meadow	SE04
3.38.2.3	Wet Alkali Hay Meadow	SE04
3.39.2.0	Wet Improved Alpine Short Grassland	E4
3.39.2.1	Wet Acid Improved Alpine Short Grassland	E4
3.39.2.2	Wet Neutral Improved Alpine Short Grassland	E4
3.39.2.3	Wet Alkali Improved Alpine Short Grassland	E4
3.400.1.0	Dry Desert	SE010
3.400.2.0	Wet Desert	SE010
3.41.1.0	Dry Improved Grassland	SE09
3.41.1.1	Dry Acid Improved Grassland	SE09
3.41.1.2	Dry Neutral Improved Grassland	SE09
3.41.1.3	Dry Alkali Improved Grassland	SE09
3.41.2.0	Wet Improved Grassland	SE04
3.41.2.1	Wet Acid Improved Grassland	SE04
3.41.2.2	Wet Neutral Improved Grassland	SE04
3.41.2.3	Wet Alkali Improved Grassland	SE04
3.42.1.0	Dry Improved Pasture	E2
3.42.1.1	Dry Acid Improved Pasture	E2
3.42.1.2	Dry Neutral Improved Pasture	E2
3.42.1.3	Dry Alkali Improved Pasture	E2
3.42.2.0	Wet Improved Pasture	SE04
3.42.2.1	Wet Acid Improved Pasture	SE04
3.42.2.2	Wet Neutral Improved Pasture	SE04
3.42.2.3	Wet Alkali Improved Pasture	SE04
3.43.1.0	Dry Improved Short Grassland	SE09
3.43.1.1	Dry Acid Improved Short Grassland	SE09
3.43.1.2	Dry Neutral Improved Short Grassland	SE09
3.43.1.3	Dry Alkali Improved Short Grassland	SE09
3.43.2.0	Wet Improved Short Grassland	SE04
3.43.2.1	Wet Acid Improved Short Grassland	SE04
3.43.2.2	Wet Neutral Improved Short Grassland	SE04
3.43.2.3	Wet Alkali Improved Short Grassland	SE04
3.44.1.1	Dry Acid Improved Short Montane Grassland	E4
3.44.2.0	Wet Improved Short Montane Grassland	E4
3.44.2.1	Wet Acid Improved Short Montane Grassland	E4
3.44.2.2	Wet Neutral Improved Short Montane Grassland	E4
3.44.2.3	Wet Alkali Improved Short Montane Grassland	E4
3.45.2.3	Wet Alkali Improved Tall Grassland	SE011
3.46.1.0	Dry Meadow	E2
3.46.1.1	Dry Acid Meadow	E2
3.46.1.2	Dry Neutral Meadow	E2
3.46.1.3	Dry Alkali Meadow	E2
3.46.2.0	Wet Meadow	SE04
3.46.2.1	Wet Acid Meadow	SE04
3.46.2.2	Wet Neutral Meadow	SE04
3.46.2.3	Wet Alkali Meadow	SE04
3.47.1.0	Dry Pasture	E2
3.47.1.1	Dry Acid Pasture	E2
3.47.1.2	Dry Neutral Pasture	E2
3.47.1.3	Dry Alkali Pasture	E2
3.47.2.0	Wet Pasture	SE04
3.47.2.1	Wet Acid Pasture	SE04
3.47.2.2	Wet Neutral Pasture	SE04
3.47.2.3	Wet Alkali Pasture	SE04
3.50.1.1	Dry Acid Semi-Arid Forest Pasture	EX
3.50.1.3	Dry Alkali Semi-Arid Forest Pasture	EX
3.500.1.0	Dry Alkali Dunes & Tidal Flats	SE012
3.500.2.0	Wet Acid Dunes & Tidal Flats	SE012
3.51.1.0	Dry Semi-Arid Grass	E1
3.51.1.1	Dry Acid Semi-Arid Grass	E1
3.51.1.2	Dry Neutral Semi-Arid Grass	E1
3.51.1.3	Dry Alkali Semi-Arid Grass	E1
3.52.1.0	Dry Semi-Arid Steppe Pasture	E1
3.52.1.1	Dry Acid Semi-Arid Steppe Pasture	E1
3.52.1.2	Dry Neutral Semi-Arid Steppe Pasture	E1
3.52.1.3	Dry Alkali Semi-Arid Steppe Pasture	E1
3.53.1.2	Dry Neutral Semi-Arid Tugai Meadow	E1
3.53.1.3	Dry Alkali Semi-Arid Tugai Meadow	E1
3.54.1.0	Dry Semi-Arid Tundra Pasture	E1
3.54.1.1	Dry Acid Semi-Arid Tundra Pasture	E1
3.54.1.2	Dry Neutral Semi-Arid Tundra Pasture	E1
3.54.1.3	Dry Alkali Semi-Arid Tundra Pasture	E1
3.55.1.0	Dry Short Grass	SE09
3.55.1.1	Dry Acid Short Grass	SE09
3.55.1.2	Dry Neutral Short Grass	SE09
3.55.1.3	Dry Alkali Short Grass	SE09
3.55.2.0	Wet Short Grass	SE04
3.55.2.1	Wet Acid Short Grass	SE04
3.55.2.2	Wet Neutral Short Grass	SE04
3.55.2.3	Wet Alkali Short Grass	SE04
3.56.1.0	Dry Short Grass Meadow	E2
3.56.1.1	Dry Acid Short Grass Meadow	E2
3.56.1.2	Dry Neutral Short Grass Meadow	E2
3.56.1.3	Dry Alkali Short Grass Meadow	E2

SEI code	SEI name	EUNIS code
3.56.2.0	Wet Short Grass Meadow	SE04
3.56.2.1	Wet Acid Short Grass Meadow	SE04
3.56.2.2	Wet Neutral Short Grass Meadow	SE04
3.56.2.3	Wet Alkali Short Grass Meadow	SE04
3.57.1.0	Dry Short Montane Grass	E4
3.57.1.1	Dry Acid Short Montane Grass	E4
3.57.1.2	Dry Neutral Short Montane Grass	E4
3.57.1.3	Dry Alkali Short Montane Grass	E4
3.57.2.0	Wet Short Montane Grass	E4
3.57.2.1	Wet Acid Short Montane Grass	E4
3.57.2.2	Wet Neutral Short Montane Grass	E4
3.57.2.3	Wet Alkali Short Montane Grass	E4
3.60.1.1	Dry Acid Steppe Meadow	SE04
3.600.2.0	Wet Acid Heath	F4
3.61.1.0	Dry Steppe Pasture	E2
3.61.1.1	Dry Acid Steppe Pasture	E2
3.61.1.2	Dry Neutral Steppe Pasture	E2
3.61.1.3	Dry Alkali Steppe Pasture	E2
3.61.2.0	Wet Steppe Pasture	SE04
3.61.2.1	Wet Acid Steppe Pasture	SE04
3.61.2.2	Wet Neutral Steppe Pasture	SE04
3.61.2.3	Wet Alkali Steppe Pasture	SE04
3.62.1.0	Dry Steppe Short Grass Pasture	E2
3.62.1.1	Dry Acid Steppe Short Grass Pasture	E2
3.62.1.2	Dry Neutral Steppe Short Grass Pasture	E2
3.62.1.3	Dry Alkali Steppe Short Grass Pasture	E2
3.62.2.1	Wet Acid Steppe Short Grass Pasture	SE04
3.62.2.2	Wet Neutral Steppe Short Grass Pasture	SE04
3.62.2.3	Wet Alkali Steppe Short Grass Pasture	SE04
3.63.1.1	Dry Acid Steppe Short Montane Grass Pasture	E4
3.63.1.2	Dry Neutral Steppe Short Montane Grass Pasture	E4
3.63.1.3	Dry Alkali Steppe Short Montane Grass Pasture	E4
3.63.2.1	Wet Acid Steppe Short Montane Grass Pasture	E4
3.63.2.2	Wet Neutral Steppe Short Montane Grass Pasture	E4
3.63.2.3	Wet Alkali Steppe Short Montane Grass Pasture	E4
3.64.1.0	Dry Steppe Tall Grass Pasture	E2
3.64.1.2	Dry Neutral Steppe Tall Grass Pasture	E2
3.64.1.3	Dry Alkali Steppe Tall Grass Pasture	E2
3.64.2.1	Wet Acid Steppe Tall Grass Pasture	SE04
3.65.1.0	Dry Tall Grass	SE09
3.65.1.1	Dry Acid Tall Grass	SE09
3.65.1.2	Dry Neutral Tall Grass	SE09
3.65.1.3	Dry Alkali Tall Grass	SE09
3.65.2.0	Wet Tall Grass	SE04
3.65.2.1	Wet Acid Tall Grass	SE04
3.65.2.2	Wet Neutral Tall Grass	SE04
3.65.2.3	Wet Alkali Tall Grass	SE04
3.68.1.2	Dry Neutral Tugai Meadow	SE04
3.68.1.3	Dry Alkali Tugai Meadow	SE04
3.700.1.0	Dry Alkali Heath Tundra	SE013
3.700.2.0	Wet Acid Heath Tundra	SE013
3.71.1.0	Dry Tundra Pasture	E2
3.71.1.1	Dry Acid Tundra Pasture	E2
3.71.1.2	Dry Neutral Tundra Pasture	E2
3.71.1.3	Dry Alkali Tundra Pasture	E2
3.71.2.0	Wet Tundra Pasture	SE04
3.71.2.1	Wet Acid Tundra Pasture	SE04
3.71.2.2	Wet Neutral Tundra Pasture	SE04
3.71.2.3	Wet Alkali Tundra Pasture	SE04
3.72.1.0	Dry Tundra Short Grass Pasture	E2
3.72.1.1	Dry Acid Tundra Short Grass Pasture	E2
3.72.1.2	Dry Neutral Tundra Short Grass Pasture	E2
3.72.1.3	Dry Alkali Tundra Short Grass Pasture	E2
3.72.2.0	Wet Tundra Short Grass Pasture	SE04
3.72.2.1	Wet Acid Tundra Short Grass Pasture	SE04
3.72.2.2	Wet Neutral Tundra Short Grass Pasture	SE04
3.72.2.3	Wet Alkali Tundra Short Grass Pasture	SE04
3.73.1.0	Dry Tundra Short Montane Grass Pasture	E4
3.73.1.1	Dry Acid Tundra Short Montane Grass Pasture	E4
3.73.1.3	Dry Alkali Tundra Short Montane Grass Pasture	E4
3.74.1.0	Dry Tundra Tall Grass Pasture	E2
3.74.1.1	Dry Acid Tundra Tall Grass Pasture	E2
3.74.1.2	Dry Neutral Tundra Tall Grass Pasture	E2
3.74.1.3	Dry Alkali Tundra Tall Grass Pasture	E2
3.74.2.1	Wet Acid Tundra Tall Grass Pasture	SE04
3.74.2.2	Wet Neutral Tundra Tall Grass Pasture	SE04
3.75.2.1	Wet Acid Unimproved Alpine Short Grassland	E4
3.75.2.2	Wet Neutral Unimproved Alpine Short Grassland	E4
3.75.2.3	Wet Alkali Unimproved Alpine Short Grassland	E4
3.76.1.0	Dry Unimproved Desert Grassland	E1
3.76.1.2	Dry Neutral Unimproved Desert Grassland	E1
3.76.1.3	Dry Alkali Unimproved Desert Grassland	E1
3.77.1.0	Dry Unimproved Grassland	SE09
3.77.1.1	Dry Acid Unimproved Grassland	SE09
3.77.1.2	Dry Neutral Unimproved Grassland	SE09
3.77.1.3	Dry Alkali Unimproved Grassland	SE09
3.77.2.0	Wet Unimproved Grassland	SE04
3.77.2.1	Wet Acid Unimproved Grassland	SE04
3.77.2.2	Wet Neutral Unimproved Grassland	SE04
3.77.2.3	Wet Alkali Unimproved Grassland	SE04
3.78.1.0	Dry Unimproved Pasture	E2
3.78.1.1	Dry Acid Unimproved Pasture	E2
3.78.1.2	Dry Neutral Unimproved Pasture	E2
3.78.1.3	Dry Alkali Unimproved Pasture	E2
3.78.2.0	Wet Unimproved Pasture	SE04
3.78.2.1	Wet Acid Unimproved Pasture	SE04
3.78.2.2	Wet Neutral Unimproved Pasture	SE04
3.78.2.3	Wet Alkali Unimproved Pasture	SE04
3.79.1.0	Dry Unimproved Short Grassland	SE09
3.79.1.1	Dry Acid Unimproved Short Grassland	SE09
3.79.1.2	Dry Neutral Unimproved Short Grassland	SE09
3.79.1.3	Dry Alkali Unimproved Short Grassland	SE09
3.79.2.0	Wet Unimproved Short Grassland	SE04
3.79.2.1	Wet Acid Unimproved Short Grassland	SE04
3.79.2.2	Wet Neutral Unimproved Short Grassland	SE04
3.79.2.3	Wet Alkali Unimproved Short Grassland	SE04
3.8.1.0	Dry Alpine Meadow Grass	E4
3.8.1.1	Dry Acid Alpine Meadow Grass	E4
3.8.1.2	Dry Neutral Alpine Meadow Grass	E4

SEI code	SEI name	EUNIS code
3.8.1.3	Dry Alkali Alpine Meadow Grass	E4
3.8.2.0	Wet Alpine Meadow Grass	E4
3.8.2.1	Wet Acid Alpine Meadow Grass	E4
3.8.2.2	Wet Neutral Alpine Meadow Grass	E4
3.8.2.3	Wet Alkali Alpine Meadow Grass	E4
3.80.1.0	Dry Unimproved Short Montane Grassland	E4
3.80.1.1	Dry Acid Unimproved Short Montane Grassland	E4
3.80.1.2	Dry Neutral Unimproved Short Montane Grassland	E4
3.80.1.3	Dry Alkali Unimproved Short Montane Grassland	E4
3.80.2.0	Wet Unimproved Short Montane Grassland	E4
3.80.2.1	Wet Acid Unimproved Short Montane Grassland	E4
3.80.2.2	Wet Neutral Unimproved Short Montane Grassland	E4
3.80.2.3	Wet Alkali Unimproved Short Montane Grassland	E4
3.800.1.0	Dry Acid Marsh	DX
3.800.2.0	Wet Acid Marsh	DX
3.81.1.0	Dry Unimproved Tall Grassland	SE09
3.81.1.1	Dry Acid Unimproved Tall Grassland	SE09
3.81.1.2	Dry Neutral Unimproved Tall Grassland	SE09
3.81.1.3	Dry Alkali Unimproved Tall Grassland	SE09
3.81.2.1	Wet Acid Unimproved Tall Grassland	SE04
3.81.2.3	Wet Alkali Unimproved Tall Grassland	SE04
3.9.1.2	Dry Neutral Alpine Short Grass	E4
3.9.1.3	Dry Alkali Alpine Short Grass	E4
3.9.2.0	Wet Alpine Short Grass	E4
3.9.2.1	Wet Acid Alpine Short Grass	E4
3.9.2.2	Wet Neutral Alpine Short Grass	E4
3.9.2.3	Wet Alkali Alpine Short Grass	E4
3.900.1.0	Dry Acid Mediterranean Scrub	FX
3.900.2.0	Wet Neutral Mediterranean Scrub	FX
4	Urban	J
5.2	Inland Water	C
5.3	Coastal Water	A

Table 3A-4 Combined EUNIS-classes with percentages.

Combined Eunis Code	EUNIS code	Percentage of Area
CE1	H	25
CE1	J	75
CE2	E2	33.33
CE2	I	33.33
CE2	J	33.33
CE3	E	50
CE3	F	50
CE4	H	50
CE5	J	50
PE1	FX	50
PE1	G1	50
SE01	D1	50
SE01	D2	50
SE02	EX	50
SE02	F1	50
SE03	EX	50
SE03	FX	50
SE04	E2	50
SE04	E3	50
SE05	FX	50
SE05	G1	50
SE06	DX	50
SE06	F2	50
SE07	DX	50
SE07	FX	50
SE08	D2	50
SE08	FX	50
SE09	E1	50
SE09	E2	50
SE10	EX	50
SE10	FX	50
SE11	E1	33.33
SE11	E2	33.33
SE11	E3	33.33
SE12	A	50
SE12	B	50
SE13	FX	50
SE13	F1	50

4. The European Background Database

Maximilian Posch, Gert Jan Reinds*

*Alterra, Wageningen University and Research Centre, Netherlands

4.1 Introduction

A main task of the Coordination Center for Effects (CCE) is to collect and collate national data on critical loads and dynamic modelling, and to provide European maps and other databases to the relevant bodies under the LRTAP Convention, especially for the purpose of integrated assessment. Ideally, all those data are based on national data submissions, provided by National Focal Centres (NFCs) upon a call for data. However, if a country does not contribute national data, values from a European background database (EU-DB), which is held and updated by the CCE, can be used for those areas.

The previous version of the European background database has been described in the 2003 CCE Status Report (Posch et al., 2003). Over the last years new databases have become available, and thus the EU-DB has been updated. As before, only forests (forest soils) are considered in the European background database. Individual tree species are not identified, but a distinction is made between coniferous, broad-leaved (deciduous) and mixed forests. In deriving variables for the EU-DB which are not directly available in existing databases, the recommendations and transfer functions in the Mapping Manual (UBA, 2004) are followed as closely as possible.

In the following sections the data sources and procedures used for deriving the variables in the European background database are described. EU-DB contains the same data as were asked from NFCs in the last call for data (see Chapter 2). Some of the variables are displayed in map or graphical format.

4.2 Map Overlays

Input data for critical load calculations and dynamic modelling include parameters describing climatic variables, base cation deposition and weathering, nutrient uptake, N transformations and cation exchange. A combined map with the information to derive the required input data was constructed by combining the following maps/databases:

(a) The harmonised land cover map produced by the CCE and SEI by combining the Corine land cover map with the SEI land cover map (see Chapter 3).

(b) A soil map at scale 1:1,000,000 for all European countries (Eurosoil, 1999); except for Russia, Belarus, Ukraine and Moldova, for which the FAO 1:5,000,000 soil map (FAO, 1981) was used.

(c) Average forest growth derived from a updated data base of the European Forest Institute (EFI), which contains growth data a variety of species and age classes in about 250 regions in Europe (Schelhaas et al., 1999).

(d) A global map of detailed elevation data (on a 30"×30" grid) from NOAA/NGDC (Hastings and Dunbar, 1998).

(e) A map with EMEP grid cells of 50×50 km^2, in which S and N deposition data are provided.

Overlaying these maps and data bases, merging polygons within every EMEP50 grid cell differing only in altitude and discarding units smaller than 1 km^2 results in about 90,000 different forest-soil combinations.

The soil maps are composed of so-called soil associations, each polygon on the map representing one association. Every association, in turn, consists of several soil typological units (soil types) that each covers a known percentage of the soil association. The soil typological units on the maps are classified into more than 200 soil types (Eurosoil, 1999).

For each soil typological unit information is available, of which soil texture and drainage classes are used here to derive other input data. Six texture classes are defined from clay and sand content and listed in Table 5.12 in the

Mapping Manual. The drainage classes, which are used to estimate the denitrification fraction, are derived from the dominant annual soil water regime (Eurosoil, 1999; FAO, 1981).

Table 4-1 shows the distribution of forest over soil types in Europe for the 10 most common forest-soil types derived from the overlay of the soil- and forest map. Most forests are located on Podzols (about 25%), especially in the Nordic countries, and to a lesser extent on Podzoluvisols (about 15%), Cambisols (about 16 %), Luvisols (about 9%) and Lithosols (about 4%). Forest soils occur mainly on coarse (texture class 1) and medium textures (class 2). Forests on the fine textures (classes 3-5) are relatively rare. About 9% of European forests are located on peat soils (histosols).

Table 4-1. Area of the 10 most common forest-soil combinations in Europe.

Soil type	Area (km^2)	% Area
Podzols (P)	698246	25.2
Cambisols (B)	430280	15.6
Podzoluvisols (D)	421249	15.2
Histosols (O)	255690	9.2
Luvisols (L)	248140	9.0
Gleysols (G)	156363	5.7
Lithosols (I)	115961	4.2
Regosols (R)	103512	3.7
Arenosols (Q)	79445	2.9
Rendzinas (E)	69388	2.5

Some inaccuracy in these estimates exists, because the soil map consists of soil associations. The map overlay thus gives a forested area for each association, not for each soil type. Forests have been assigned evenly to all soil types within the association, which in reality will not always be the case.

4.3 Input data for critical loads and dynamic modelling

All calculations were done by assuming a soil depth (rooting zone) of 0.5 m.

Precipitation surplus and soil water content

To compute the concentration and leaching of compounds in the soil, the annual water flux through the soil has to be known. To this end meteorological data are needed. Long-term (1961-1990) average monthly temperature, precipitation and cloudiness were derived from a high resolution European data base (Mitchell et al., 2004) that contains monthly values for the years 1901-2001 for land-based grid-cells of 10'×10' (approximately 15×18 km in central Europe). For sites east of 32° a 0.5°×0.5° global database from the same authors was used.

Actual evapotranspiration was calculated according to a model used in the IMAGE global change model (Leemans and Van den Born, 1994) following the approach by Prentice et al. (1993). Potential evapotranspiration was computed from temperature, sunshine and latitude. Actual evapotranspiration was then computed using a reduction function for potential evapotranspiration based on the available water content in the soil, described by Federer (1982). Soil water content is in turn estimated using a simple bucket-like model that uses water holding capacity (derived from the available soil texture data) and precipitation data. A complete description of the model can be found in Annex 4 of Reinds et al. (2001).

These computations also yield the annual average soil water content θ.

The available water content (AWC) was estimated as a function of soil type and texture class according to Batjes (1996) who provides texture class dependent AWC values for FAO soil types based on an extensive literature review.

Base cation and chloride deposition

The total depositions of Ca, Mg, K and Na onto forests have recently been modelled by EMEP/MSC-W on the EMEP50 grid (Van Loon et al., 2005). Chloride deposition was assumed equal to the Na deposition.

Base cation weathering

Weathering of base cations, BC_w, was computed as a function of parent material class and texture class and corrected for temperature, as described in the Mapping Manual (UBA, 2004).

Weathering rates of Ca, Mg, K and Na as fractions of BC_w were estimated as a function of clay and silt content (in %) for texture classes 2 to 5 (Van der Salm, 1999) and as fixed fractions of total weathering for texture class 1 (De Vries, 1994).

Nutrient uptake

Net uptake of base cations and nitrogen was computed by multiplying the estimated annual average growth of stems and branches with the element contents of base cations and N in these compartments. Wood densities of 450 kg/m^3 and 650 kg/m^3 as well as branch-to-stem ratios of 0.15 and 0.20 for coniferous and deciduous trees, respectively, have been used. For mixed forests the average of these values were applied.

Forest growth was derived from the EFI database mentioned above (Schelhaas et al., 1999). Growth was assessed by taking from the database the average growth over all age classes for the combination of region and tree species group.

Contents of N, Ca, Mg and K in stems and branches of coniferous and deciduous forests are derived from Table 5.8 in the Mapping Manual UBA (2004), which is based on data from a literature study by Jacobsen et al. (2002). The average values of spruce and pine were assigned to conifers and the average of oak and beech to deciduous forests. Again, an average of these was used for mixed forests.

Denitrification and N immobilisation

The denitrification fraction, f_{de}, was computed as a function of drainage status, which is known for each soil type and is given in Table 5.9 of the Mapping Manual (UBA, 2004).

N immobilisation consists of a constant (time-independent) part, which is the same as used in critical load calculations (1 kg N ha^{-1}a^{-1}) and a time-dependent part, which is computed as a function of the prevailing C:N ratio of the top soil. This C:N ratio is estimated from a transfer function by Klap et al. (2002) which can also be found in the Mapping Manual (UBA, 2004). This transfer function computes the C:N ratio as a function of soil texture, forest type, climate variables and the N deposition of the relevant year (1995). The speed of change of the C:N ratio depends on the size of the C pool in the topsoil. This C pool for the top 20 cm is estimated from the organic carbon content (available for every soil type) and bulk density.

The bulk density ρ of the soil was computed from a transfer function using clay and organic carbon content, derived from data by Hoekstra and Poelman (1982) and Van Wallenburg (1988; see also UBA, 2004). Clay content is an attribute to the soil map, carbon content for each soil type was derived from a European database on forest soils (Vanmechelen et al., 1997).

Al-H relationship and organic acids

The Al concentration is computed from a gibbsite equilibrium (i.e. α=3) and the equilibrium constant is estimated from simultaneous measurements of [Al] and pH at about 150 forest monitoring plots as a function of soil texture class (De Vries et al., 2003).

Dissociation of organic acids was modelled by assuming them as mono-protic with a dissociation constant of pK=4.5 (see eqa.5.46 in UBA, 2004). The DOC concentration was estimated from a linear regression with soil pH and texture using data from European Intensive Forest Monitoring plots. A charge density m=0.023 mol/molC was used throughout.

Cation exchange capacity and base saturation

Cation exchange capacity (CEC) was computed as a function of clay content, organic carbon content and soil pH according to a transfer function by Helling et al. (1964; see also UBA, 2004).

Base saturation for the reference year (1995) was estimated from a transfer function derived by Klap et al. (2002; see also UBA, 2004). This transfer function computes the base saturation as a function of soil texture, forest type

as well as the S, N and base cation deposition. The base saturation values were used to calibrate the exchange constants of the H-Al-Bc exchange.

4.4 Results

The EU-DB obtained from the data(bases) and transfer functions described above can be used to compute critical loads of S and N acidity and nutrient N. Critical loads have been computed with the Simple Mass Balance (SMB) model, using a critical Al:Bc ratio of 1 mol mol^{-1} for all forests and soils, except for peat soils (Histosols), for which a critical molar Bc:H ratio is used (1 for conifers, 1/3 for deciduous forests and an average value of 2/3 for mixed forests). Several of the input variables as well as critical loads are displayed as cumulative distribution functions in Chapter 2, where they are compared to data from countries which have submitted national data in response to the recent call.

In Figure 4-1 the 5th percentiles of the maximum critical load of S acidity, $CL_{max}(S)$, and the critical load for nutrient N, $CL_{nut}(N)$, are displayed on the EMEP50 grid. The maps clearly show that in most grid cells (the 5th percentile of) the critical load for nutrient N is smaller than that of $CL_{max}(S)$.

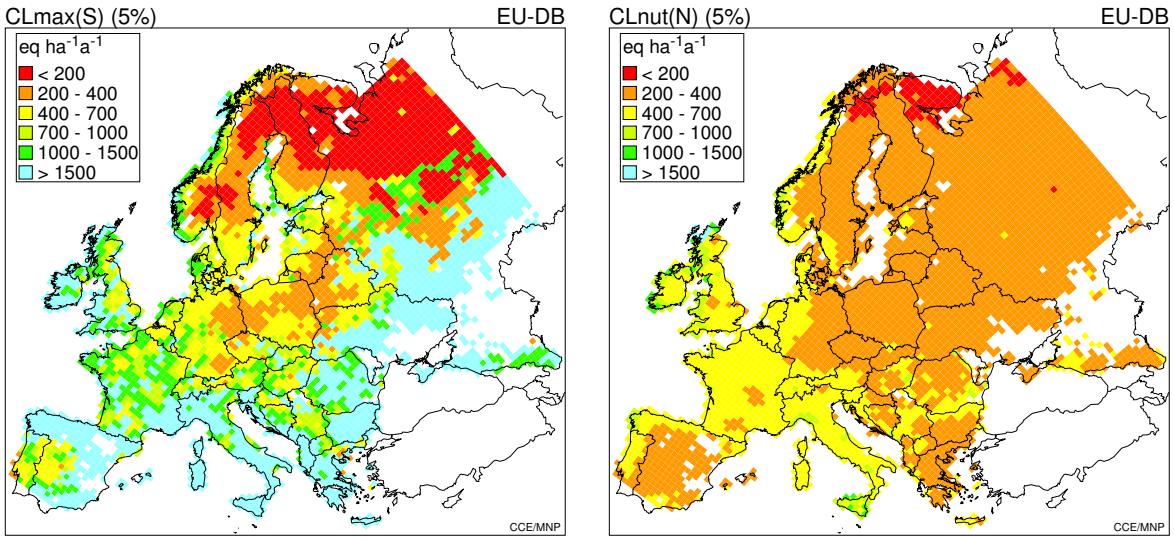


Figure 4-1. The 5th percentile of $CL_{max}(S)$ and $CL_{nut}(N)$ on the EMEP50 grid, computed from the European background database.

The exceedance of the acidity and nutrient N critical loads for the year 2010 is shown in Figure 4-2. In this scenario the implementation of the current legislation (the Gothenburg Protocol and the EU NEC Directive) is assumed. The forest-specific deposition has been provided by the EMEP/MSC-W (Tarrasón et al., 2004). As can be seen, acidification is a substantial problem only in some parts of central Europe, whereas eutrophication is a much more wide-spread and severe problem. These maps should be compared with the exceedance maps in Chapter 1.

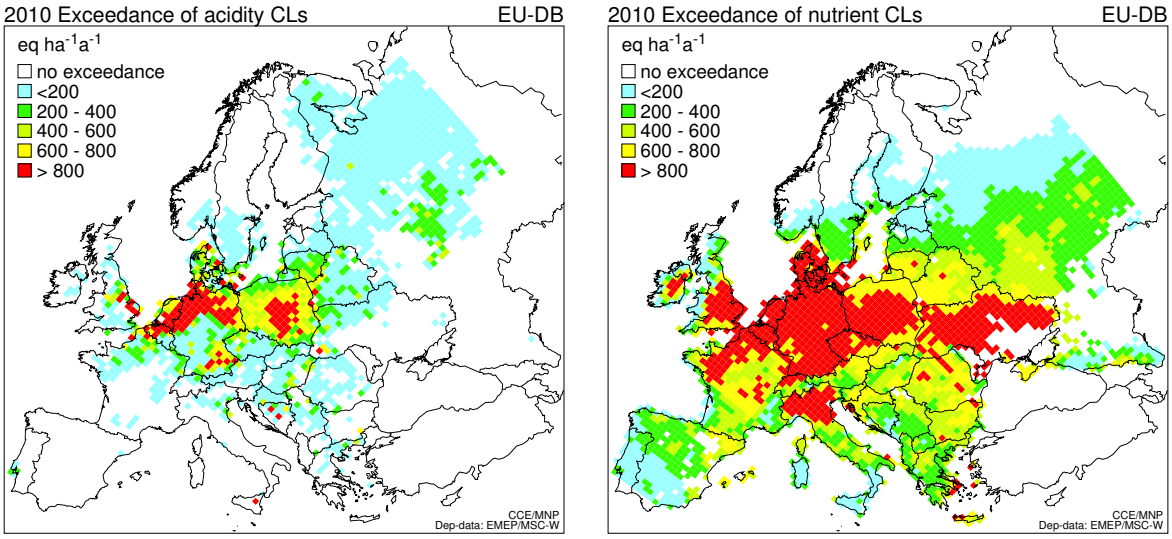


Figure 4-2. The average accumulated exceedance (AAE) of the acidity critical loads (left) and the critical loads of nutrient nitrogen (right), using the deposition to forests in 2010, assuming the implementation of current legislation (Gothenburg Protocol and EU NEC Directive).

Not only critical loads can be calculated with the European background database, also simulations with the dynamic soil acidification model VSD (Posch and Reinds, 2005), which has used by many European countries (see Part II), have been carried out. Figure 4-3 shows the temporal development of two major soil variables, pH and base saturation between 1990 and 2100 after running the VSD model on each of the circa 90,000 forest sites with S and N deposition constant after 2010 at 'Gothenburg level' (as used in Figure 4-2). The figure shows the temporal development of some percentiles ('percentile traces') of the distribution of those variables over the 110 years of simulation. As can be seen, the temporal development is rather unspectacular, which is not surprising for the pH, since for a constant deposition the soil solution concentrations will soon be in equilibrium with the deposited ions. Rather more surprising are the very minor changes occurring in the European distribution of base saturation, which is a slowly reacting soil variable. However, small changes in the distribution do not necessarily mean small changes at individual sites, decreases in some regions could be compensated by increases in others.

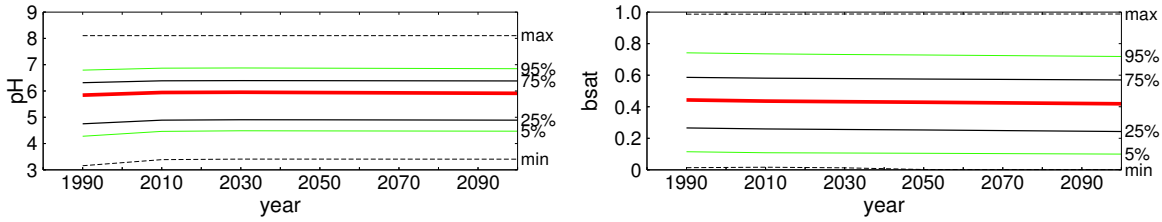


Figure 4-3. Temporal development (1990-2100) of some percentiles of pH (left) and base saturation (right) of the about 90,000 forest sites of the European background DB, when the VSD model is run with the 'Gothenburg deposition' after 2010.

Not only the variables themselves and their distributions are of interest, but also the relationship between them. Two key variables in any dynamic acidification model are the pH of the soil solution and the base saturation of the cation exchange complex. In Figure 4-4 the correlation between these two variables is shown for the year 2100, i.e. the last year of the simulation shown in Figure 4-3. The about 90,000 data points are shown in three colours, depending on the magnitude of the Gapon exchange constant for the Al-Bc exchange, K_{AlBc}. Since this is generally unknown, it is calibrated so that at every site a prescribed base saturation is obtained in 1995. The red dots in Figure 4-4 show sites for which $\log_{10}K_{AlBc}<0$, the blue dots sites for which $\log_{10}K_{AlBc}>2$, and the green ones with values between those two limits. Especially for sites with values of K_{AlBc} in the range between 0 and 2, the relationship between pH and base saturation shows an S-shaped pattern which has also been observed and/or modelled by Reuss (1983), Bloom and Grigal (1985) and De Vries et al. (1989).

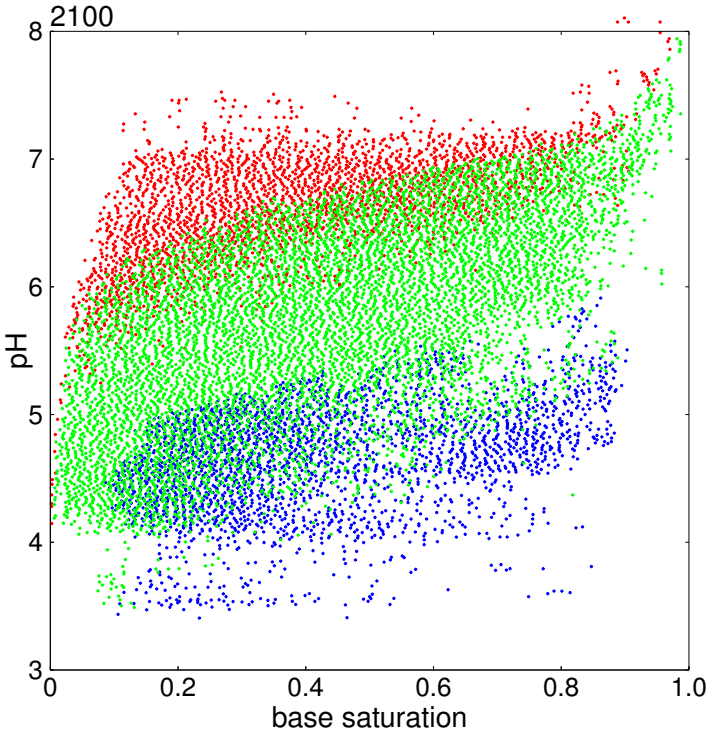


Figure 4-4. Correlation between base saturation and soil solution pH in 2100 for about 90,000 sites of the EU-DB. Red: sites with $log_{10}K_{AlBc}<0$, green: $0 \leq log_{10}K_{AlBc} \leq 2$, blue: $log_{10}K_{AlBc}>2$, where K_{AlBc} is the Al-Bc Gapon exchange constant.

In Figure 4-5 shows the correlation between two more pairs of variables at the end of the simulation of the about 90,000 European sites in 2100. The left panel illustrates, as expected, that high [Al]:[Bc] ratios are more likely to occur in soils with low base saturation; and the right panel confirms that the leaching of N is generally higher in soils with a low C:N ratio, i.e. soils which approach N saturation.

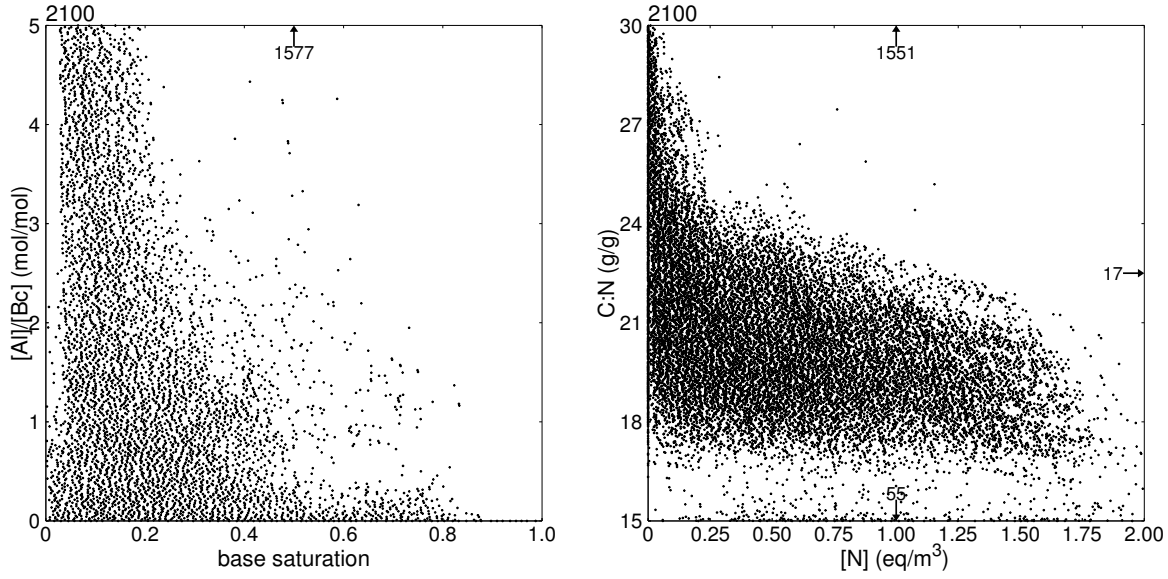


Figure 4-5. Correlation between base saturation and molar Al:Bc ratio (left) and between total N concentration in soil solution and the C:N ratio in the top soil layer (right) in 2100 for about 90,000 sites of the EU-DB.

The European background database has not only been used to compute critical loads and simulate the time development of the soils, but also to compute target loads and delay times. For acidification target loads are characterised not by a single number but by a function – very much like acidity critical loads. In Figure 4-6 the 5th percentile of the $TL_{max}(S)$ – the quantity of a target load function corresponding to $CL_{max}(S)$ in the critical load function – is displayed for the target years 2030 and 2050. By definition, a target load cannot be greater than a critical load, and for ecosystems for which no target load has to be calculated (e.g. an ecosystem which never experienced exceedance) the critical load function is, by definition, used a target load function. Thus the number of ecosystems in every grid cell is the same for critical load and target load statistics. The black-shaded grid cells in Figure 4-6 indicate cells in which for at least 5% of the ecosystem area no target loads can be calculated, i.e. even a reduction of the acidifying deposition to zero does not lead to a recovery of the ecosystem in the target year. Figure 4-6 should be compared to Figure 4-1 (left) to get an impression of the stringency of the target load as compared to the critical load.

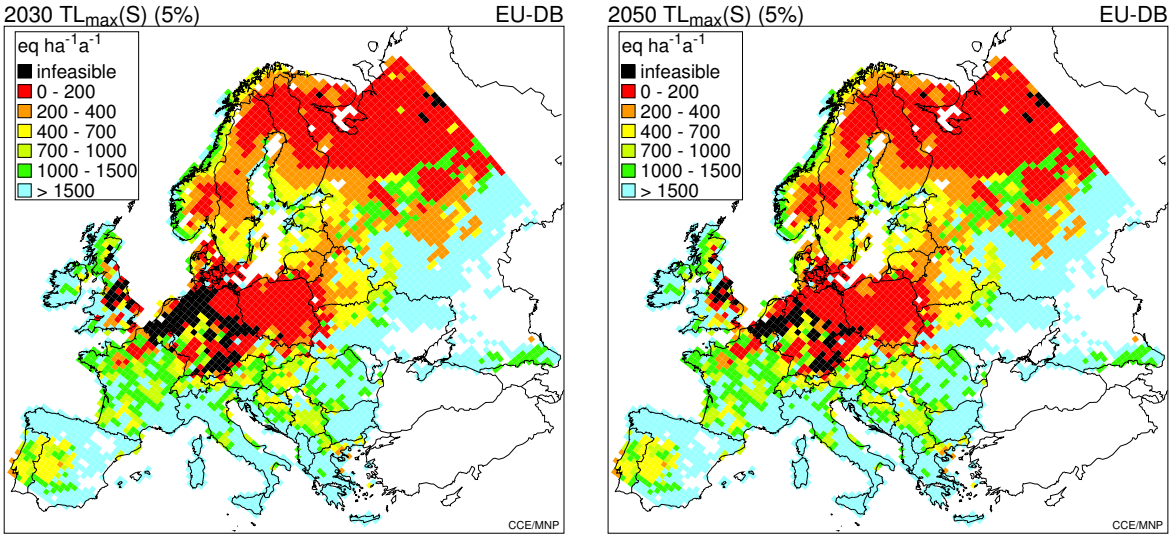


Figure 4-6. The 5th percentile of target loads $TL_{max}(S)$ for the years 2030 (left) and 2050 (right) on the EMEP50 grid, computed from the European background database.

4.5 Concluding remarks

The European background database (EU-DB) has been updated for use by the CCE to fill in gaps left by countries which do not deliver data as well as for possible studies on a European scale. The EU-DB includes the latest available data on a European scale for the calculation of critical loads and for running simple dynamic models. The database, however, is not a final product; it will be checked and updated, whenever inconsistencies in the existing data are found or new data become available.

References

Batjes NH (1996) Development of a world data set of soil water retention properties using pedotransfer rules. Geoderma 71: 31-52

Bloom PR, Grigal DF (1985) Modeling soil response to acidic deposition in nonsulfate adsorbing soils. Journal of Environmental Quality 14(4): 489-495

De Vries W, Posch M, Kämäri J (1989) Simulation of the long-term soil response to acid deposition in various buffer ranges. Water, Air and Soil Pollution 48: 349-390

De Vries W (1994) Soil response to acid deposition at different regional scales. Doctoral dissertation, Agricultural University Wageningen, Wageningen, Netherlands, 487 pp.

De Vries W, Reinds GJ, Posch M, Sanz MJ, Krause GHM, Calatayud V, Renaud JP, Dupouey JL, Sterba H, Vel EM, Dobbertin M, Gundersen P, Voogd JCH (2003) Intensive Monitoring of Forest Ecosystems in Europe. Technical Report 2003, EC-UNECE, Brussels and Geneva, 161 pp.

Eurosoil (1999) Metadata: Soil Geographical Data Base of Europe v. 3.2.8.0. Eurosoil, Ispra, Italy

FAO (1981) FAO-Unesco Soil Map of the World, 1:5.000.000; Volume V (Europe), Unesco, Paris, 199 pp.

Federer CA (1982) Transpirational supply and demand: Plant, soil, and atmospheric effects evaluated by simulation. Water Resour. Res. 18(2): 355-362

Hastings DA, Dunbar PK (1998) Development & assessment of the Global Land One-km Base Elevation Digital Elevation Model (GLOBE). ISPRS Archives 32(4): 218-221

Helling CS, Chesters G, Corey RB (1964) Contribution of organic matter and clay to soil cation exchange capacity as affected by the pH of the saturating solution. Soil Sci. Soc. Am. J. 28: 517-520

Hoekstra C, Poelman JNB (1982) Density of soils measured at the most common soil types in the Netherlands (in Dutch). Report 1582, Soil Survey Institute, Wageningen, Netherlands, 47 pp

Jacobsen C, Rademacher P, Meesenburg H, Meiwes KJ (2002) Element contents in tree compartments – Literature study and data collection (in German). Report, Niedersächsische Forstliche Versuchsanstalt, Göttingen, Germany, 80 pp

Klap JM, Brus DJ, De Vries W, Reinds GJ (2002) Assessment of site-specific estimates of critical deposition levels for nitrogen and acidity in European forest ecosystems using measured and interpolated soil chemistry. (in prep)

Leemans R, Van den Born GJ (1994) Determining the potential distribution of vegetation, crops and agricultural productivity. Water Air Soil Pollut. 76: 133-161

Mitchell TD, Carter TR, Jones PD, Hulme M, New M (2004) A comprehensive set of high-resolution grids of monthly climate for Europe and the globe: the observed record (1901-2000) and 16 scenarios (2001-2100). Tyndall Centre Working Paper 55, Norwich, United Kingdom, 30 pp.www.cru.uea.ac.uk/cru/data/hrg.htm

Posch M, Hettelingh J-P, Slootweg J, Downing RJ (eds) (2003) Modelling and mapping of critical thresholds in Europe. Status Report 2003, Coordination Center for Effects, RIVM Report 259101013, Bilthoven, Netherlands, iv+132 pp www.mnp.nl/cce

Posch M, Reinds GJ (2005) VSD - User Manual of the Very Simple Dynamic soil acidification model. Coordination Center for Effects, MNP, Bilthoven, Netherlands (in prep.)

Prentice IC, Sykes MT, Cramer W (1993) A simulation model for the transient effects of climate change on forest landscapes. Ecol. Model. 65: 51-70

Reinds GJ, Posch M, De Vries W (2001) A semi-empirical dynamic soil acidification model for use in spatially explicit integrated assessment models for Europe. Alterra Report 084, Alterra Green World Research, Wageningen, Netherlands, 55 pp

Reuss JO (1983) Implications of the calcium-aluminum exchange system for the effect of acid precipitation on soils. Journal of Environmental Quality 12(4): 591-595

Schelhaas MJ, Varis S, Schuck A, Nabuurs GJ (1999) EFISCEN's European Forest Resource Database, European Forest Institute, Joensuu, Finland, www.efi.fi/projects/eefr/

Tarrasón L et al. (2004) Transboundary acidification, eutrophication and ground level ozone in Europe. EMEP Status Report 1/2004, Norwegian Meteorological Institute, Oslo. www.emep.int

UBA (2004) Manual on methodologies and criteria for modelling and mapping critical loads & levels and air pollution effects, risks and trends. Umweltbundesamt Texte 52/04, Berlin. www.icpmapping.org

Van der Salm C (1999) Weathering in forest soils. Doctoral dissertation, University of Amsterdam, Amsterdam, 288 pp

Vanmechelen L, Groenemans R, Van Ranst E (1997) Forest soil condition in Europe. Results of a large-scale soil survey. EC/UNECE, Brussels, Geneva, 261 pp

Van Loon M, Tarrasón L, Posch M (2005) Modelling base cations in Europe. EMEP/MSC-W & CCE Note 2/05, Norwegian Meteorological Institute, Oslo, 58 pp

Van Wallenburg C (1988) The density of peaty soils (in Dutch). Internal Report, Soil Survey Institute, Wageningen, Netherlands, 5 pp

5. Use of Critical Loads in Integrated Assessment Modelling

Maximilian Posch, Jean-Paul Hettelingh, Chris Heyes*

*Centre for Integrated Assessment Modelling (CIAM) at IIASA, Laxenburg, Austria

5.1 Introduction

Critical loads and their exceedances have been used in integrated assessment (IA) modelling since the negotiations leading to the Second Sulphur Protocol (Oslo, 1994). To be useable in IA models such as RAINS, the critical load information on the (currently) about 1.2 million ecosystems covering Europe has to be condensed and adapted. Since the deposition of sulphur and nitrogen species is computed on the EMEP grid, critical load information has been provided by the CCE in the form of protection and exceedance percentiles and isolines for this grid system. The methods for deriving such isolines are summarised in Chapter 8 of the Mapping Manual (UBA, 2004).

The change from the 150×150 to the 50×50 EMEP grid increased the number of grid cells by almost an order of magnitude. The distinction between different ecosystem classes (such as forests, semi-natural vegetation and surface waters) further enlarged the amount of data to be derived for IA modelling. This increase in the amount of data poses some problems for including critical loads in optimisation exercises carried out in IA modelling. Since it is not individual grids but countries that matter – after all, the grid system and size are to some extent arbitrary – , and since other pollutants (e.g. particulate matter) had to be included into the optimisation framework, the methodology for computing changes in exceedances due to changes in emissions has been simplified. The new approach has been inspired by the Life Cycle Impact Analysis (LCIA) community, which uses the simplest approach possible, i.e. a linear relationship between emission (change) and impact (change). We adopt this approach for including critical load and exceedance information into IA modelling, and in the following sections we define and derive the respective models and factors.

5.2 Methodology

In the IA modelling the average accumulated exceedance (AAE) has been used as the measure to compare emission reductions to critical load exceedances. The definitions and methods for calculating the AAE for acidity and nutrient N critical loads can be found in Chapter 7 of the Mapping Manual (UBA, 2004). And the simplest assumption (model) is that the change in the AAE for a receptor area (country) k is linearly related to the changes in all emissions of all pollutants involved, i.e.:

$$(1) \qquad AAE_{0,k} - AAE_k = f \cdot \sum_{p=1}^{P} \sum_{j=1}^{N_p} a_{p.k.j} \cdot \left(E_{0,p,j} - E_{p,j}\right), \quad k = 1,...K$$

where AAE_k is the AAE in receptor k for the new (or to be determined) emissions $E_{p,j}$ of pollutant p in emitter area j; $AAE_{0,k}$ is the AAE for the reference emissions $E_{0,p,j}$; N_p is the number of emitter regions for pollutant p, P is the number of pollutants, f is a unit conversion factor, and K is the number of receptor areas. Finally, $a_{p,k,j}$ are the coefficients determining the linear model, characterising the 'strength' of the relationship between emissions of pollutant p in country j and AAE in region k. We call the coefficients $a_{p,k,j}$ (region-to-country) *impact factors* (of pollutant p).

Eq.1 holds for the AAE of both nutrient N (eutrophication) critical loads and critical loads of acidity. In the first case the number of pollutants is P=2, namely NO_x and NH_3, whereas in the latter P=3, where the third pollutant is SO_2. Note that despite the fact that only total N deposition is needed in the calculation of exceedances, NO_x and ammonia emissions have to be considered separately, since they contribute in different ways to total N deposition (different sources and different behaviour in the atmosphere).

In mathematical terms, eq.1 is nothing but the linear term in the Taylor expansion of AAE_k, as a function of the emissions, around a given point ($\boldsymbol{E}_0$, $AAE_{0,k}$) with $\boldsymbol{E}_0=(E_{0,1,1}, \ldots, E_{0,P,Np})$. Thus the expression is, by definition, exact for $\boldsymbol{E}=\boldsymbol{E}_0$, and the smaller the deviations in the emissions from $\boldsymbol{E}_0$ the better the approximation will be. The task is (a) to select proper reference points ($\boldsymbol{E}_0$, $AAE_{0,k}$), (b) to derive the set of impact factors $a_{p,k,j}$, and (c) to determine the range of applicability of the model, i.e. estimate the error made in comparison to exceedance calculations with the exact model.

Before carrying out these steps, the relationship to the factors used in LCIA shall be shortly discussed: In LCIA one is interested in the overall (ideally: global) impact of the change in one unit of emission. Here this would be the change in AAE in the whole of Europe which is obtained by summing over all K countries:

$$AAE = \sum_{k=1}^{K} AAE_k \qquad (2)$$

and AAE_0 is defined analogously. Summing over k in eq.1 yields then:

$$AAE_0 - AAE = f \cdot \sum_{p=1}^{P} \sum_{j=1}^{N_p} c_{p.j} \cdot \left(E_{0,p,j} - E_{p,j}\right) \qquad (3)$$

where we have defined the coefficients:

$$c_{p,j} = \sum_{k=1}^{K} a_{p,k,j} \qquad (4)$$

and it is these coefficients the LCIA community is interested in. These coefficients are variably called (site-dependent) ‘characterisation’, ‘damage’ or ‘impact’ factors. A recent example, using the accumulated exceedance (AE) as ‘impact category indicator’, can be found in Seppälä et al. (2005). Keeping in mind the definition of a critical load, the most obvious indicator would be ecosystem area protected, and it has been studied as well (e.g., Krewitt et al., 2001; Hettelingh et al., 2005). However, it turns out that the linearity assumption is not always fulfilled in this case, and caution should be exercised when using a linear model for ‘protected ecosystem area’ as impact category indicator.

5.3 Results

The choice of reference emissions $\boldsymbol{E}_0$ for the linear model is limited: It has to be emissions for which the (ecosystem-specific) deposition fields have been computed with the full atmospheric transport model, the Unified Model of EMEP/MSC-W in this case (see Tarrasón et al., 2004), thus allowing AAE_0 to be computed exactly. And the emissions should not be too far away from the expected (new) emissions, for which the model is used, in order to increase the probability that the linear model is a good approximation of ‘reality’. Therefore we used the country emissions for the year 2010 from the so-called baseline scenario ‘current legislation’ (‘BL_CLE’), which has been prepared for the EU’s Clean Air for Europe (CAFE) programme (Amann et al., 2005). The impact factors $a_{p,k,j}$ are then computed by changing the emission of pollutant p in source region j, leaving the emissions of the other pollutants and all other source regions unchanged. With this special emission vector the corresponding exceedances AAE_k are computed. Then this special case is inserted into eq.1, leaving only a single term on the right-hand side, from which the impact factors for every receptor country k can be obtained as:

$$a_{p,k,j} = \frac{AAE_{0,k} - AAE_k}{E_{0,p,j} - E_{p,j}}, \quad k = 1,\ldots,K \qquad (5)$$

For every such emission change the corresponding AAE_k’s have to be computed, and this means running the exact atmospheric transport model, or having an approximate version available, such as the source-receptor matrices in case of the old EMEP lagrangian model. Due to the inherent non-linearities in the Unified Model, no such general source-receptor matrices exist. But the Unified Model has been run for a 15% emission reduction for each pollutant in each of the 51 source regions. And thanks to this database the impact coefficients can be computed without approximations. It should be noted, that the (weak) cross-correlations, e.g., the change in ammonium

deposition due to changes in sulphur emissions have been neglected here (although there is no principal problem to include them).

Since there are critical loads data for 36 receptor countries, the calculations result in (51+46+51)×36= 5328 impact coefficients for acidification and (51+46)×36=3492 coefficients for nutrient N. Tabulating these almost 9,000 values with sufficient precision, would result in quite unwieldy tables, making a comparison and interpretation almost impossible. However, this is facilitated with the aid of the graphical representations shown in Figures 5-1 and 5-2. Every cell in the matrices represents an impact coefficient for the respective source-receptor combination for the chosen pollutant and effect. The colour represents the size class (see legend in Figure 5-2) with darker/redder colours indicating higher values. The cells are identified by the ISO 3166 2-letter country codes (ISO, 2005); the 3-letter codes ASI and NOA are for the remaining Asian and African areas within the EMEP modelling domain, respectively; and 5 sea areas: ATL=Atlantic, BAS=Baltic Sea, BLS=Black Sea, MED=Mediterranean, NOS=North Sea. The coefficients are in meq $ha^{-1}kt^{-1}$, i.e. if emissions are given in kt a^{-1} of NO_2, NH_3 or SO_2, respectively, one has to set $f=10^{-3}$ in eq.1 to obtain the AAE in the customary units of eq $ha^{-1}a^{-}1$.

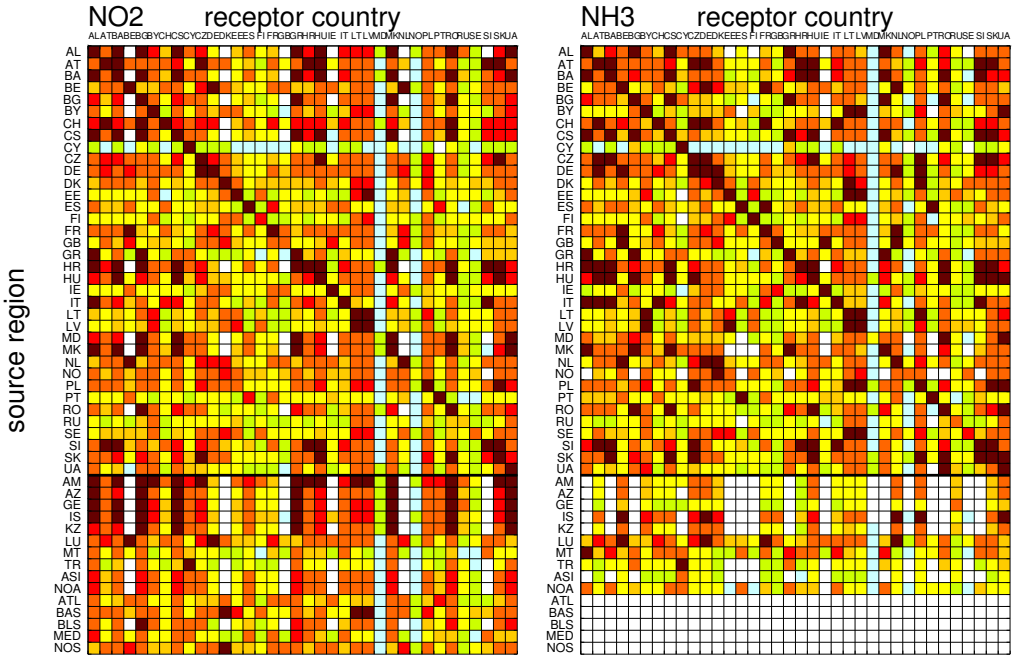


*Figure 5-1. Graphical representation of the impact factors for **eutrophication** for the emissions of NO_2 and NH_3. The upper square represents the source-receptor relationship for the alphabetically ordered 36 countries for which critical loads data are available (see Figure 5-2 for the legend and the text for the codes).*

The generally more reddish colour of the eutrophication panels (Figure 5-1) compared with the acidification panels (Figure 5-2) clearly indicates that exceedances of nutrient N are higher and more widespread than exceedances of acidity critical loads, which is confirmed by the maps in Chapter 1. A white column indicates that critical loads are not (any more) exceeded in that country in the reference year (here: 2010). The upper square delimited by the thick horizontal line in Figures 5-1 and 5-2 represents the AAE source-receptor relationship for the 36 countries for which critical loads data are available. Since these countries are sorted alphabetically both vertically and horizontally, the diagonal-dominance – i.e. the darker colours in the diagonal from upper left to lower right – shows that generally most of the contribution to its exceedance comes from the countries themselves. But also other sources can have a large contribution to a country's exceedance: e.g. the SO_2 emissions from international shipping in the North Sea to the exceedance of acidity critical loads in the Netherlands.

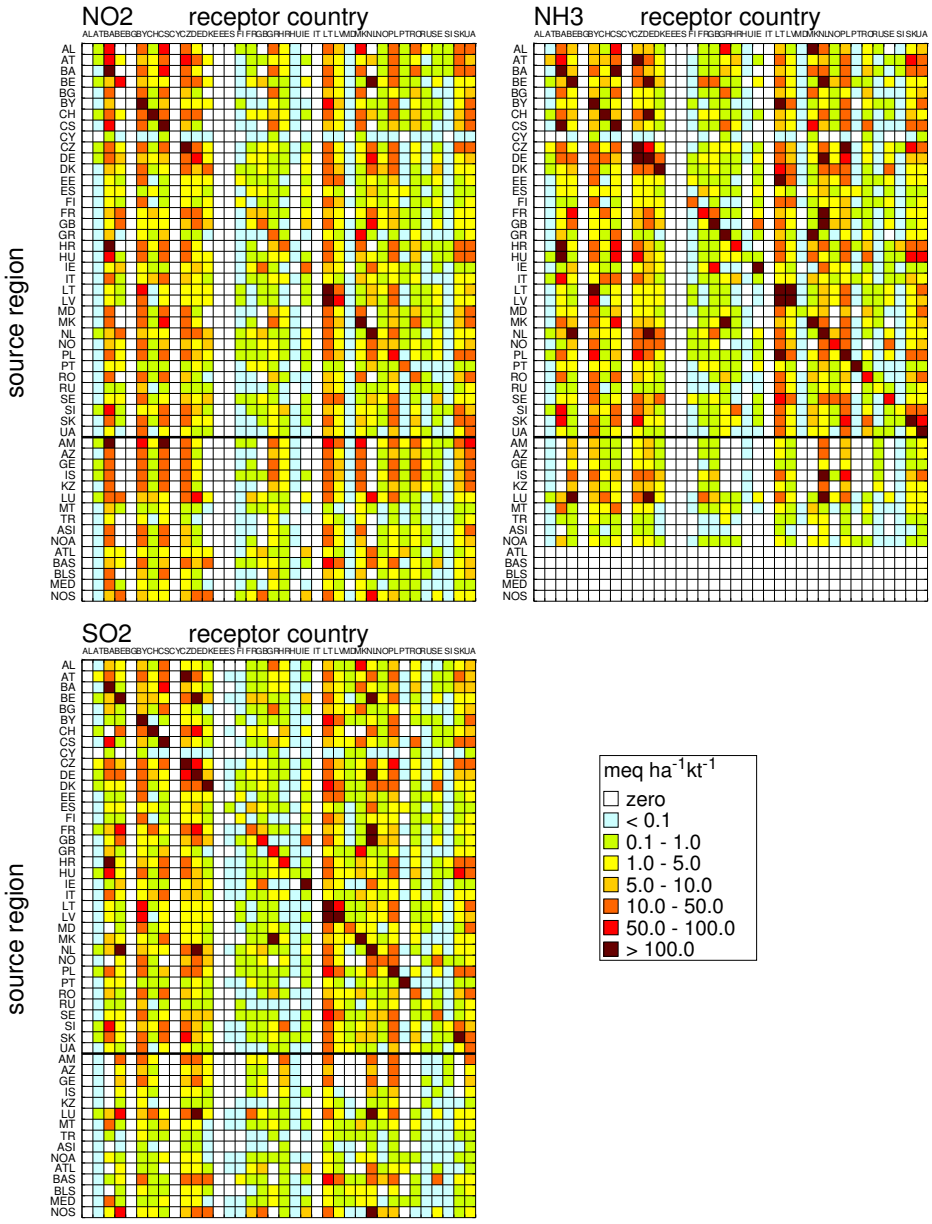


*Figure 5-2. Graphical representation of the impact factors for **acidification** for the emissions of NO_2, NH_3 and SO_2. The upper square represents the source-receptor relationship for the alphabetically ordered 36 countries for which critical loads data are available (see the text for the codes).*

5.4 How good are the linear approximations?

The use of the linear model derived above, e.g. in the optimisation mode of the RAINS model, inevitably raises the question of how much it deviates from exact calculations (within the foreseeable range of application). First we investigate how much the exceedance in a country differs from linearity as a function of the emission changes in a single source region. This is done by computing the AAE with the full model and check 'how linear' the results are. This is illustrated in Figure 5-3; for two countries it shows the AAE as a function of the reduction in a single pollutant (NO_2 and NH_3 in the case of eutrophication, SO_2 in addition for acidification) in one source region. It can be seen that for emission reductions up to 50% the relationship is quite linear. In fact, in all cases displayed each correlation coefficient for the ten sets of 51 data points is above –0.999.

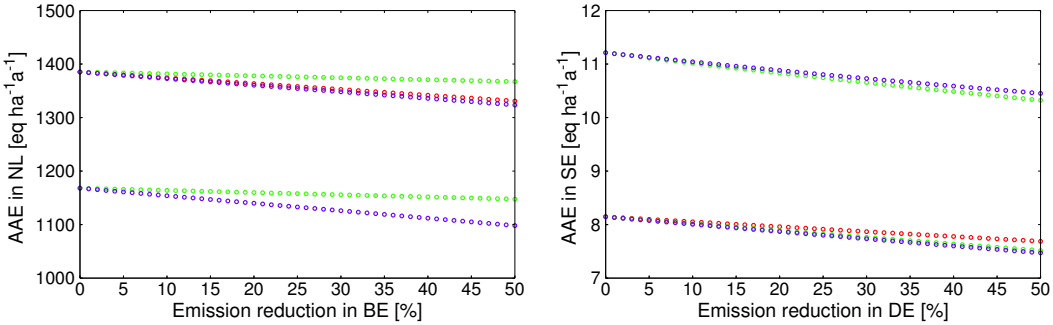


Figure 5-3. Acidification and eutrophication AAE in the Netherlands (left) and Sweden (right) as a function of emission changes in Belgium and Germany, resp. Calculations are shown in steps of 1% reduction of SO_2 (red circles), NO_2 (green) and NH_3 (blue). The data points strongly suggest in all cases a linear relationship over the whole range shown.

Changing the emissions in a single source region (as shown in Figure 5-3) is, in general, a small overall change and thus linearity might be expected for these so-called marginal changes. A sterner test of the linearity assumption is to change the emissions in *all* source regions simultaneously. Figure 5-4 shows the AAE for acidification and eutrophication in the United Kingdom and Europe as function of simultaneous percent emission reductions in all source regions. Also shown are the straight lines resulting from the linear model derived in this chapter. The graphs indicate that for reductions up to at least 20% the linear model provides a very good approximation. It is also clear from general considerations – and the graphs support this – that the linear model fails if one gets closer to zero exceedance: While the exact calculations will never yield a negative AAE, the linear model intersects at some point with the x-axis, and thus for all reduction beyond that point would yield a negative AAE. To avoid negative values, the left-hand side of eq.1 has to be set to zero if AAE_k becomes greater than $AAE_{0,k}$.

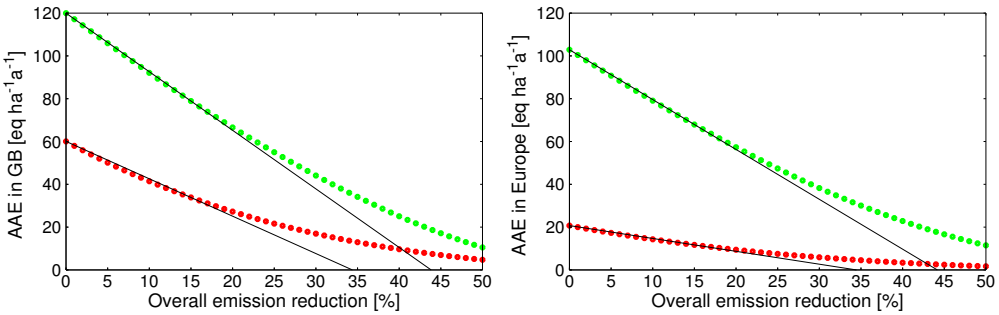


Figure 5-4. AAE in the United Kingdom (left) and Europe (right) for acidification (red) and eutrophication (green) as a function of equal percent emission reductions in all source regions and for all pollutants. The black straight lines show the linear model derived above.

5.5 Future work

The linear model to compute the AAE in European countries for emission reduction scenarios turns out to be a very good approximation as long as the reductions stay below 20%, and are still acceptable in many cases for higher reduction percentages. However, to gain more confidence, and possibly improve the model, the following points should be considered:

- To make optimal use of the model, the reference case ($\boldsymbol{E}_0$, AAE_0) should be taken as close as possible to investigated scenarios, thus minimising the error made due to the linearization. E.g., one could take

emissions which are, say, 20% below the 2010 emissions as reference case. Any expected change from 2010 emissions would then probably be close to this reference case.

- The investigation of the error made by the linearization should be made more systematic, i.e. all source-receptor relationship should be investigated.
- The inclusion of cross-correlations between the pollutants, i.e. the influence of a reduction in X on the deposition of Y, should be considered.
- To better capture the approach to zero AAE, one could investigate some simple non-linear (e.g. second-order) model. However, any such increase in complexity has to be carefully balanced with its impact on the optimisation routines used in integrated assessment.

It should be kept in mind that the linear model for calculating exceedances will always result in approximations. Thus it is strongly recommended to check any final result by an *ex-post* calculation using the exact procedures.

References

Amann M, Bertok I, Cabala R, Cofala J, Heyes C, Gyarfas F, Klimont Z, Schöpp W, Wagner F (2005) A final set of scenarios for the Clean Air For Europe (CAFE) Programme. Final Report to the European Commission, International Institute for Applied Systems Analysis, Laxenburg, Austria, 103 pp. www.iiasa.ac.at/rains

Hettelingh J-P, Posch M, Potting J (2005) Country-dependent characterisation factors for acidification in Europe – A critical evaluation. International Journal of Life-Cycle Assessment 10(3):177-183 <DOI: http://dx.doi.org/10.1065/lca2004.09.182>

ISO (2005) www.iso.org/iso/en/prods-services/iso3166ma/02iso-3166-code-lists/list-en1.html

Krewitt W, Trukenmüller A, Bachmann TM, Heck T (2001) Country-specific damage factors for air pollutants: a step towards site dependent life cycle impact assessment. International Journal of Life-Cycle Assessment 6(4): 199-210

Seppälä J, Posch M, Johansson M, Hettelingh J-P (2005) Country-dependent characterisation factors for acidification and terrestrial eutrophication based on accumulated exceedance as an impact category indicator. International Journal of Life-Cycle Assessment, OnlineFirst <DOI: http://dx.doi.org/10.1065/lca2005.06.215>

Tarrasón L et al. (2004) Transboundary acidification, eutrophication and ground level ozone in Europe. EMEP Status Report 1/2004, Norwegian Meteorological Institute, Oslo. www.emep.int

UBA (2004) Manual on methodologies and criteria for modelling and mapping critical loads & levels and air pollution effects, risks and trends. Umweltbundesamt Texte 52/04, Berlin. www.icpmapping.org

6. Dynamic Modelling of Lakes in Eastern Canada

J. Aherne[1], T.A. Clair[2], I.F. Dennis[2], M. Gilliss[3], S. Couture[4], D. McNicol[5], R. Weeber[5], P.J. Dillon[1], W. Keller[6], D.S. Jeffries[7], S. Page[8], K. Timoffee[9], B.J. Cosby[10]

[1]Environmental and Resource Studies, Trent University, Peterborough, Ontario, Canada
[2]Environment Canada, Atlantic Region, Sackville, New Brunswick, Canada
[3]New Brunswick Environment Department, Fredericton, New Brunswick, Canada
[4]Environnement Canada, Centre Saint Laurent, Montréal, Québec, Canada
[5]Environment Canada, Ontario Region, Nepean, Ontario, Canada
[6]Ontario Ministry of the Environment, Sudbury, Ontario, Canada
[7]Environment Canada, National Water Research Institute, Burlington, Ontario, Canada
[8]Fisheries and Oceans Canada, Freshwater Institute, Winnipeg, Manitoba, Canada
[9]Environment Canada, National Capital Region, Gatineau, Québec, Canada
[10]University of Virginia, Charlottesville, Virginia, United States

6.1 Introduction

Critical loads have been widely accepted in Europe as a basis for the development of air pollution control strategies, as evidenced by the Second Sulphur Protocol and the Gothenburg Protocol (see Gregor et al., 2001). The concept owes its origin to the 'target loading' concept proposed by Canadian scientists, in relation to deposition of sulphates to aquatic systems, during transboundary pollution control negotiations with the USA in the early 1980s. This target load concept has been used in Canada to design an emission reduction programme (RMCC, 1990; Jeffries and Lam, 1993). More recently, critical loads have been determined and mapped for waters (Hindar et al., 2001; Henriksen et al., 2002; Aherne et al., 2004; Watmough et al., 2005; Dupont et al., 2005) and forest soils (Arp et al., 1996; Moayeri et al., 2001; Ouimet et al., 2001; Watmough and Dillon, 2003) for a number of regions in eastern Canada. Much of this work is summarised and presented along with steady-state critical load maps for eastern Canada in the 2004 Canadian Acid Deposition Science Assessment (Jeffries and Ouimet, 2004).

In recent years, there has been increasing recognition of the importance of dynamic models in developing emission reduction policies. Under the LRTAP Convention, work is currently underway to apply dynamic models on a European scale to support the review and possible revision of the Gothenburg Protocol. Recently, dynamic soil chemical models have been used in eastern Canadian to assess the impact of proposed sulphur emission reductions on future lake water chemistry (Aherne et al., 2003; Clair et al., 2003; Larssen et al., 2003).

This chapter describes the application of a dynamic soil-chemical model (MAGIC; Cosby et al., 2001) to 502 lakes in eastern Canada. The objective of the research was to model the past and future acidification-status for acid-sensitive lakes in eastern Canada.

6.2 Methods

Study area

Long-term monitoring of lakes and rivers for acidification effects has been conducted in Canada by the Federal Environment and Fisheries Departments, as well as by a number of provincial governmental organisations. Using these databases, lake water chemistry data were collated for 502 lakes from five provinces (Ontario, Quebec, New Brunswick, Nova Scotia and Newfoundland) across eastern Canada, with 65% of the lakes located in Ontario (Table 6-1). In order to be selected, the lakes needed to have information on catchment characteristics (lake and catchment area, lake mean depth, catchment runoff) in addition to annual water chemistry data. The study lakes span a 3000 km transect across eastern Canada reflecting a strong east to west gradient in climate, meteorology and acid deposition (Figure 6-1). However, most of the selected sites were located on acid-sensitive terrain such as the granitic Canadian Shield, slates and shales (Shilts, 1981).

Table 6-1. Mean catchment characteristics and lake chemistry summarised by province and all study lakes (DOC = dissolved organic carbon).

	New Brunswick	Newfoundland	Nova Scotia	Ontario	Quebec	All Lakes
Number of lakes (n)	72	27	66	327	10	502
Lake area (ha)	42.1	84.0	132.8	100.2	14.2	93.6
Catchment area (ha)	747.5	586.4	3058.9	1253.1	99.1	1354.8
Mean lake depth (m)	3.2	3.3	2.5	6.2	7.1	5.2
Runoff (m)	0.82	1.01	1.06	0.45	0.74	0.62
pH	6.56	5.76	5.31	5.99	5.92	5.97
Ca^{2+} ($\mu mol_c\ L^{-1}$)	118.45	51.68	38.24	126.96	71.17	108.91
Mg^{2+} ($\mu mol_c\ L^{-1}$)	33.32	25.39	42.27	54.87	23.90	47.92
Na^{+} ($\mu mol_c\ L^{-1}$)	61.15	75.87	149.28	36.43	22.26	56.65
K^{+} ($\mu mol_c\ L^{-1}$)	8.79	5.39	7.65	8.81	4.94	8.40
NH_4^{+} ($\mu mol_c\ L^{-1}$)	0.00	0.00	0.00	2.92	1.96	1.94
SO_4^{2-} ($\mu mol_c\ L^{-1}$)	51.93	24.21	47.84	133.55	59.83	103.23
Cl^{-} ($\mu mol_c\ L^{-1}$)	31.15	68.66	146.76	18.52	7.52	39.67
NO_3^{-} ($\mu mol_c\ L^{-1}$)	0.56	0.35	0.18	3.17	2.72	2.24
DOC ($mg\ L^{-1}$)	5.63	5.83	7.29	4.73	4.57	5.25

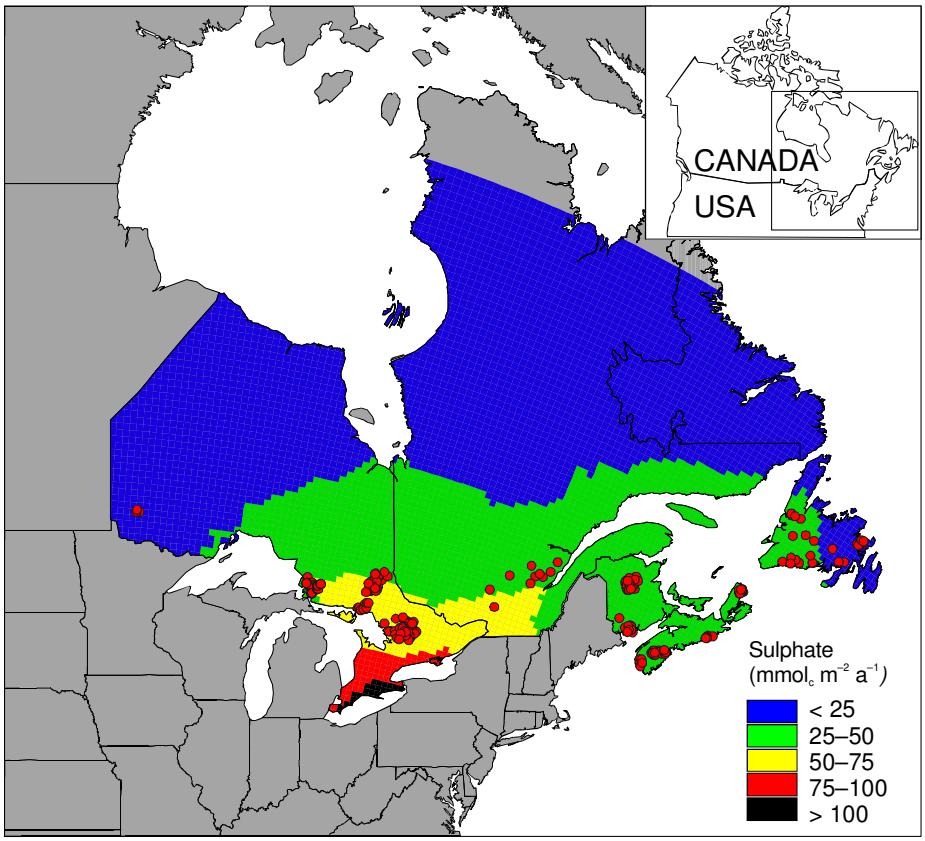


Figure 6-1. Location of 502 study lakes (red dots) in the provinces of Ontario, Quebec, New Brunswick, Nova Scotia and Newfoundland in eastern Canada. Total (wet and dry) deposition of sulphate in eastern Canada is also shown.

Model of Acidification of Groundwater in Catchments

The model of acidification of groundwater in catchments (MAGIC) is a lumped-parameter model of intermediate complexity, developed to predict the long-term effects of acidic deposition on soil and surface water chemistry. As such, the principal drivers are the time-series inputs of atmospheric (wet+dry) deposition. The model is

calibrated using observed (or 'target') values of surface water and soil chemistry for a specified period (calibration year). A detailed description of MAGIC is given by Cosby et al. (1985, 2001). In the current study, simulations were carried out using an annual time-step, with a number of simplifying assumptions applied consistently across the region. It was assumed that forests were at steady state and harvesting removals were negligible. Discharge was described using long-term means with 100% routed to the lake.

Catchment data

Annual average lake concentration data (targets) for model calibration were derived from the most recent consecutive three-year period, with each lakes having at least two years of available data (Table 6-1). Lake characteristics showed considerable variation across each province with mean lake area ranging from 14.2 (Quebec) to 132.2 (Nova Scotia) ha and long-term annual average runoff ranging from 0.45 (Ontario) to 1.06 (Nova Scotia) m. Lake chemistry showed similar variation, with sulphate concentrations in lake water ranging from 24.21 (Newfoundland) to 133.55 (Ontario) $\mu mol_c\ L^{-1}$. New Brunswick was the only province with a mean pH greater than 6.0; however, in general lake pH was normally distributed with a median pH of ~6.0 for the study lakes (Figure 6-2). The majority of lakes had low buffering, with calcium concentrations showing considerable skewness to lower values (Figure 6-2).

Information on catchment soils (bulk density, cation exchange capacity and exchangeable base cation fraction) were generalised from soils maps and limited sampling programs at specific long-term study sites across eastern Canada.

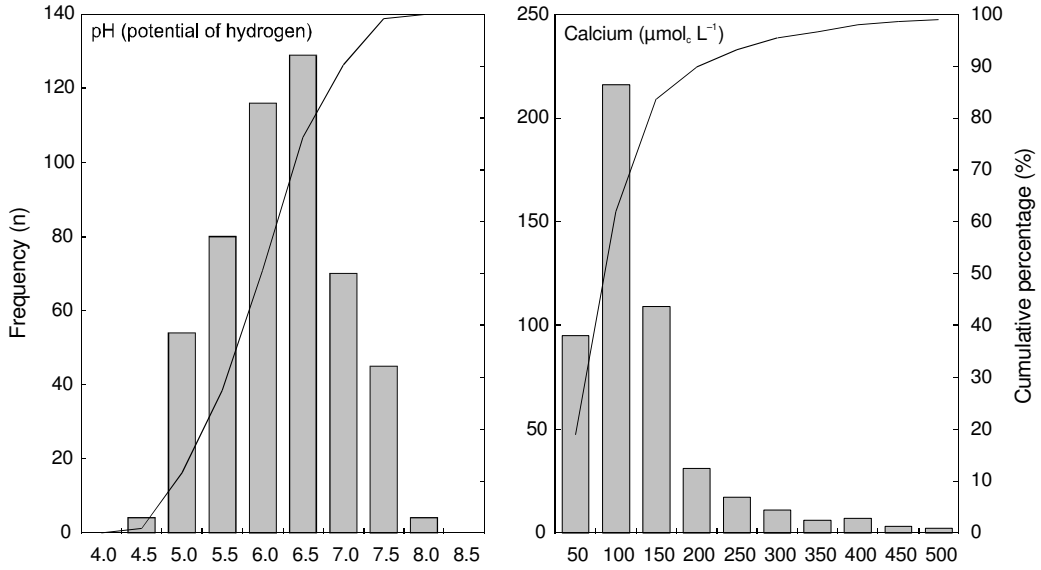


Figure 6-2. Histogram and cumulative distribution for pH and calcium in the study lakes.

Deposition data

Annual average wet and dry deposition fields (1994–1998) for the major ions in precipitation across eastern Canada (Ro and Vet, 2003; Vet and Shaw, 2004) were used to estimate current deposition to each lake. Wet deposition (at a resolution of approximately 45 km by 45 km) and dry deposition (at a resolution of approximately 35 km by 35 km) were interpolated to a common grid resolution (25 km by 25 km) and combined to produce total deposition estimates for each ion (see Figure 6-1).

Historic sulphate deposition history was reconstructed from sulphur emission inventories (1850–1940: Husar, 1994; Lefohn et al., 1999; 1940–1980: EPA, 2000) and observed data (Figure 6-3). Similarly, nitrate deposition history was reconstructed from emission inventories and observed data. North American emission inventories for ammonia are rather scarce. As such, a simplified ammonium deposition sequence was constructed from observed data and nitrate emission data in combination with global emission estimates of ammonia (Galloway, 1995).

Future sulphate deposition was derived from recently proposed emission reduction estimates using the Acid Deposition and Oxidant Model (ADOM; WxPrime, 2004). The future scenario 'NOX3P' is entirely sectorial based and includes reductions in nitrogen oxide emissions. NOX3P includes all Canadian and United States control programs legislated as of 2003 and the Canadian post-2000 Acid Rain and United States Clear Skies programs. The scenario approximates to a 45% reduction in sulphur and 68% reduction in nitrogen oxide emissions by 2020 from 1989 baselines. Sulphate and nitrate deposition was assumed constant thereafter (Figure 6-3). Deposition forecasts for ammonium were assumed to remain constant at current levels. In addition, deposition sequences for all other ions were assumed to be constant throughout the simulation period.

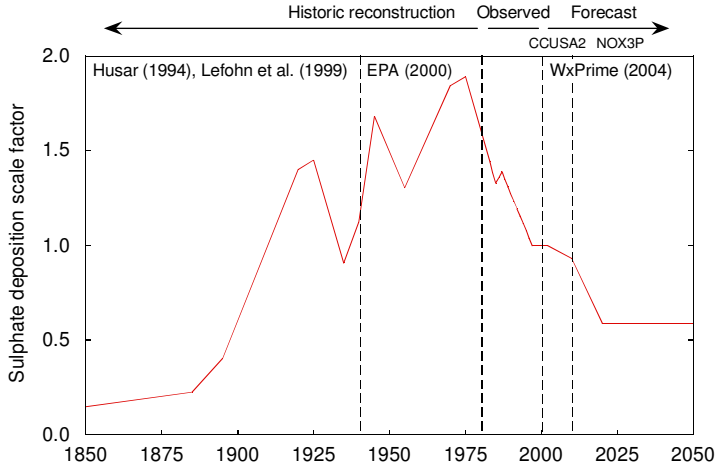


Figure 6-3. Estimated historic and future sulphate deposition (scale factor with current deposition equivalent to a factor of 1.0) for the period 1850–2050. The broken lines separate the different data sources used to construct the deposition sequence.

Model calibration

Site-specific parameter files were prepared using lake water and soil physico-chemical characteristics (lake area, lake retention time, soil bulk density, soil cation exchange capacity, etc) and considered 'fixed' in the model. In addition, a number of default parameter values were uniformly applied across the region, e.g., the partial pressure of carbon dioxide in the soil (p_{CO2}) was set at ~15 times atmospheric. Chloride and sulphate were assumed to be in steady state with respect to input-output fluxes. The excess of outputs over inputs was attributed to unmeasured dry deposition. The assumption that sulphate is conservative appears to be reasonable for eastern Canada (Figure 6-4). Detailed process-oriented nitrogen dynamics were not modelled, rather, nitrogen (nitrate and ammonium) transformation and uptake was described as a catchment net retention calculated simply as the difference between input and output flux during the calibration year. This percentage was assumed to be constant throughout the simulation.

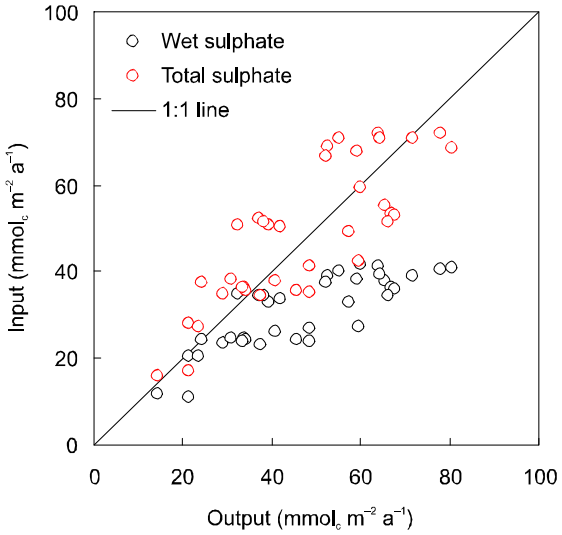


Figure 6-4. Wet and total sulphate input versus output for lakes in eastern Canada. Sulphate input was derived from mapped deposition fields (25 by 25 km grids) across eastern Canada (see Figure 6-1). Sulphate output was estimated as the average for all lakes within each deposition mapping grid (with a minimum of four lakes per deposition grid).

Base cation weathering rates and initial soil exchangeable fractions (and exchange constants) were calibrated to lake water and soil chemistry observations using an iterative automated optimisation procedure. To account for uncertainty in a number of the fixed parameters, a 'fuzzy' optimisation method was employed. In addition, uncertainty bands (or tolerance levels) were also applied to the target lake water (± 2 $\mu mol_c\ L^{-1}$) and soil chemistry (± 0.2 %) variables. For each study lake, 10 calibrations were attempted; any simulation that reproduced all target variables was considered successful. Finally, hindcast and forecast simulations were carried out for each lake using all successful calibrations. Multiple simulation results for each lake were combined using median statistics to predict regional lake water chemistry for the period 1850–2050.

6.3 Results

Multiple calibrations for each lake were performed on simulations from 1850 to 2000 using historical deposition sequences. In total, 498 lakes were successfully calibrated. The number of successful calibrations per study lake ranged from 1–10, with the majority of lakes having 10 successful calibrations (98%). The generalised soil data used in the current assessment can lead to soils having calibrated selectivity coefficients outside the range that has generally been observed (De Vries and Posch, 2003). As a further quality control, only those lakes with calibrated logarithmic soil selectivity coefficients for calcium and magnesium between –3.5 and +3.5 were selected for model simulations. This left 398 lakes, for which soil and lake water chemistry was simulated for the period 1850–2050. The trends in lake acidification and recovery were evaluated using time-series' for pH and acid neutralising capacity (ANC; estimated as the difference between base cations and acid anions). The regional trends for eastern Canada are presented as percentile time-series (Figures 6-5).

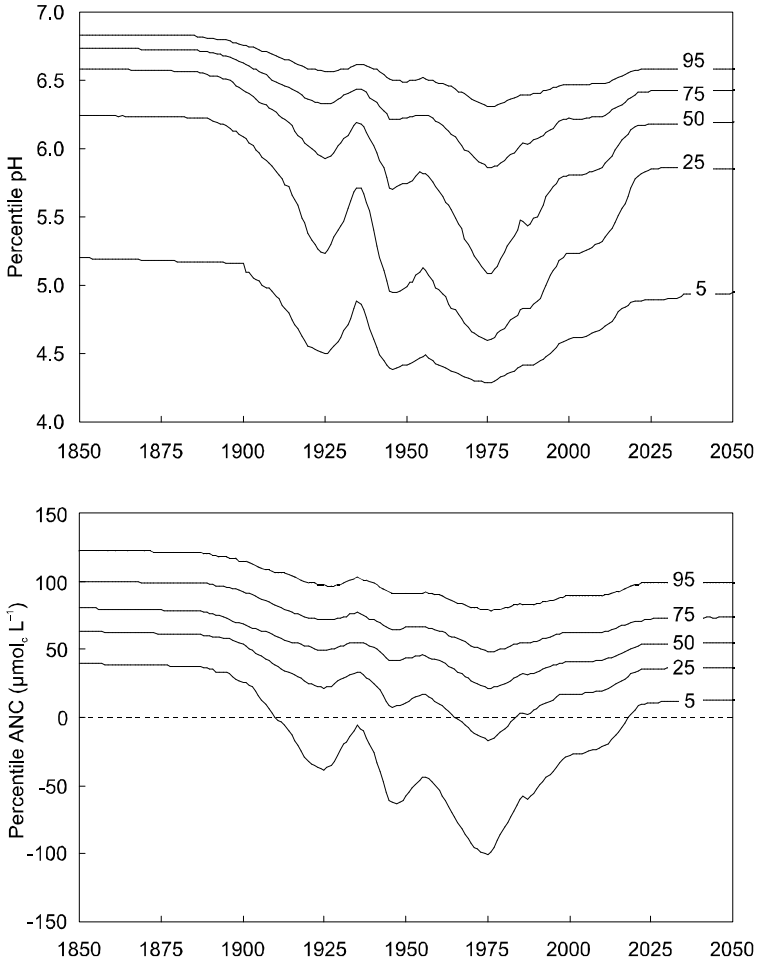


Figure 6-5. Simulated percentile time-series for pH and acid neutralising capacity (ANC) during the period 1850–2050. The 5th, 25th, 50th, 75th and 95th percentiles are shown (small numbers in figure).

In 1850, historic lake pH ranged from 5.20–6.80. Regional values for pH we generally static until deposition started to change dramatically after 1900 (Figure 6-5). In the time period between 1950 and 1975, when acid load peaked, pH decreased by an average of 0.4 pH units. The lower percentiles reflect lake catchments with high concentrations of organic acids. As a result, the increase in acid deposition during the mid-1970s is somewhat buffered in these lakes. During peak depositions, 80% of the lakes fell below pH 6.0. The decline in acid deposition from the late 1970s, and under the proposed future scenario, has a substantial affect on the pH. Significant recovery is predicted by 2050, with quartile (25th percentile) pH values estimated at 5.86. ANC follows a similar pattern to pH (Figure 6-5). All lakes had positive ANC until the early 1900s, and by the mid-1970s ~35% had ANC < 0 µmol$_c$ L^{-1}. However, by 2050 97% of the lakes had ANC > 0 µmol$_c$ L^{-1}. A small number of lakes had high ANC values (95th percentile) reflecting those catchments with higher weathering rates. In general, both ANC and pH show a recovery potential under the current deposition scenario, and by 2050 concentrations levels have recovered to values predicted for the early 1900s.

Although ANC shows a recovery potential for lakes in eastern Canada, the response is not uniform across all regions (Figure 6-6). The largest changes in ANC occurred in central Ontario (Sudbury and Muskoka), while the smallest were in Nova Scotia and Newfoundland, which are more influenced by organic acids. Though it is perhaps unrealistic to expect water chemistry conditions to return to pre-acidification levels, it is nevertheless important to know whether future conditions will be sufficient to allow aquatic communities to recover. An ANC value of 40 µmol$_c$ L^{-1} has generally been used as a critical limit for aquatic organisms in eastern Canada (Henriksen et al., 2002; Dupont et al., 2005). Historic simulations indicate that lakes in every region of the country had chemical conditions suitable for healthy aquatic communities before acidification began, with the exception of a few sites in Newfoundland where highly dilute, organic waters caused unusual conditions. Future

simulations (2030), indicate that ANC levels should be suitable at more than 90% of the lakes in each region except for Ontario (Sudbury, Muskoka), Quebec, Nova Scotia and Newfoundland. The Sudbury region is still sensitive due to a long history of intensive deposition, while Quebec has soils with very low buffering capacity. In contrast, water chemistry in Nova Scotia and Newfoundland is controlled in large part by extremely low soil buffering capacity (see Figure 6-2) and natural organic acids which tend to naturally depress pH.

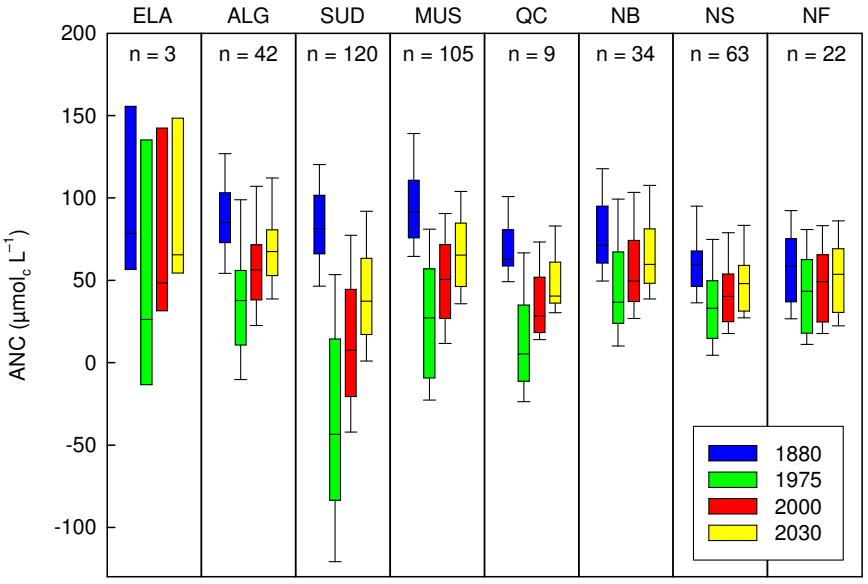


Figure 6-6. Box plot showing median, quartile and 95th percentile values of acid neutralising capacity (ANC) during 1880 (blue), 1975 (green), 2000 (red) and 2030 (yellow) for ELA (Experimental Lakes Area, western Ontario), ALG (Algoma, north-central Ontario), SUD (Sudbury, central Ontario), MUS (Muskoka, south-central Ontario), QC (Québec), NB (New Brunswick), NS (Nova Scotia) and NF (Newfoundland). Note: the years 1880, 1975, 2000 and 2030 roughly correspond to pre-acidification, worst case, current and future lake chemistry, respectively.

6.4 Conclusions

Hindcast simulations provide a stark picture of water chemistry conditions that probably existed in eastern Canada during the mid-1970s. The large reductions in sulphur emissions have caused measurable improvements, but these have not been enough to return the water chemistry in a large portion of the lakes to levels conducive for unimpaired ecosystem function. Emission control agreements that are in place, or are currently proposed, will not be sufficient to return ecosystem function to acceptable levels in all parts of eastern Canada within the next 20 years. In order to reach this goal, further reductions will have to be made in acid emissions in central and eastern North America.

References

Aherne J, Dillon PJ, Cosby BJ (2003) Acidification and recovery of aquatic ecosystems in south-central Ontario, Canada: regional application of the MAGIC model. Hydrology and Earth Systems Science 7: 561–573

Aherne J, Posch M, Dillon PJ, Henriksen A (2004) Critical loads of acidity for surface waters in south-central Ontario, Canada: regional application of the First-order Acidity Balance (FAB) Model. Water Air Soil Pollution: Focus 4: 25–36

Arp PA, Oja T, Marsh M (1996) Calculating critical S and N loads and current exceedances for upland forests in southern Ontario, Canada. Canadian Journal of Forest Research 26: 696–709

Clair TA, Dennis IF, Cosby BJ (2003) Probable changes in lake chemistry in Canada's Atlantic Provinces under proposed North American emission reductions. Hydrology and Earth Systems Science 7: 574–582

Cosby BJ, Ferrier RC, Jenkins A, Wright RF, (2001) Modelling the effects of acid deposition: refinements, adjustments and inclusion of nitrogen dynamics in the MAGIC model. Hydrology and Earth Systems Science 5: 499–517

Cosby BJ, Hornberger GM, Galloway JN, Wright RF (1985) Modeling the effects of acid deposition: assessment of a lumped parameter model of soil water and streamwater chemistry. Water Resources Research 21: 51–63

De Vries W, Posch M (2003) Derivation of cation exchange constants for sand loess, clay and peat soils on the basis of field measurements in the Netherlands. Report 701, Alterra, Wageningen, The Netherlands, 50 pp

Dupont J, Clair TA, Couture S, Estabrook R, Gagnon C, Godfrey PJ, Jeffries DS, Kahl JS, Khan H, Nelson S, Peckenham J, Pilgrim W, Stacey P, Taylor D, Van Arsdale A (2005) Critical loads of acidity and water sensitivity in New England States and eastern Canadian Provinces. Environmental Monitoring & Assessment (in press)

EPA (2000) National Air Pollutant Emission Trends: 1900–1998. EPA-454/R-00-002, United States Environmental Protection Agency, North Carolina; www.epa.gov/ttn/chief/trends/trends98

Galloway JN (1995) Acid deposition: perspectives in time and space. Water Air Soil Pollution 85: 15–24

Gregor H-D, Nagel H-D, Posch M (2001) The UN/ECE international programme on mapping critical loads and levels. Water Air Soil Pollution: Focus 1: 5–19

Henriksen A, Dillon PJ, Aherne J (2002) Critical loads of acidity to surface waters in south-central Ontario, Canada: regional application of the steady-state water chemistry model. Canadian Journal of Fisheries and Aquatic Science 59: 1287–1295

Hindar A, Posch M, Henriksen A (2001) Effects of in-lake retention of nitrogen on critical load calculations. Water Air Soil Pollution 130: 1403–1408

Husar R (1994) Sulphur and Nitrogen Emission Trends for the United States: An Application of the Materials Flow Approach. In, R.U. Ayres and U.E. Simonis (eds.), Industrial Metabolism: Restructuring for Sustainable Development, United Nations University Press. 390pp; www.unu.edu/unupress/unupbooks/80841e/80841e00.htm

Jeffries DS, Lam DCL (1993) Assessment of the effect of acidic deposition on Canadian lakes: determination of critical loads for sulphate deposition. Water Science Technology 28, 183–187

Jeffries DS, Ouimet R (2004) Critical Loads: Are They Being Exceeded? In, 2004 Canadian Acid Deposition Science Assessment. Environment Canada

Larssen T, Brereton C, Gunn JM (2003) Dynamic modeling of recovery from acidification of lakes in Killarney Park, Ontario, Canada. Ambio 32: 244–248

Lefohn AS, Husar JD, Husar RB (1999). Estimating historical anthropogenic global sulfur emission patterns for the period 1850–1990. Atmospheric Environment 33: 3435–3444; data: www.asl-associates.com/sulfur1.htm

Moayeri M, Meng F-R, Arp PA, Foster NW (2001) Evaluating critical soil acidification loads and exceedances for a deciduous forest at the Turkey Lakes watershed. Ecosystems 4: 555–567

Ouimet R, Duchesne L, Houle D, Arp PA (2001) Critical loads of atmospheric S and N deposition and current exceedances for Northern temperate and boreal forests in Quebec. Water Air Soil Pollution: Focus 1: 119–134

RMCC (1990) The 1990 Canadian Long-range Transport of Air Pollutants and Acid Deposition Assessment Report, Part 4: Aquatic Effects', Federal/Provincial Research and Monitoring Coordinating Committee, Ottawa, Ontario, 151 pp

Ro CU, Vet RJ (2002) Analyzed data fields from the National Atmospheric Chemistry Database (NAtChem) and Analysis Facility. Air Quality Research Branch, Meteorological Service of Canada, Environment Canada, Toronto, Ontario

Shilts WW (1981) Sensitivity of bedrock to acidification: modification by glacial processes. Technical Report, Geological Survey of Canada, Paper 81–14, Natural Resources Canada, Ottawa, ON, Canada

Vet RJ, Shaw M (2004) 1994–1998 average dry deposition velocities calculated using the MSC Air Quality Research Branch dry deposition model (RDM). Meteorological Service of Canada, Environment Canada, Toronto, Ontario

Watmough SA, Aherne J, Dillon PJ (2005). Effect of declining lake base cation concentration on freshwater critical load calculations. Environmental Science and Technology 39: 3255–3260

Watmough SA, Dillon PJ (2003) Do critical load models adequately protect forests? A case study in south-central Ontario. Canadian Journal of Forest Research 33: 1544–1556

WxPrime (2004) Emissions-Scenario Simulations of Potential Nitrogen Emission Reductions Using the Acid Deposition and Oxidant Model (ADOM). WxPrime Corporation, Toronto, 51 pp

Part II. National Focal Centre Reports

This part consists of reports on national data on critical loads and dynamic modelling calculations submitted to the Coordination Center for Effects by the National Focal Centres (NFCs).

Countries which updated their data on critical loads for *heavy metals* after the CCE workshop (Berlin, April 2005) were asked to add a paragraph to the national report describing the update.

The NFC reports received were edited for format and clarity, but have not been further reviewed.

AUSTRIA

National Focal Centre

Christian Nagl
Umweltbundesamt GmbH
Department of Air Quality Control
Spittelauer Lände 5
1090 Vienna
tel: +43-1-313 04 5866
fax: +43-1-313 04 5400
christian.nagl@umweltbundesamt.at
www.umweltbundesamt.at

Collaborating institutions

Erik Obersteiner
Umweltbundesamt Gmbh
Department of Terrestrial Ecology
Spittelauer Lände 5
1090 Vienna
tel: +43-1-31 304-3690
fax: +43-1-31 304-3700
erik.obersteiner@umweltbundesamt.at
www.umweltbundesamt.at

Austrian Federal Office and Research Centre for Forests
Franz Mutsch
Department of Forest Ecology
Klemens Schadauer
Department of Forest Inventory
Seckendorff-Gudent-Weg 8
1131 Vienna
tel: +43-1-87 838-0
http://bfw.ac.at

Status

In response to the call for data of November 2004 a new dataset of critical loads and dynamic modelling is provided. Changes to the 2003 dataset are:

- The acceptable N leaching is set to 4 kg N in the lowlands (500 m a.s.l.), decreasing to 2 kg N at 2000 m a.s.l.
- New deposition data for base cations, sulphur and nitrogen are used.
- The denitrification fraction f_{de} is based on soil moisture classes instead of clay content classes.
- Carbon pool and C:N ratio are calculated for the organic layer + mineral topsoil (0–10 cm) only
- Ecosystem type G3.1B is introduced to indicate unmanaged protection forests, where no nutrient uptake takes place.
- Runoff calculation is based on equation 5.91b in Chapter 5.5 of the Mapping Manual (UBA, 2004).

Data sources

Soils: Soil information is based on the Austrian Forest Soil Inventory from Austrian Federal Office and Research Centre for Forests (Forstliche Bundesversuchsanstalt, 1992). About 500 sample plots were collected in an 8.7 × 8.7 km grid between 1987 and 1990. Most of the soil input parameters to critical loads and target loads calculation were taken from this dataset. The data are part of the BORIS soil information system run by the Federal Environment Agency.

Nutrient uptake: Information on biomass uptake comes from the Austrian Forest Inventory, sampled by the Austrian Federal Office and Research Centre for Forests - BFW (Schieler et al., 2001). Mean harvesting rates for the years from 1986 to 1996 were aggregated on EMEP grid cell basis. Grid cells with too few sample points were combined with neighbouring cells. Base cation and nitrogen content were taken from Jacobsen et al. (2002). No nutrient uptake takes place at unmanaged protection forests.

Ecosystem: Four forest ecosystem types have been investigated according to EUNIS classification: G1 (*Fagus sylvatica*, *Quercus robur*), G3 (*Picea abies*, *Pinus sylvestris*, *Larix decidua*), G4 and G3.1B, which is used to indicate unmanaged protection forests. Ecosystem area was identified by dividing the known ecosystem area per grid cell (from forest inventory) by the number of soil inventory points falling in this ecosystem type.

Depositions:

Sulphur and nitrogen deposition time series provided by the CCE 2004 (included with the database-file)

Base cation depositions: Van Loon et al. (2005)

Calculation Methods

The calculations and assumptions made are generally in accordance with the Mapping Manual (UBA, 2004) and CCE Status Reports. A detailed description of the parameters and the data and methods used for their derivation is given in Table AT-1.

The Access version of VSD was used for critical loads calculation and dynamic modelling. For the cation exchange the Gapon model was used, the exchange constants were calibrated. Soil density (Theta) was set to 0.3 m^3 m^{-3}, CN_{min} and CN_{max} were set to be 10 respectively 40. Oliver constants for the organic acid dissociation model were set to be 4.5, 0, and 0.

Base cations were included lumped in the Ca column for weathering and uptake. Due to the lack of spatial distributed information on organic acids, default values for all records were used.

Calcareous soils occur at 30% of the sample points representing about 40% of the ecosystem area.

Table AT-1. Data description, methods and sources.

Variable	Explanation and Unit	Description
EcoArea	Area of the ecosystem within the EMEP grid cell (km^2)	calculated from Austrian forest inventory data
CLmaxS	Maximum critical load of sulphur (eq ha^{-1} a^{-1})	calculated by VSD
CLminN	Minimum critical load of nitrogen (eq ha^{-1} a^{-1})	calculated by VSD
CLmaxN	Maximum critical load of nitrogen (eq ha^{-1} a^{-1})	calculated by VSD
CLnutN	Critical load of nutrient nitrogen (eq ha^{-1} a^{-1})	Mapping Manual 5.3.1.1, Eq. 5.5
nANCcrit	The quantity –ANCle(crit) (eq ha^{-1} a^{-1})	calculated by VSD
Nleacc	Acceptable nitrogen leaching (eq ha^{-1} a^{-1})	decreasing from 4 kg N in the lowlands (500 m a.s.l.) to 2 kg N at 2000 m a.s.l. (see Swiss NFC Report in Posch et al., 2001)
crittype	Chemical criterion used	used: molar Al/Bc (1)
critvalue	Critical value for the chemical criterion	used: 1
thick	Thickness of the soil (m)	mostly 0.5 m, sometimes less, depending on soil inventory data
bulkdens	Average bulk density of the soil (g cm^{-3})	Mapping Manual 6.4.1.3 Eq. 6.27
Cadep	Total deposition of calcium (eq ha^{-1} a^{-1})	total depositions for forest ecosystems (Van Loon et al., 2005)
Mgdep	Total deposition of magnesium (eq ha^{-1} a^{-1})	total depositions for forest ecosystems (Van Loon et al., 2005)
Kdep	Total deposition of potassium (eq ha^{-1} a^{-1})	total depositions for forest ecosystems (Van Loon et al., 2005)
Nadep	Total deposition of sodium (eq ha^{-1} a^{-1})	total depositions for forest ecosystems (Van Loon et al., 2005)
Cldep	Total deposition of chloride (eq ha^{-1} a^{-1})	= 1.166·Nadep
Bcwe	Weathering of base cations (eq ha^{-1} a^{-1})	Mapping Manual 5.3.2.3, Eq. 5.39; Table 5-14 (WRc = 20 for calcareous soils; factor 0.8 for Na reduction)
Bcupt	Net growth uptake of base cations (eq ha^{-1} a^{-1})	[average yearly yield rate * base cation content], data from Austrian forest inventory, base cation contents from Jacobsen et al. 2002 (no uptake by unmanaged protection forests)

Qle	Amount of water percolating through the root zone (mm a^{-1})	Mapping Manual 5.5.2.1.3, Eq. 5.91b (Precipitation data from Hydrological Atlas of Austria; $f_{E,zb}$ = 1)
lgKAlox	Equilibrium constant for the Al-H relationship (log10)	used: 8 (gibbsite equilibrium)
expAl	Exponent for the Al-H relationship	used: 3 (gibbsite equilibrium)
pCO2fac	Partial CO_2-pressure in soil solution as multiple of the atmospheric CO_2 pressure (-)	[$\log_{10}p_{CO2}$ = –2.38 + 0.031·Temp (°C)]; atmospheric CO_2 pressure = 0.00037 atm; equation recommended by CCE
cOrgacids	Total concentration of organic acids (m*DOC) (eq m^{-3})	used: 0.01 (recommended by M. Posch)
Nimacc	Acceptable amount of nitrogen immobilised in the soil (eq ha^{-1} a^{-1})	see German NFC Report in Posch et al. (2001), p.142, Table DE-7
Nupt	Net growth uptake of nitrogen (eq ha^{-1} a^{-1})	[average yearly yield rate * N content], data from Austrian forest inventory, N contents from Jacobsen et al. (2002)
fde	Denitrification fraction ($0<=f_{de}<1$) (-)	from 0.1 (dry) to 0.8 (wet) according to soil moisture class; information from soil inventory
CEC	Cation exchange capacity (meq kg^{-1})	information from soil inventory; calibrated to pH 6.5 (Mapping Manual 6.4.1.3 Eq. 6.29)
bsat	Base saturation (-)	information from soil inventory
yearbsat	Year in which the base saturation was determined	year of soil inventory (1987-1990)
lgKAlBc	Exchange constant for Al vs. Bc (log10)	calibrated by VSD; starting value 0
lgKHBc	Exchange constant for H vs. Bc (log10)	calibrated by VSD; starting value 3
Cpool	Initial amount of carbon in the topsoil (g m^{-2})	[*thick* * *bulkdens* * C_{org}(%) * 10 000]; for mineral topsoil (0-10 cm) + organic layer; information from soil inventory
CNrat	C:N ratio in the topsoil	*Cpool* / *Npool*
yearCN	Year in which the C:N ratio and *Cpool* were determined	year of soil inventory (1987-1990)
EUNIS code	EUNIScode of ecosystem	G1, G3, G4, G3.1B (unmanageded protection forests)

References

BMLFUW - Bundesministerium für Land- und Forstwirtschaft, Umwelt und Wasserwirtschaft (eds) (2003) Hydrologischer Atlas Österreichs. 1. Lieferung, BMLFUW, Wien

Forstliche Bundesversuchsanstalt (eds) (1992) Österreichische Waldboden-Zustandsinventur. Ergebnisse, Mitteilungen der Forstlichen Bundesversuchsanstalt, Wien

Jacobsen C, Rademacher P, Meesenburg H, Meiwes KJ (2002) Gehalte chemischer Elemente in Baumkompartimenten. Niedersächsische forstliche Versuchsanstalt Göttingen

Posch M, De Smet PAM, Hettelingh J-P, Downing RJ (eds) (2001) Modelling and mapping of critical thresholds in Europe. CCE Status Report 2001. Report 259101010/2001, Coordination Center for Effects, RIVM, Bilthoven, The Netherlands

Posch M, Hettelingh J-P, Slootweg J, Downing RJ (eds) (2003) Modelling and Mapping of Critical Thresholds in Europe: CCE Status Report 2003. Report 259101013/2003, Coordination Center for Effects, RIVM, Bilthoven, The Netherlands

Schieler K, Schadauer K (2001) The Austrian Forest Inventory 1992-96. online-publication http://fbva.forvie.ac.at/700/1891.html, Austrian Federal Office and Research Centre for Forests, Vienna

UBA (2004) Manual on Methodologies and Criteria for Modelling and Mapping Critical Loads & Levels and Air Pollution Effects, Risks and Trends. Umweltbundesamt, Berlin, www.icpmapping.org

Van Loon M, Tarrason L, Posch M (2005) Modelling Base Cations in Europe. EMEP/MSC-W & CCE Note 2/2005, Norwegian Meteorological Institute, Oslo, Norway, 47 pp

BELARUS

National Focal Centre

Oleg Bely, Natalia Lysukha
Belarussian Research Centre 'Ecology'
31A Horuzhaya Str.
220002 Minsk
tel.: +375-17-234-70-65
fax: +375-17-234-80-72
belnic@tut.by, promeco@tut.by

Calculation methods

Critical loads of sulphur and nitrogen have been calculated for terrestrial ecosystems in Belarus using modified Steady-State Mass Balance (SSMB) equations. The corresponding algorithms described below have been suggested by Bashkin (1997).

The parameters used to calculate critical loads include:

- ANC_l = acid-neutralizing capacity of soil
- BC_d = base cation deposition
- BC_u = base cation uptake
- BC_w = base cation weathering
- *CNrat* = C:N ratio in the upper soil layer
- C_N = critical content of nitrogen in surface water
- C_b = coefficient of biogeochemical turnover
- C_t = active temperature coefficient (ratio of temperature sum> 5^{o}C to total annual sum)
- d = upper soil layer depth
- K_{gibb} = gibbsite coefficient
- *NBCrat* = ratio of N to BC in plant tissue
- N_{de} = denitrification of soil N
- N_{de}* = denitrification of deposition N
- N_i = immobilization of soil N
- N_i* = immobilization of deposition N
- N_{le} = N leaching
- *NMC* = nitrogen mineralization capacity of soil (eq ha^{-1} a^{-1})
- N_{td} = total N deposition, wet+dry (NO_x+NH_x)
- N_u = uptake of soil N
- N_u* = uptake of deposition N
- N_{upt} = annual N uptake
- Q = surface runoff
- *We* = chemical weathering of soil (eq ha^{-1} a^{-1} at 1m depth)

The **minimum critical load of nitrogen** has been calculated as:

$$CL_{min}(N) = N_i^* + N_u^*$$

where:

$$N_i^* = \begin{cases} 0.15 \cdot \text{Ntd} \cdot \text{Ct} / \text{Cb} & \text{if CNrat} > 10 \\ 0.25 \cdot \text{Ntd} \cdot \text{Ct} / \text{Cb} & \text{if } 10 \le \text{CNrat} < 14 \\ 0.30 \cdot \text{Ntd} \cdot \text{Ct} / \text{Cb} & \text{if } 14 \le \text{CNrat} < 20 \\ 0.35 \cdot \text{Ntd} \cdot \text{Ct} / \text{Cb} & \text{if CNrat} \ge 20 \end{cases}$$

and:

$$N_u^* = N_{upt} - N_u$$

and the annual N uptake has been defined as:

$$N_{upt} = \begin{cases} K \cdot \text{Nupt} \cdot (1 - 1/\text{Cb}) & \text{if Cb} > 1 \\ K \cdot \text{Nupt} \cdot (1 - 1/\text{Cb}) & \text{if Cb} \le 1 \end{cases}$$

The constant K=1.2 for deciduous forest, and 0.8 for coniferous forests.

Uptake of nitrogen from the soil, N_u, is calculated as:

$$N_u = (NMC - N_i - N_{de}) \text{ᴝ} C_t$$

where:

$$N_i = \begin{cases} 0.15 \cdot \text{NMC/Cb} & \text{if C : N} > 10 \\ 0.25 \cdot \text{NMC/Cb} & \text{if } 10 \le \text{C : N} < 14 \\ 0.30 \cdot \text{NMC/Cb} & \text{if } 14 \le \text{C : N} < 20 \\ 0.35 \cdot \text{NMC/Cb} & \text{if C : N} \ge 20 \end{cases}$$

and:

$$N_{de} = \begin{cases} 0.145 \cdot \text{NMC} + 0.9 & \text{if NMC} < 10 \\ 0.145 \cdot \text{NMC} + 0.605 & \text{if } 10 \le \text{NMC} \le 60 \\ 0.145 \cdot \text{NMC} + 6.477 & \text{if NMC} > 60 \end{cases}$$

The **critical load of nutrient nitrogen** has been calculated as:

$$CL_{nut}(N) = CL_{min}(N) + N_l + N_{de}^*$$

where:

$$N_l = Q \cdot C_N$$

$$N_{de}^* = N_{td} \cdot C_t \cdot N_{de} / NMC$$

The **maximum critical load of sulphur** has been calculated as:

$$CL_{max}(S) = C_t \cdot (BC_w - ANC_l) + (BC_d - BC_u)$$

where:

$$BC_w = Wr \cdot d$$

$$BC_u = N_u^* \cdot NBCrat$$

$$ANC_l = Q \cdot ([\text{H}] + [\text{Al}])$$

with [Al]=0.2 and $[\text{H}] = ([\text{Al}]/K_{gibb})^{1/3}$

The **maximum critical load of nitrogen** has been calculated as:

$$CL_{max}(N) = CL_{max}(S) + CL_{min}(N)$$

Data sources

Description of the main data sources is given in Table BY-1.

Table BY-1. Primary parameters for calculating critical loads.

Parameters	Min. value	Max. value	Data sources
CNrat – C:N ratio in the upper soil layer	7.2	25	National data on different soil types
Cb – coefficient of biogeochemical turnover	0.8	20	Data of national studies
Ct – active temperature coefficient	0.49	0.57	Data of national studies
NMC – nitrogen mineralization capacity of soils (eq ha^{-1} a^{-1})	18	90	Published data on different soil types. (Bashkin, 1997), data of national studies and calculations.
N_{upt} – annual N uptake (kg ha^{-1} a^{-1})	0	75	National data on annual uptake
N_{td} – total N deposition, wet+dry (NO_x+NH_x) (kg ha^{-1} a^{-1})	5.33	11.26	Results of EMEP/MSC-W calculations, 2002
BC_d – base cations deposition (eq ha^{-1} a^{-1})	303	2420	Data from monitoring stations in the south of Belarus were used to calculate the base cation deposition (2000 – 2001)
BC_u – base cations uptake (eq ha^{-1} a^{-1})	100	1750	Minimum value – uptake for moss-pine forest Maximum value – uptake for eagle fern-bilberry oak forest. Data of national studies.
BC_W – base cations weathering (eq ha^{-1} a^{-1})	250	2250	Minimum value: for peat soils. Maximum value: for humus calcareous soils (Rendzinas). Recommended in mapping Manual (Hettelingh and de Vries, 1992)
ANC_l – acid-neutralizing capacity of soil (eq ha^{-1} a^{-1})	1020	30	Critical concentrations for Al+ and H+ were derived from the soil acidity (Hettelingh and de Vries)
Q – surface runoff (m)	0.01	0.34	The precipitation surplus values (Q) were derived as the difference between the precipitation and evatransporation. Data of national studies.

Figure BY-1 shows the distribution of terrestrial ecosystem of Belarus in the EMEP grid.

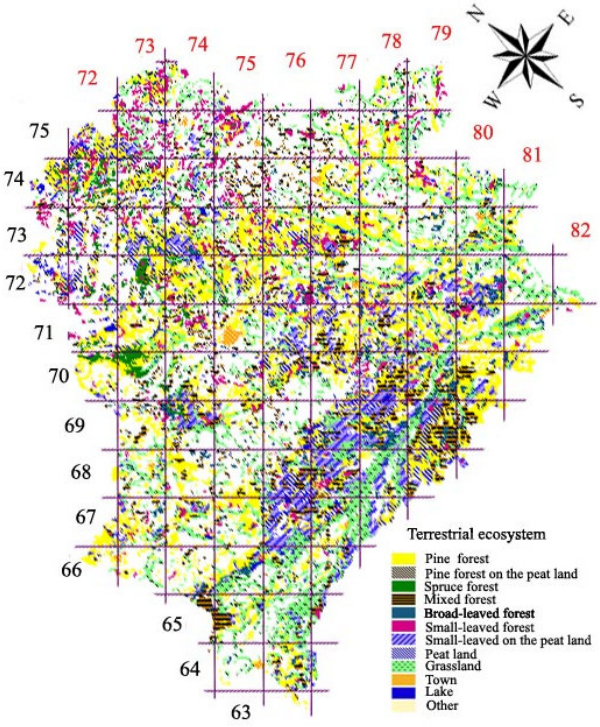


Figure BY-1. Terrestrial ecosystems of BELARUS.

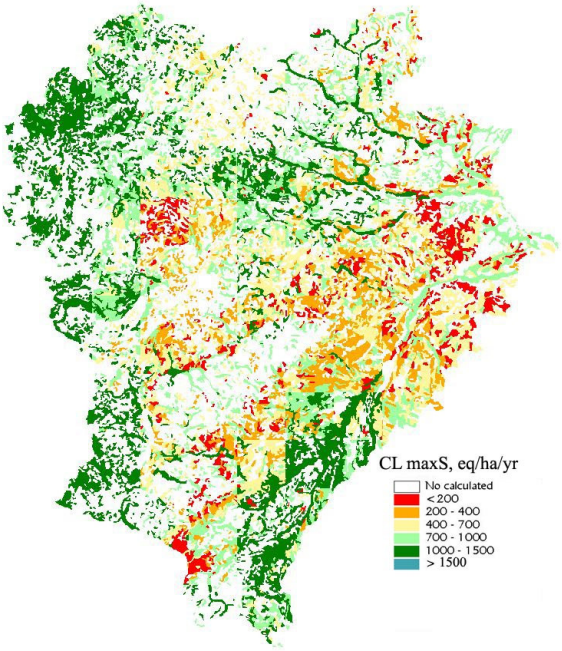


Figure BY-2. Maximum critical loads of sulphur.

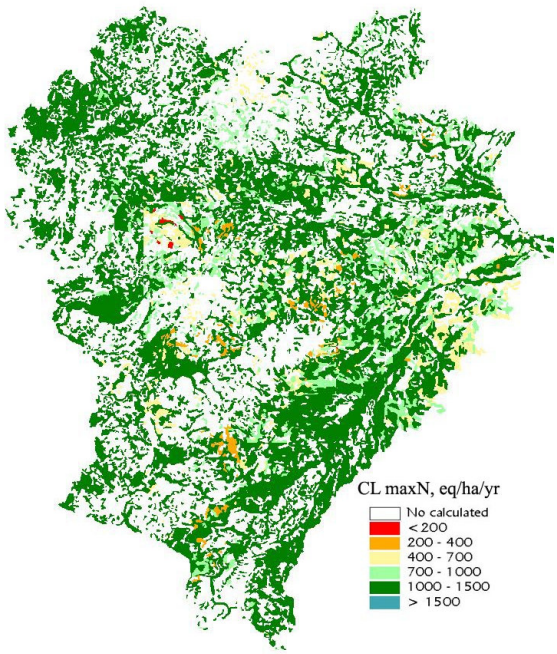


Figure BY-3. Maximum critical loads of nitrogen.

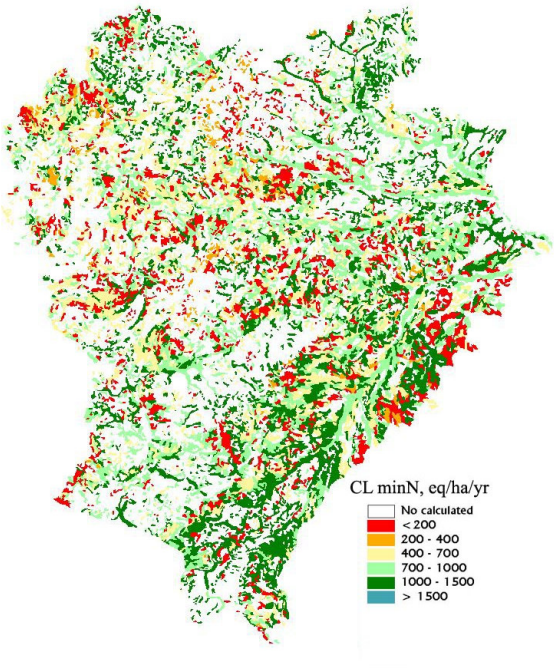


Figure BY-4. Minimum critical loads of nitrogen.

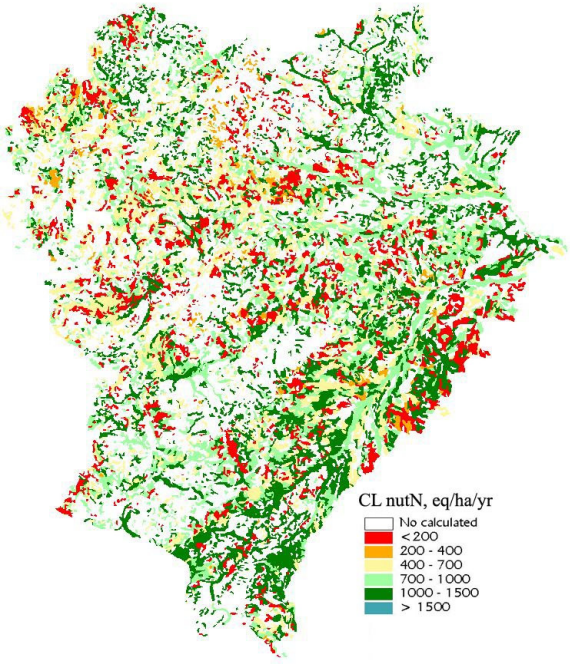


Figure BY-5. Critical loads of nutrient nitrogen.

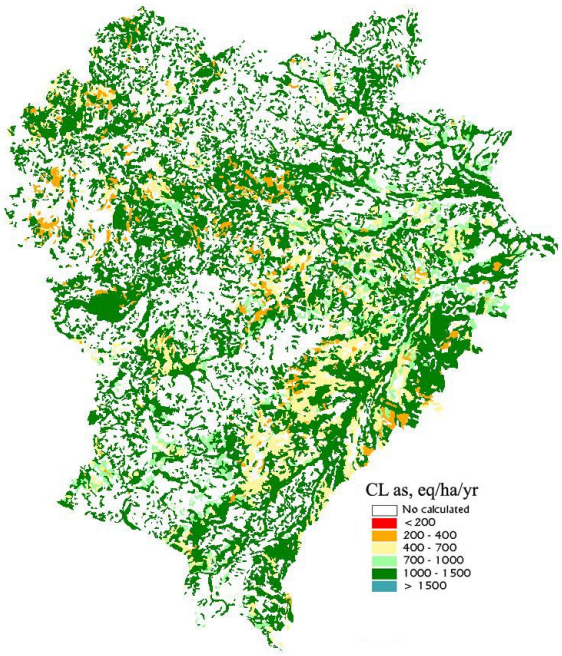


Figure BY-6. Critical loads of acidification.

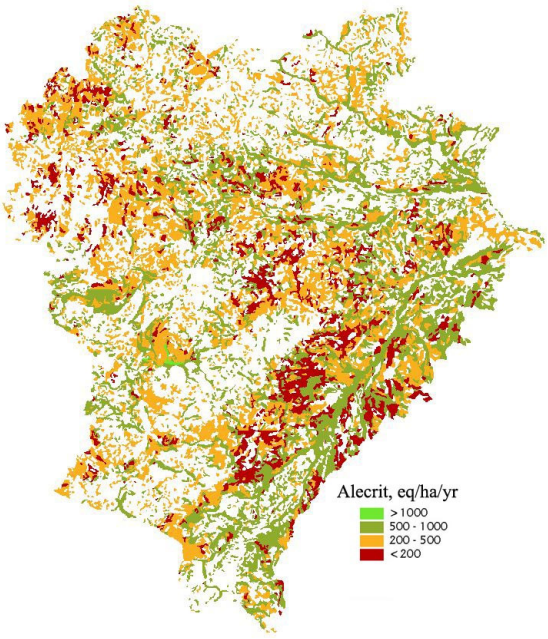


Figure BY-7. Critical ANC leaching.

Table BY-2. Summary critical load values for different terrestrial ecosystems.

Critical loads parameters [eq ha^{-1} a^{-1}]	Forest ecosystem			Grassland			Peat land		
	Min. value	Max. value	Average value*	Min. value	Max. value	Average value*	Min. value	Max. value	Average value*
$Cl_{max}(S)$	1.6	2563.2	686.5	51.5	2809.0	1256.6	24.7	2710.7	1130.4
$Cl_{max}(N)$	114.7	7428.5	1396.6	270.5	3148.2	1524.2	464.7	7428.5	2595.3
$Cl_{min}(N)$	24.7	6786.5	710.1	10.3	1668.7	267.7	77.7	6786.5	1464.9
$Cl_{nut}(N)$	27.4	6801.4	719.5	11.5	1678.5	269.5	80.7	6801.4	1479.9

* - Average value without taking account areas of polygons

Results and conclusions

The values of $CL_{max}(S)$, $CL_{max}(N)$ $CL_{min}(N)$ and $CL_{nut}(N)$ for terrestrial ecosystems are summarized in Table BY-2 and illustrated in Figures BY-2 to BY-5.

Calculated values of $CL_{max}(S)$ range between 1.6 and 2563.2 eq ha^{-1} a^{-1}, the values $CL_{max}(S)$>= 2000 are for bottomland grassland and grassland under calcic podzoluvisoils, $CL_{max}(S)$<200 are for bilberry pine forests and lichens forests on the peat lands. The lowest critical loads of $CL_{min}(N)$ are for forest ecosystem, where annual production is low, such as pine forest on the high peat lands (24-57 eq ha^{-1} a^{-1}), mixed forests on the carr lands and fen peat lands (118-570 eq ha^{-1} a^{-1}) and lichens pine forests (79-241 eq ha^{-1} a^{-1}). For other ecosystems (spruce forests, small-leaved and broad-leaved forests) $CL_{min}(N)$ range between 100 and 3700 eq ha^{-1} a^{-1}. As the most ecosystems of Belarus are formed in conditions of nitrogen deficit, the tendency for $CLnut(N)$ are similar to the above-stated. The values of $CL_{max}(N)$>500 eq ha^{-1} a^{-1} (5th percentile) are for 97% terrestrial ecosystems.

The critical ANC leaching is shown in Figure BY-7.

Critical loads of acidification, characterized resistance of ecosystems to acidify, are illustrated in Figure BY-6.

It can be concluded that the calculated values for acidity, sulfur and nitrogen give a good initial indication of the spatial variability of ecosystem sensitivity to acidification in Belarus.

Acknowledgments

The Belarussian NFC wishes to thank the Russian, German, Dutch, Polish, and Bulgarian colleagues, MSC-W, MSC-E, and the RIVM for their collaboration. The authors gratefully acknowledge S.Tsyro (Meteorological Synthesizing Centre-West) for providing modelling deposition data for the territory of Belarus for 2002, W. Mill (NFC Poland) for providing critical load database for Eastern Poland ecosystems in the EMEP grid, Prof. V. Bashkin (Russia), and Prof. H.-D. Gregor, J. Slootweg and G. Schütze for methodological support in works of critical load calculation and mapping.

Reference

Bashkin VN (1997) The critical load concept for emission abatement strategies in Europe: a review. Environ. Conserv. 24(1): 5-13

Bashkin VN, Kasimov NS (2004) Biogeochemistry – Moscow: Scientific World, pp. 527 -585

De Smet PAM, Heuvelmans E (1997) Development of the European Land Use Data Base. In: Posch et al.1997, op.cit., pp. 41-46

EMEP/MSC-W (1998) Transboundary acidifying air pollution in Europe, MSC-W Status Report 1998 – Parts 1 and 2. EMEP/MSC-W Report 1/98, Norwegian Meteorological Institute, Oslo, Norway

Hettelingh J-P, Posch M, Slootweg J (eds) (2004) Critical Loads and Dynamic Modelling results: CCE Progress Report 2004. RIVM Report 259101014, Bilthoven, The Netherlands

Lysukha N, Zalygina I (2002) The state of critical load calculation and mapping in Belarus. Proceedings of 4th training workshop on the calculation and mapping of critical loads for air pollutants for the UNECE LRTAP Convention on in East and South East European countries (Sudak, Ukraine (Crimea). 27-31 October 2002) pp. 62 -67

Lysukha NA, Zubrytski VS (2003) Methodological approaches to calculation and mapping of critical loads from oxidizing pollutants in Belarus and initial information for calculations. Proceeding 5th subregional meeting of ICPs and training-workshop on the calculation and mapping of critical loads for air pollutants relevant for the UN/ECE Convention on LRTAP in East and South East European countries, Minsk, Belarus, 24 – 26 September 2003, Minsk, 2003, pp. 57 -60

Posch M, De Smet PAM, Hettelingh J-P, Downing RJ (eds) (1999) Calculation and mapping of critical thresholds in Europe: Status Report 1999. RIVM Report 259101009, Biilthoven, The Netherlands

Posch M, De Smet PAM, Hettelingh J-P, Downing RJ (eds) (2001) Modelling and mapping of critical thresholds in Europe: Status Report 2001. RIVM Report 259101010, Biilthoven, The Netherlands

Posch M, Hettelingh J-P, Slootweg J, Downing RJ (eds) (2003) Modelling and mapping of critical thresholds in Europe: Status Report 2003. RIVM Report 259101013, Biilthoven, The Netherlands

Sidorovitch EA, Rupasova ZhA, Busko EG (1985) The functioning of forest communities under anthropogenic impact. Minsk: Nauka i Tekhnika, pp. 76-125

Sidorovitch EA, Alechno AI, Busko EG (1985) The ecological monitoring of forest communities in the Belorussia. Minsk: Nauka i Tekhnika, pp. 133-175

UBA (1996) Manual on Methodologies and Criteria for Mapping Critical Levels/Loads and geographical areas where they are exceeded. UN/ECE Convention on Long-range Transboundary Air Pollution. Federal Environmental Agency (Umweltbundesamt), Texte 71/96, Berlin

UBA (2004) Manual on methodologies and criteria for MODELING AND MAPPING CRITICAL LOADS AND LEVELS and Air Pollution Effects, Risks and Trends. UNECE Convention on Long-range Transboundary Air Pollution

BELGIUM

Flanders

National Focal Center

S. Overloop, M. Van Steertegem
Flemish Environment Agency
Van Benedenlaan 34
B-2800 Mechelen
tel: +32-15-451471
fax: +32-15-433280
s.overloop@vmm.be
www.vmm.be

Wallonia

National Focal Center

A. Fourmeaux, M. Loutsch
Ministry of Walloon Region, DGRNE
Avenue Prince de Liège 15
B-5100 Namur
tel: +32 -81-325784
fax: +32-81-325784
M.Loutsch@mrw.wallonie.be

Collaborating institutions

V. Vanderheyden, J-F. Kreit
SITEREM S.A.
Cour de la Taillette, 4
B-1348 Louvain-la-Neuve
info@siterem.be

S. Eloy
Scientific Institute for Public Services (ISSEP)
Rue du Chera, 200
B-4000 Liège
s.eloy@issep.be

University of Liège :
E. Everbecq, J. Smitz, JF. Deliège
Environmental center, Sart Tilman B5
cenv@ulg.ac.be
V. Gennotte, A Bertrand, JP Thomé, A. Goffart
Aquapôle, Quai Van Beneden,22
A.Goffart@ulg.ac.be

Catholic University of Louvain :
B. Delvaux, F. Ducarme, M. Goffin
Dept. of Soil Science
Delvaux@pedo.ucl.ac.be

Heavy Metals

The fish species considered for the health aspect in relation to atmospheric deposition of Hg is a 1 kg. pike, and therefor the TF_{HgBio} is set to 1.

BULGARIA

National Focal Centre

Yavor Yordanov
Executive Environment Agency
Tzar Boris III Str. 136
BG-1618 Sofia
tel: +359 2 9406473
fax: +359 2 9559015
landmon@nfp-bg.eionet.eu.int

Collaborating institutions

Nadka Ignatova
University of Forestry
Department of Chemistry and Biochemistry
Kitka Jorova
University of Forestry
Department of Soil Science
Kliment Ochridsky Street 10
1756 Sofia
tel: +359 2 91907 (351) (N I)
+359 2 91907 (360) (K J)
+359 2 91907 (357) (I M)
fax: +359 2 62 28 30
nadia_ignatova@hotmail.com

Maria Groseva
Department of Soil Science
Forest Research Institute
Kliment Ochridsky Street 136
1756 Sofia
tel: +359 2 62 29 61
fax: +359 2 62 29 65

Radka Fikova
Central Laboratory of Total Ecology
Bulgarian Academy of Sciences
Gagarin Street 2
1300 Sofia
tel: +359 2 719195

National maps produced

In present submission the critical loads ware mapped for main forest ecosystem types in Bulgaria: coniferous woodland and broadleaved deciduous woodland. The distributions of these ecosystems were defined from the new CORINE land cover 2000 data set (CLC, 2000). The CLC 2000 data set was used for spatial identification of receptors and determination of ecosystems area in each observed EMEP 50×50 km^2 grid cell.

Critical loads are mapped for coniferous and broadleaved ecosystems in three forest monitoring stations under ICP Forest level-II situated in three different EMEP 50×50 km^2 grid cells.

Calculation methods

Critical loads of acidity, sulphur and nitrogen were calculated for forest soils under main forest tree species using the steady-state mass balance approach and the latest recommendations provided in Mapping Manual 2004.

Table BG-1. Critical load data and computation approaches.

Parameter	Unit	Method	Source
		Critical load database and computation approaches	
$CL(A)$	eq ha^{-1} a^{-1}	$= BC_w - ANC_{le(crit)}$	Mapping Manual
$CL_{max}(S)$	eq ha^{-1} a^{-1}	$= CL(A) + BS_{dep} - BC_u$	Mapping Manual
$CL_{min}(N)$	eq ha^{-1} a^{-1}	$= N_u - N_i$	Mapping Manual
$CL_{max}(N)$	eq ha^{-1} a^{-1}	$= CL_{min}(N) + CL_{max}(S)$	Mapping Manual
$CL_{nut}(N)$	eq ha^{-1} a^{-1}	$= N_u + N_i + N_{le(crit)}$	Mapping Manual
BC_{dep}	eq ha^{-1} a^{-1}	National Forest Monitoring Data.	
BC_u	eq ha^{-1} a^{-1}	Data from national observations for main tree species Grozeva (1986), Trashliev and Ninov (1971).	
BC_w	eq ha^{-1} a^{-1}	Weathering rates of base cations for soil units in each observed EMEP grid cell – Soil map FAO, Mapping Manula (UBA, 1996).	
$ANC_{le(crit)}$	eq ha^{-1} a^{-1}	$= Al_{le(crit)} + H_{le(crit)}$	
K_{gibb}	m^6 eq^2	= 300	Mapping Manual
$N_{le(crit)}$	eq ha^{-1} a^{-1}	$= Q * [N]_{acc}$	Mapping Manual

Most of data needed for VSD running was computed and prepared regarding to Mapping Manual and national observed data. The CL and TL functions were computed for three forest monitoring stations and for dominant soil types under coniferous and broadleaved ecosystems (G1 - *Fagus sylvatica*, *Quercus frainetto*, *Quercus cerris*; G3 - *Picea abies*, *Abies alba*).

Table BG-2. Dynamic modelling data and computation approaches.

Parameter	Unit	Method	Source
		Dynamic modelling data and computation approaches	
Thick	m	Soil-dependent	National Forest Monitoring Data.
Bulkdens	g cm^{-3}	Soil-dependent	National Forest Monitoring Data
CEC	meq kg^{-1}	$(0.44.pH+3.0).clay+(5.1.pH-5.9).Corg$	Mapping manual
C_{pool}	g m^{-2}	$= 10^6.\rho_{top}.z_{top}.C_{om}.OMC$	
CNrat	Transfer function from Mapping manual		
BSat	Transfer function from Mapping manual		

Data sources

Soils: Soil type and soil property was defined from soil profiles inventory in each observed EMEP 50×50 km grid cells. The dominant soil types under main tree species was taking into account in Critical loads computation.

Weathering rate: The weathering rate in 50 cm root zone was derived as average sum of base cations, regarding to soil type observed in any of forest sites.

Table BG-3. Weathering rates for observed sites.

Site	Vitinia	Yundola	Staro Oriahovo
Weathering rate [eq ha^{-1} a^{-1}]	540	545	1170

Precipitation: Precipitation data ware derived from the map of average precipitation measured in Bulgaria by the national weather service and by directly measurements in observed sites.

Net growth uptake of base cations and nitrogen: Nitrogen and base cations net uptake rates were obtained by multiplying the element contents of the stems (N, Ca, K, Mg and Na) with average annual harvest/growth rate. Data on biomass removal for forest have been derived from the National Forest Survey Agency. The content of base cations and nitrogen in the biomass has been taken from the literature for different harvested parts (stem and bark) of the plants (Jorova, 1992; Ignatova et al., 2001; De Vries and Bakker, 1998; De Vries et al., 2001.)

Depositions: The data for base cation depositions, sulphur and nitrogen were collected from open fields and under canopy measurements in all the year round in each of observed sample plots. The air pollutant data was obtained from hourly automatic measurements under ICP Forest IInd level stations located in Vitinia, Yundola and Staro Oriahovo sample plots.

Ecosystem identification: The new CORINE Land Cover data set was used for clear spatial identification of the observed forest ecosystems and area measurements.

Results

Regarding to sulphur and nitrogen deposition data and local soil conditions, the highest levels of $CL_{max}(S)$ and $CL_{max}(N)$ was calculated in Staro Oriahovo sample plot under broadleaved receptors (*Quercus frainetto Ten*; *Quercus cerris L.*). On the other hand the lowest levels of $CL_{max}(S)$ and $CL_{max}(N)$ were found in Yundola sample plot under coniferous receptors (*Picea abies*, *Abies alba*).

The $CL(A)$ has a maximum value in Staro Oriahovo sample plots (4890 eq ha^{-1} a^{-1}) and the minimum value in Yundola sample plot (3354 eq ha^{-1} a^{-1}).

The exceedances of critical loads were not found in any of observed forest districts.

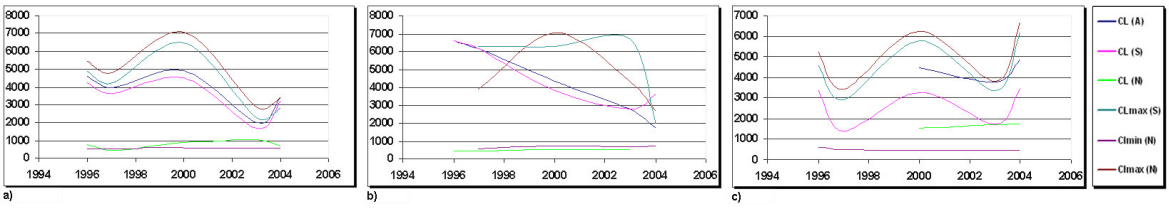


Figure BG-1. Time development of Critical loads for Vitinia –a), Yundola –b) and Staro Oriahovo –c) forest sample plots.

A complete set of the parameters for Very Simple Dynamic (VSD) model was prepared. The dynamic model 'VSD Studio 2.0' was applied for all observed forest sample plots. The CL and TL functions were computed for all three sites with pH value as a criterion. Regarding to present data and VSD outputs there is no violation of the criterion and all sites are in safe and will be in safe in asked years (2030, 2050 and 2100 – Figure BG-2).

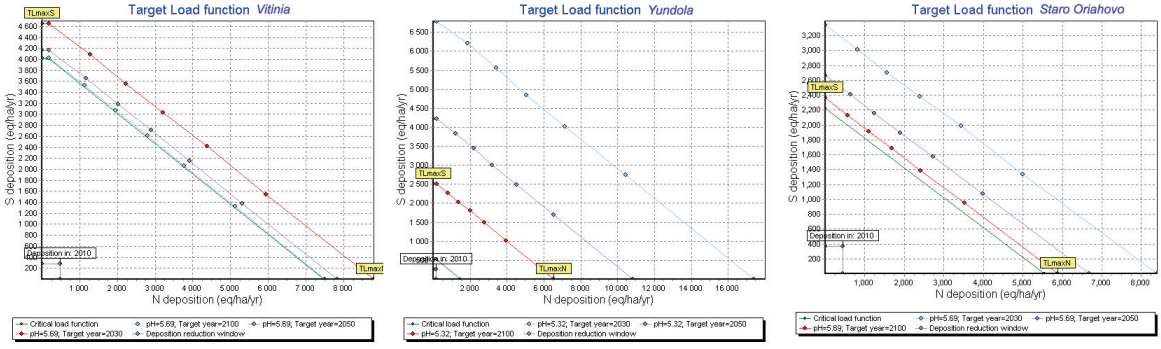
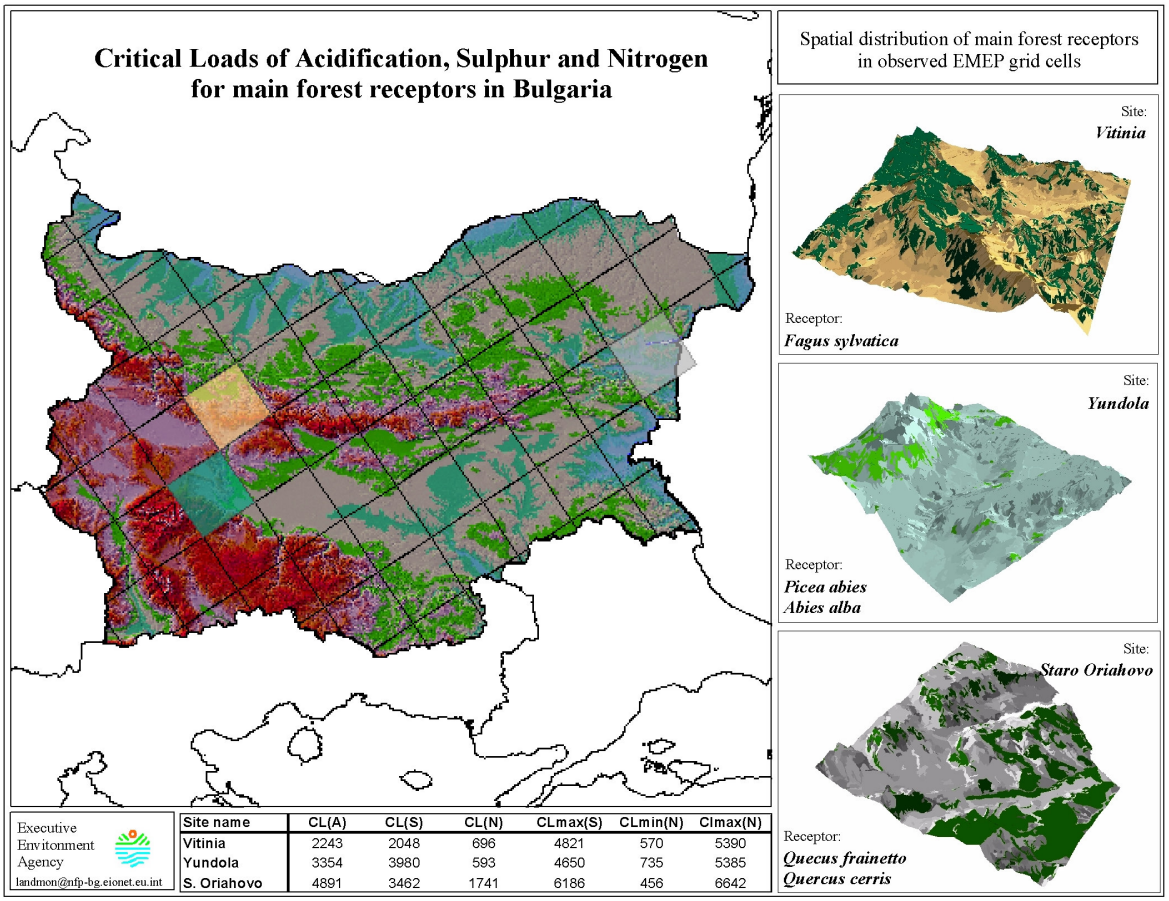


Figure BG-2. Target Load function as an output from VSD Studio 2.0 for three observed sites.



Site name	CL(A)	CL(S)	CL(N)	CLmax(S)	CLmin(N)	Clmax(N)
Vitinia	2243	2048	696	4821	570	5390
Yundola	3354	3980	593	4650	735	5385
S. Oriahovo	4891	3462	1741	6186	456	6642

Figure BG-3. Critical loads of acidification, sulphur and nitrogen.

References

De Vries W (1988) Critical deposition levels for nitrogen and sulfur on Dutch forest ecosystems. Water Air Soil Pollut. 42:221-239

De Vries W (1993) Average critical loads for nitrogen and sulfur and its use in acidification abatment policy in the Netherlands. Water Air Soil Pollut. 68: 399-434

Downing R, Hettelingh J-P, De Smet PAM (eds) (1993) Calculation and mapping of critical loads in Europe: Status Report 1993. RIVM Report 259101003, Bilthoven, The Netherlands

Ganev C (1990) Modern soil chemistry. Science and art, 372 pp

Hettelingh J-P, Downing RJ, De Smet PAM (eds) (1991) Calculation and Mapping of Critical Loads in Europe: CCE Technical Report No 1. RIVM Report 259101001, Bilthoven, The Netherlands

Hettelingh J-P, Posch M, De Smet PAM, Downing RJ (eds) (1995). The use of critical loads in emission reduction agreements in Europe. Water Air Soil Pollut. 85: 2381-2388

Hettelingh J-P, De Vries W (1992) Mapping Vademecum. RIVM Report 259101002, Bilthoven, The Netherlands

Ignatova N, Jorova K, Grozeva M, Stanev I, Kehaiov T, Trendafilov K, Tintchev G (1997) Calculation and mapping of critical loads for acid pollutants in Bulgaria.
Report 28/587. Ministry of Environment, Sofia, 93 pp. (in Bulgarian)

Ignatova N, Jorova K, Grozeva M, Trendafilov K, Tintchev G, Petkova T (1998) Manual on Methodologies for calculation and mapping of critical loads for acidity, sulfur and nitrogen for soils in Bulgaria. S., Iriss, 49 pp. (in Bulgarian)

Ignatova N, Fikova R, Jorova K, Grozeva M (1999) Comparative calculations of critical loads, using depositions in coniferous and deciduous forests. Proceedings of Training workshop on critical loads calculations for air pollutants, 27 September-2 October 1999, Pushcino, Russia, pp.100-110

Ignatova N, Jorova K, Fikova R (2000) Effect of receptors at the catchment on critical loads values of acid deposition. Proc. of 75 years LTU conf. pp. 321-330 (in Bulgarian)

Ignatova N, Jorova K, Grozeva M, Kechajov T, Stanev I (2001) Calculation and mapping of critical thresholds in Europe. Bulgaria. In: Posch et al., op. cit. pp. 114-120

Kehayov T (1986) Undergrowth waters in Bulgaria, mapping in 1:2 000 000, Vol. V, 304–307, S. BAS

Mapping Manual (2004) Manual on methodologies and criteria for MODELLING AND MAPPING CRITCAL LOADS & LEVELS and Air Pollution Effects, Risk and Trends.

Posch M, Hettelingh J-P, De Smet PAM, Downing RJ (eds) (1997) Calculation and mapping of critical thresholds in Europe. RIVM Report 259101007, Bilthoven, The Netherlands

Posch M, De Smet PAM, Hettelingh J-P, Downing RJ (eds) (1999) Calculation and mapping of critical thresholds in Europe. RIVM Report 259101009, Bilthoven The Netherlands

UBA (1996) Manual on Methodologies and Criteria for Mapping critical Levels/Loads and geographical areas where they are exceeded. UNECE Convention on Long-range Transboundary Air Pollution. Umweltbundesamt, Texte 71/96. Berlin.

CZECH REPUBLIC

National Focal Centre

Irena Skořepová, Stanislav Beneš and Ivan Pařízek
Czech Environmental Institute
Vršovická 65
CZ-100 10 Praha 10
tel: +420-2-67225270
fax: +420-2-71737721
irena.skorepova@ceu.cz

Collaborating institutions

Pravoslav Pokorný
Forest Management Institute
Nábřežní 1326
CZ-250 01 Brandýs nad Labem

Miloš Zapletal
Ekotoxa – Opava
Horní nám. 2
CZ-746 01 Opava

National maps produced

The database involves critical loads of sulphur (maximum), nitrogen (maximum and minimum), nutrient nitrogen and related data (Table CZ-1). In addition the soil parameters needed for a dynamic model application are included. The evaluation of critical loads was carried out for forest ecosystems. Three forest ecosystem types have been investigated (prevailing tree types):

- coniferous forest ecosystems – 'G3'(*Picea abies, Pinus sylvestris, Larix decidua*),
- broadleaved deciduous forest ecosystems – 'G1'(*Fagus sylvatica, Quercus robur, Quercus petraea, Carpinus betulis*),
- mixed forest ecosystems – 'G4'.

The geographic coordinates for forest ecosystems represent the polygons of the CORINE map with related soil data based on actual measured soil data were provided by the Forest Management Institute in Brandys nad Labem. Data processing includes combining the soil data with GIS layers such as temperatures, precipitation amounts, runoff, and base cation depositions. The following maps were produced:

- Maximum critical loads of sulphur
- Minimum critical loads of nitrogen
- Maximum critical loads of nitrogen
- Critical loads of nutrient nitrogen

Table CZ-1. Values involved in the database.

Variable	Name	In units
Longitude	Co-ordinate	Decimal degrees
Latitude	Co-ordinate	Decimal degrees
I50	EMEP50 horizontal coordinate	
J50	EMEP50 vertical coordinate	
EcoArea	Real area of a polygon	km^2
CLmaxS	Maximum critical loads of S	Eq ha^{-1} a^{-1}
CLminN	Minimum critical load of N	eq ha^{-1} a^{-1}
ClmaxN	Maximum critical load of N	eq ha^{-1} a^{-1}
CLnutN	Critical load of nutrient N	eq ha^{-1} a^{-1}
nANCcrit	Critical leaching of alkalinity	eq ha^{-1} a^{-1}
Nleacc	Critical nitrogen leaching	eq ha^{-1} a^{-1}
crittype	2; 1 (for peat soils)	
critvalue	0.02 eq Al^{3+} per m^3; 1 Al/BC ratio	

Variable	Name	In units
thick	Thickness of the soil	m
bulkdens	Average bulk density of the soil	g m^{-3}
Cadep	Total deposition of calcium	eq ha^{-1} a^{-1}
Mgdep	Total deposition of magnesium	eq ha^{-1} a^{-1}
Kdep	Total deposition of potassium	eq ha^{-1} a^{-1}
Nadep	Total deposition of sodium	eq ha^{-1} a^{-1}
Cldep	Total deposition of chloride (set to 50)	eq ha^{-1} a^{-1}
Cawe	Weathering of calcium	eq ha^{-1} a^{-1}
Mgwe	Weathering of magnesium	eq ha^{-1} a^{-1}
Kwe	Weathering of potassium	eq ha^{-1} a^{-1}
Nawe	Weathering of sodium	eq ha^{-1} a^{-1}
Caupt	Net growth uptake of calcium	eq ha^{-1} a^{-1}
Mgupt	Net growth uptake of magnesium	eq ha^{-1} a^{-1}
Kupt	Net growth uptake of potassium	eq ha^{-1} a^{-1}
Qle	Amount of water percolating through the root zone	mm a^{-1}
lgKAlox	Equilibrium constant for Al-H relationship (log_{10})	
expel	Exponent for Al-H relationship	-
pCO2fac	Partial CO_2 pressure in soil solution (as multiple)	-
cOrgacids	Total concentration of organic acids (m*DOC)	eq m^{-3}
Nimacc	Acceptable nitrogen immobilisation	eq ha^{-1} a^{-1}
Nupt	Net growth nitrogen uptake	eq ha^{-1} a^{-1}
Fde	Denitrification fraction	-
Nde	Amount of nitrogen denitrified	eq ha^{-1} a^{-1}
CEC	Cation exchange capacity	meq kg^{-1}
Bsat	Base saturation	-
yearbsat	Year of the base saturation determination	
lgKAlBc	Exchange constant for Al vs Bc (lg)	
lgKHBc	Exchange constant for H vs Bc (lg)	
Cpool	Amount of carbon in the top soil	g m^{-2}
Cnrat	C:N ratio in the top soil	g g^{-1}
yearCN	Year of the CNrat determination	
DMstatus		
EUNIScode	EUNIS code	

Calculation methods

Three values characterising the critical load function of acidifying S and N have been evaluated – $CL_{max}(S)$, $CL_{min}(N)$ and $CL_{max}(N)$. The critical load preventing eutrophication has been represented as the critical load of nutrient nitrogen – $CL_{nut}(N)$. Land use map classes have been used for describing forest ecosystems. The soil parameters needed for the dynamic modelling (*pH*, *Bsat*, *CNrat*, *Corg*, clay and sand compositions) have been taken from the forest soil database structured into 41 unique forest areas (forest-soil combinations?- js). The measured data have been converted to a depth of 0.5 m of the soil profile (with few exeptions). The forest soil database contains 2257 soil analyses. The equilibrium constants for Al-BC, BC-H and Al-H ion exchanges have been joined to the main soil types (sand, loess, clay and peat soils) according to the Manual for Dynamic Modelling. Soil texture characteristics have been used for the derivation of the denitrification factor f_{de}.

In addition the database comprises the assessment of weathering rates based on the local observations of rock types and related silicate analyses from the database (Skořepová et al., 1998, based on archive data from the Geological Survey, Prague). Runoff represents the amount of water percolating through the soil profile. The relationship for the assessment of 'precipitation surplus' has been used for the calculation (UBA, 2004; chapter

5.5). The critical uptakes of nitrogen, N_{upt}, and base cations, BC_{upt}, represent the average actual uptakes in the period 1990–1999 (Pondělíčková and Henžlík, 2000). The Mapping Manual (UBA, 2004) and the Manual for Dynamic Modelling (Posch et al., 2003) are the main methodological sources for the evaluation of critical loads and related data given in the CL-database.

The simple mass balance method summarised in the Mapping Manual (UBA, 2004) has been used to calculate the critical loads. The calculation of critical loads includes the following equations (the meaning of used symbols is in Table CZ-1):

$CL_{max}(S) = BC_{we} + BC_{dep} - Cl_{dep} - Bc_{upt} - (-ANC_{crit})$

$CL_{min}(N) = N_{upt} + N_{im,acc}$

$CL_{max}(N) = CL_{min}(N) + CL_{max}(S)/(1-f_{de})$

$CL_{nut}(N) = N_{upt} + N_{im,acc} + N_{le(acc)}/(1-f_{de})$

where

$ANCcrit = -Q^* ((\ [Al]_{crit} / K_{gibb}\ )^{1/3} + [Al]_{crit})$

$[Al]_{crit} = 0.02$ eq m^{-3}

For estimating the CO_2 partial pressure (Brook et al., 1983) and the organic acid concentrations (Römkens et al., 2004) in the forest soils the following equations have been used:

$\text{Log}\ (p_{CO2}) = -2.38 + 0.031 * T$,

where T = temperature of the soil (^oC)

$\text{Log}(DOC) = 2.66 + 0.7 * \log(OM) - 0.15 * pH + 1.52 * \log(solid/solution)$,

where DOC = dissolved organic carbon (mg l^{-1}),

OM = organic matter content in the soil (%),

$Solid/solution$ = dimensionless ratio of the soil solid fraction and the soil solution expressed on mass basis

Data sources

Table CZ-2. Sources of used data.

Map	Scale	Source	Updated
CORINE map		Ministry for the Environment of the Czech Republic, 2000	yes
Annual mean base cation deposition	2×2 km^2	Czech Hydrometeorological Institute, Prague (Fiala and Livorova, 2003)	no
Annual mean temperature	1:500 000	Czech Hydrometeorological Institute, Prague (Kveton et al., 1999)	no
Annual mean precipitation	1:500 000	Czech Hydrometeorological Institute, Prague (Kveton et al., 1999)	no
Database			
Soil measured data (1990 – 2000)	Localities (2257)	Forest Management Institute, Brandýs n.L. (Pokorny et al., 2001)	no
Rock composition	Localities (7228)	Czech Environmental Institute, Prague (Skorepova et al., 1998)	no

Comments and Conclusions

In comparison to evaluation of critical loads for sulphur and nitrogen published in the CCE Status Report 2003 the national database of critical loads involves only the data based on the actual measured values on soil properties

and chemistry at present. These parameters enable to apply the dynamic modelling more easily than before. The results reflect not only the actual state of the forest soils in the Czech Republic but also their relatively high spatial distribution and historical development of atmospheric deposition.

Acknowledgement

I would like to thank very much the Coordination Center for Effects, to J.-P. Hettelingh, J. Slootweg and M. Posch, for their help in dynamic modelling, processing of maps and target load calculations. The Czech NFC is moving at present from the Czech Environmental Institute for the re-organization to CENIA.

Heavy Metals

Data submission

The data involve critical loads of cadmium, lead and mercury for forest ecosystems. Human health effects due to drinking waters have been used for the calculation (Mapping Manual, 2004). The quality criteria for drinking water are taken from WHO (2004). The critical loads represent the sum of tolerable outputs from the ecosystems in terms of net metal uptake and metal leaching.

Calculation methods

Equation (1) for the evaluation of heavy metal critical loads is based on the assumption of steady-state conditions in the ecosystem. The simple mass balance model presented in the Mapping Manual (2004) can be described as:

$$CL(M) = M_u + M_{le(crit)} \quad (1)$$

where $CL(M)$ in $g.ha^{-1}.a^{-1}$ is the critical load of the heavy metal (HM), M_u is the removal of the HM by the biomass from forest ecosystems and $M_{le(crit)}$ is the critical leaching of the HM from the soil layer (0.5 m). Biomass removal represents the average actual uptake in the period of 1990 – 1999 (Pondělíčková – Henžlík eds., 2000) and the data on metal contents in harvestable biomass $[M]_{ha}$ provided in the Mapping Manual have been used in the calculation of the flux M_u (table CZ-3).

Table CZ-3. Contents of Cd, Pb and Hg in the biomass for all types of forest ecosystems.

Metal	Cd	Pb	Hg
[M]ha in mg kg^{-1} dw	0.25	1.0	0.025

The critical leaching $M_{le(crit)}$ refers to the total vertical leaching rate and it is based on the critical concentrations of heavy metals for drinking waters $M_{ss(crit)}$ (Table CZ-4) and the runoff of water percolating through the soil profile. The relationship for the assessment of 'precipitation surplus' has been used for the calculation of the runoff (UBA, 2004; chapter 5.5).

Table CZ-4. Critical concentrations for Cd, Pb and Hg used in the calculation of critical loads.

Metal	Cd	Pb	Hg
Mss(crit) in mg m^{-3}	3	10	1

Data Sources

Table CZ-5. Layers used in the evaluation of the critical loads of HM.

Map	Scale	Source
CORINE map		Ministry for the Environment of the Czech Republic, 2000
Annual mean temperature	1 : 500 000	Czech Hydrometeorological Institute, Prague (Kveton et al., 1999)
Annual mean precipitation	1 : 500 000	Czech Hydrometeorological Institute, Prague (Kveton et al., 1999)

Comments and Conclusions

Critical loads of cadmium and lead for forest ecosystems are in the ranges of 0.6 – 30 g $ha^{-1}a^{-1}$ and 2.2 – 100 g $ha^{-1}a^{-1}$, respectively. Critical loads of mercury are lower relatively and range from 0.13 to 10 g $ha^{-1}a^{-1}$. The runoff of waters percolating the soil profiles has the main influence in the all values of critical loads.

References

Pondělíčková A, Henžlík V (2000) Zpráva o stavu lesního hospodářství České republiky – stav ke dni 31.12. 1999. Ministerstvo zemědělství ČR, Lesnická práce, s.r.o., ISBN 80-86386-06-6, Praha, Česká republika (in Czech)

Posch M, Hettelingh J-P, Slootweg J (eds.) (2003) Manual for Dynamic Modelling of Soil Response to Atmospheric Deposition. CCE, RIVM, The Netherlands

Römkens PFAM, Groenenberg JE, Bonten LTC, De Vries W, Brill, J (2004) Derivation of partition relationships to calculate Cd, Cu, Ni, Pb and Zn solubility and activity in soil solutions. Alterra-report 305, Alterra, Wageningen

Skořepová I, Beneš S, Roušarová Š, Withers RH (1998) Klasifikace obsahů Cr, Cu, Ni, Zn, Pb, Fe, Al, Mg, Ca, Na, K a P v horninách ČR jako podklad pro mapování kritických zátěží těžkých kovů na území ČR. Závěrečná zpráva úkolu Kritické zátěže, Český ekologickýc ústav, Praha, Česká republika (in Czech)

UBA (1996) Manual on Methologies and Criteria for Mapping Critical Levels/Loads and Geographical Areas where they are exceeded. Federal Environmental Agency text 71/96, ISSN 0722-186X, Berlin, Germany (updated in 2004)

UBA (2004) Manual on Methologies and Criteria for Modelling and Mapping Critical Loads & Levels and Air Pollution Effects, Risks and Trends. Federal Environmental Agency Texte 52/04, ISSN 0722-186X, Berlin

GERMANY

National Focal Centre

OEKO-DATA
Hans-Dieter Nagel
Hegermuehlenstr. 58
D-15344 Strausberg
tel.: +49-3341-3901920
fax: +49-3341-3901926
hans.dieter.nagel@oekodata.com
www.oekodata.com

Calculation methods

The German NFC provides an update of the national critical load data (steady-state mass balance approach), input data for the application of the dynamic model VSD, and resulting target load functions for Germany. Critical loads are calculated in accordance to the methods described in the Mapping Manual (UBA, 2004). The German critical load database consists of 104,195 records; a detailed description of the data and the methods for derivation is given in Table DE-1.

Table DE-1. National critical load database and calculation methods / approaches.

Parameter	Variable	Unit	Description
Critical load of acidity	CLmaxS	eq ha^{-1} a^{-1}	Manual, equation 5.22
	ClminN	eq ha^{-1} a^{-1}	Manual, equation 5.25
	ClmaxN	eq ha^{-1} a^{-1}	Manual, equation 5.26
Critical load of nutrient nitrogen	ClnutN	eq ha^{-1} a^{-1}	Manual, equation 5.5
Acid neutralisation capacity leaching	nANCcrit	eq ha^{-1} a^{-1}	Manual; the minimum value of the following approaches using different chemical criteria was taken for the calculation (see crittype in the call for data): 1 [Al]:[Bc] equation 5.31 2 [Al] Derived from $Al_{le(crit)}$ in equation 5.32-5.34 by Al_{le}/Q_{le} 4 pH equation 5.35 (see Table DE-2) 6 [Bc]:[H] equation 5.36 All approaches include effects of bicarbonate leaching and dissociation of organic acids (eq. 5.43 – 5.47)
Acceptable nitrogen leaching	Nleacc	eq ha^{-1} a^{-1}	Manual, equation 5.6; see Table DE-3 for $[N]_{crit}$ values
Thickness of the soil layer	thick	m	Actually rooted zone, depending on vegetation and soil type
Bulk density of the soil	bulkdens	g cm^{-3}	German general soil map (BUEK, 1000), Hartwich et al. (1995)
Bc and Cl deposition	Cadep, Mgdep, Kdep, Nadep, Cldep	eq ha^{-1} a^{-1}	National total deposition data for the year(s) 1999 (Bc) and 1997-99 (Cl), Gauger et al. (2003)
Weathering of base cations	Cawe; Mgwe and Kwe = 0	eq ha^{-1} a^{-1}	Manual, equation 5.39, Manual, table 5.12-5.14
Weathering of Na	Nawe	eq ha^{-1} a^{-1}	Manual 5.3 p. 23
Uptake of base cations by vegetation	Caupt; Mgupt and Kupt= 0	eq ha^{-1} a^{-1}	Manual, equation 5.8 (without branches) Manual, table 5.8 for element contents, Jacobsen et al. (2002)
Amount of water percolating through the root	Qle	mm a^{-1}	German hydrological atlas BGR (2002)

Parameter	Variable	Unit	Description
zone			
Gibbsite equilibrium constant	lgKAlox (Kgibb)	(m^6 eq^{-2})	Manual 5.3 p.21 (constant $\log_{10}(10^8$ m^6 $eq^{-2})$)
Partial CO_2-pressure in soil solution in relation to the atmospheric CO2 pressure	pCO2fac		Manual, equation 5.44
Total concentration of organic acids	cOrgacids	eq m^{-3}	Manual equation 5.46 with values for DOC by De Vries et al. (2004): Calculation of critical loads for cadmium, lead and mercury. Table A11.1
Nitrogen immobilisation	Nimm	eq ha^{-1} a^{-1}	Vegetation period dependent, coniferous forest and heaths 2-5 kg ha-1 a-1, all other vegetation types 1-4 kg ha-1 a-1
Nitrogen uptake by vegetation	Nupt	eq ha^{-1} a^{-1}	Manual, equation 5.8 (without branch) Manual, table 5.8 for element contents, Jacobson et al 2002
Denitrification factor	fde	-	Depending on pore volume for pF>4.2, influence of (ground) water on the horizons and nutrient availability according to Manual Table 5.9
Cation exchange capacitiy	CEC	meq kg^{-1}	Bodenkundliche Kartieranleitung (1994)
Base saturation	bsat		Based on Level I forest soil inventory in Germany
Exchange constant for Al vs. Bc	lgKAlBc		Gapon, based on Manual, Table 6.4
Exchange constant for Al vs. H	lgKAlH		Gapon, based on Manual, Table 6.4
Initial amount of carbon in the topsoil	Cpool	g m^{-2}	Based on Level I forest soil inventory in Germany
C:N ratio in the topsoil	Cnrat		Based on Level I forest soil inventory in Germany
EUNIS code	EUNIScode		Schlutow (2004)

Most of the data are based on soil properties described for the reference profiles of the units of the General Soil Map of Germany (BUEK, 1000; Hartwig et al., 1995). Climate data were provided by German Weather Services. Both the precipitation and temperature are 30 year means (1971–2000).

Table DE-2. Buffer substance systems and their lowest acceptable base saturation (Ulrich 1985, adapted).

Buffer substance system	lowest acceptable pH	BUEK-unit Legend-No.
Carbonate buffer ($CaCO_3$)	6.2	54
Silicate buffer (primary silicates)	5.0	2, 3, 4, 5, 8, 9, 11, 12, 13, 14, 15, 21, 22, 29, 35, 36, 37, 38, 39, 40, 41, 44, 47, 48, 49, 68, 69
Exchange buffer (clay minerals)	4.5	18, 24, 42, 45, 46, 50, 51, 52, 53
Manganese oxides/ clay minerals	4.2	10, 19, 23, 26, 28, 43
Aluminum buffer (n $[Al(OH)_x^{(3-x)+}]$, Aluminum hydroxosulfates)	4.0	65, 66, 67, 70
Aluminum/iron buffer (Aluminum buffer, plus 'soil-$Fe(OH)_3$')	3.8	1, 6, 7, 16, 17, 20, 25, 27, 30, 31, 32, 55, 56, 58, 64
Iron buffer (iron hydrite)	3.2	33, 34, 57, 59, 60, 61, 62, 63, 71

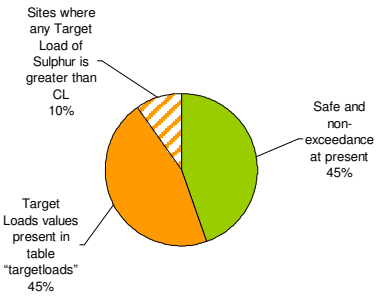
The pH in soil solution should not have values below the lower limit of the recent buffer system.

Table DE-3. Acceptable nitrogen concentrations (according to Mapping Manual Table 5.7).

vegetation type	[N]crit
deciduous forest	0.0276
coniferous forest	0.0143
mixed forest	0.02142
heats	0.02142
bogs	0.0143

Table DE-4. Status of the target load calculation in Germany.

No. of Sites (=km²)	
Sites calculated with SMB:	104,195
Sites calculated with VSD:	104,195
Results for all sites:	
Sites safe and non-exceedance at present:	46,556
Target Loads values present in table 'targetloads'	57,639
Sites where any Target Load of Sulphur is greater than CL	10,260
Potential valid Target Loads in table 'targetloads'	47,379



Status of the Target Loads in target years

Target year 2030	
Non-exceedance & non-violation in Target year	12,458
TL function present	33,856
Target load not feasible	1,438
Target load for Sulphur greater than CLmax(S)	9,887
Target year 2050	
Non-exceedance & non-violation in Target year	12,771
TL function present	34,026
Target load not feasible	1,225
Target load for Sulphur greater than CLmax(S)	9,617
Target year 2100	
Non-exceedance & non-violation in Target year	13,072
TL function present	34,262
Target load not feasible	837
Target load for Sulphur greater than CLmax(S)	9,468



Heavy Metals

Rather than a default value (15 *atmospheric), p_{CO2} is set according equation 5.44 from the Manual.

References

Bodenkundliche Kartieranleitung (1994) Hrsg.: Bundesanstalt für Geowissenschaften und Rohstoffe und Geologische Landesämter, 4. Auflage

De Vries W, Bakker DJ (1998) Manual for calculation critical loads of heavy metals for terrestrial ecosystems, DLO Winand Staring Center. Report 166

De Vries W, Posch M (2003) Derivation of cation exchange constants for sand loess, clay and peat soils on the basis of field measurements in the Netherlands. Alterra-Rapport 701, Alterra Green World Research, Wageningen, The Netherlands, 50 pp

Gauger Th, Anshelm F, Schuster H, Erisman JW, Vermeulen AT, Draaijers GPJ, Bleeker A, Nagel HD (2003) Mapping of ecosystem specific long-term trends in deposition loads and concentrations of air pollutants in Germany and their comparison with Critical Loads and Critical Levels, Part 1: Deposition Loads 1990 – 1999, Final Report UBA 299 42 210, Institut für Navigation der Universität Stuttgart, on behalf of the Federal Environmental Agency (Umweltbundesamt), Berlin

Hartwich R, Behrens J, Eckelmann W, Haase G, Richter A, Roeschmann G, Schmidt R (1995) Bodenübersichtskarte der Bundesrepublik Deutschland 1 : 1 000 000. Karte mit Erläuterungen, Textlegende und Leitprofilen. Bundesanstalt für Geowissenschaften und Rohstoffe, Hannover (BÜK 1000) und Daten der Schätzprofile für die Leitböden

Jacobsen C, Rademacher P, Meesenburg H, Meiwes KJ (2002) Element contents in tree compartments – Literature study and data collection (in German). Report, Niedersächsische Forstliche Versuchsanstalt, Göttingen, Germany, 80 pp

Schlutow A (2004), CORINE Land Cover application for assessment and mapping of critical loads in Germany, Proceedings of the CORINE workshop, Berlin, 21.01.2004

Schöpp W, Posch M, Mylona S, Johansson M (2003) Long-term development of acid deposition (1880-2030) in sensitive freshwater regions in Europe. Hydrology and Earth System Sciences 7(4): 436-446

UBA (2004): Manual on Methodologies and Criteria for Modelling and Mapping Critical Loads & Levels and Air Pollution Effects, Risks and Trends. Federal Environmental Agency (Umweltbundesamt) Berlin, UBA-Texte 52/04 (download via internet: www.icpmapping.org)

FRANCE

National Focal Centre

Anne Probst
David Moncoulon
Laboratoire des Mécanismes de Transferts en Géologie
LMTG
UMR 5563 CNRS/UPS/IRD
14, avenue Edouard Belin
F-31400 Toulouse
aprobst@lmtg.obs-mip.fr
dmoncou@lmtg.obs-mip.fr

Jean-Paul Party
Sol-Conseil
251 rte La Wantzenau - Robertsau
F-67000 Strasbourg

Collaborating institutions

Laurence Galsomiès
Christian Elichegaray
ADEME
Centre de Paris - Vanves
Département Air
27, rue Louis Vicat
F-75737 Paris cedex 15

Erwin Ulrich
Luc Croisé
Office National des Forêts
Direction Technique
Département Recherche et Développement
Réseau RENECOFOR
Boulevard de Constance
F-77300 Fontainebleau

Louis-Michel Nageleisen
Ministère de l'Agriculture, de l'Alimentation, de la Pêche et des Affaires Rurales (DGFAR)
Département de la Santé des Forêts Antenne Spécialisée
Cenre INRA de Nancy
F-54280 Champenoux

Anne-Christine Le Gall
Direction des Risques Chroniques
Unité MECO
INERIS BP N°2
F-60550 Verneuil en Halatte

Marc Rico
Monique Allaux
Ministère de l'Ecologie et du Développement Durable
Bureau de la pollution atmosphérique, des équipements énergétiques et des transports
Direction de la Pollution et de la Prévention des Risques
20, avenue de Ségur
F-75007 Paris

Introduction

The French ecosystem classification was updated in 2003 for calculation and mapping of the critical loads of acidity and nutrient nitrogen (Probst et al., 2003; Moncoulon et al., 2004). A first critical loads database for

acidity and nutrient nitrogen corresponding to this new classification was sent in 2003 to the Coordination Center for Effects. In 2004, the French NFC has provided updated calculations of critical loads and input data required for dynamic modelling. Preliminary results on target loads calculation were also sent to the Coordination Center for Effects (Probst et al., 2004).

In 2005, the French National Focal Centre provided an update of the national critical load data:

- updated critical load values for acid nitrogen and sulphur;
- updated critical load values for nutrient nitrogen;
- new calculations of target loads using dynamic modelling.

For nutrient nitrogen, following a regional meeting for comparison of critical loads of adjacent countries, an important work has been provided on nitrogen uptake values for updating critical load of nutrient nitrogen. For dynamic modelling, updated data for soil parameters and atmospheric deposition data were used as basic parameters.

The studied area, representing French forest and natural vegetation ecosystems, consists of 180,101 km^2, i.e. 32% of France total area.

Calculation method

Steady state critical loads

The Steady State Mass Balance (SSMB) model was applied on the soil top layer (0-20 cm) as described in Posch et al. (1995). All calculations have been made by the French NFC and compared with VSD model (Posch et al., 2003) outputs of critical loads. The critical loads for sulphur (Eq. 1), acid nitrogen (Eq. 2, 3) and nutrient nitrogen (Eq. 4) were calculated as follows:

$$CL_{max}(S) = BC_{dep} + BC_w - BC_u + ANC_{le}(crit) \quad \text{(Eq. 1)}$$

$$CL_{min}(N) = N_i + N_u \quad \text{(Eq. 2)}$$

$$CL_{max}(N) = CL_{min}(N) + CL_{max}(S)/(1-f_{de}) \quad \text{(Eq. 3)}$$

$$CL_{nut}(N) = N_i + N_u + N_{le}/(1-f_{de}) \quad \text{(Eq. 4)}$$

BC_{dep}, BC_w and BC_u are respectively the atmospheric deposition, the weathering rate and the vegetation uptake for base cations. $ANC_{le(crit)}$ is the critical leaching of acid neutralising capacity. N_i, N_u, N_{le} are respectively the immobilisation, uptake and leaching rate of total nitrogen. f_{de} is the denitrification factor.

Dynamic modelling

The objective of the 2005 call for data is (i) to apply dynamic modelling to determine the ecosystem response to variation in acid atmospheric deposition (ii) to calculate target loads. Among the available dynamic models, VSD model (Posch et al., 2003) application has been compared with that of SAFE model (Sverdrup et al., 1995) on French ecosystems (Probst et al., 2003; Moncoulon et al., 2003).

For acid ecosystems (eolian sandy soil, sandstones, schists of Britanny), acceptable differences were observed between the 2 model outputs. For soils with higher buffering capacity, significant differences appeared between the model outputs.

In order to derive target loads on French ecosystems, VSD model has been calibrated with the SAFE model outputs. However, since target loads are only calculated on the most sensitive ecosystems, VSD outputs are reasonably consistent with the other models outputs.

Several NFCs from adjacent countries met in the early 2005 to compare critical loads and input data from boundary regions. One of the most important conclusions of this meeting was the need for improvement of consistency between the adjacent countries. VSD model is the model which application is the easiest because it does not need lot of basic data and provides relative consistency most easy. However, an important calibration work is necessary for its application.

Input data for dynamic modelling

Table FR-1. Critical loads and dynamic modelling parameters used for 2005 calculations.

Parameter	Unit	Description
Chem. criterion used and critical value		See table 3
$N_{le(acc)}$	$eq.ha^{-1}.a^{-1}$	0 for plain decideous forest; 50 for plain coniferous forest; 100 for mountain forest ecosystems (Party and Thomas, 2000)
Bc_{dep}	$eq.ha^{-1}.a^{-1}$	RENECOFOR network measurements extrapolated at the national scale (Ulrich et al., 1998 ; Croisé et al., 2002)
Bc_{we}	$eq.ha^{-1}.a^{-1}$	PROFILE simulations (Party, 1999)
Bc_{upt}	$eq.ha^{-1}.a^{-1}$	Calculated from [BC] in vegetation (Party, 1999) and net uptake of biomass by harvesting (IFN, 2002)
N_u	$eq.ha^{-1}.a^{-1}$	Calculated from [N] in vegetation (Party and Thomas, 2000) and net uptake of biomass by harvesting (IFN, 2002)
f_{de}	$eq.ha^{-1}.a^{-1}$	Extrapolated from Guidance manual data (UBA, 1996) to french soil conditions (see table FR-2)
All soil parameters		From RENECOFOR network data (Brethes and Ulrich, 1997) and CCE network data (Badeau and Peiffer, 2001). See table FR-4 (Brethes and Ulrich, 1997)

Table FR-2. Denitrification factor values (adapted from UBA, 2004).

Soil type	f_{de}
Non hydromorphic soil	0.05 to 0.2
Hydromorphic silt or sandy soil	0.3
Hydromorphic clay	0.4
Peat soil and marshes	0.5

Table FR-3. Critical limit value.

Soil and bedrock type	ANC criteria	Critical limit value
Soft calcareous sediments	Al/BC	1.2
Hard calcareous sediments	Al/BC	1.2
Soft acid sediments		
Sands	pH	4.6
Sandy silex formations	pH	4.6
Others	Al/BC	1.2
Hard acid sediments		
Schists	pH	4.6
Sandstones	pH	4.6
Others	Al/BC	1.2
Metamorphic rocks		
Acid granite	pH	4.6
Others	Al/BC	1.2
Volcanic rocks	Al/BC	1.2

Table FR-4. Soil parameters.

	Units	Min	Max	Median
Bulk density	$g.cm^{-3}$	0.732	1.4	0.915
Conc. Org. Acids	$eq.m^{-3}$	0	0.02436	3.5×10^{-5}
CEC	$meq.kg^{-1}$	1	38	20
Base saturation	-	0.12	1	0.78
Carbon	$g.m^{-2}$	3920	14000	9878
C:N ratio		12	28	15

The total concentration of organic acids in soil solution is calculated from DOC (Dissolved Organic Carbon) which is estimated from pH and clay content in soil layer. To be consistent with critical load calculations, only one soil layer (the top layer) must be taken into account to compute target loads. Therefore all French soils were assumed to consist of a single soil layer. For French forest soils, the first 20 centimetres were considered as the receptor for target loads (which is consistent with critical loads methodology). Due to the lack of data, only one value (5 atm) was considered for p_{CO2} in the topsoil.

Results

Critical loads of nutrient nitrogen

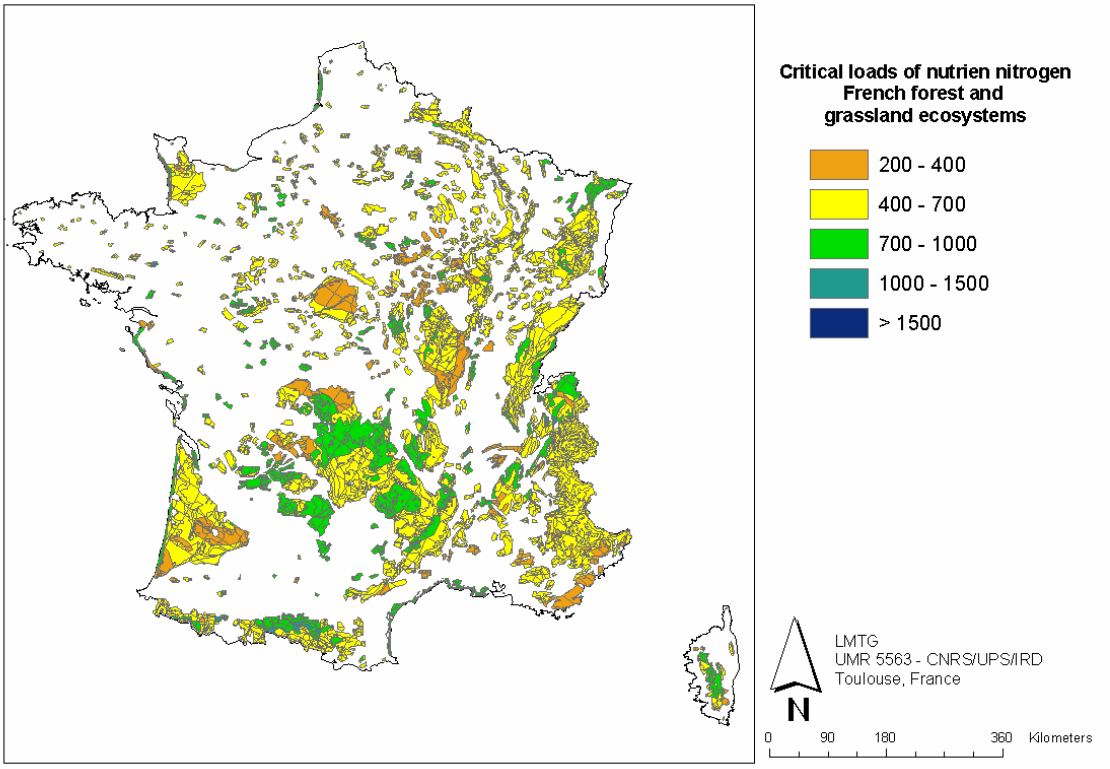


Figure FR-1. Forest and grassland ecosystems: Critical Loads of nutrient nitrogen.

The most sensitive areas for nitrogen eutrophication are located in the Sologne (Centre part of France) and the Landes marshes (SW), the northern part of Massif Central and the eastern Mediterranean area (Figure FR-1). Empirical values for critical loads of nutrient nitrogen have been applied to costal zones (EUNIS code B1.4) and are thus different from 2003 values (which were more sensitive).

The critical loads of nutrient nitrogen show a global sensitivity of the French ecosystems. The lowest critical load values larger than 400 eq $ha^{-1}a^{-1}$ or < 5.6 kgN $ha^{-1}a^{-1}$) represent 24,927 km^2 (13.8% of the studied area). Critical load values smaller than 700 eq $ha^{-1}a^{-1}$ (< 9.8 kgN $ha^{-1}a^{-1}$) represent 143,117 km^2 (79.4% of the studied area, i.e. forests and natural grasslands).

Total nitrogen deposition in France is estimated by EMEP model in 1995 to:

- 4 to 10 kgN.ha^{-1}.a^{-1} in the southern half part of the territory (approximately south of the Loire river);
- 10 to 20 kgN.ha^{-1}.a^{-1} in the northern half part of the territory (north of the Loire river).

Total nitrogen deposition in France calculated and extrapolated from RENECOFOR network (Croisé et al., 2002) indicates a:

- global deposition level for France: 9 to 12.5 kgN ha^{-1} a^{-1};
- highest deposition: 12.5 to 15.8 kgN ha^{-1} a^{-1} located in the Pyrenées, the Massif Central, the northern Alps, the Jura and the Vosges mountains;
- lowest deposition: 6.8 to 9 kgN $ha^{-1}a^{-1}$ located in Mediterranean area, the southern Alps, the coastal Corse and the southern Brittany.

Depending on the deposition data sources, EMEP or RENECOFOR, the deduced exceedances will be significantly different. However, regarding both network data, it appears that the entire territory is exposed to high deposition and exceedances.

Critical loads of nutrient nitrogen calculated with the Simplified Mass Balance equation are very sensitive, comparing with empirical critical loads (Party and Thomas, 2000).

Critical loads of sulphur

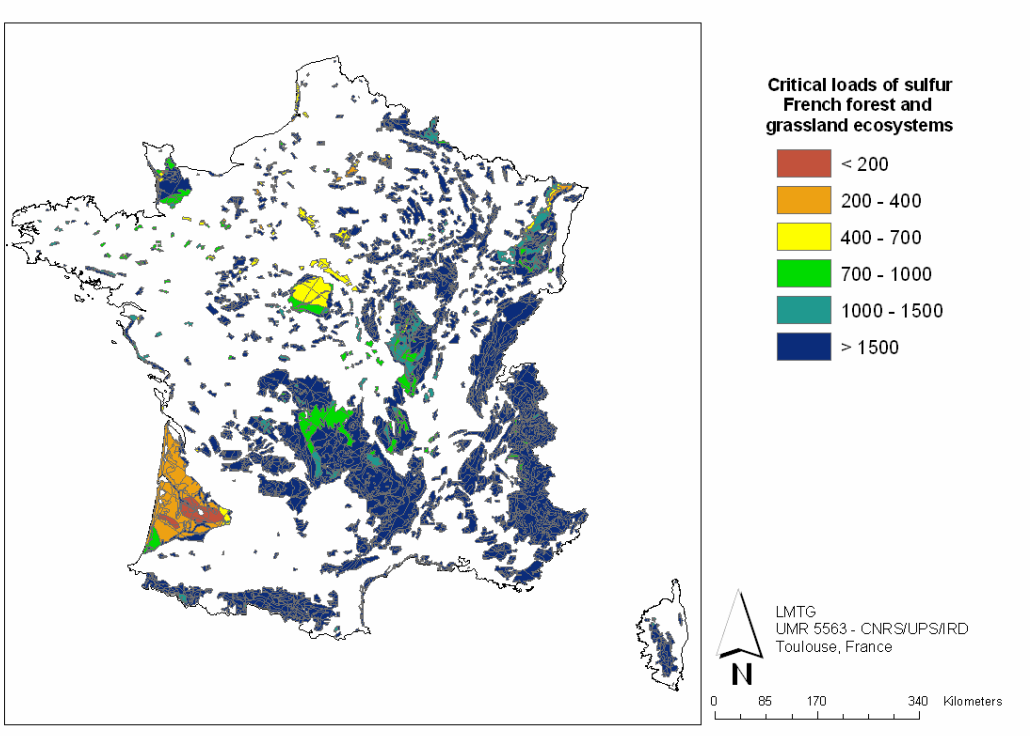


Figure FR-2. Forest and grassland ecosystems: Critical loads of sulphur.

Critical loads of sulphur have been updated in 2005 (Figure FR-2) by recalculation of cations throughfall deposition, taking into account the cycle between biomass uptake and re-deposition. The only significant

differences between 2004 and 2005 critical loads appear in the granite of Massif Central (more sensitive) and in the granite of the Vosges mountains (more sensitive).

Target loads of sulphur and nitrogen

Between 1880 and 2010, exceedance occurred on 387 out of 4145 ecosystems. The total exceeded surface represents 21,537 km^2 (12% of the forest and grassland area or 3.8% of the national area).

Exceedances concerns mostly (see also Figure FR-3):

- southwest of France : acid sands of the Landes forest and marshes;
- granitic ecosystems of the Massif Central;
- granitic and sandstone ecosystems on the Vosges mountains;
- eolian sands in the centre and north of France;
- the Ardennes mountains;
- shist of Brittany and Normandy.

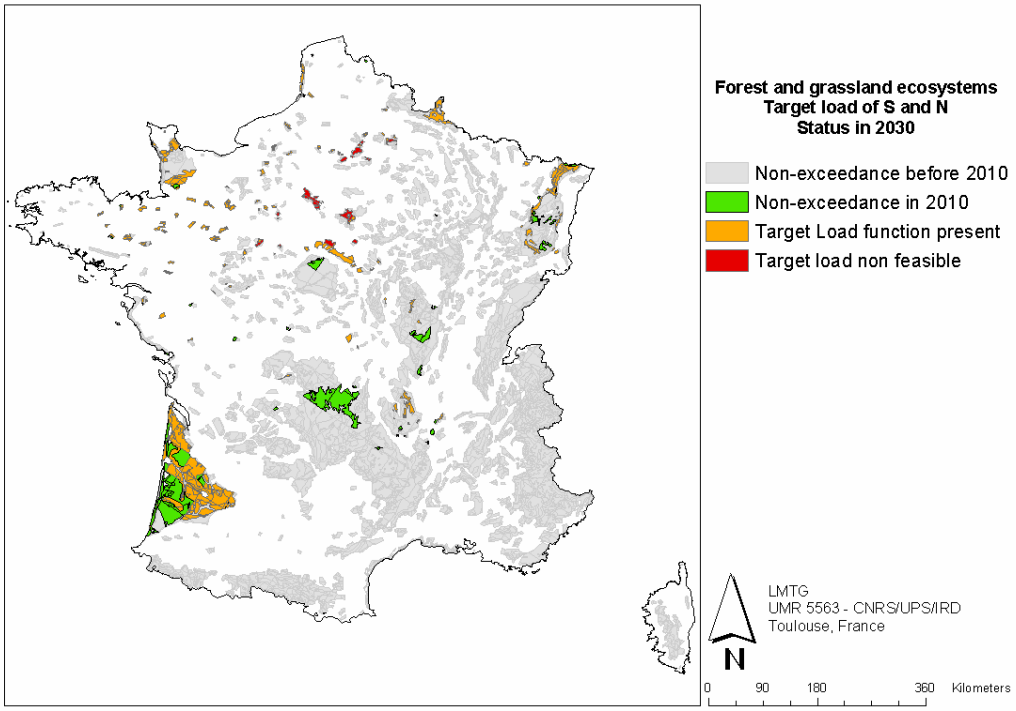


Figure FR-3. Forest and grassland ecosystems: Target Loads of S and N. Status in 2030.

Among these areas, according to the Gothenburg protocol for reduction of acid deposition, some ecosystems located in the south of the Landes, north and north-east of the Massif Central, and the Sologne marshes will not be exceeded in 2010, as predicted by the model outputs.

Among the ecosystems which will still be exceeded in 2010, target loads can be calculated. The implementation year fixed for this call for data is 2020: deposition linearly decreases from 2010 Gothenburg protocol deposition to 2020 target load value.

With 2020 deposition value fixed to zero as a test, a few ecosystems will not even recover : all the concerned ecosystems are located in the vicinity of Paris: the oak forest and beech forest on acid sands in the Parisian bassin and the north of Paris ; the oak forest on silt formations in the north of Paris.

Target loads are finally calculated for the following ecosystems:

- pine forest and marshes on acid eolian sands in the north of the Landes;
- oak and beech forest on schists in Brittany and Normandy;
- oak forest on tertiary sands near Sologne marshes;
- oak forest on shists in the Ardennes mountains;
- beech or spruce forest on sandstone or granitic ecosystems in the Vosges mountains;
- beech forest on acidic granites in the northern part of Massif Central.

On these ecosystems, further reductions have to be added to critical load values to reach a safe state in the target year: 2030, 2050 and 2100.

References

Badeau V, Peiffer M (2001) Base des données écologiques des placettes françaises du Réseau Européen de suivi des dommages forestiers (réseau 16 x 1-km). Premier inventaire: juillet 1993 – Octobre 1994 Deuxième inventaire: mai à août 1999. Département Santé des Forêts Antenne Spécialisée. 17pp

Brêthes A, Ulrich E (1998) RENECOFOR: Caractéristiques pédologiques des 102 peuplements du réseau. Office National des Forêts, Département des Recherches Techniques, 573 pp

Croise L, Duplat P, Jaquet O, Ulrich E (2002) Deux approches indépendantes pour l'estimation des dépôts atmosphériques totaux hors couvert forestier sur le territoire français en vue d'établir des cartes d'excès de charges critiques d'acidité. Rapport ADEME définitif n°99 62 008. 105pp

Inventaire Forestier National (2002) Synthèse par département. Internet site: www.ifn.fr/pages/index-fr.html

Moncoulon D, Probst A, Party JP (2004) Critical loads of acidity: importance of weathering, atmospheric deposition and vegetation uptake for ecosystem sensitivity determination. C.R. Geoscience 336: 1417-1426

Party JP (1999) Acidification des sols et des eaux de surface des écosystèmes forestiers français : facteurs, mécanismes et tendances. Taux d'altération sur petits bassins versants silicatés. Application au calcul des charges critiques d'acidité. Thèse de Doctorat, Université Louis Pasteur de Strasbourg. 233 pp

Party JP, Thomas AL (2000) Cartographie de la végétation et charges critiques azotées pour la France. Rapport ADEME définitif (marché n°99 62 020)

Posch M, De Vries W, Hettelingh J-P (1995) Critical loads of sulfur and nitrogen. In: Posch M, De Smet PAM, Hettelingh J-P, Downing RJ (eds) Calculation and mapping of Critical Tresholds in Europe: Status Report 1995. RIVM Report 259101004, Bilthoven, Netherlands. 182pp

Posch M, Reinds GJ (2003) VSD - User Manual of the Very Simple Dynamic soil acidification model. Coordination Center for Effects (RIVM), Bilthoven, The Netherlands (in prep.)

Probst A, Moncoulon D, Party JP (2003) French National Focal Center report. In: M. Posch, J-P Hettelingh, J Slootweg, RJ Downing (eds), Modelling and Mapping of Critical Treshold in Europe: CCE Status Report 2003. RIVM Report 259101013, Bilthoven, The Netherlands, pp. 73-80

Sverdrup H, Warfinge P (1995) Estimating field weathering rates using laboratory kinetics. Reviews in mineralogy, vol. 31. Chap 11, 485-541.

UBA (1996) Manual on methodologies and criteria for mapping critical levels/loads and geographical areas where they are exceeded. UNECE Convention on Long Range Transboundary Air Pollution. Federal Environmental Agency (Umweltbundesamt), Berlin

UBA (2004): Manual on Methodologies and Criteria for Modelling and Mapping Critical Loads & Levels and Air Pollution Effects, Risks and Trends. Federal Environmental Agency (Umweltbundesamt) Berlin, UBA-Texte 52/04 (download via internet: www.icpmapping.org)

Ulrich E, Lanier M, Combes D (1998) RENECOFOR – Dépôts atmosphériques, concentrations dans les brouillards et dans les solutions de sol (sous-réseau CATAENAT) – Rapport scientifique sur les années 1993 à 1996. Editeur : Office National des Forêts, Département des Recherches Techniques, ISBN 2-84207-134-4, 135 pp

HUNGARY

National Focal Centre

Miklós Dombos, László Pásztor, József Szabó
Research Institute for Soil Science and Agricultural Chemistry
Hungarian Academy of Sciences
1022 Budapest Herman Ottó u. 15
tel: +36-1-3564682
fax: +36-1-3564682
dombos@rissac.hu

Introduction

Critical loads for the Hungarian forest ecosystems have been updated in 2003. The database provided in 2003 has been derived from the AGROTOPO soil database and the CORINE Land Cover database linked to additional information on spatial distribution of forests. To improve critical load modelling further database has been involved. The Hungarian Soil Monitoring Database (TIM) used in last year fulfilled the requirements of input parameters of the models (e.g. MakeDep, SAFE). However results of modelling have to be tested further thus critical data for acidification provided in 2004 are still valid until the next call.

Data sources

Soil Information and monitoring system (TIM).

Based on physiographical-soil-ecological units 1236 representative observation points were selected of which 183 sites are in forests. Monitoring was in 1992, measurements are repeated 1, 3 or 6 years depending on the stability of soil variables. Most of the soil parameters in the model have been gathered from measured data (Table HU-1).

Biomass variables were derived from ICP sites (nutrient content) except the actual biomass, which was measured in sites (estimated from standing biomass classes) (Table HU-2).

Mineralogical data was gathered from a mineralogical map. This is the weakest point of the data acquisition, because of the spatial resolution and the method of the estimation of mineral composition (Table HU-3).

Results

Cumulative distributions of some input parameters have been showed in figure HU-1. Values of these parameters are measured or estimated at sites. Histogram of base saturation differs significantly from dataset used in last years having a lower range. In Figure HU-2 time series of modelled response variables, like pH, base saturation and Bc:Al ratios have been illustrated in one site as an example. These curves are produced in all calibrated sites.

Figure HU-3 shows the results of critical load modelling. The most inner points show the exceedance of critical loads; red points correspond to the occurrence of an exceedance, sites with blue points are not exceedance and grey points indicate that the calibration failed. The outside circles show the base saturation and pH in the three soil layers. An earlier assessment of the soil acidification is illustrated in the background of the maps, showing the susceptibility of soil acidification in ordinal scale. Red and brawn patches are higher susceptibility to acidification, whereas blue patches are calcareous soils.

Conclusions:

- Hungarian soil monitoring database fulfilled the input requirements of MakeDep/SAFE models.

- 183 forest sites were enough to characterize the spatial heterogeneity of soil acidification status in country scale.
- Calibration failed at several sites that are to be checked later on.
- In many sites the results of the earlier soil susceptibility map and the critical load exceedances were consistent although output inconsistencies occurred at several sites. This might be explained by the nutrient nitrogen exceedances that are in the focus of the next modelling goals.

Table HU-1. Soil parameters of the SAFE model.

Soil parameters	
layers	3 layers according to the soil genetic classification
layer thickness	Measured
Evaporation fraction	0.2
Lateral flow	0 –not estimated
rel Bc uptake	Derived according to measured Bc concentrations in layer solution
rel N uptake	Derived according to measured NO3 conc. in layer solution
soil bulk density	Measured
soil moisture content	According to the potential plant available soil moisture content /measured values of pF=4.2-pF=2.5/
mineral surface area	Derived from particle size distribution (Xi) that are measured at sites Mineral surface area = 0.3*Xsand+2.2*Xsilt +6*Xclay)*Bulk density*1000
cation exchange capacity	Measured
E Ca	Measured
E Mg	Measured
E K	Measured
soil solution DOC	Arbitrary according to layers: in A layer =20, B = 5, C = 2
soil solution p_{CO2}	Arbitrary according to layers: in A layer =2, B = 5, C = 10
Al solubility coefficient	-
SO_4 to H ratio	-
q SO_4	-
p1 SO_4	-
p2 SO_4	-
field capacity	-
wilting point	-

Table HU-2. Biomass parameters of the SAFE model.

Biomass parameters	
Stem mass	Estimated by forest yield classes
Branch and Canopy mass	Estimated from measured values at ICP sites, derived according to tree species and the estimated stem biomass
Mineralization rate	0.15
LF miner rate	0.95
Coniferous Deciduous ratio	0 or 1
Deciduous litter fraction	1
Coniferous litter fraction	0.14
Growth func. N	2.4551
Growth func. K for stem	61.937
Growth func. K for root	-
Growth func. K for bark	-
Growth func. K for branch	61.937
Growth func. K for canopy	20.65
Ca, Mg, K, Na contents in stem, branch and canopy:	Measured in ICP sites, derived according to tree species

Table HU-3. Clay mineral composition used in modelling.

Mineral composition types	'K-Feldspar:'	'Plagioclase:'	'DutchClay:'	'Smektite:'	'Muscovite:'	'illite-1:'	'illite-2:'	'illite-3:'	'Mg-Chlorite:'	'illite-verm:'	'Biotite:'	'Verm-1:'	'Verm-2:'	'Verm-3:'
1	0	0	0	0.25	0	0.5	0	0	0.250		0	0	0	0
2	0	0	0	0.1	0	0.4	0	0	0.4	0	0	0.1	0	0
3	0	0	0	0.1250		0.250		0	0.250	.1250		0.250		0
4	0	0	0	0.4	0	0.3	0	0	0.3	0	0	0	0	0
5	0	0	0	0.35	0	0.350		0	0.1	0.1	0	0.1	0	0
6	0	0	0	0.25	0	0.2	0	0	0.250	.1	0	0.2	0	0
7	0	0	0	0.3	0	0.250		0	0.1	0.1	0	0.250		0
8	0	0	0	0.55	0	0.150		0	0.150		0	0.150		0
9	0	0	0	0.5	0	0	0	0	0	0	0	0	0	0

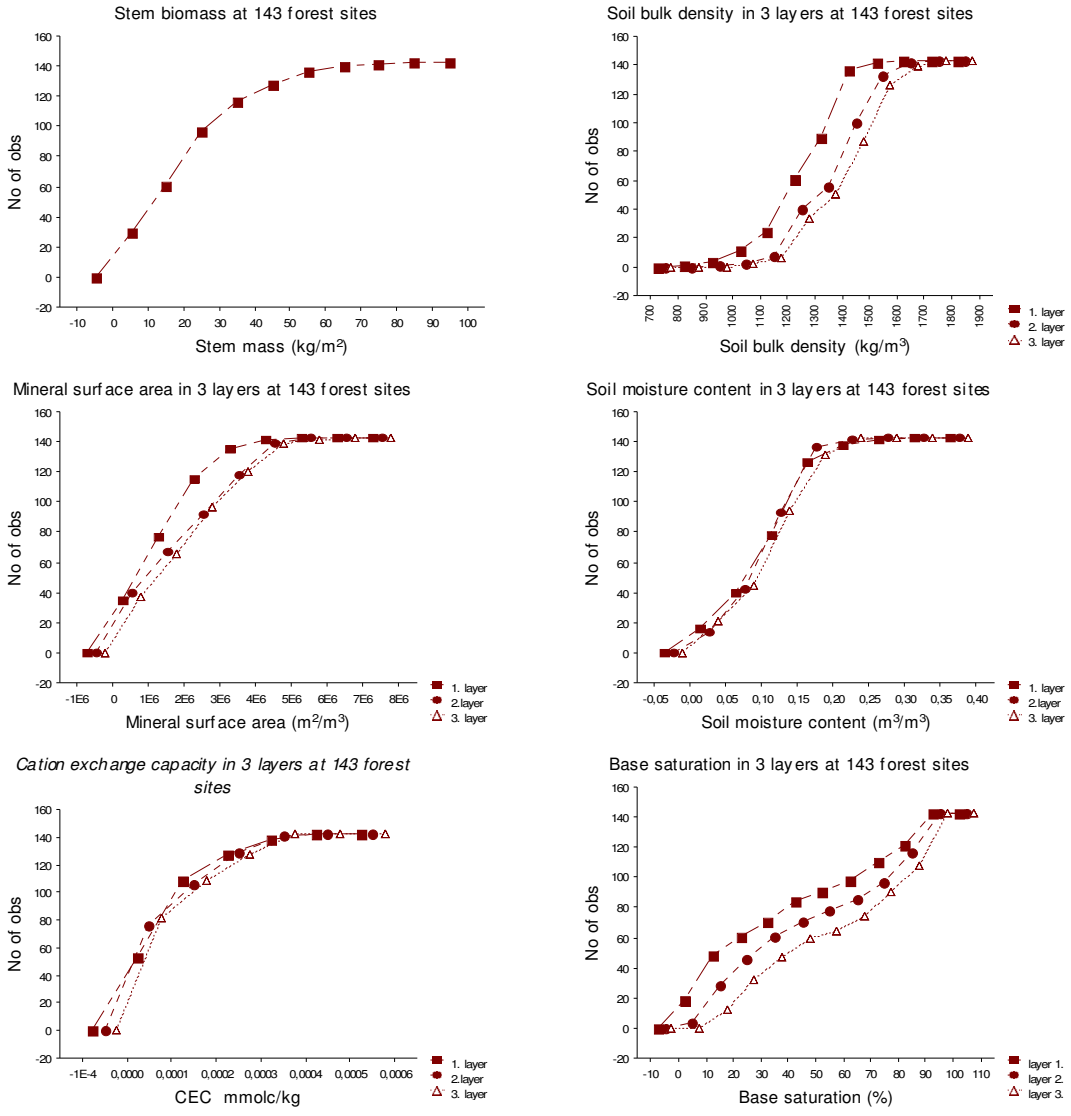


Figure HU-1. Cumulative histograms of stem biomass, soil bulk density, mineral surface area, soil moisture content, cation exchange capacity, and base saturation.

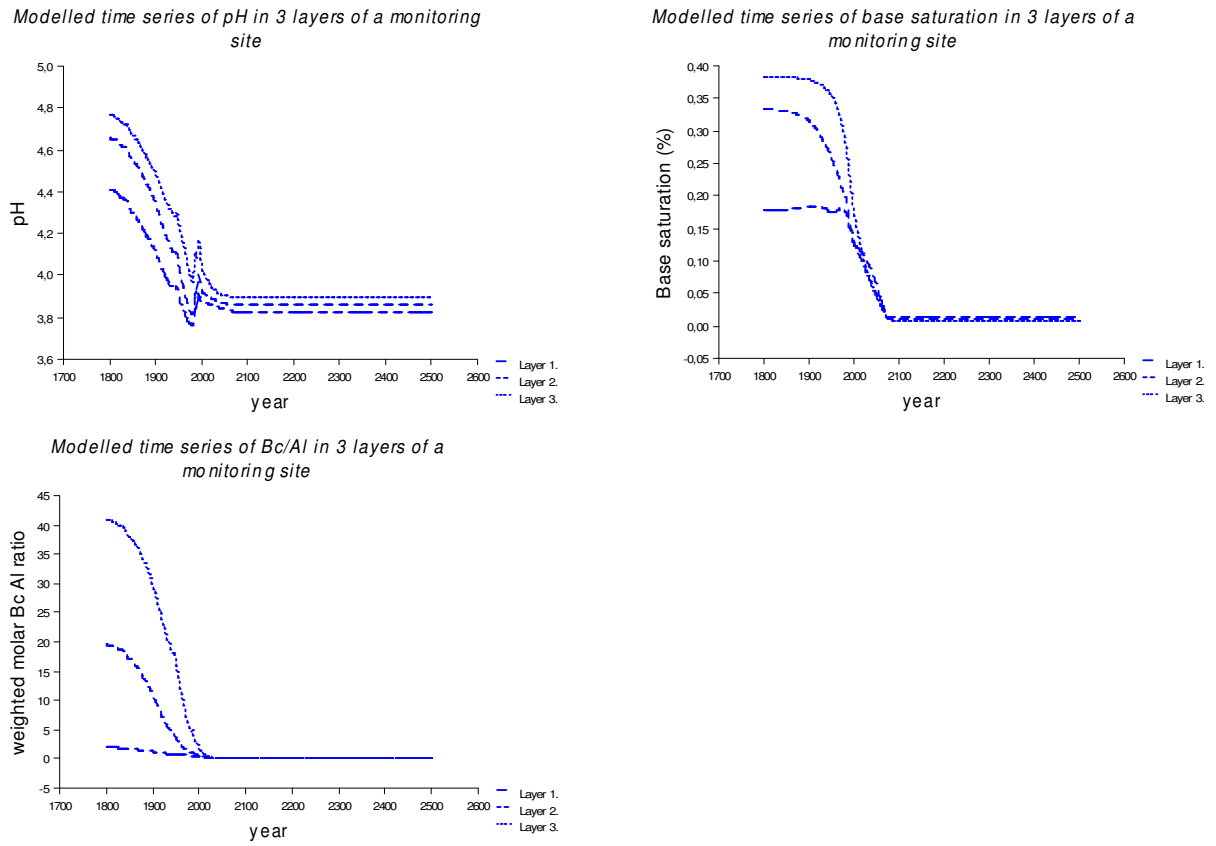
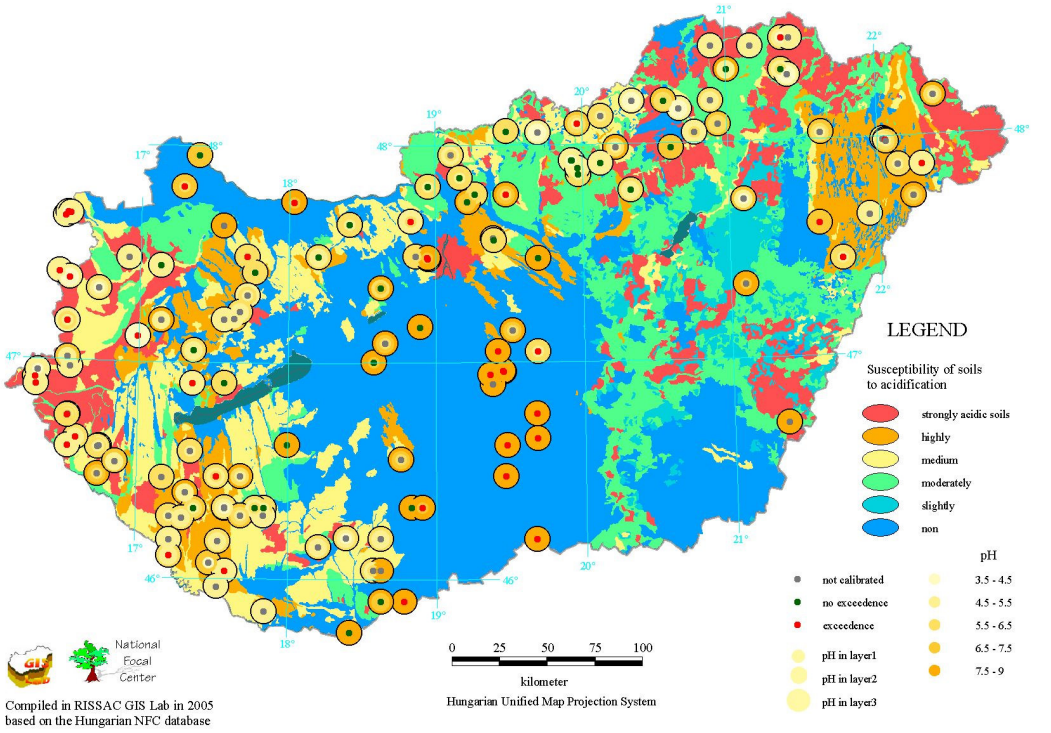


Figure HU-2. Modelled time series of soil pH, base cation /Al ratios in soil solution and base saturation.



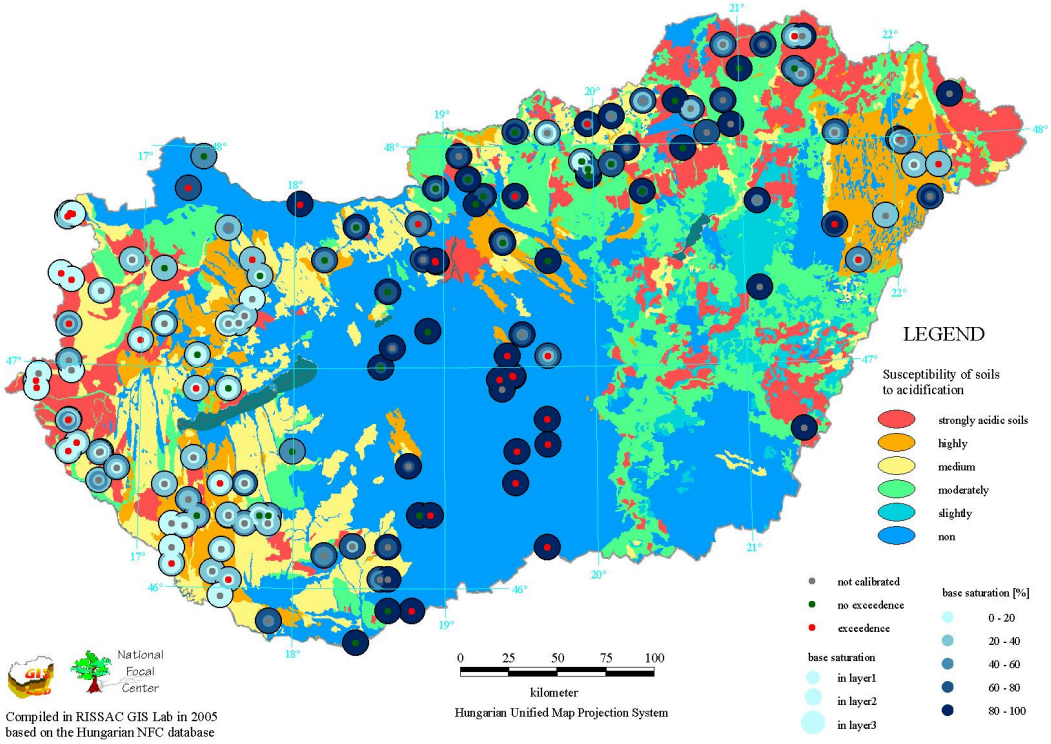


Figure HU-3. Critical load exceedances in Hungarian Soil Monitoring forest sites calculated by the SAFE model.

IRELAND

National Focal Centre

Michael McGettigan
Environmental Protection Agency
McCumiskey House
Richview, Clonskeagh Road
Dublin 14
tel: +353 1 268 0100
fax: +353 1 268 0900
m.mcgettigan@epa.ie

Collaborating institutions

Julian Aherne
Environmental and Resource Studies
Trent University, 1600 West Bank Drive
Peterborough, Ontario, K9J 7B8
Canada
tel: +1 705 748 1011 extn 5351
fax: +1 705 748 1569
julian.aherne@ucd.ie

Calculation methods

Critical loads and target loads were estimated for four ecosystems: coniferous forests (2449 km^2), deciduous forests (1805 km^2), natural grasslands (2050 km^2) and heathlands (2631 km^2). The methodology and model input parameters for Irish ecosystems have been updated in accordance with the latest version of the Mapping Manual (www.icpmapping.org), and to ensure consistency between critical loads and target loads. All critical loads and dynamic (target loads and scenario simulations) modelling were carried out using the Very Simple Dynamic (VSD) model (Posch et al., 2001).

The general soil map of Ireland (Gardiner and Radford, 1980) was the principal data source for all soil related model input parameters. The weathering rate of base cations is based on a Skokloster classification (Nilsson and Grennfelt, 1988; Hornung et al., 1995) of the general soil map of Ireland. By assigning a Skokloster critical load range to the principal soil of each association on the general soil map of Ireland a weathering rate map has been produced (Aherne and Farrell, 2000a, 2000b). The critical leaching of Acid Neutralising Capacity is calculated as described by Hettelingh et al. (1991), page 35. A pH of 4.2 was selected as the H^+ concentration limit and subsequently used to estimate the Al^{3+} critical limit via the gibbsite relationship (Aherne et al., 2001; Aherne and Farrell, 2002). The H^+ critical limit of pH = 4.2 is based on work by Ulrich (1987).

A detailed description of the data and methods is given in Table IE-1; soil input parameters required for dynamic modelling are given in Table IE-2. For further discussion on data sources and methods see Aherne and Farrell (2000a,b, 2002) and Aherne et al. (2001).

Data sources

Soils: 1:575,000 general soil map of Ireland and the accompanying soil survey bulletin (Gardiner and Radford, 1980). Additional soil information was supplied by Jim Collins, University College Dublin (personal communication).

Land cover: 1:100,000 CORINE land cover project, Ireland (OSI, 1993).

Precipitation: Interpolation (kriging) of long-term mean annual precipitation volume for approximately 600 sites for the period 1951–1980 (Fitzgerald, 1984).

Precipitation surplus: Precipitation minus evapotranspiration and surface runoff. Evapotranspiration is estimated from interpolation (kriging) of long-term mean annual evapotranspiration volume, 1951–1980 (14 sites, see Aherne and Curtis, 2003). Surface runoff is inferred from soil permeability classes derived from the general soil map of Ireland.

Base cation deposition: Interpolation (kriging) of mean annual non-marine bulk precipitation chemistry concentrations for approximately 20 sites for the period 1985–1994. The minimum sampling period is not less than 3 years. Total base cation deposition was estimated using a filter factor of 2.0 for forests and 1.5 for heathlands (Aherne and Farrell, 2000b).

Nutrient uptake: It is assumed that all coniferous trees are Sitka Spruce; yield class is the average for Sitka Spruce in Ireland (COFORD, 1994) and stem concentrations are for Sitka Spruce in Wales (Emmett and Reynolds, 1996).

Table IE-1. Irish critical load database: calculation methods and data sources.

Variable	Calculation method and data source	Justification
EcoArea	Database describing the percentage cover of each land cover type in every 1 km^2 (OSI, 1993).	CORINE land cover
$Cl_{max}(S)$ $Cl_{min}(N)$ $Cl_{max}(N)$ $Cl_{nut}(N)$	VSD model (Microsoft Access version).	Mapping manual and to ensure consistency between critical and target loads
$nANC_{crit}$	$= Q \times ([Al]_{crit} + [H]_{crit})$ A pH of 4.2 was selected for [H]crit and [Al]crit estimated via the gibbsite relationship.	Mapping manual Ulrich (1987)
$N_{le(acc)}$	$= Q_{le} \times [N]_{acc}$ A value of 0.0143 eq m^{-3} was set for $[N]_{acc}$.	Mapping manual
crittype *critvalue*	pH was selected as the chemical criterion with a critical value of 4.2 (Aherne et al., 2001; Aherne and Farrell, 2002). The critical limit is based on work by Ulrich (1987).	Mapping manual Ulrich (1987)
thick	Sum of O/A/E/B horizons for the modal profile of the principal soil for each soil associations on the general soil map of Ireland, see Table IE-2.	Gardiner and Radford (1980)
bulkdens	Average bulk density estimated from percent organic carbon in each horizon and weighted by depth for each profile.	Gardiner and Radford (1980); Posch et al. (2003)
Ca_{dep} Mg_{dep} K_{dep} Na_{dep} Cl_{dep}	Estimated from interpolated (kriging) point source non-marine bulk concentration measurements and interpolated rainfall volumes. A filter factor of 2 was used to scale from bulk to total deposition for forest and 1.5 for heathlands.	Aherne and Farrell (2000b); modelled EMEP base cation deposition is unreliable for western Europe
Ca_{we} Mg_{we} K_{we} Na_{we}	Skokloster classification: the mid-value of each of the five classes is used to define soil weathering, except for the final (non-sensitive) class, which is set at 4000.	Nilsson and Grennfelt (1988) Hornung et al. (1995) Aherne and Farrell (2000a)
Ca_{upt} Mg_{upt} K_{upt}	Coniferous forest: minimum of available base cations (= Bcwe + Bcdep – Bcle) and estimated uptake (= yield class × wood density × stem concentration). Other ecosystems: fixed removal (45 eq ha^{-1} a^{-1}) via occasional grazing.	COFORD (1996) Emmett and Reynolds (1996)
Q_{le}	30-year mean annual precipitation minus evapotranspiration and surface runoff (derived from soil type). Meteorological data source: Met Éireann	Aherne and Curtis (2003)
LgKAlox *expAl*	Gibbsite (Kgibb) equilibrium relationship with exponent equal to 3. Kgibb was based on soil type: 9.5 m^6 eq^{-2} for organic soils, 100 m^6 eq^{-2} for peaty podzols and peaty gleys, and 300 m^6 eq^{-2} for the remaining soils.	Mapping manual
pCO_2fac	For consistency with previous critical load estimates, set to a default value of 1.0, which effectively turns off the process in the VSD model.	Not important for soils with pH < 5.0

Variable	Calculation method and data source	Justification
cOrgacids	For consistency with previous critical load estimates, set to a default value of 0.001, which effectively turns off the process in the VSD model.	Limited data
$N_{im(acc)}$	Set to a default value of 71 eq ha^{-1} a^{-1} for all ecosystems.	Mapping manual
N_{upt}	Coniferous forests: See base cation uptake comments. Other ecosystems: fixed removal (71 eq ha^{-1} a^{-1}) via occasional grazing.	COFORD (1996) Emmett and Reynolds (1996)
f_{de}	Based on drainage class of each soil association on the general soil map of Ireland, see Table IE-2.	Mapping manual
CEC *Bsat* *yearbsat*	Based on the modal profile of the principal soil for each association on the general soil map of Ireland. Variables were weighted by depth and bulk density for O and/or A horizons only (see Table IE-2). Sample year was set to 1980.	Gardiner and Radford (1980)
LgKAlBc *lgKHBc*	VSD model (Microsoft Access version). Gapon exchange equations were used.	Mapping manual; Posch et al. (2003)
Cpool *CNrat* *yearCN*	Based on the modal profile of the principal soil for each association on the general soil map of Ireland. Variables were weighted by depth and bulk density (see Table IE-2). Sample year was set to 1980.	Gardiner and Radford (1980)
EUNIScode	Simplified to four codes representing coniferous (G3), mixed deciduous (G4), grassland (E3) and heathland (F4).	

Table IE-2. Soil variables for the principal soil of each association (ID) on the general soil map of Ireland (Gardiner and Radford, 1980). See Table IE-1 for explaination of table headings.

ID	*thick* m	*bulkdens* g cm^{-3}	f_{de}	*CEC* meq kg^{-1}	*Bsat* %	*Cpool* g m^{-2}	*CNrat*	*Clay* %	*Sand* %	C_{org} %
1	0.55	0.800	0.2	286	0.10	14326	35.8	10.2	24.7	4.2
2	0.83	1.290	0.7	376	0.44	4896	25.5	59.8	2.6	1.5
3	1.00	0.100	0.8	640	0.23	15279	26.9			52.2
4	0.05	1.075	0.0	152	0.22	3280	30.5	8.0	23.0	6.1
5	1.10	0.095	0.8	960	0.20	14362	26.9			52.2
6	0.50	1.347	0.1	116	0.45	12726	13.2	16.2	21.9	2.3
7	0.18	0.845	0.0	552	0.55	16984	9.9	29.8	13.8	11.2
8	0.65	1.339	0.1	200	0.34	7926	17.3	10.5	15.4	2.4
9	0.50	1.112	0.1	147	0.23	19807	13.0	23.3	7.3	5.5
10	1.04	1.490	0.1	153	0.42	9747	9.7	18.8	20.2	0.9
11	0.41	1.310	0.7	161	0.72	14869	9.3	30.0	27.0	2.8
12	0.70	1.395	0.1	164	0.25	12532	13.8	8.8	21.0	1.8
13	0.41	1.371	0.1	104	0.61	10793	11.3	15.4	21.0	2.1
14	0.40	1.342	0.1	225	0.52	11504	13.9	26.8	8.2	2.4
15	0.86	1.365	0.1	140	0.46	11497	12.0	13.5	22.1	2.1
16	0.57	1.461	0.0	62	0.48	9773	10.0	8.0	16.6	1.2
17	0.60	1.265	0.1	366	0.64	18333	13.0	28.5	33.3	3.3
18	0.70	1.446	0.1	175	0.23	7334	8.7	24.1	17.7	1.3
19	0.30	1.104	0.1	285	0.32	14217	13.3	32.8	10.8	5.6
20	0.37	1.252	0.1	115	0.21	13815	13.5	25.7	7.3	3.5
21	0.81	1.486	0.7	71	0.84	9353	10.4	23.1	18.3	1.0
22	0.58	1.434	0.7	126	0.75	10758	8.8	34.7	11.5	1.5

ID	*thick* m	*bulkdens* g cm^{-3}	f_{de}	*CEC* meq kg^{-1}	*Bsat* %	*Cpool* g m^{-2}	*CNrat*	*Clay* %	*Sand* %	C_{org} %
23	0.20	0.200	0.4	888	0.57	9520	27.4	10.0	68.0	23.8
24	0.50	0.100	0.8	1030	0.28	20372	26.9			52.2
25	0.53	1.423	0.4	154	0.56	10626	9.9	27.4	20.2	1.6
26	0.40	1.219	0.7	417	0.82	19038	10.0	49.0	18.4	3.9
27	0.52	1.421	0.7	202	0.87	7445	9.2	41.1	9.5	1.6
28	0.64	1.453	0.2	147	0.62	9377	8.0	23.7	26.6	1.3
29	0.95	1.271	0.1	290	0.33	22667	13.3	22.5	15.0	3.2
30	0.84	1.468	0.1	127	0.98	10780	8.6	14.8	21.6	1.1
31	0.40	1.415	0.1	115	0.88	7725	8.4	21.7	21.4	1.6
32	1.12	1.452	0.1	84	0.88	14361	11.9	30.0	14.2	1.3
33	0.20	1.091	0.0	281	0.86	7486	13.1	14.7	27.2	5.8
34	1.00	1.481	0.1	116	0.88	11152	9.0	25.0	21.8	1.0
35	0.46	1.516	0.0	152	0.82	3945	7.7	17.9	37.8	0.7
36	0.95	1.506	0.1	100	0.63	8324	8.8	16.1	22.3	0.8
37	1.01	1.475	0.2	145	0.52	12106	12.0	25.9	17.0	1.1
38	0.82	1.474	0.2	140	0.63	7409	8.3	30.0	21.2	1.1
39	1.22	1.449	0.7	118	0.97	19482	9.3	45.1	8.9	1.3
40	0.58	1.375	0.4	138	0.66	12939	9.6	34.5	13.3	2.0
41	0.41	1.319	0.7	488	0.86	11420	14.0	50.6	19.0	2.7
42	0.90	1.455	0.7	158	0.63	12213	11.4	36.2	14.6	1.2
43	0.75	1.324	0.7	137	0.94	13985	12.4	24.9	11.5	2.6
44	1.18	0.061	0.8	1400	0.43	7626	23.7			47.5

ID refers to the soil association number (Gardiner and Radford, 1980). Additional soil information was supplied by Jim Collins, University College Dublin (personal communication).

References

Aherne J, Farrell EP (2000a) Assessment of the application of empirical critical loads of acidity to Irish soils. Irish Journal of Agricultural and Food Research 39(3): 349–358

Aherne J, Farrell EP (2000b) Final Report: Determination and Mapping of Critical Loads for Sulphur and Nitrogen and Critical Levels for Ozone in Ireland. Environmental Protection Agency, Dublin, Ireland, 225 pp

Aherne J, Farrell EP, Hall J, Reynolds B, Hornung M (2001) Using multiple chemical criteria for critical loads of acidity in maritime regions. Water, Air and Soil Pollution: Focus 1: 75–90

Aherne J, Farrell EP (2002) Steady-state critical loads of acidity for sulphur and nitrogen: a multi-receptor, multi-criterion approach. Science of the Total Environment 288(3): 183–197

Aherne J, Curtis CJ (2003) Critical loads of acidity for Irish lakes. Aquatic Sciences 65(1): 1–15

COFORD (1994) Pathway to Progress: A Programme for Forest Research and Development. National Council for Forest Research and Development, University College Dublin, Ireland, 132 pp

Emmett B, Reynolds B (1996) Nitrogen critical loads for spruce plantations in Wales: is there too much nitrogen? Forestry 69(3): 205–214

Fitzgerald D (1984) Monthly and Annual Averages of Rainfall for Ireland 1951–1980. Climatological Note No. 7, Irish Meteorological Service, Dublin, Ireland

Gardiner M, Radford J (1980) Soil Associations of Ireland and their Land Use Potential. Soil Survey Bulletin No. 36, An Foras Taluntais, Dublin, Ireland.

Hettelingh JP, Downing RJ, De Smet PAM (1991) Mapping Critical Loads for Europe: CCE Technical Report No. 1. RIVM Report 259101001, Bilthoven, The Netherlands

Hornung M, Bull KR, Cresser M, Hall J, Langan SJ, Loveland P, Smith C (1995) An empirical map of critical loads of acidity for soils in Great Britain. Environmental Pollution 90(3): 301–310

Nilsson J, Grennfelt P (eds.) (1988) Critical loads for Sulphur and Nitrogen. Miljörapport 1988:15, Nordic Council of Ministers, Copenhagen, Denmark

OSI (1993) 1:100,000 CORINE land cover project (Ireland), Ordnance Survey of Ireland, Phoenix Park, Dublin, Ireland

Posch M, Hettelingh J-P, Slootweg J (2003) Manual for Dynamic Modelling of Soil Response to Atmospheric Deposition. RIVM Report 259101012, Bilthoven, The Netherlands, 71 pp

Ulrich B (1987) Stability, Elasticity, and the Resilience of Terrestrial Ecosystems with Respect of Matter Balance. Ecological Studies 61, Springer-Verlag Berlin-Heidelberg, Germany

ITALY

National Focal Centre

Mara Angeloni
Ministry for the Environment
Via Cristoforo Colombo
I-00147 Rome
tel: + 39-6-5722 8113
angeloni.mara@minambiente.it

Collaborating institutions

Patrizia Bonanni
Valerio Silli
APAT (National Agency for Environmental Protection and Technical Services)
Via Vitaliano Brancati, 48
I-00144 Rome
tel: +39-6-5007 2800
+39-6-5007 2801
fax: +39-6-5007 2986
bonanni@apat.it
silli@apat.it

Roberto Daffinà
APAT Consultant
Via Vitaliano Brancati, 48
I-00144 Rome
tel: +39-6-5007 2410
fax: +39-6-5007 2986
daffina@apat.it

Armando Buffoni
APAT Consultant
Via Pergolesi 2
20124 Milano
tel/fax: 02 66713184
ab-mi@libero.it

INTRODUCTION

Critical loads were calculated according to the SMB methodology described in the Mapping Manual 2004 (UBA, 2004) or in its old version (UBA, 1996). The most relevant changes to the input data are listed below:

Receptors mapped: The CORINE Land use database has been adopted. Receptors are defined geometrically by the CORINE database while vegetation characteristics were defined by intersection with a vegetation map provided by the Ministry for Environment.

Meteorology: Datasets regarding the annual mean temperature and precipitation were updated by means of data provided by Climate Research Unit of the University of East Anglia.

Soil parameters: Soil parameters were derived from the European database EUsoils.

In order to carry out statistical analysis, EUNIS level 3 ecosystems considered in critical load calculation (Table IT-1) were aggregated to the second level.

Table IT-1. Ecosystem types (EUNIS habitats) considered in the Italian critical loads.

Level 1	Level 2	Habitat
A4	A4.5	Shallow sublittoral sediments dominated by angiosperms
B1	B1.4	Coastal stable dune grassland
B3	B3.3	Rock cliffs, ledges and shores, with halophytic angiosperms
C1	C1.2	Permanent mesotrophic lakes, ponds and pools
C3	C3.2	Water-fringing reedbeds and tall helophytes other than canes
E2	E2.3	Mountain hay meadows
E1	E1.2	Perennial calcareous grassland and basic steppes
	E1.3	Mediterranean xeric grassland
	E1.5	Mediterraneo-montane grassland
	E1.8	Mediterranean dry acid and neutral closed grassland
E4	E4.3	Acid alpine and subalpine grassland
	E4.4	Calciphilous alpine and subalpine grassland
F2	F2.3	Subalpine and oroboreal bush communities
F3	F3.1	Temperate thickets and scrub
	F3.2	Mediterraneo-montane broadleaved deciduous thickets
F5	F5.2	Maquis
F7	F7.4	Hedgehog-heaths
G1	G1.1	Riparian [Salix], [Alnus] and [Betula] woodland
	G1.5	Broadleaved swamp woodland on acid peat
	G1.6	[Fagus] woodland
	G1.7	Thermophilous deciduous woodland
	G1.8	Acidophilous [Quercus]-dominated woodland
G2	G2.1	Mediterranean evergreen [Quercus] woodland
G3	G3.1	[Abies] and [Picea] woodland
	G3.2	Alpine [Larix] - [*Pinus cembra*] woodland
	G3.4	[*Pinus sylvestris*] woodland south of the taiga
	G3.5	[*Pinus nigra*] woodland
	G3.7	Lowland to montane mediterranean [Pinus] woodland (excluding [*Pinus nigra*])
G4	G4.6	Mixed [Abies] - [Picea] - [Fagus] woodland

EUNIS	km^2	%
G1	60355	48%
G1.1	1868	1%
G1.6	12638	10%
G1.7	40783	33%
G1.8	5059	4%
G3	13514	11%
E1	11587	9%
G2	10130	8%
E4	9958	8%
F3	7675	6%
G4	5561	4%
F2	3882	3%
E2	1478	1%
F5	1212	1%

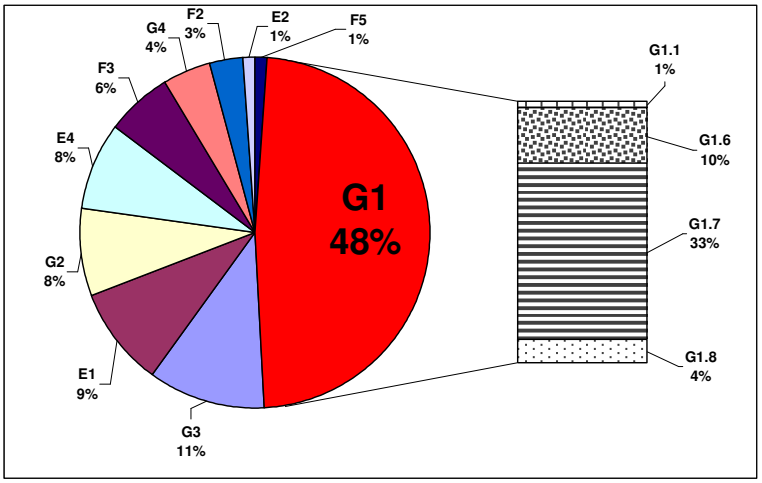


Figure IT-1. The areas of the ecosystems for which critical loads and dynamic modelling calculations have been executed

Table IT-2. Minimum, maximum and median value for all CL and DM variables.

	G1	G3	E1	G2	E4	F3	G4	F2	E2	F5	B1	B3	C3	F7	A4	C1	E3
area	48%	11%	9%	8%	8%	6%	4%	3%	1%	1%	0%	0%	0%	0%	0%	0%	0%
EcoArea [km^2]																	
min	1.0	1.0	1.0	1.0	1.0	1.0	1.0	1.0	4.0	1.0	1.0	1.0	12.0				
med	182.9	68.9	92.7	70.8	211.9	62.9	123.6	69.3	123.2	39.1	29.4	18.7	27.0	53	35	6	4
max	1275	1032	474.0	1010	588.0	328.0	588.0	342.0	608.0	195.0	79.0	87.0	42.0				
Nleacc [eq ha^{-1} a^{-1}]																	
min	71.4	35.7	71.4	35.7	71.4	35.7	104.7	35.7	72.1	35.7	71.4	47.2	160.7				
med	139.6	47.3	110.3	47.9	152.3	47.5	192.0	54.3	145.1	66.0	105.5	86.6	181.5	192.7	71.4	71.4	46.9
max	285.7	71.4	231.4	71.4	214.3	95.2	285.7	71.4	214.3	150.1	154.8	173.0	202.4				
Thick [m]																	
min	0.2	0.1	0.1	0.2	0.1	0.2	0.2	0.2	0.2	0.2	0.2	0.2	0.3				
med	0.5	0.5	0.5	0.5	0.4	0.5	0.4	0.5	0.5	0.5	0.4	0.6	0.4	0.5	1	0.2	0.7
max	1.2	1.2	1.2	3.0	1.1	1.1	1.2	1.2	1.2	1.0	1.0	1.0	0.5				
Bulkdens [g.cm^{-3}]																	
min	0.7	0.7	0.7	0.7	0.7	0.7	0.7	0.7	0.7	0.7	0.7	0.7	0.8				
med	1.0	1.0	1.0	1.0	0.9	0.9	0.8	1.0	1.1	1.1	1.0	0.9	0.8	0.7	0.7	1.6	1.2
max	1.6	1.6	1.6	1.6	1.6	1.6	1.6	1.6	1.6	1.6	1.6	1.6	0.9				
Cadep [eq.ha^{-1} a^{-1}]																	
min	252.0	250.0	302.0	249.5	472.0	320.0	467.2	473.3	475.4	361.6	572.4	371.6	918.5				
med	785.3	742.8	778.2	693.4	716.0	800.0	728.9	684.9	701.2	777.3	659.2	685.7	1081	1001	586	568.1	1046
max	1487	1402	1261	1342	1159	1334	1070	1045	903.2	1143	862.0	1324	1243				
Mgdep [eq.ha^{-1} a^{-1}]																	
min	78.0	50.0	92.0	72.0	107.6	116.0	107.1	107.6	120.7	135.6	163.5	142.8	263.1				
med	263.9	241.7	272.7	248.9	171.1	274.7	177.9	166.6	175.1	294.2	210.5	241.2	302.5	273	222	221	403
max	582.4	515.8	499.3	524.3	296.6	521.0	276.8	272.1	231.3	444.0	312.9	515.8	342.0				
Kdep [eq.ha^{-1} a^{-1}]																	
min	17.6	17.5	21.1	17.5	33.0	22.4	32.7	33.1	33.3	25.3	40.7	26.0	64.3				
med	61.0	56.8	61.3	55.8	50.1	61.9	51.0	47.9	49.1	66.0	47.8	56.7	75.6	70	52.7	51.1	94.1
max	133.8	126.1	113.6	120.8	81.1	120.1	74.9	73.2	63.2	102.8	60.3	119.1	87.0				
Nadep [eq.ha^{-1} a^{-1}]																	
min	81.8	110.6	151.0	102.0	122.0	162.0	93.0	113.1	140.6	210.0	210.0	215.0	500.8				
med	584.0	506.4	624.0	565.0	232.5	616.3	241.3	218.5	236.1	723.1	414.3	517.9	588.1	483.4	468.6	456	1055
max	1611	1510	1338	1442	572.5	1430	442.9	432.5	357.3	1173	782.5	1415	675.5				
Cawe [eq.ha^{-1} a^{-1}]																	
min	238.5	70.5	681.9	477.4	67.0	687.7	238.5	67.0	238.5	687.7	1021	763.0	1303				
med	1955	1707	1946	1729	1410	1857	1396	1722	1985	2084	1967	2496	1753	1928	1964	777	2670
max	5144	5152	4582	3844	4838	5152	4050	4838	3913	3965	4353	4504	2204				
Mgwe [eq.ha^{-1} a^{-1}]																	
min	108.4	9.4	151.4	63.6	9.0	222.6	108.4	9.0	108.4	222.6	228.8	460.9	541.7				
med	997.1	892.9	1025	933.3	723.3	950.5	708.4	738.3	758.9	1075	739.9	1162	711.5	1138	944	448	1614
max	2454	2322	2695	2322	1818	2322	1900	1908	1908	2093	1865	2322	881.4				
Kwe [eq.ha^{-1} a^{-1}]																	
min	91.6	49.4	164.9	164.9	47.0	164.9	91.6	47.0	98.9	165.1	341.6	164.9	468.9				
med	562.0	475.0	541.2	474.9	399.7	526.8	406.2	591.9	772.3	597.8	712.3	792.3	599.4	443	558	180	577
max	2568	2200	1687	1333	2525	2200	1709	2525	1826	1332	1363	2255	729.9				
Nawe [eq.ha^{-1} a^{-1}]																	
min	128.7	22.2	198.2	154.6	21.0	227.3	128.7	21.0	128.7	227.3	299.2	595.2	662.8				
med	1276	1123	1308	1158	926.3	1203	914.5	978.2	1040	1395	984.9	1538	903.7	1451	1222	579	2082
max	2999	2999	3503	2999	2347	2999	2454	2468	2468	2788	2416	2999	1145				
Qle [mm a^{-1}]																	
min	60.0	52.0	56.5	52.0	239.6	50.0	345.8	238.0	246.7	63.0	202.5	66.0	992.8				
med	538.0	543.0	473.3	333.7	863.5	535.0	857.6	796.1	780.5	330.0	401.5	391.4	1316.9	1304	227	199	557
max	1593.0	1951.6	1512.0	987.0	1998.5	1591.0	1771.6	1688.9	1400.0	837.3	672.5	949.0	1640.9				
pCO2 [* atm. Press.]																	
min	16.3	16.3	17.0	20.7	16.3	17.1	17.0	16.3	17.4	20.0	27.7	24.6	21.3				
med	25.9	25.9	26.6	30.7	19.0	26.1	21.3	21.1	23.7	30.5	32.0	32.3	21.7	19.49	26.8	37.76	30.4
max	40.4	45.8	41.0	45.8	29.7	40.4	29.7	29.7	29.7	40.5	37.8	37.9	22.1				
cOrgacids [eq m^{-3}]																	
0.01																	
Nimacc [eq.ha^{-1} a^{-1}]																	
min	23.6	16.3	11.8	0.0	32.1	2.0	5.0	10.9	32.1	3.7	14.8	14.8	41.5	39.2	57	23.6	49.7
med	86.3	96.1	84.9	66.9	44.8	30.3	59.5	23.6	42.6	58.5	40.2	67.8	42				
max	346.7	324.4	328.1	349.2	72.1	210.2	65.6	126.5	66.2	307.6	80.3	293.7	42.6				
Nupt [eq.ha^{-1} a^{-1}]																	
min	0.0	64.8	0.0	53.1		12.8	123.9	12.8		10.0	10.0	10.0					
med	543.4	604.2	13.1	269.4	10	63.9	590.0	64.7	10	41.8	113.3	135.2	10	10	10	462	573
max	908.8	705.0	418.9	409.9		64.8	824.5	81.0		64.8	733.4	573.2					
fde																	
min	0.0	0.0	0.0	0.0	0.1	0.0	0.1	0.0	0.2	0.2	0.4	0.4	0.3				
med	0.4	0.4	0.4	0.4	0.3	0.4	0.4	0.4	0.4	0.4	0.5	0.5	0.4	0.4	0.5	0.5	0.3

	G1	G3	E1	G2	E4	F3	G4	F2	E2	F5	B1	B3	C3	F7	A4	C1	E3
area	48%	11%	9%	8%	8%	6%	4%	3%	1%	1%	0%	0%	0%	0%	0%	0%	0%
max	1.3	0.5	0.5	0.5	0.5	0.6	1.3	1.5	0.5	0.5	0.5	0.5	0.4				
CEC [meq kg^{-1}]																	
min	38.4	35.8	90.53	104.7	119.4	57.0	114.7	113.8	119.8	114.9	138.1	119.6	136.3				
med	166.2	155.7	165.3	174.6	202.5	165.1	175.7	218.2	189.1	159.2	273.7	177.6	165.5	196.8	157.3	133.4	106
max	495.1	415.0	495.1	485.1	312.4	461.9	292.3	417.6	278.1	317.5	439.7	364.3	194.8				
Bsat																	
min	0.3	0.3	0.3	0.3	0.3	0.3	0.3	0.3	0.3	0.3	0.3	0.0	0.5				
med	0.6	0.6	0.6	0.6	0.6	0.6	0.6	0.6	0.8	0.7	0.6	0.5	0.6	0.3	0.6	0.3	0.6
max	1.0	1.0	1.0	1.0	1.0	1.0	1.0	1.0	1.0	1.0	1.0	1.0	0.6				
Cpool [g m^{-2}]																	
min	654	1033	1068	630	2371	1159	1050	1050	3695	1161	2100	1050	3306				
med	6651	6176	5932	6751	6098	5679	5423	6616	6650	6237	4837	6490	5341	2987	10556	4800	8050
max	76800	76800	33600	58679	25897	24000	28000	26303	12650	14044	8000	11412	7377				
lgKAlBc																	
min	-0,5	-0,2	-0,2	-0,2	0,2	2,5	0,2	0	0	-0,2	0,6	0,6	0,4				
med	0,8	0,9	0,8	0,9	1,2	3,7	1	1,1	0,6	0,8	0,8	0,9	0,5	0,7	1,7	0,6	2,0
max	2,3	2,6	2,1	2,6	2,6	4,8	2,1	2,6	1,9	1,8	1,5	1,7	0,6				
lgKHBc																	
min	2,1	2,1	2,1	2,1	2,5	2,5	2,5	2,5	3,3	2,1	3,4	3,5	3,8				
med	3,8	3,7	3,7	3,7	4	3,7	3,9	4	4,2	3,6	3,7	4	3,9	3,8	3,8	3,7	4,7
max	5,0	5,5	4,8	5,5	5,5	4,8	5,1	5,5	5	4,8	4,3	4,4	3,9				
lgKAlox																	
8																	
expAl																	
3																	
Cnrat																	
30																	
CLmax(S) [eq.ha^{-1} a^{-1}]																	
min	2231.1	2150.5	3911.5	2784.8	1963.4	5226.1	2488.5	1943.3	3001.4	4473.4	5893.4	5204.2	8426.5				
med	10494	9333.1	10648	9426.5	8104.3	10315	7922.1	9129.7	10240	11214	9913.5	12344	10679	11372	9866	5118	14564
max	20746	20193	21219	17666	19923	20482	17111	19929	17171	18534	19953	19042	12932				
CLmin(N) [eq.ha^{-1} a^{-1}]																	
min	57.7	142.9	193.6	36.4	332.5	134.4	370.2	351.8	369.0	196.7	352.3	62.2	588.8				
med	501.6	500.6	473.9	399.0	612.8	444.2	632.4	592.1	605.3	377.9	521.5	432.2	823.0	798.9	333.7	266.8	374.7
max	1207.2	1491.4	877.9	938.5	1242.2	1038.8	1150.6	1061.6	1009.7	735.7	679.8	833.2	1057.3				
CLmax(N) [eq.ha^{-1} a^{-1}]																	
min	2602.7	2684.1	4105.1	3114.4	2528.7	5550.9	2966.8	2295.1	3518.7	4670.1	6441.0	5546.1	9015.3				
med	10996	9833.7	11122	9825.4	8717.0	10759	8554.5	9721.8	10845	11592	10435	12776	11502	12171	10200	5385	14938
max	21359	20721	21828	17940	20349	21024	17665	20469	17540	18771	20633	19743	13989				
CLnut(N) [eq.ha^{-1} a^{-1}]																	
min	262.4	193.2	76.6	196.8	140.0	117.4	616.0	187.3	142.5	64.8	117.9	72.2	462.5				
med	880.0	949.9	322.8	498.6	420.3	343.1	1046.7	438.6	426.2	260.5	361.2	403.4	667.5	612	186.4	595.4	842.3
max	1664.5	1940.1	719.6	1085.2	1030.1	900.3	1610.0	940.5	830.8	549.6	1173.8	1181.1	872.5				
nANCcrit [eq.ha^{-1} a^{-1}]																	
min	655.0	813.3	2217.6	1411.2	1193.2	2925.3	1028.9	1140.3	1789.7	2519.3	3356.9	2987.1	4862.6				
med	5541.7	4842.9	6014.0	5131.4	4629.0	5802.4	4095.8	5139.5	5793.6	6295.4	5510.7	6828.8	6151.3	6516	5535	2596	7809
max	11221	10702	11406	9634.1	11002	11273	9014.3	10965	9528.6	10250	11132	10162	7440.0				

References

Bonanni P, Brini S, Buffoni A, Stella G, Vialetto G (2001) Acidificazione ed eutrofizzazione da deposizioni atmosferiche: le mappe nazionali dei carichi critici. ANPA 14/2001

De Vries W, Posch M, Reinds GJ, Kämäri J (1993) Critical loads and their exceedance on forest soils in Europe.Report 58, DLO Winand Staring Centre, Wageningen, The Netherlands, 116 pp

Downing RJ, Hettelingh J-P, De Smet PAM (eds) (1993) Calculation and Mapping of Critical Loads in Europe: CCE Status Report 1993. RIVM Report 259101003, Bilthoven, The Netherlands

FOEFL (eds) (1994) Critical Loads of Acidity for Forest Soils and Alpine Lakes - Steady State Mass Balance Method. Environmental Series No. 234, Federal Office of Environment, Forests and Landscape, Bern, 68 pp

Hettelingh J-P, Downing RJ, De Smet PAM (eds) (1991) Mapping Critical Loads for Europe. CCE Technical Report No.1, RIVM Report 259101001, Bilthoven, The Netherlands

Posch M., Hettelingh J-P, Slootweg J (eds) (2003) Manual for dynamic modelling of soil response to atmospheric deposition.CCE Technical Report 259101012, Bilthoven, The Netherlands

Reinds GJ, Posch M, De Vries W (2001) A semi-empirical dynamic soil acidification model for use in spatially explicit integrated assessment models for Europe.Report 084, Alterra,Wageningen,The Netherlands, 55 pp

UBA (1996) Manual on Methodologies and Criteria for Mapping Critical Levels/Loads and geographical areas where they are exceeded. UN/ECE Convention on Long-range Transboundary Air Pollution. Federal Environmental Agency, Texte UmweltBundesAmt 71/96, Berlin

UBA (2004) Modelling and Mapping Critical Loads & Levels and Air Pollution Effects, Risks and Trends. UmweltBundesAmt, Texte 52/04, Berlin

Van der Salm C, Kohlenberg L, De Vries W (1998) Assessment of weathering rates in Dutch loess and river-clay soils at pH 3.5 using laboratory experiments. Geoderma 85: 41–62

NETHERLANDS

National Focal Centre

Arjen van Hinsberg
Netherlands Environmental Assessment Agency (MNP)
P.O.Box 303
NL-3720 AH Bilthoven
tel: +31-30-2743062
fax: +31-30-2744419
arjen.hinsberg@mnp.nl

Collaborating institutions

Gert Jan Reinds, Hans Kros, Wim de Vries
Alterra (WUR)
P.O.Box 47
NL-6700 AA Wageningen
Tel: +31-317 474697
Fax: + 31- 317 419000
gertjan.reinds@wur.nl

Calculation Methods

Critical loads

Critical loads are calculated for the protection of:

- Forests (soils) against root damage due to elevated Al:Bc ratios and soil quality by requiring no changes in pH (or base saturation) and/or readily available Al (critical acid load).
- Plant species composition in terrestrial ecosystems (forests and other semi-natural vegetations) against eutrophication (critical N load) and acidification (critical acid load).
- Plant species composition in small heath land lakes against eutrophication (critical N load).

The methods to calculate these critical loads are described in a report the evaluation of the Dutch acid rain abatement strategies (Albers et al., 2001) and in various CCE reports since 2001. Critical acid loads for the protection of forest soils were calculated with SMB, as described in the CCE progress report of 2003 (Van Hinsberg and de Vries, 2003). Critical loads for the protection of heath land lakes were calculated with the dynamic model, AquAcid (Albers et al., 2001). The procedure for calculating the critical loads for the protection of terrestrial vegetations have been improved since last year. Previously, critical loads were computed with regression equations based on forward SMART2 simulations using constant deposition at various levels (Van Hinsberg and Kros, 2001). This old procedure introduced additional uncertainty from the regression functions. Moreover, for a substantial number of ecosystems, the method did not yield (positive) critical loads. In this case empirical critical loads for nitrogen were used and no target loads could be computed. In the new calculation procedure we used a steady-state version of SMART2 (Reinds et al., in prep.) to overcome these problems. Furthermore, updated critical limits for pH and nitrogen availability were obtainable for some terrestrial ecosystems (Van Dobben et al., 2004). We made use of empirical critical loads for calibration and validation only (Table NL-1).

Table NL-1. Empirical critical loads (Bobbink et al., 2002), modelled critical loads(CL) and target loads(TL) for 2030 and 2100 (in kg $ha^{-1}a^{-1}$) for EUNIS classes.

EUNIS class	Empirical CL	n[1)]	Modelled CL [2)]	Modelled TL (2030)	Modelled TL (2100)
Forest (G1)	10-20	38939	16.8 (12.9 - 18.2)	8.4 (7.4 – 16.8)	14.0 (13.0 – 16.8)
Forest (G4.1, G1.2)	-	3737	35.0 (13.0 – 43.1)	35 (25.0 – 43.1)	35 (14.5 - 43.1)
Raised bogs and wet heaths (D1)	5-10	526	6.1 (6.1 – 6.1)	4.5 (3.8 – 6.1)	5.7 (5.0 – 6.1)
Salt marsh (A2.64/65)	30-40	633	30.0 (30.0 – 34.1)	33.7 (29.9 – 33.9)	34.1 (34.0 – 34.1)
Semi-dry calcareous grasslands (E1.26)	15-25	6	12.4 (12.4 – 12.4)	-	-
Dry and neutral grasslands (E1.7)	10-20	2662	8.0 (8.0 – 8.0)	1.4 (0.2 – 3.1)	7.9 (4.4 – 10.9)
Inland dune siliceous	10-20	850	13.8 (13.8 - 13.8)	11.9 (11.5 – 12.9)	13.5 (13.5 – 13.7)

EUNIS class	Empirical CL	n[1)]	Modelled CL [2)]	Modelled TL (2030)	Modelled TL (2100)
grasslands (E1.95)					
Hay meadows (E.2.2)	10-20	4208	8.0 (8.0 - 21.7)	2.8 (1.1 – 17.)	7.5 (1.1 – 16.7)
Moist and wet oligotrophic grasslands (E3.5)	10-20	3621	12.6 (12.6 – 12.6)	1.4 (0.5 – 6.7)	1.2 (0.4 – 12.6)
Coastal stable dune grasslands (B1.4)	10-20	3267	10.7 (4.4 – 12.6)	-	-
Coastal dune heaths (B1.5)	10-20	63	15.5 (14.4 – 15.5)	3.3 (3.1 – 5.0)	12.9 (12.6 – 12.9)
Moist to wet dune slacks (B1.8 en A2.64)	10-25	1185	15.5 (7.2 – 23.6)	1.1 (0.4 – 1.2)	7.2 (1.1 – 7.2)
Dry heaths (F4.2)	10-20	5427	19.8 (9.4 – 17.1)	19.8 (17.0 – 19.8)	19.8 (18.5 – 19.8)
Soft-water lakes[3)] (C1.1)	4-10	417	4.7 (1.2 – 12.4)	-	-

[1)] Number of modelled sites
[2)] Values in brackets refer to the 5 and 95 percentiles
[3)] Calculated with AquAcid

As in earlier data submissions to the CCE, the critical load for nitrogen as nutrient was calculated as the nitrogen deposition that leads to the desired nitrogen availability (Van Hinsberg and de Vries, 2001). The critical load function for acidity was derived so that each combination of S and N deposition on this function would lead to the desired pH in a steady state. In earlier submissions to the CCE, the parameters were back-calculated using fixed ratios between N and S depositions as well as assuming a negligible N uptake, a low constant N immobilization of 1 $kg.ha^{-1}.a^{-1}$ and a low constant denitrification fraction of 0.1 (Van Hinsberg and de Vries, 2001). For a limited number of sites the new method still did not yield realistic critical loads (> 100 $eq.ha^{-1}.a^{-1}$) for either nitrogen or acidity. A study will be conducted to investigate whether this is due to the model concept, the input data or the imposed critical limits for pH and/or nitrogen availability.

Target loads

The target loads for protection of forest soils were computed with the VSD model using a critical [Al]:[Bc] criterion (Van Hinsberg et al., 2004). Target loads for the protection of plant species composition in terrestrial ecosystems were computed with the SMART2 model, using critical limits for both pH and nitrogen availability (Van Hinsberg and Kros, 2001).

Both VSD and SMART2 were calibrated, with simulations starting in 1880; exchange parameters were adjusted so that base saturation in 1995 was correctly simulated. Base saturation in 1995 was assigned to each 250×250 m grid cell using a transfer function with soil type, vegetation type and groundwater regime. For VSD, the C:N ratio and the carbon pool too were back-calculated, whereas for SMART2, the amount of litter was calibrated within defined limits by adjusting the litterfall rate and/or mineralization constant.

The target loads computed with VSD were compared to critical loads based on the [Al]:[Bc] criterion and to critical loads based on the concept of requiring no changes in pH or base saturation (a criterion for which no meaningful target loads can be computed). The minimum of the three functions was submitted. In other words, for som ecosystems the target load for [Al]:[Bc] is submitted, although the critical load for a constant pH is lower than the critical load for [Al]:[Bc]. For such ecosystems, obtaining a certain [Al]:[Bc] ratio in a specific year will simply require more deposition reduction aimed at no pH change on an infinite time scale.

Target loads for plant species composition were computed with SMART2, so that protection of the ecosystem would be achieved for both pH and N availability simultaneously. For a number of ecosystems (about 5%), the model did not produce a target load function leading to the desired pH and N availability for any of the three target years (2030, 2050, 2100), although a valid critical load function exists. Since pH recovery of these systems is extremely slow, it would take more than a century to achieve the desired pH and N availability. Because we

doubt the validity of this result, it was decided to leave out the dynamic modelling results (target loads and time development) for the ecosystems for which no valid target load had been computed in any of the three years (2030, 2050 and 2100). Further analysis will be carried out to reveal the causes of this slow recovery.

Data derivation

All critical loads and target loads were calculated for 250×250 m grid cells. Specifying the terrestrial vegetation–soil combination in the 250×250 m grid cells was achieved using an overlay of the 1:50,000 soil map and a vegetation map based on both satellite observations, along with several detailed vegetation surveys. Five types of terrestrial vegetation and 16 major soil types were specified. With respect to vegetation types, we distinguished three groups of tree species (deciduous forests, pine forests and spruce forests), and grassland and heath land (CCE, 2001). Calculated critical loads for nitrogen as a nutrient in small heath land lakes were calculated separately with AquAcid and added to the final database later on.

Soil types were differentiated into 16 major groups, including two non-calcareous sandy soils and one calcareous sandy soil, three loess soils, four non-calcareous clay soils, one calcareous clay soil and five peat soils (Van der Salm, 1999). All these soil types were further sub- divided into five hydrological classes, depending on the seasonal fluctuations of the groundwater table. Parameterization of processes included in both VSD and SMART2 was kept uniform.

Derivation of data needed for critical load calculations and target loads (dynamic modelling)

Data sets and model parameters used to calculate the critical load and target loads are described in the status report of 2003 (Van Hinsberg and de Vries, 2003), while an overview of the SMART2 model, along with its parameterization, is provided in Kros (1998). Target loads and critical loads were calculated using earlier described data, except for the amount of litterfall and N content in the litterfall. In contrast to earlier calculations, the amount of litterfall in steady state was assumed to vary among different combinations of nature targets and soil types. For forests, data was derived from the SUMO model, which uses tree-species dependent litterfall. For grasslands, maximum litterfall was assumed to be linearly related to the above-ground biomass (which could be calculated for different nature types using Ellenberg indicators; Van Hinsberg et al., 2002) multiplied by a factor indicating the litterfall production. This factor was set at 0.75 in grasslands, based on measurements in Molinea grasslands (Berendse, 1988), and at 0.20 in heath lands (Berendse, 1988).

References

Albers R, Beck J, Bleeker A, Van Bree L, Van Dam J, Van der Eerden L, Freijer J, Van Hinsberg A, Marra M, Van der Salm C, Tonneijck A, De Vries W, Wesselink L, Wortelboer F (2001) Evaluatie van de verzuringsdoelstellingen: de onderbouwing. RIVM Report 725501001, Bilthoven, The Netherlands

Berendse F (1988) De nutriëntenbalans van droge zandgrondvegetaties in verband met de eutrofiëring via de lucht. University of Wageningen, Wageningen, The Netherlands

Bobbink R, Ashmore M, Braun S, Flückiger W, Van den Wyngaert IIJ (2002) Empirical nitrogen critical loads for natural and semi-natural ecosystems: 2002 update. In: Empirical critical loads for nitrogen, B.A.A.R. Bobbink (ed.), Swiss Agency for Environment, Forest and Landscape SAEFL, Berne, pp. 43-170

Kros J (1998) Verbetering, verfijning en toepassing van het model SMART2 - De modellering van de effecten van verzuring, vermesting en verdroging voor bossen en natuurterreinen ten behoeve van de Milieubalans. SC-DLO MBP Report 3, Wageningen, The Netherlands

Reinds GJ, Posch M, Kros H (2005) Steady state version of the SMART2 model. Alterra Report (in prep)

Van der Salm C (1999) Weathering in forest soils. PhD Thesis, University of Amsterdam, Amsterdam

Van Dobben H, Schouwenberg EPAG, Mol JP, Wieggers HJJ, Jansen M, Kros J, De Vries W (2004) Simulation of critical loads for nitrogen for terrestrial plant communities in the Netherlands. Alterra Report 953, Wageningen, the Netherlands, 84 pp

Van Hinsberg A, Kros J (2001) Dynamic modelling and the calculation of critical loads for biodiversity. In: Posch et al. (eds): Modelling and Mapping of Critical Thresholds in Europe, CCE Status Report 2001, pp. 73-80

Van Hinsberg A, De Vries W (2001) Netherlands. In: Posch et al. (eds): Modelling and mapping of critical thresholds in Europe: CCE Status Report 2001. RIVM Report 259101010, Bilthoven, The Netherlands, pp. 73-80

Van Hinsberg A, Van Dobben H, Kros J (2003) Possibilities asd use of multi-species models for the calculation of critical loads for nitrogen for (semi-)natural ecosystems. In: B Achermann, R Bobbink (eds) Empirical Critical Loads for Nitrogen. Swiss Agency for Environment, Forest and Landscape, Berne, pp. 213-225

Van Hinsberg A, De Vries W (2003) Netherlands. In: Posch et al. (eds) Modelling and mapping of critical thresholds in Europe: CCE Status Report 2003. RIVM Report 259101013, Bilthoven, The Netherlands, pp. 93-97

Van Hinsberg A, Reinds GJ, Kros H, De Vries W (2004) The Netherlands. In: Hettelingh et al. (eds): Critical loads and dynamic modelling results: CCE Progress Report 2004. RIVM Report 259101014, Bilthoven, The Netherlands, pp. 91-95

NORWAY

National Focal Centre

Thorjørn Larssen
Norwegian Institute for Water Research
P.O. Box 173 Kjelsås
0411 Oslo
tel: +47 22185194
fax: +47 22185200
thorjorn.larssen@niva.no

Collaborating institutions

Norwegian Institute for Air Research
P.O. Box 100
2007 Kjeller

Norwegian Institute for Nature Research
Tungasletta 2
7485 Trondheim

Norwegian Institute for Land Inventory
P.O. Box 115
1431 Aas

Calculation of Target Load Functions (TLFs)

We have calculated target load functions for surface waters, according to the specifications in the call. The calculations are based on a population of 131 lakes in southern Norway. These are lakes included in the national monitoring program and are those for which we have sufficient data to calculate target load functions with the dynamic model MAGIC. Due to resource limitations we have confined our work at this time to lakes south of 62.5 degrees latitude. Target loads were not calculated for lakes having measured ANC values in 1995-1997 (average) higher than ANC_{limit}. The variable ANC_{limit} was calculated in accordance with the Mapping Manual, except that BC^*_0 was taken from the calibrated initial concentrations from the MAGIC model calibration. 83 of the lakes had ANC below ANC_{limit} and TLFs was calculated.

Ranges of model inputs and parameters and comments on their sources and justifications are listed in Table NO-1.

Table NO-1. Model inputs and parameters.

Var	Unit	Min	Max	Assumptions, data sources and justifications
EcoArea	%	100%	100%	We consider 100% of the land area to contain watersheds for lakes and rivers. We have not calculated the area of the EMEP grid cells, which should be given here (minus the part of the cell covering ocean).
CLmaxS	eq ha^{-1} a^{-1}	5.36	73.24	Calculated with FAB model (according to Mapping Manual, except BC^*_0 taken from MAGIC calibrations (1860)
CLminN	eq ha^{-1} a^{-1}	3.20	42.32	
CLmaxN	eq ha^{-1} a^{-1}	11.78	118.42	
CLnutN				Not applicable
crittype		6	6	ANC is used as criterion for all lakes
critvalue	µeq L^{-1}	1.27	18.15	Variable ANC_{limit}
SoilYear		1995	1995	Same year (1995) used for all soil analyses
ExCa	%	2.17	40.41	Taken from nearest relevant soil sampling locations or as a combination of nearest forested and non-forested soil sampling location. Data from forested catchments from the National Forest Inventory; data from non-forested catchments from different research and monitoring projects.
ExMg	%	0.69	24.47	
ExNa	%	0.75	6.75	
ExK	%	0.26	7.43	
thick	m	0.03	0.89	
BulkDens	kg m^{-3}	192.3	906.98	
CEC	meq kg^{-1}	12.31	242.52	
Cpool	g m-2	2080	85371	
Npool	g m-2	99	4914	
Porosity	%	50	50	Assumption. Constant value used for all sites.
Nimacc	eq ha^{-1} a^{-1}	34	34	Default values for FAB model from Mapping Manual
UptCa	meq m^{-2} a^{-1}	0.00	29.74	Based National Forest Inventory.

Var	Unit	Min	Max	Assumptions, data sources and justifications
UptMg	meq m^{-2} a^{-1}	0.00	5.61	
UptK	meq m^{-2} a^{-1}	0.00	6.44	
UptNa	meq m^{-2} a^{-1}	0.00	1.06	
UptSO4	meq m^{-2} a^{-1}	0.00	0.00	
UptNH4	meq m^{-2} a^{-1}	0.00	0.00	
HlfSat	µeq L^{-1}	100	100	Assumption. Constant value used for all sites.
Emx	meq kg^{-1}	1.00	1.00	Assumption. Constant value used for all sites.
Nitrif	%	100	100	Assumption based on the fact that ammonium concentrations are very low.
Denitrf	%	0.00	0.00	
CNRange		11.00	11.00	Constant range based on empirical data from [1]
CNUpper		10	73.4	Calibrated
DepYear		1995	1995	
Cldep	eq ha^{-1} a^{-1}	66.78	5366	Deposition flux of Chloride, sat equal to catchment output flux
Cadep	eq ha^{-1} a^{-1}	2.47	198.6	
Mgdep	eq ha^{-1} a^{-1}	13.09	1039.8	Calculated from [Cl^-] using standard sea salt ratios and assuming no non-sea salt deposition
Nadep	eq ha^{-1} a^{-1}	57.30	4363	
Kdep	eq ha^{-1} a^{-1}	1.20	96.60	
NH4dep	eq ha^{-1} a^{-1}	74.04	811.0	Calculated from observed ratios in deposition to SO4.
NO3dep	eq ha^{-1} a^{-1}	74.77	695.5	SO4 deposition was calculated from runoff flux assuming geological contribution and background deposition as described in mapping manual.
LakeYear		1995	1995	
Calake	µmol L^{-1}	2.99	39.25	
Mglake	µmol L^{-1}	1.78	37.43	
Nalake	µmol L^{-1}	7.39	247.94	
Klake	µmol L^{-1}	1.02	16.37	Lake chemistry taken from the National Lake Monitoring Program [2]. Average for 1995-1997 was used.
NH4lake	µmol L^{-1}	0.00	0.00	
SO4lake	µmol L^{-1}	4.51	68.36	
Cllake	µmol L^{-1}	8.46	302.75	
NO3lake	µmol L^{-1}	1.38	34.76	
DOC	µmol L^{-1}	0.73	31.96	Organic acid fraction of DOC assuming tri-protic acid and charge density of 10.2 µeq/mg C (From [3])
RelArea	%	0.41	36.36	Data for each catchment taken from maps
RelForArea				
RetTime	a	0.50	0.50	Assumption. Constant value used for all sites.
Qs	m	0.41	4.49	Runoff taken from digital 30-year normal runoff database.
expAllake		3.00	3.00	Assumption. Constant value used for all sites.
pCO2	%	0.05	0.05	Assumption. Constant value used for all sites.
Nitrifilake	%	100	100	Assumption. Constant value used for all sites.
Cased	m a^{-1}	0.00	0.00	
Mgsed	m a^{-1}	0.00	0.00	
Nased	m a^{-1}	0.00	0.00	Assumption. Constant value used for all sites.
Ksed	m a^{-1}	0.00	0.00	
SO4sed	m a^{-1}	0.00	0.00	
Clsed	m a^{-1}	0.00	0.00	
NH4sed	m a^{-1}	5.00	5.00	Assumption, based on generalization described in Mapping Manual
NO3sed	m a^{-1}	5.00	5.00	
UptNH4lake	%	0.00	0.00	Assumption. Constant value used for all sites.
UptNO3lake	%	0.00	0.00	Assumption. Constant value used for all sites.
Sdep2010	eq ha^{-1} a^{-1}	80.43	621.5	Calculated from estimate of total input in 1995 and Current Legislation forecast scenarios taken from [4].
NOxdep2010	eq ha^{-1} a^{-1}	49.35	459.0	
NH3dep2010	eq ha^{-1} a^{-1}	71.08	778.6	

Calculation of Critical Loads

Surface waters

The critical loads for waters were calculated for all lakes were TLFs were calculated using the FAB model and data corresponding to those used in the TLF calculations. BC^*_0 was taken from the initial (1869) value of the MAGIC model calibrations.

The Norwegian critical loads database is available on a grid basis, each grid covering 1/4 times 1/8 degree. For all the grid cells not having a lake where TLFs were calculated, the CLs from the database was used. The CL database for surface water has been updated with digital runoff data since previous calls. The data are described in [5] and [6].

Forest soils

The critical loads for forest soils were calculated using the SMB model. They are not updated since reported to CCE in the 2003 Call for data [4]. The methods and data are described in [6].

Nutrient effects on vegetation

The critical loads for nutrient effects on vegetation are considerable updated [7, 8]. Empirical critical loads are used, with the lowest value of the range for each vegetation type from [9]. Data are taken from the national 3x3 km^2 sampling grid of the National Forest Survey. Critical loads were determined for ten natural and semi-natural ecosystems. Rural habitats were excluded. The following ecosystems and values were used:

1	Ombrotrophic mire (bog) and lowland mires without further information.	500 mg N/m^2
2	Freshwater and river	500 mg N/m^2
3	Glacier	500 mg N/m^2
4	Alpine vegetation	500 mg N/m^2
5	Poor fen and alpine mires without further information	1000 mg N/m^2
6	All types of forest	1000 mg N/m^2
7	Treeless vegetation below forest limit, coastal heath	1000 mg N/m^2
8	Grazing land	1000 mg N/m^2
9	Intermediate and rich fen	1500 mg N/m^2
10	Cultural landscapes without further information	2000 mg N/m^2
11	Rural areas, technical impediment	none

Assignment of areas to the different critical loads

The area assigned to the surface water critical load and target load data for each data point (grid) approximately adds up to the total area of Norway (approximately 323,000 km^2). The total area for the grids with forest soils critical loads adds up to the total area of productive forest (72,700 km^2). For the nutrient nitrogen to vegetation critical loads, the data points are located in a 3x3 km^2 grid, thus the area of each grid are sat to 9 km^2. The area for all grids adds up to approximately the total area of the country.

References

Aarrestad PA, Bruteig I (2005) Updated Critical Loads for Atmospheric Deposition of Nitrogen for Nutrient Effects on Vegetation. Norwegian Institute for Nature Research (in prep)

Achermann B, Bobbink R (eds) (2003) Empirical critical loads for nitrogen. Expert workshop Berne 11-13 Nov. 2002. Swiss Agency for the Environment: Berne, Switzerland

Gundersen P, Callesen I, De Vries W (1998) Nitrate leaching in forest ecosystems is controlled by forest floor C/N ratio. Environmental Pollution 102: 403-407

Henriksen A, Buan AK (2000) Critical Loads and exceedances of Critical Loads for Surface Water, Soils and Vegetation in Norway (In Norwegian). Norwegian Institute for Water Research, Oslo, 29 pp

Hruska J, et al. (2003) Is a universal model of organic acidity possible: Comparison of the acid/base properties of dissolved organic carbon in the boreal and temperate zones. Environmental Science and Technology 37: 1726-1730

Knudsen S, et al. (2005) EIF Air Phase II Report. Norwegian Institute for Air Research, 67 pp

Larssen T, Høgåsen T (2003) Critical Loads and Exceedances of Critical Loads in Norway (In Norwegian). Norwegian Institute for Water Research. 24 pp

Schöpp W, et al. (2003) Long-term development of acid deposition (1880-2030) in sensitive freshwater regions in Europe. Hydrology and Earth System Sciences 7: 436-446

SFT (2004) Norwegian monitoring programme for long-range transported air pollutants. Annual report - Effects 2003. The Norwegian Pollution Control Authority (SFT), Oslo, Norway, 172 pp

POLEN

National Focal Centre

Wojciech A. Mill, Adrian Schlama
Institute of Environmental Protection
Section of Integrated Modelling
Grunwaldzka Str. 7B/2
PL-41-106 Siemianowice Śl.
tel/fax: +48 32 2281482
mill@silesia.top.pl

Collaborating institutions

Anna Pasieczna, Jozef Lis
Polish Geological Institute
Environmetal Geology Department
Rakowiecka Str. 4
PL-00-975 Warszawa
tel: +48 22 8495351
apas@pgi.waw.pl
jlis@pgi.waw.pl

Dorota Rzychoń, Adam Worsztynowicz
Institute for Ecology of Industrial Areas
Kossutha 6
PL-40-881 Katowice
Tel: +48 32 2546031
rzychon@ietu.katowice.pl
worsztynowicz@ietu.katowice.pl

State Inspectorate of Environmental
Protection, Department of Monitoring
Contractor:
Ryszard Twarowski, Jan Błachuta
Institute of Meteorology
and Water Management
the Wrocław Branch
Parkowa Str. 30
PL-51-616 Wrocław
tel: +48 71 3281446

Krzysztof Okła, Jolanta Starzycka
General Directorate of the State Forests
Spatial Information System
Wawelska Str. 52/54
PL-00-922 Warszawa
okla@lasypanstwowe.gov.pl,
j.starzycka@lasypanstwowe.gov.pl

Calculation methods

Critical loads

Basically critical loads were calculated in accordance with the methodology presented in the latest version of the Mapping Manual and implemented in the SONOX software (Mill, 2000).

Broadleaved (EUNIS class G1) and coniferous (EUNIS class G3) forest ecosystems were the receptors mapped. The Polish critical loads database consists of 88,383 records representing grid cells of 1×1 km^2 size covering about 30% of the country's area.

Target loads

The target loads for protection of forest soils were computed with the Access version of the VSD model (Posch and Reinds, 2005). For the cation exchange the Gapon model was used.

Revisions made to input data

The following changes to critical loads input data have been made since the last update:

Chemical criterion

A test has been performed to compare the effect of different chemical criteria on critical loads for Polish forest soils. The Al criterion produced the lowest $CL_{max}(S)$ values and was accepted for critical and target loads calculations instead of previously used Bc/Al criterion.

Base cation deposition data

The bulk deposition data for base cations produced by the Institute of Meteorology and Water Management – the Wrocław Branch under the State Monitoring of Environment authority were compared with the recently distributed EMEP base cations maps. Taking into account some model uncertainties, difference in spatial replication (50×50 km^2 EMEP grids vs determined spatial points), contribution of local sources in monitored values basically not considered by EMEP model (the monitored depositions are systematically higher than modelled) a conclusion may be drawn that in general the correspondence of the monitored and modelled depositions might be considered satisfactory.

To calculate critical loads for Polish forest ecosystems national base cation deposition data monitored for 2003 were applied.

Denitrification fraction

Denitrification fraction values f_{de} were assigned to soil clay content according to empirical relationship given in German NFC Report in Posch et al. (2001).

Sea salt correction

Within this critical loads update the base cations deposition was corrected for sea salt contribution. No significant changes to critical load values have been observed.

No changes to additional soil data needed for target loads calculations have been made within this update.

Summary of Polish critical loads data

Summary of $CL_{max}(S)$, $CL_{min}(N)$, $CL_{max}(N)$ and $CL_{nut}(N)$ as well as corresponding input data is given in Table PL-1

Maps submitted

Based on the results of critical load calculations updated maps of $CL_{max}(S)$, $CL_{min}(N)$, $CL_{max}(N)$ and $CL_{nut}(N)$ for Polish forests were submitted - Figures PL 1-2.

Dynamic modelling results

The dynamic model VSD (Very Simple Dynamic model) has been used to generate target load functions for 88,383 forest sites. Target load functions are submitted for the target years 2030, 2050 and 2100. A summary of the results is presented in Table PL-2.

Table PL-1. Summary of Polish critical load data.

Parameter	EUNIS code	Min value	Mean value	Max value	Methods used	Description
$Cl_{max}(S)$ [eq $ha^{-1}yr^{-1}$]	G1	409	1574	4970	$CL_{max}(S)=BC_{dep}+BC_w-BC_u-ANC_{le(crit)}$	Calculated by SONOX
	G3	530	1577	5039		
$Cl_{min}(N)$ [eq $ha^{-1}yr^{-1}$]	G1	219	743	1321	$Cl_{min}(N)=N_i+N_u$	Calculated by SONOX
	G3	219	421	896		
$CL_{max}(N)$ [eq $ha^{-1}yr^{-1}$]	G1	990	2994	>9,999	$CL_{max}(N)=CL_{min}(N)+CL_{max}(S)/(1-f_{de})$	Calculated by SONOX
	G3	990	2357			
$CL_{nut}(N)$ [eq $ha^{-1}yr^{-1}$]	G1	257	800	1501	$CL_{nut}(N)=N_i+N_u+N_{le}(acc)/(1-f_{de})$	Calculated by SONOX
	G3	257	491	1566		
Bc_{dep} [eq $ha^{-1}yr^{-1}$]	G1	208	438	694	The bulk deposition values of base cations were estimated from the reported wet deposition data multiplied by dry deposition factors derived from throughfall data provided by the integrated monitoring surveys	Monitoring network operated by the Institute of Meteorology and Water Management – Wroclaw Branch under the authority of Main Inspectorate of Environment Protection
	G3	208	441	840		
BC_u [eq $ha^{-1}yr^{-1}$]	G1	72	344	572	Uptake of base cations related to deciduous and coniferous trees was calculated as the minimum of growth limited uptake and nutrient limited uptake.	Elements content in stems and branches was provided by the Polish Academy of Science – Institute of Dendrology (Fober, 1986). The forest growth rates were obtained from the Forest Management and Geodesy Office.
	G3	72	186	409		
BC_w [eq $ha^{-1}yr^{-1}$]	G1	218	566	2558	Calculated according to Mapping Manual. Also PROFILE model has been applied for limited number of sites.	Soil samples delivered by the Forest Research Institute (Wawrzoniak et al., 2000) Mineral composition analysis (Stępniewski, 1998)
	G3	218	466	2558		
Q_{le} [mm yr^{-1}]	G1	5	167	1366	According to Mapping Manual, calculated as the difference between 30- year mean atmospheric precipitation and evapotranspiration	Hydrological Atlas of Poland (Stachy et al., 1986)
	G3	5	152	1360		
K_{gibb} [m^6eq^{-2}]	G1		300		Following the Mapping Manual recommendation the value 300 for mineral soils was chosen.	Mapping Manual
	G3		300			
$ANC_{le(crit)}$ [eq $ha^{-1}yr^{-1}$]	G1	14.2	479	3897	Calculated via SMB equation with Bc:Al ratios differentiated due to 6 tree species.	Mapping Manual
	G3	14.2	432	3865		
N_i [eq $ha^{-1}yr^{-1}$]	G1	71	157	356	A temperature dependent long-term immobilization factor was applied, ranging from 71 to 356 eq $ha^{-1}yr^{-1}$	CCE Status Report 2001
	G3	71	138	356		
N_u [eq $ha^{-1}yr^{-1}$]	G1	112	587	965	Uptake of nitrogen related to six major tree species was calculated as the minimum of growth limited uptake and nutrient limited uptake.	Elements content in stems and branches was provided by the Polish Academy of Science – Institute of Dendrology (Fober, 1986). The forest growth rates were obtained from data bank of the Forest Management and Geodesy Office.
	G3	112	283	540		
f_{de}	G1	0.1	0.17	0.8	Depending on soil clay content values from 0.1 to 0.8 were applied	CCE Status Report 2001
	G3	0.1	0.13	0.8		
$N_{le}(acc)$ [eq $ha^{-1}yr^{-1}$]	G1	1.1	35.1	286	For coniferous: 0.0143 eq/m3· Qle for deciduous: 0.02 eq/m3 ·Qle	Mapping Manual
	G3	1.8	53.9	480		

Table PL-2. Summary of target loads calculations for Polish forest ecosystems.

Status	Target Year	Number of sites	%
TLF present	2030	38767	43.86
	2050	39175	44.32
	2100	39107	44.25
TL not feasible	2030	604	0.68
	2050	83	0.09
	2100	0	0.00
Not exceeded in 2010	2030	9368	10.60
	2050	9481	10.73
	2100	9632	10.90
Exceeded at present		48739	55.15

Heavy Metals

Since the 15th CCE workshop in Berlin the following two changes have been made to the Polish heavy metals database:

- Soil pH values measured in KCl extract were corrected to soil solution pH according to the regression function given in Table 5.23 in the Manual on Methodologies and Criteria for Modelling and mapping Critical loads & Levels and Air Pollution Effects, Risks and Trends.
- Annual mean precipitation surplus values were determined by empirical relationship combining long-term mean annual values of temperature, precipitation and potential evapotranspiration. This relationship is given in the Manual as equation 5.91b.

The two corrected input parameters were entered into the heavy metals database and calculations of critical loads of cadmium, lead and mercury were repeated. The corrections done resulted in a further improvement of the accordance of the Polish critical loads of the all considered metals with relevant critical loads in neighboring countries.

References

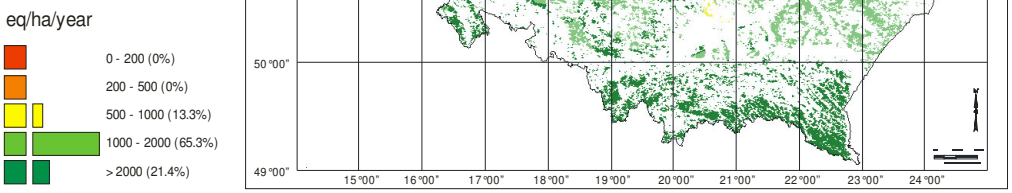
Fober H (1986) Nasze drzewa leśne (ed) Białobok S, PWN, Warszawa
Mill W (2000) Integrated modelling of acidification effects to forest ecosystems – model SONOX. Water, Air and Soil Pollution 130: 1289-1294
Posch M, Hettelingh J-P, De Smet PAM, Downing RJ (eds) (2001) Calculation and Mapping of Critical Thresholds in Europe: CCE Status Report, RIVM Report No.259101009, Bilthoven, The Netherlands
Posch M, Reinds GJ (2005) VSD – User Manual of the Very Simple Dynamic soil acidification model. Coordination Center for Effects, RIVM, Bilthoven, The Netherlands (in prep.)
Stachy J (1986) Atlas hydrologiczny Polski, Wydawnictwa Geologiczne, Warszawa
Stępniewski M (1998) Mineralogical composition of selected forest soils. Manuscript. State Institute of Mineralogy, Warsaw
Wawrzoniak J, Małachowska J, Wójcik J, Liwińska A (2000) Stan uszkodzenia lasów w Polsce w 1999 r. na podstawie badań monitoringowych, Biblioteka Monitoringu Środowiska PIOŚ, Warszawa

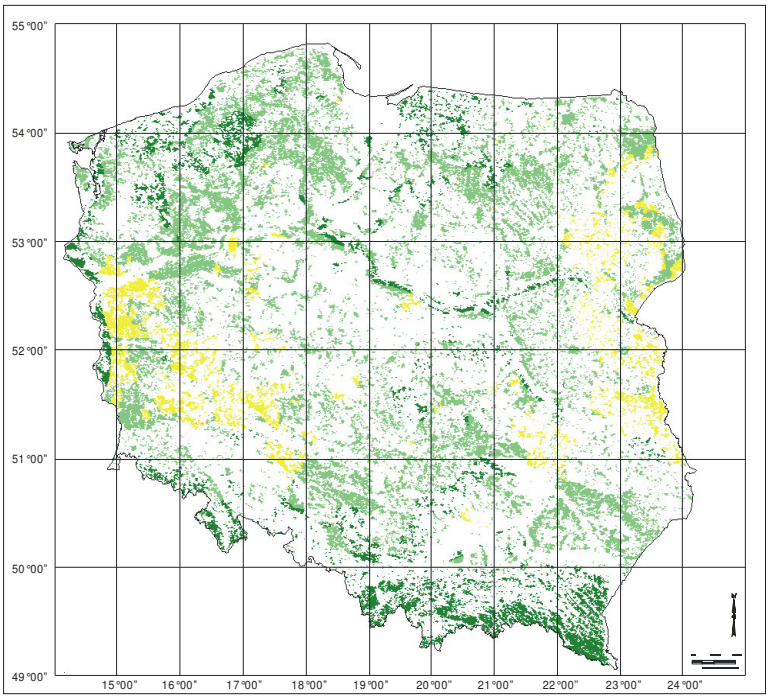
Figure PL-1. Critical loads.

Institute of Environmental Protection
Department of Environmental Policy - Section of Integrated Modelling
Grunwaldzka Str. 7b/2, 41-106 Siemianowice Sl., Poland

Maximum critical loads of sulphur

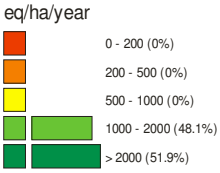
2005





Maximum critical loads of nitrogen

2005



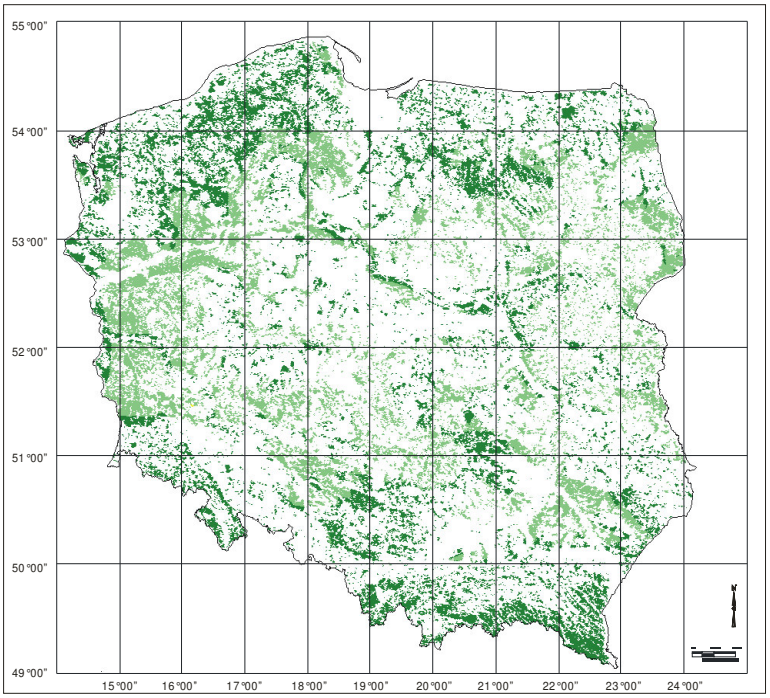
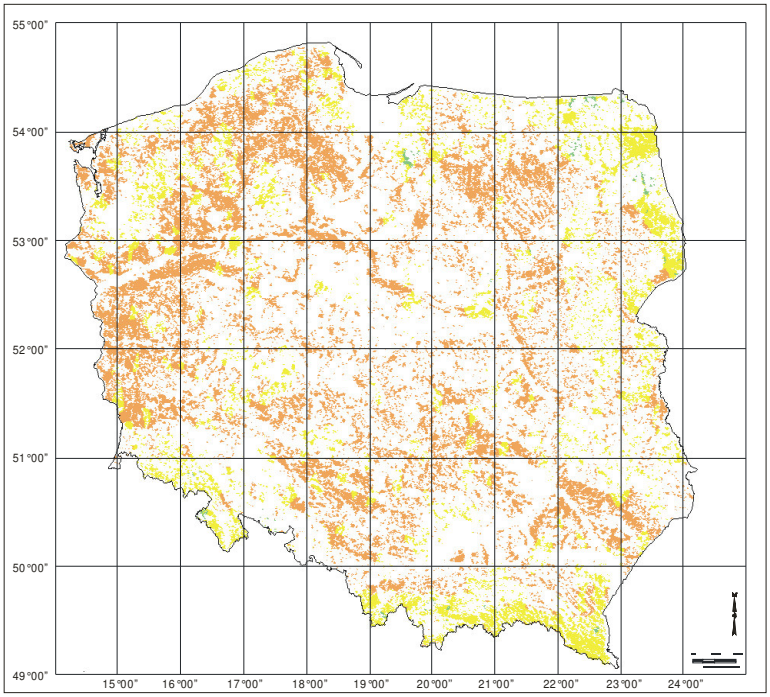


Figure PL-2. Critical loads.

Institute of Environmental Protection
Department of Environmental Policy - Section of Integrated Modelling
Grunwaldzka Str. 7b/2, 41-106 Siemianowice Sl., Poland

Minimum critical loads of nitrogen

2005

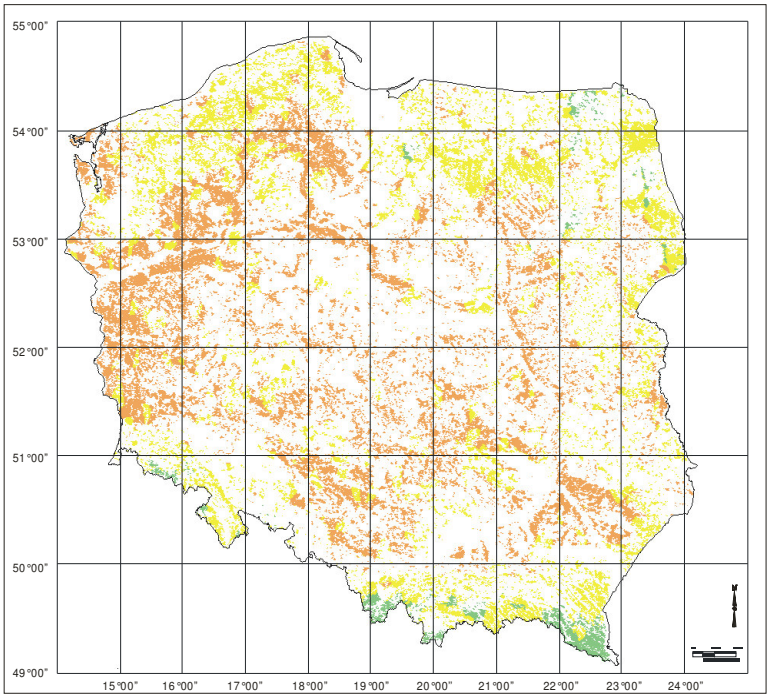


eq/ha/year

- 0 - 200 (0%)
- 200 - 500 (69.7%)
- 500 - 1000 (29.7%)
- 1000 - 2000 (0.5%)
- > 2000 (0%)

Critical loads of nutrient nitrogen

2005



eq/ha/year

- 0 - 200 (0%)
- 200 - 500 (55.1%)
- 500 - 1000 (40.8%)
- 1000 - 2000 (4.1%)
- > 2000 (0%)

SLOVAKIA

National Focal Centre

Dusan Závodský
Slovak Hydrometeorological Institute
Jeséniova 17
SK-833 15 Bratislava
tel: +421 7 5941 5377
fax: +421 7 5477 5670
zavodsky@mail.shmu.sk

Collaborating institution

Jozef Mindas
Forest Research Institute
T.G.Masaryka 22
SK-960 92 Zvolen
tel: +421 855 5314 206
fax: +421 855 5321 833
mindas@fris.sk

Heavy Metals

For mercury the metal content in wood and bark used to calculate the metal uptake has been set to the default value of 0.03 mg kg^{-1} dw. The critical total dissolved metal concentration in the soil solution has been slightly modified.

SWEDEN

National Focal Centre

Ulla Bertills
Swedish Environmental Protection Agency
SE-106 48 Stockholm
tel: +46 8 698 1502
ulla.bertills@naturvardsverket.se

Håkan Staaf
Swedish Environmental Protection Agency
SE-106 48 Stockholm
tel: +46 8 698 1442
hakan.staaf@naturvardsverket.se

Collaborating institutions

Cecilia Akselsson
Department of Chemical Engineering
University of Lund
P.O. Box 124
SE-221 01 Lund
tel: + 46 46 222 4866
cecilia.akselsson@chemeng.lth.se

Mattias Alveteg
Department of Chemical Engineering
University of Lund
P.O. Box 124
SE-221 01 Lund
tel: + 46 46 222 3627
mattias.alveteg@chemeng.lth.se

Veronika Kronnnäs
Swedish Environmental Research Institute
P.O. Box 5302
SE-400 14 Göteborg
tel: +46 31 725 6278
veronika.kronnas@ivl.se

Filip Moldan
Swedish Environmental Research Institute
P.O. Box 5302
SE-400 14 Göteborg
tel: +46 31 725 6231
filip.moldan@ivl.se

Lars Rapp
Swedish University of Agricultural Sciences
Environmental Data Centre
P.O. Box 7062
SE-750 07 Uppsala
tel: + 46 18 673826
lars.rapp@md.slu.se

Harald Sverdrup
Department of Chemical Engineering
University of Lund
P.O. Box 124
SE-221 01 Lund
tel: + 46 46 222 8274
harald.sverdrup@chemeng.lth.se

Introduction

In response to the call for data November 2004, the following datasets have been produced:

- Updated critical loads for acidity of forest and freshwater ecosystems
- Target load functions for forest and freshwater ecosystems 2030, 2050, 2100
- Values of chemical variables for Go (Gothenburg) and Bg (background) scenarios for forest and freshwater ecosystems

Calculation methods

Critical loads and target loads

Forest ecosystems

For forest ecosystems critical loads were calculated with either a steady-state or a dynamic approach, depending on data availability. In the steady-state approach, critical loads were calculated as described in Sverdrup et al. 2002, using the PROFILE model. Calculations were performed for a 50 cm soil profile, divided into four layers (O, A/E, B, C), assuming an average stone/rock content of 30% in the mineral soil and using rate controlled nitrogen immobilisation.

Where data availability allowed for dynamic assessment, critical loads and associated target loads were calculated using the SAFE model setup. MAKEDEP (Alveteg et al., 2002) was used to derive site specific time series of deposition, nutrient uptake and nutrient cycling for the simulation period 1800-2500. The SAFE model (Alveteg, 1998; Warfvinge et al., 1993) includes chemical weathering, nitrification, Gapon type cation exchange, empirical aluminium concentration control and soil solution equilibria. The soil profile was divided into three to five layers and for some sites even seven layers, based on available measurements of exchangeable cations. The model is calibrated against present base saturation only by varying the initial base saturation. As the model is initialized at year 1800 assuming steady-state, varying the initial base saturation is equivalent to varying the Gapon selectivity coefficient.

To allow for calculations of critical loads and target loads the future scenario was averaged based on the next forest rotation, rather than the present forest rotation as done in VSD. In both the steady-state and dynamic calculations an adaptive uptake scheme was used for distributing uptake between soil layers (Martinsson et al., 2005). In the steady-state approach a weighted Bc:Al ratio was used as the chemical criterion, whereas molar $Bc:Al^{3+}$ ratio was used in the dynamic approach. The critical limit was set to 1 in both cases. For sites where critical loads were calculated with both methods the dynamic results were chosen for inclusion in the reporting. Climate parameters were kept constant throughout the modelling period. SAFE was run with sulphate adsorption and rate-controlled nitrogen immobilisation turned off. Nitrogen deposition was never reduced below the calculated average future net uptake. Nutrient uptake, nutrient circulation as well as deposition of other elements than S and N were averaged for upcoming forest rotation and were kept constant in the TL and CL runs after 2010. An average value was approached from the value in 2000 by linear interpolation. It should be noted that the background scenario affected the model calibration for some sites and that consequently even 1990 values differ in the two scenarios (Bg and Go). Many sites also differ between the two scenarios for 2010 since the average uptake is approached linearly prior to 2010. The background scenario implicitly assumes a change in forestry practice for many sites. On the other hand, a change might be needed from a sustainability perspective, i.e. reducing removal of base cations, according to previous studies.

Freshwater ecosystems

For freshwaters the critical loads were calculated using the first-order acidity balance (FAB) model as described in Henriksen et al. (1993), Posch (1995) and Rapp et al. (2002). Dynamic modelling was performed using the MAGIC model (Cosby et al., 1985; 2001).

In order to make the critical load calculations consistent with the MAGIC model, the weathering rate, calculated by MAGIC, was used in FAB. When no MAGIC weathering was available, the FAB weathering was based on a regression between pre-industrial [BC]*, calculated by MAGIC, and contemporary [BC]*. Thus the F-factor for estimating the pre-industrial lake chemistry was not used. Existing MAGIC calibration (Moldan et al., 2004) had to be modified to make the dynamic model calculations consistent with calculations of critical loads by FAB with respect to historical forest uptake. Since the lakes' catchments are not at risk of becoming nitrogen saturated before 2100, nitrogen dynamics in the modelling were turned off. The value of N deposition of the second points of the target load functions, the equivalent to the $Cl_{min}(N)$ of the critical load function, was set equal to N-immobilisation.

The chemical threshold, ANC_{limit}, was set to 20 (eq l^{-1} in cases where $[BC^*_o] > 25$ (eq l^{-1}. In other cases, ANC_{limit} was set to $0.75[BC^*_o]$ to allow for naturally low ANC concentrations. The N-immobilisation was set to a maximum of 2 kg N $ha^{-1}a^{-1}$ (terrestrial) and then weighted to land use types within the catchment. The average denitrification fraction for each catchment was related linearly to the fraction of peat lands in the catchment area ($f_{de}=0.1+0.7f_{peat}$) as suggested in Posch et al. (1997). In contrast to the mapping manual, the net uptake of base cations was taken into account when calculating $CL_{max}(S)$.

Data sources

Deposition

Historical deposition data was derived from updated EMEP150 grid specific deposition histories 1880- 2030 over Europe according to Schöpp et al. (2003). The deposition curves were scaled to fit the present deposition (1998) of the 50×50 km^2 of the investigated forests and lakes. The deposition histories were supplemented with an estimated deposition pattern between 1800 and 1880, scaled to fit the individual sites.

Present day deposition data was estimated from the MATCH model (Robertson et al., 1999, www.smhi.se) in a 20×20 km^2 grid over Sweden for the year 1998. However, for base cations (Ca, Mg, K) data for 1997 was used. For the lakes, the deposition was scaled to the calibration year and adjusted using the observed lake water chemistry to account for the local variation within the 20×20 km squares (Moldan et al., 1997). The total deposition of Cl^-, SO_4^{2-} and base cations was adjusted at each site using lake water chemistry. It was assumed that, as a result of the declining SO_4^{2-} deposition in the years 1985 to 2000, an estimated percentage of the output flux of SO_4^{2-} from the lakes had been desorbed from catchment soils or, in lakes with large retention time, from the lake water itself. The percentage was 35% for the TID124 lakes, calibrated in 1997, and 20% for the VG57 lakes, calibrated in 2000. In 1985, for the HA56 lakes, no desorbtion was assumed. The modelled deposition of N species was adjusted to account for variations in dry deposition of by assuming that the ratio between the adjusted deposition and the deposition given by SMHI was the same for the N species and SO_4^{2-} at each lake.

Forest ecosystems

For calculating critical loads of forest ecosystems, data on soil mineralogy was calculated using a normalisation procedure for total elemental soil data from 25,442 till sites supplied by the Swedish Geological Survey (SGU), The Swedish National Inventory of Forests, RIS (www-ris.slu.se) and from the Terra Mining (Akselsson et al., 2004). General soil and forest stand characteristics for these sites were achieved by interpolation using data from 17,019 forest sites in RIS, and these data were also used for calculating uptake of nitrogen and base cations in biomass (Akselsson et al., 2004). Data on mean annual temperature, precipitation and runoff were achieved from SMHI (The Swedish Meteorological and Hydrological Institute).

From the Swedish critical loads data base of 1883 forest sites used in earlier reporting (Posch et al., 2001; Sverdrup et al., 2002) 656 sites with the additional information needed were selected for dynamic modelling, together with 16 ICP Forests level II monitoring sites. Of these, in total 671 sites, forest growth was successfully reconstructed by MAKEDEP for 656 sites, for the remainder MAKEDEP could not explain estimates of currently accumulated biomass nitrogen. Critical loads were in turn successfully calculated by SAFE for 542 sites, and these are included in the critical loads database. The sites which SAFE fails to calculate critical loads typically have very low simulated base cation concentrations.

For dynamic modelling, biomass and litter fall data have been derived from Marklund (1988) and element concentrations in different components from various inventories and experimental sites. Soil mineralogy was derived according to Warfvinge and Sverdrup (1995) and data on root depth were used according to Rosengren and Stjernquist (2004).

Freshwaters

Water chemistry data originate from the Swedish national monitoring program and from regional surveys. The dynamic modelling was carried out for 234 lakes. The lakes come from three sets of lake calibrations; 56 lakes in the county of Halland in south-western Sweden (HA56), from a regional survey in 1985, 57 lakes in Västra Götaland county, to the north of Halland (VG57), from a regional survey in 2000, and 121 lakes in a national monitoring programme (TID124). Measurements from 1985, 1997 and 2000 were used. Lakes for which only critical loads are reported are based on the 1995 Lake Survey, in total 2909 lakes. Critical loads are reported for a total of 3143 lakes. Limed lakes were corrected by assuming a constant Ca:Mg ratio for nearby lakes and assuming that the Mg concentration was not affected by liming. Long-term averages (1961-1990) of runoff volumes provided by the Swedish Meteorological Institute (SMHI) were used. Land use data were taken from the Swedish National Land Survey. Long-term averages of nutrient uptake were derived from the Swedish Forest Inventory 1983-92 for the TID124 lakes and from the ASTA database for the HA56 and VG57 lakes. Pre-industrial nutrient uptake was set to 0.5 times present day for lake catchments in southern Sweden and zero for 64 of the TID124 lakes in northern Sweden, based on existing information about Swedish forests and forestry from the 1870/80-ies.

Soil data for the lake catchments were derived from The National Survey of Forest Soils and Vegetation, a subprogramme within RIS (www-ris.slu.se). Soil depth, amount of exchangeable Ca^{2+}, Mg^{2+}, Na^{+} and K^{+} per mass of soil, CEC, soil pH and amount of C and N were vertically aggregated for the profiles of each soil sample included for a lake. Soil bulk densities were estimated by Karltun (1995) and averaged over the profiles. Soil water DOC was assumed to be 8 mg l^{-1} for all catchments (based on data from permanent forest monitoring plots in Sweden, ICP Forests, level II).

Comments and conclusions

The Swedish database for critical loads calculated with the steady-state approach has been updated for both forest ecosystems and freshwaters. For forest ecosystems the number of sites has increased 10-fold compared to the 2003 report, from 1883 to 25,442 sites. A comparison between critical loads data from the two data sets are given in Table SE-1.

Dynamic modelling with SAFE was reported for 542 forest sites, evenly distributed over Sweden. Of these, target load functions existed for 179 sites. A comparison between critical loads calculated using PROFILE and SAFE are shown in Figure SE-1.

For freshwaters, critical loads were calculated using data from 3143 lakes, including 2909 from the 1995 national lake survey. The 234 lakes used for dynamic modelling with MAGIC represent more acid lakes and about half of them are located in south-western Sweden. The median value of the critical loads for the 234 lakes is slightly lower than that of the 2909 lake population (Table SE-2). Target load functions existed for 25 of the lakes used for dynamic modelling.

Critical loads calculated with MAGIC were compared with critical loads from the modified FAB for the 234 lakes population (Figure SE-2). Weathering rates calculated in MAGIC were also used in FAB. There is a fairly good agreement between the two data sets although the modified FAB model tends to predict somewhat higher critical loads.

Table SE-1. Crititical loads for forest ecosystems in Sweden calculated using the 1883 sites database (2003) and the 25 442 sites database (2005) in meq m-2 a-1.

Percentile	2003 database			2005 database		
	$CL_{max}(S)$	$CL_{min}(N)$	$Cl_{max}(N)$	$CL_{max}(S)$	$CL_{min}(N)$	$CL_{max}(N)$
min	0	7.4	7.4	2.7	5.7	23.2
10th	9.0	11.9	37.6	26.7	10.2	47.1
50th	**48.7**	**24.4**	**72.8**	**47.8**	**19.0**	**68.4**
90th	145.9	40.7	178.7	110.1	37.4	149.3
max	604.2	72.77	668.7	714.3	74.1	816.8

Table SE-2. A comparison between critical loads estimated for the 234 lake population used for dynamic modelling and the remaining 2909 lake population used for critical loads only. In both cases the modified FAB model is used (in eq ha^{-1} a^{-1}).

Percentile	234 population (DM)			2909 population (CL)		
	$CL_{max}(S)$	$CL_{min}(N)$	$CL_{max}(N)$	$CL_{max}(S)$	$CL_{min}(N)$	$CL_{max}(N)$
min	0	109	126	0	23	23
5th	138	138	511	117	121	422
25th	348	169	1151	404	160	929
50th	**535**	**299**	**1657**	**652**	**217**	**1476**
75th	878	827	2409	1180	275	2640
95th	1996	1225	5190	3783	360	8031
max	3588	1558	10175	44662	634	154367

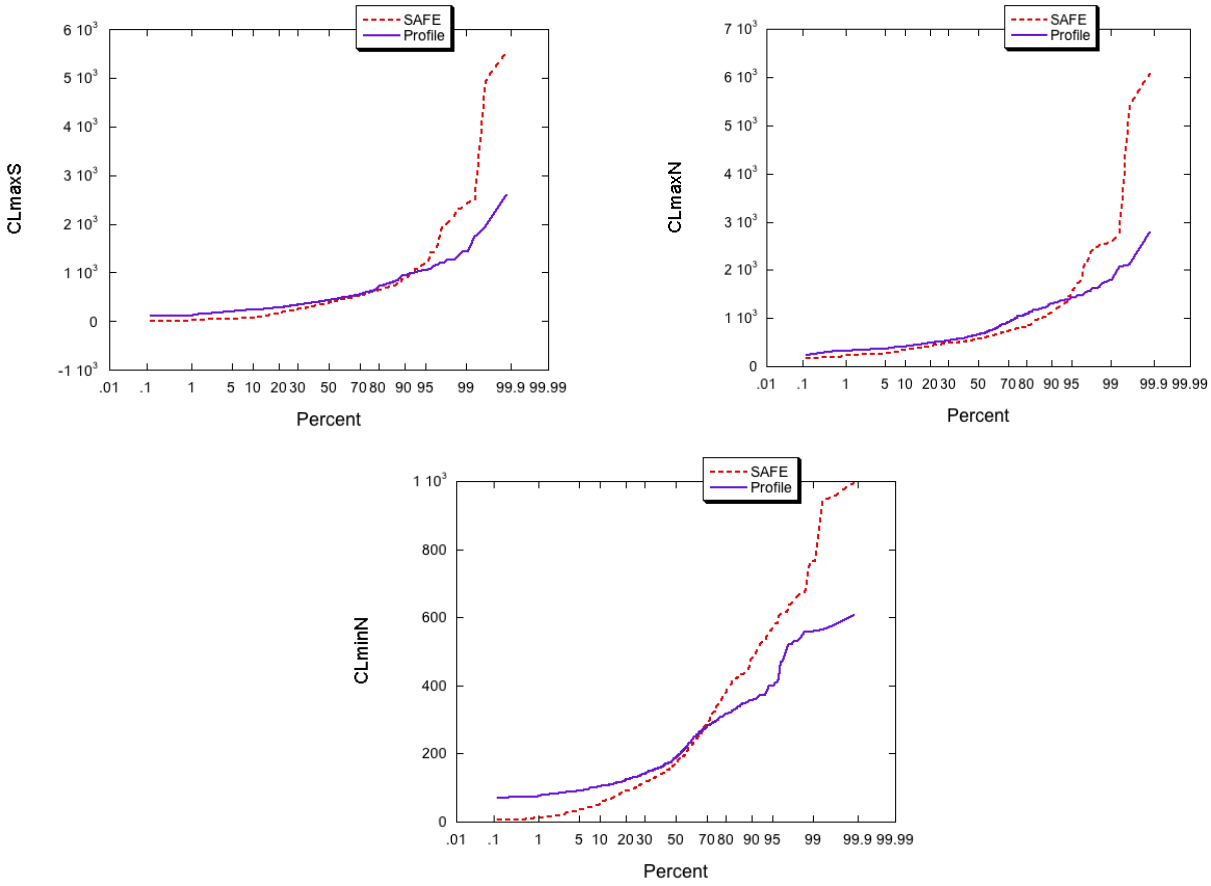


Figure SE-1. Comparison of cumulative distribution functions for sites where $CL_{max}(S)$, $CL_{min}(N)$ and $CL_{max}(N)$ (eq ha^{-1} a^{-1}) were successfully calculated with both PROFILE and SAFE.

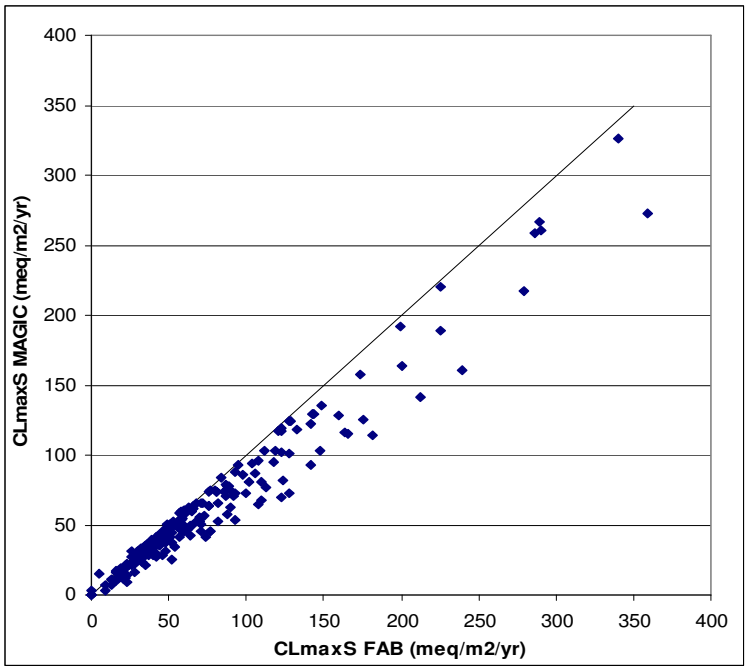


Figure SE-2. Comparison between critical loads for the 234 lake population calculated by the MAGIC and the FAB models respectively (meq m^{-2} a^{-1}). The weathering rate calculated by MAGIC was also used in FAB.

References

Akselsson C, Holmqvist J, Alveteg M, Kurz D, Sverdrup H (2004) Scaling and mapping regional calculations of soil chemical weathering rates in Sweden. Water, Air, and Soil Pollution: Focus 4: 671-681

Alveteg M (1998) Dynamics of forest soil chemistry. PhD dissertation. Lund University, Lund

Alveteg M, Kurz D, Becker R (2002) Incorporating nutrient content elasticity in the MAKEDEP model, Reports in ecology and environmental engineering 1, 52-67

Cosby BJ, Hornberge GM, Galloway JN, Wright RF (1985) Time scales of catchmen acidification: a quantitative model for estimating freshwater acidification. Environ. Sci. Technol. 19:1144-1149

Cosby B, Ferrier RC, Jenkins A, Wright RF (2001) Modelling the effects of acid deposition: refinements, adjustments and inclusion of nitrogen dynamics in the MAGIC model. Hydrol. Earth Syst. Sci. 5: 499-517

Henriksen A, Forsius M, Kämäri J, Posch M, Wilander A (1993) Exceedance of Critical Loads for lakes in Finland, Norway and Sweden: Norwegian Institute for Water Research, Report 32/1993, Oslo.

Karltun E (1995) Acidification of forest soils on glacial till in Sweden. Report 4427, 1-76. Swedish Environmental Protection Agency, Solna, Sweden

Marklund LG (1988) Biomass functions for pine, spruce and birch in Sweden. Report 45, Swedish University of Agricultural Scienecs, Dept of Forest Survey

Martinsson L, Alveteg M, Kronnäs V, Sverdrup H, Warfvinge P, Westling O (2005) A regional perspective on present and future soil chemistry at 16 Swedish forest sites. Water, Air and Soil Pollution. (accepted for publication)

Moldan F, Kronnäs V, Wilander A, Karltun E, Cosby BJ (2004) Modelling acidification and recovery of Swedish lakes. WASP Focus.

Posch M (1995) Critical Loads for Aquatic Ecosystems. In: Mapping and Modelling of Critical Loads for Nitrogen: a workshop report, Proceedings of the Grange-Over-Sands Workshop 24-26 October 1994

Posch M, Kämäri J, Forsius M, Henriksen A, Wilander A (1997) Exceedance of critical loads for lakes in Finland, Norway, and Sweden. Reduction requirements for acidifying nitrogen and sulfur deposition. Environmental Management 21: 291-304

Posch M. De Smet PAM, Hettelingh J-P, Downing RJ (2001) Modelling and Mapping of critical thresholds in Europe. Status report 2001. RIVM Report No 259101010, Bilthoven, the Netherlands

Rapp L, Wilander A, Bertills U (2002) Kritisk belastning för försurning av sjöar. In: Kritisk belastning för svavel och kväve. Swedish Environmental Protection Agency. Report 5174, pp 81-106 (in Swedish)

Robertson L, Langne J, Engard M (1999) An Eulerian limited-area atmospheric transport model. J. Appl. Meteor. 38: 190-210

Rosengren U, Stjernquist I (2004) Gå på djupet. The SUFOR Research Programme. (www.sufor.se)

Schöpp W, Posch, M, Mylona S, Johansson M (2003) Long term development of acid deposition (1880-2030) in sensitive freshwater regions in Europe. Hydrology and Earth System Sciences 7: 436-446

Sverdrup H, Rapp L, Staaf H, Alveteg. M (2002) Kritisk belastning för försurning av skogsmark. In: Kritisk belastning för svavel och kväve. Swedish Environmental Protection Agency. Report 5174, pp 53-80 (in Swedish)

Warfvinge P, Sverdrup H (1995) Critical Loads of Acidity to Swedish Forest Soils, Methods data and results, Reports in ecology and environmental engineering, Report 5:1995, Lund University, Department of Chemical Engineering II

Warfvinge P, Falkengren-Grerup U, Sverdrup H, Andersen B (1993) Modelling long-term cation supply in acidified forest stands. Environ. Pollut. 80: 209 -221

SWITZERLAND

National Focal Centre

Swiss Agency for the Environment, Forests and Landscape (SAEFL)
Air Pollution Control Division
Beat Achermann
CH-3003 Bern
tel: +41-31-3229978
fax: +41-31-3240137
beat.achermann@buwal.admin.ch

Collaborating institutions

METEOTEST
Beat Rihm
Fabrikstrasse 14
CH-3012 Bern
tel: +41-31-3072626
fax: +41-31-3072610
office@meteotest.ch

EKG Geo-Science

Daniel Kurz
Ralligweg 10
CH-3012 Bern
tel: +41-31-3026867
fax: +41-31-3026825
geoscience@swissonline.ch

Overview

The Swiss data set on critical loads of acidity and nutrient nitrogen is compiled from the output of four modelling and mapping approaches (see Figure CH-1):

1. The dynamic models SAFE and VSD (very simple dynamic model) were used for assessing acidifying effects of air pollutants on forest soils. The multi-layer model SAFE was calibrated and applied on 260 sites, where full soil profiles were available. For calculating critical loads of acidity and target loads, the input data of SAFE were aggregated to one layer in order to run the VSD model.
2. The SMB method for calculating critical loads of nutrient nitrogen ($CL_{nut}(N)$) was applied on 10,434 forest sites (managed forests) of the National Forest Inventory (LFI 1990/92), which is based on a 1×1 km^2 raster.
3. The empirical method for mapping $CL_{nut}(N)$ includes different natural and semi-natural ecosystems, such as raised bogs, fens, species-rich grassland, alpine heaths and poorly managed forest types with rich ground flora. The mapping was done on a 1×1 km raster combining several input maps of nature conservation areas and vegetation types. The total sensitive area amounts to 16,373 km^2.
4. Critical loads of acidity were calculated for 100 sensitive alpine lakes in Southern Switzerland applying a generalized version of the FAB model (first order acidity balance).
5. The data layers of the SMB method and the empirical method partially cover the same areas. Therefore, the results of both methods were combined by choosing the minimum $CL_{nut}(N)$ per grid cell. The final data set contains 22,790 records with $CL_{nut}(N)$ on the 1×1 km raster.

The main results of the four modelling approaches are shown in Figure CH-2 as cumulative frequency distributions: $CL_{nut}(N)$ for forests (SMB method), $CL_{nut}(N)$ for (semi-)natural ecosystems (empirical method) as well as the maximum critical load of sulphur, $Cl_{max}(S)$, for forests (SAFE/VSD models) and Alpine lakes (FAB model).

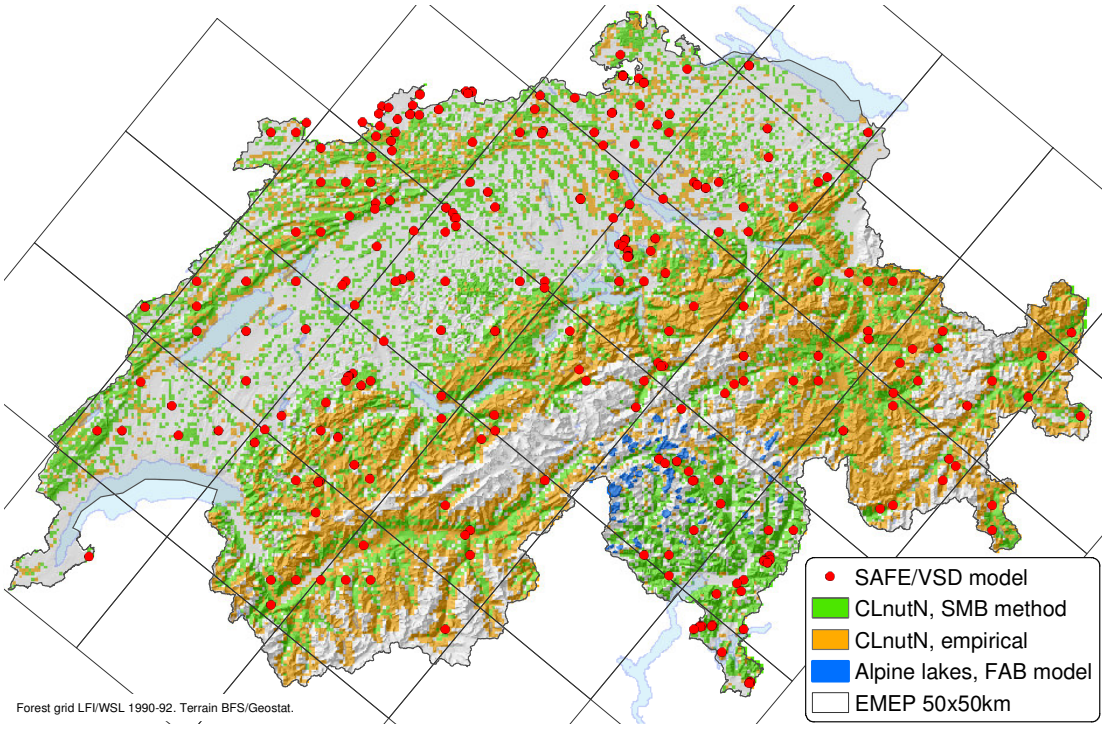


Figure CH-1. Overview of sensitive habitats and modelling sites in Switzerland.

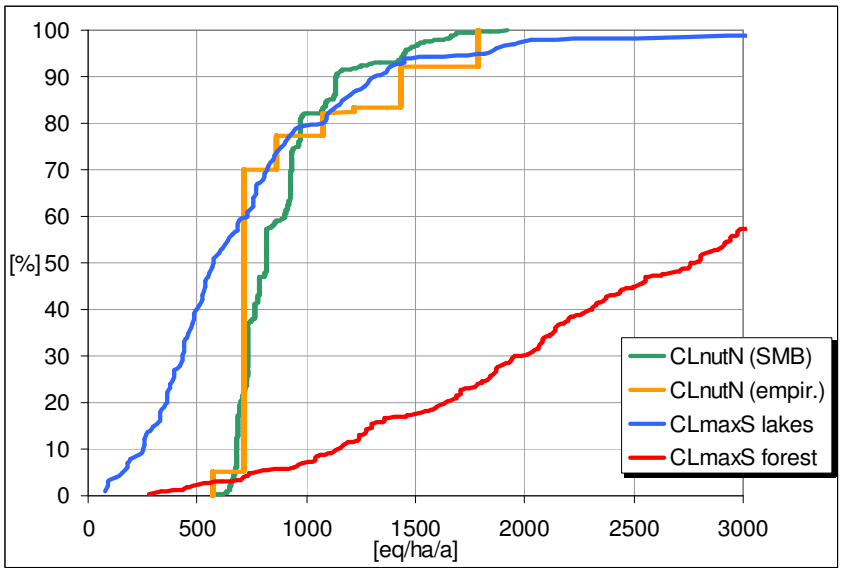


Figure CH-2. Cumulative frequency distributions of $CL_{nut}(N)$ (SMB and empirical method) and Clmax(S) (forests and Alpine lakes).

Input for dynamic modelling of soil acidification

The dynamic modelling of critical loads and target loads of acidity was based on samples from 260 soil profiles consisting of 2 to 9 layers each. Table CH-1 lists the sources of all input data required for the SAFE model runs. At 21 sites, also measurements of soil water chemistry are available (Braun, 2004). Those were used to check plausibility of the results for single soil layers. The multi-layer data were transformed to the one-layer input files

for VSD according to Kurz and Posch (2002). VSD was used to calculate critical loads, target loads and scenarios demanded by the data call.

The sampling sites are not regularly distributed within the country (Figure CH-1). Therefore, the area of forest represented by one site (EcoArea) was calculated per EMEP-cell dividing the total forested area by the number of sampling points.

*Table CH-1. Data sources for the SAFE/VSD model application. Abbreviations: *: time-series parameter; #: soil layer specific parameter.*

Parameter	Comments/Derivation method	Sources
	Climate parameters	
infiltration rate (P)* percolation rate (Q)*	• amount of precipitation infiltrating the soil and amount of water leaving the soil at the base of the soil profile (or rooting zone), respectively • site specific time series for the period 1969-1998 from the hydrological model WAWAHAMO • P and Q extended to the past and future using the average of the modelled period • for CL/TL calculations P is the average P of the rotation period containing the biomass key year (1995)	• base data from Zierl (2000) • processed data
evapo-transpiration fraction#	• (time-invariant) fraction of evapotranspiration from a particular soil layer • estimated from classified fine-root distribution; transfer function	• base data (fine-root distribution) from Zimmermann (2004) and Braun (2004)
soil moisture#	• layer specific bulk soil water content • calculated from layer specific available water capacity (AWC) which in turn is estimated according to AG Bodenkunde; transfer function	• Arbeitsgruppe Bodenkunde (1982) • base data (AWC) from Zimmermann (2004) and Braun (2004)
soil temperature	• average annual soil temperature at 0.2 m soil depth • extrapolated from measurements as a function of altitude; transfer function	• FOEFL (1994, p. 45) • processed data
	Deposition parameters	
wet and dry deposition	• see following chapter on deposition data	• processed data
throughfall deposition (key year)	• mean annual throughfall deposition for a specified year • estimated by means of a regression model (Ca, Mg, K) or a fraction of the deposition (NO_x, NH_y); key year 2000 • for SO_x, Cl and Na, troughfall deposition equals total deposition	• SAEFL (1998, Table 3.3, p.37)
canopy exchange (key year)	• mean annual canopy exchange for a specified year • calculated by PRESAFE from wet, dry and throughfall deposition input	• Alveteg et al. (2002)
'sea-salt' correction	• not considered in Switzerland	• Alveteg et al. (2002)
total deposition time series*	• annualized gridded (EMEP50) average total deposition time-series for all ions (absolute or relative figures) and the simulation period • SO_x, NO_x and NH_y deposition trends 1880-2030 after Schöpp et al. (2003). Constant background deposition prior to 1700 (smoothly approached from 1880 values). Constant 2010 deposition after 2010	• Schöpp et al. (2003); Slootweg (2004) • BUWAL (1995)

Parameter	Comments/Derivation method	Sources
	• Cl deposition trends adopted from Cl emission trends compiled in BUWAL (1995). Trends outside of the investigated period as for SO_x, NO_x and NH_y • 80% of Bc and Na deposition kept constant (national average). 20% varied according to total dust emission trends from BUWAL (1995). Trends outside of the investigated period SO_x, NO_x and NH_y	
	Vegetation parameters	
biomass	• any year(s) (growing) biomass for minimum 2 (lumped wood and canopy) up to 5 tree compartments (e.g. stem, root, bark, branch and canopy) of 2 (coniferous and deciduous) or more tree species groups • for sites not on the National Forest Inventory grid intersections, the nearest meaningful (regarding altitude) neighbour is allocated • 'species' mass data are lumped to stand and compartment specific biomass	• base data (compartment masses for 12 Swiss major tree species) from Kaufmann (WSL, 2004)
nutrient content	• minimum and maximum Ca-, Mg-, K- and N-contents of the tree compartments considered • foliage macro nutrient content ranges generalized from measurements and literature for species with no available measurements • empirically derived proportionality factors to estimate nutrient contents in wood compartments from foliage levels • the 5 (compartments) times 12 (species) times 8 (min/max macro-nutrients) matrix recalculated to stand and compartment specific min/max nutrient contents	• measurements from Braun (2004) • Bergmann (1993)
logistic growth function bonity	• bonity and respective n and k values of a n^{th} order Mikaelis-Menten equation fitted to the data of respective yield tables (bonity and n are site and species specific while k ('half-time') is additionally compartment specific) • n and k of the Mikaelis-Menten function fitted to the tabulated values in yield tables for managed spruce (coniferous) and beech (deciduous) stands with different bonity • all compartments are modelled with the same n (stem) but different k which are (empirical, fixed) fractions of k (stem)	• Badoux (1966-1969) • bonity from LFI data extract (WSL, 2004) and Braun (2004)
land-use history*	• annualized national, regional or local fraction of the stands' (growing) biomass cut down and removed from the stand, respectively, for all compartments and the simulation period, assuming all stem wood felled removed from the stand and compartment removal as fraction of the material of the other compartments • national stem removal trends from SAEFL (1998) updated with recent years harvesting figures • average regional harvesting rates (from NFI 1982-1986) scaled with national stem removal trends (continuous harvesting) • removal of other compartments than stem simplified from SAEFL (1998) • stands assumed to be forested since 1600	• SAEFL (1998)

Parameter	Comments/Derivation method	Sources
litterfall fraction	• site specific average fraction of canopy shed every year • assumed base rates: 1.0 (deciduous canopies) and 0.143 (coniferous canopies) • base rates corrected for nutrient retention before leaf/needle fall (-30% for deciduous and -10% for coniferous canopies)	• measured nutrient contents of fresh foliage and leaf litter from Braun (2004)
mineralization rate harvest litter canopy litter	• site specific annual average fraction of pooled harvest residues and pooled canopy litter mineralized • assumed base rates: 0.10 (harvest litter) and 0.70 (canopy litter) at an average annual air temperature of 7°C • base rates corrected for site specific annual average air temperature	• average annual air temperature from Zierl (2000)
relative base cation uptake# relative nitrogen uptake#	• base cation and nitrogen uptake in each soil layer within the rooting zone as fraction of total base cation and nitrogen uptake • estimated from classified fine-root distribution; transfer function (cp. evapotranspiration fraction)	• base data (fine-root distribution) from Zimmermann (2004) and Braun (2004)
	Soil parameters	
layer thickness#	• 'field' (bulk) thickness of a soil layer considered • adopted from field measurements	• base data from Zimmermann (2004) and Braun (2004)
bulk soil density# (fine-earth density#)	• (dry) density of the bulk soil of a layer considered • estimated from measured densities of the bulk soil or fine earth and classified layer specific coarse contents • missing densities of the fine earth are estimated using curve fits (power functions) derived from classified (BEK) measurements	• base data from Zimmermann (2004) and Braun (2004)
coarse content#	• layer specific content (volume fraction) of inorganic components > 2 mm ('stones') in the (bulk) soil • derived from field classification	• base data from Zimmermann (2004) and Braun (2004)
grain size distribution#	• layer specific relative contents (wt. fraction) of sand (2000 - 50 µm), silt (50 - 2 µm) and clay (< 2 µm) in the inorganic fine-earth • measured according to Gee and Bauder (1986)	• Gee and Bauder (1986). • base data from Zimmermann (2004) and Braun (2004)
surface area#	• (total) mineral surface area subject to chemical weathering in a soil layer considered • calculated from grain size distribution using a sieve curve to surface area transfer function • corrected (lowering) for high clay contents • adjusted to the bulk framework	• Jönsson et al. (1995)
cation exchange capacity#	• (any years) cation exchange capacity (CEC) of a soil layer considered • contents of the fine-earth's exchangeable Al, Fe, Ca, Mg, K and Na measured after ammonium-chloride extraction • contents of the fine-earth's exchangeable acidity • missing values either adopted from the above or below layer or, in case of H^+, estimated from the relationship of measured exchangeable acidity with pH($CaCl_2$) • CEC adjusted to the bulk framework	• Yuan (1959) • base data from Zimmermann (2004) and Braun (2004)
base saturation# (*)	• (any years, see below) base saturation for all soil layers considered	• base data from Zimmermann (2004) and

Parameter	Comments/Derivation method	Sources
soil sampling year	• fraction of exchangeable cations Ca, Mg and K in respect of CEC • key year to which the base saturation refers to is the soil sampling year	Braun (2004)
mineral contents#	• layer specific quantitative mineralogical composition of the fine-earth (up to 14 weatherable minerals) • derived from total elemental analysis of the fine earth, qualitative mineralogy and assumed mineral stoichiometries using a mass balance method • extra parameters used for this procedure: total elemental analysis (e.g. SiO_2, TiO_2, Al_2O_3, Fe_2O_3, MnO, MgO, CaO, Na_2O, K_2O, P_2O_5, LOI); qualitative mineralogy (e.g. from thin section analysis) oxalate-extractable Al and Fe; HNO_3-extractable Ca and Mg of calcareous soils mineral stoichiometry database. • quantitative mineralogy corrected for mineral specific surface area and adjusted to the bulk framework	• total elemental analyses from Zimmermann (2004) and Braun (2004)
soil solution DOC#	• mean (annual) dissolved organic carbon (DOC) concentration in the soil solution of all layers • forcing function; based on generalized data from a Ticino research site	• measurements from Blaser (1993)
soil solution pCO_2#	• mean (annual) layer specific soil partial CO_2 pressure (expressed as multiple of the ambient pCO_2) • generalized forcing function (polynomial) fitted to literature data (ref)	• basic values from Solomon and Cerling (1987)
soil solution $logK_{Gibb}$#	• soil-layers specific log of apparent gibbsite equilibrium constant • generalized forcing function in relation to organic matter content	• basic values from Mapping Manual, UBA (1996)
type of layer#	• type of layer according to field classification • used as classification variable	• base data from Zimmermann (2004) and Braun (2004)
BEK classification	• classification of the sites according to the Map of Suitability of Soils of Switzerland 1:200:000	• EJPD, EVD and EDI (1980) • base data from Zimmermann (2004) and Braun (2004)

Input for critical loads of nitrogen ($Cl_{nut}(N)$)

The SMB method was applied for forests according to the Mapping Manual with the input data listed in Table CH-2.

Table CH-2. Input data for calculating Clnut(N) with the SMB method (FOEFL 1996, with updates).

Parameter	Values	Comment
f_{de}	0.3 dry soils 0.5 moist soils 0.7 moderate wet s. 0.8 wet soils	data from soil map 1:200,000 (EJPD, EVD and EDI 1980)
$N_{le(acc)}$	4 kg N ha^{-1} a^{-1} at 500m altitude, 2 kg N ha^{-1} a^{-1} at 2000m altitude	linear interpolation in-between. Acceptable leaching mainly occurs by management (after cutting), which is more intense at lower altitudes. Q and $[N]_{acc}$ are not used.
N_i	3 kg N ha^{-1} a^{-1} at 500m altitude, 5 kg N ha^{-1} a^{-1} at 1500m altitude	linear interpolation in-between. At high altitudes the decomposition of organic matter slows down due to lower temperatures and therefore the accumulation rates of N and C are naturally higher.
N_u	0.7 – 7.0 kg N $ha^{-1}a^{-1}$	present uptakes calculated on the basis of estimated long-term harvesting rates and average element contents in stems

The application of the empirical method is based on vegetation data compiled from various sources (Hegg et al., 1993; EDI, 1991; WSL, 1993). 25 Sensitive vegetation types were identified and included in the critical load map (Table CH-3). If more than one type occurs within a 1×1 km grid-cell the lowest value of $Cl_{nut}(N)$ was selected for this cell.

Table CH-3. The empirical method: selected ecosystems, critical load values applied in Switzerland (kg N ha^{-1} a^{-1}) and EUNIS codes.

Ecosystem	CLN range	Relevant vegetation types in Switzerland	$Cl_{nut}(N)$	EUNIS code
Acidic coniferous forests	10-20	Molinio-Pinetum (Pfeifengras-Föhrenwald)	17	G3.44
		Ononido-Pinion (Hauhechel-Föhrenwald)	12	G3.43
		Cytiso-Pinion (Geissklee-Föhrenwald)	12	G3.4
		Calluno-Pinetum (Heidekraut-Föhrenwald)	12	G3.3
Acidic deciduous forests	10-20	Quercion robori-petraeae (Traubeneichenwald)	15	G1.7
Calcareous forests	10-20	Quercion pubescentis (Flaumeichenwald)	15	G1.71
		Fraxino orno-Ostryon (Mannaeschen-Hopfenbuchwald)	15	G1.73
		Erico-Pinion mugi (Ca) (Erika-Bergföhrenwald aufKalk)	15	G3.44
		Erico-Pinion sylvestris (Erika-Föhrenwald)	15	G3.44
Arctic and alpine heaths	5-15	Juniperion nanae (Zwergwacholderheiden)	10	F2.23
		Loiseleurio-Vaccinion (Alpenazaleenheiden)	10	F2.21
Calcareous species-rich grassland	15-25	Mesobromion (erecti) (Trespen-Halbtrockenrasen)	20	E1.26
Neutral-acid species-rich grassland	15-25	Molinion (caeruleae) (Pfeifengrasrieder)	25	E3.51
Montane-(sub)alpine	10-20	Chrysopogonetum grylli (Goldbart-	15	E1.2

grassland		Halbtrockenrasen)		
		Seslerio-Bromion (Koelerio-Seslerion) (Blaugras-Trespen-Halbtrockenrasen)	12	E1.2
		Festucetum paniculatae (Goldschwingelrasen)	12	E4.3
		Stipo-Poion molinerii (Engadiner Steppenrasen), alpine	10	E1.24
		Elynion (Nacktriedrasen), alpine	10	E4.42
		Seslerion (variae) (Blaugrashalden), alpine	10	E4.43
		Caricion ferrugineae (Rostseggenhalden), alpine	10	E4.41
Poor fens	10-20	Scheuchzerietalia (Scheuchzergras)	20	D2.21
Rich fens	15-25	Caricion fuscae (Braunseggenried)	25	D2.2
		Caricion davallianae (Davallsseggenried)	25	D4.1
Ombrotrophic bogs	5-10	Sphagnion fusci (Hochmoor)	8	D1.1
Shallow soft-water bodies	5-10	Littorellion (Strandling-Gesellschaften)	8	C1.1

Critical loads for alpine lakes

In 2004, critical loads of acidity for alpine lakes were calculated with a generalised FAB-model (Posch, 2004) and supplied to the CCE (see CCE Progress Report, 2004). The model was run for the catchments of 100 lakes in Southern Switzerland at altitudes between 1650 and 2700 m (average 2200 m).

By the end of February 2005, a revised data set was supplied with improved input data, i.e. deposition, BC uptake, catchment borders.

Deposition data

The deposition of BC, N and S was calculated with a generalised combined approach (FOEFL, 1994 and 1996; Thimonier et al., 2004), for the reference year 2000.

Wet deposition is calculated by combining the concentration field of sulphate, nitrate and ammonium compounds in rain water with a precipitation map. Wet concentration measurements are relatively homogenous below an altitude of 1000 m. At higher altitudes concentrations decrease. In southern Switzerland, a detailed study on wet deposition patterns was carried out (SAEFL, 2001).

Resistance analogue models are used for assessing the dry deposition of NH_3 and NO_2 gas and aerosols. For these compounds, the concentration fields are calculated from emission inventories with a resolution of 200m (NH_3 100m) by applying statistical dispersion models (e.g. Thoeni et al., 2004). For HNO_3, the concentration field is calculated as a function of altitude. For SO_2, the concentration field is determined by geo-statistical interpolation of monitoring results. For BC, gridded bulk deposition data from CCE are used in combination with filtering factors for forests and average ratios of individual base cations in bulk deposition measurements.

The concentration fields are multiplied by deposition velocities, which depend on the reactivity of the pollutant, surface roughness and climatic parameters. Deposition velocity values were taken from literature (FOEFL, 1996, with modifications).

As an example, Fig. CH-3 shows the resulting spatial pattern of total nitrogen deposition, characterised by a general decrease with altitude, relatively low deposition in inner-Alpine valleys and areas with high depositions due to local ammonia emissions (e.g. in central Switzerland) or by import (in southern Switzerland).

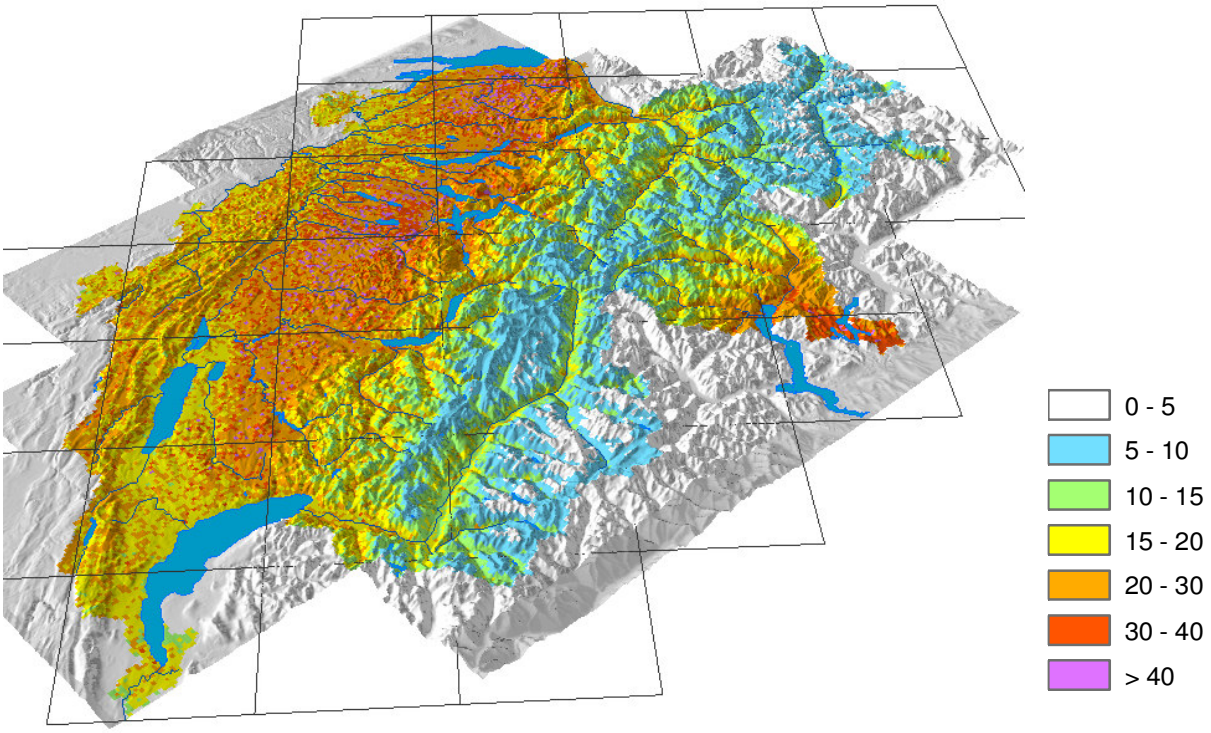


Figure CH-3. Nitrogen deposition (in kg N ha^{-1} a^{-1}) for the year 2000 in a perspective view (model results with a resolution of 1×1 km^2 ; the EMEP 50×50km^2 grid is drawn at an altitude of 1000 m).

Acknowledgements

This work is financed by the Swiss Agency for the Environment, Forest and Landscape (National Focal Centre for modelling and mapping activities under the Convention on Long-range Transboundary Air Pollution).

For the implementation of the VSD- and generalized FAB-model, M. Posch from the CCE provided helpful support and Fortran routines. We thank Stefan Zimmermann (WSL) and Sabine Braun (IAP) for supplying the soil profile data as well as Edgar Kaufmann (WSL) for calculating the biomass in tree compartments.

References

Alveteg M, Kurz D, Becker R (2002) Incorporating nutrient content elasticity in the MAKEDEP model. Reports in Ecology and Environmental Engineering, 1: 52-67

Arbeitsgruppe Bodenkunde (1982) Bodenkundliche Kartieranleitung, Geologische Landesämter und Bundesanstalt für Geowissenschaften und Rohstoffe (Hg.) Hannover, 3. Aufl., 331pp

Badoux E (1966-1969) Ertragstafeln für Fichte, Tanne, Buche und Lärche. Eidg. Anst. forstl. Versuchswes. (WSL), Birmensdorf.

Bergmann W (1993) Ernährungsstörungen bei Kulturpflanzen, 3. Aufl., Fischer-Verlag Jena

Blaser P (1993) Dissolved organic carbon (DOC) concentrations in soil layers. Swiss Federal Research Institute WSL, Birmensdorf, pers. comm.

Braun S (2004) soil profile data for 82 sites and soil solution (lysimeter) data for 21 sites in Switzerland, measured minimum and maximum Ca-, Mg-, K- and N-contents of tree compartments, measured nutrient contents of fresh foliage and leaf litter. Institute for Applied Plant Biology (IAP), Schönenbuch, pers. comm.

BUWAL (ed) (1995) Vom Menschen verursachte Luftschadstoff-Emissionen in der Schweiz von 1900 bis 2010, Schriftenreihe Umwelt Luft, 256 pp

EDI (1991) Bundesinventar der Hoch- und Uebergangsmoore von nationaler Bedeutung. (Federal Inventory of Raised and Transitional Bogs of National Importance). Appendix to the Federal Ordinance on the Protection of Raised Bogs. Eidgenössisches Departement des Innern (EDI), Bern

EJPD, EVD and EDI (eds) (1980) Bodeneignungskarte der Schweiz (Map of suitability of soils in Switzerland) 1:200'000 (BEK). Eidgenössische Drucksachen- und Materialzentrale, Bern. In digital form: BFS/GEOSTAT, Neuchâtel

FOEFL (ed) (1994) Critical loads of acidity for forest soils and alpine lakes - steady state mass balance method. Environ. Ser. Air, 234. Swiss Agency for the Environment, Forests and Landscape (SAEFL, former FOEFL), Bern

FOEFL (ed) (1996) Critical Loads of Nitrogen and their Exceedances - Eutrophying Atmospheric Deposition. Environmental Series No. 275, Federal Office of Environment, Forests and Landscape, Berne, 74 pp

Gee GW, Bauder JW (1986) Particle-size Analysis. In: A. Kluthe (ed) Methods of Soil Analysis, Part 1 - Physical and Mineralogical Methods, ASA-SSSA, Madison, USA, Agronomy Monograph 9, 2nd edition

Hegg O, Béguin C, Zoller H (1993) Atlas schutzwürdiger Vegetationstypen der Schweiz (Atlas of Vegetation Types Worthy of Protection in Switzerland). Edited by Federal Office of Environment, Forests and Landscape, Bern

Jönsson C, Warfvinge P, Sverdrup H (1995) Application of the SAFE model to the Solling spruce site. Ecological Modeling, 83: 85-96

Kurz D, Posch M (2002) A comparison of the SAFE and VSD Soil Dynamic Models Using Swiss Data. Bern & Bilthoven
LFI (1990/92) Schweizerisches Landesforstinventar (LFI), Datenbankauszüge vom 30. Mai 1990 und vom 8. Dezember 1992. Birmensdorf, Eidg. Forschungsanstalt für Wald, Schnee und Landschaft (WSL)
Posch M (2004) The generalised First-order Acidity Balance (genFAB) model. (pers. comm. 12.03.2004)
SAEFL (ed) (1998) Acidification of Swiss Forest Soils – Development of a Regional Dynamic Assessment. Environmental Documentation Air/Forest No. 89. Swiss Agency for the Environment, Forests and Landscape (SAEFL), Bern, 115 pp
SAEFL (ed) (2001) Acidifying Deposition – Southern Switzerland. Environmental Documentation No. 134. Swiss Agency for the Environment, Forests and Landscape (SAEFL), Berne, 113 pp
Schöpp W, Posch M, Mylona S, Johansson M (2003) Long term development of acid deposition (1880-2030) in sensitive freshwater regions in Europe, Hydrology and Earth System Sciences 7(4): 436-446
Slootweg J (2004) Data delivery of annualized gridded (EMEP50) average total deposition time-series for all ions (after Schöpp et al. 2003). Coordination Center for Effects (CCE), Bilthoven, NL.
Solomon DK, Cerling TE (1987) The annual carbon dioxide cycle in a montane soil: observations, modeling and implications for weathering, Water Resources Research, 23: 2257-2265
Thimonier A, Schmitt M, Waldner P, Rihm B (2004) Atmospheric deposition on Swiss Long-term Forest Ecosystem Research (LWF) plots. Environmental Monitoring and Assessment (in press)
Thöni L, Brang P, Braun S, Seitler E, Rihm B (2004) Ammonia monitoring in Switzerland with passive samplers: Patterns, determinants and comparison with modelled concentrations. Environmental Monitoring and Assessment 98: 95-107
UBA (2004) Modelling and Mapping Critical Loads & Levels and Air Pollution Effects, Risks and Trends. UmweltBundesAmt, Texte 52/04, Berlin
WSL (1993) Federal Inventory of Fenlands of National Importance. Pers. comm. from A. Grünig and P. Schönenberger, Swiss Federal Institute for Forest, Snow and Landscape Research, Birmensdorf. The inventory was published in 1995 as an Appendix to the Federal Ordinance on the Protection of Fenlands
WSL (2004) Schweizerisches Landesforstinventar LFI, Datenbankauszug der Erhebung 1993-1995, vom 25. Oktober 2004. Ulrich Ulmer. Eidg. Forschungsanstalt WSL, Birmensdorf
Yuan (1959) Determination of exchangeable hydrogen in soils by a titration method. Soil Sci. 88:164-167
Zierl B (2000) WAWAHAMO a hydrological model to simulate drought in forested ecosystems. PhD, Eidgenössische Forschungsanstalt WSL, Birmensdorf, Switzerland
Zimmermann S (2004) Soil profile data for 178 forest sites in Switzerland. Swiss Federal Research Institute WSL, Birmensdorf (pers. comm.)

UNITED KINGDOM

National Focal Centre

Jane Hall, Jackie Ullyett
Centre for Ecology and Hydrology
Monks Wood, Abbots Ripton
Huntingdon PE28 2LS
tel: +44 1487 772429
fax: +44 1487 773467
jrha@ceh.ac.uk, jmu@ceh.ac.uk
http://critloads.ceh.ac.uk

Collaborating institutions

Dynamic modelling:
Chris Evans, Edwin Rowe
Centre for Ecology and Hydrology
Orton Building
Deiniol Road
Bangor LL57 2UP
tel: +44 1248 370045
fax: +44 1248 355365
cev@ceh.ac.uk, ecro@ceh.ac.uk

Julian Aherne
c/o Macaulay Institute
Craigiebuckler
Aberdeen AB15 8QH
julian.aherne@ucd.ie

Rachel Helliwell, Bob Ferrier
Macaulay Institute
Craigiebuckler
Aberdeen AB15 8QH
tel: +44 1224 498200
fax: +44 1224 311556
r.helliwell@macaulay.ac.uk,
r.ferrier@macaulay.ac.uk

Alan Jenkins, Mike Hutchins
Centre for Ecology and Hydrology
Maclean Building
Crowmarsh Gifford
Wallingford OX10 8BB
tel: +44 1491 838800
Fax: +44 1491 692424
jinx@ceh.ac.uk, mihu@ceh.ac.uk

Introduction

In 2004 the UK updated their steady-state critical loads of acidity and nutrient nitrogen (Hall et al., 2004a,b). The steady-state data for terrestrial habitats remain unchanged and the 2004 data sets should be used. For the freshwater habitats (EUNIS classes C1 and C2) the steady-state data are also unchanged but are re-submitted together with updated results from UK dynamic modelling activities. The MAGIC model has now been applied to 320 UK surface water sites for which FAB critical loads were submitted in 2004. This report focuses on the further development and application of MAGIC in the UK.

The methodology used for the calibration of MAGIC has been updated to a) maximise consistency with the steady-state model, FAB; b) incorporate nitrogen dynamics and run Target Load Functions (TLFs) for all sites; and c) include improved input data based on new soil measurements and databases.

Site selection for dynamic modelling

MAGIC has been calibrated to a total of 320 sites, based on a number of regional water surveys undertaken between 1995 and 2002, and forming part of the UK freshwater critical loads dataset (Table UK-1). All regions are considered acid-sensitive, but span a range of sulphur and nitrogen deposition from the Cairngorms (low) to the South Pennines (high). Site-selection protocols varied by region; in the Cairngorms, Galloway and Mourne Moutains, all standing waters were sampled. In the Lake District and South Pennines, standing waters located on areas of acid-sensitive geology were sampled. In the larger Welsh regions, a subset of streams and standing waters located on acid-sensitive geology were sampled. Lakes were sampled on between one and four occasions over one year, while the Welsh stream sites were all sampled monthly over one year. Detailed descriptions of the regional datasets used are given in Evans et al. (2001) and Helliwell et al. (in prep). Note that two regions included in the previous call for data were not re-calibrated and included in the current model runs: (i) the Trossachs (central Scotland) were excluded because they do not contain any sites with present-day ANCs below critical thresholds; (ii) the majority of sites in Dartmoor (Devon) to which MAGIC has previously been applied are not incorporated in the freshwater steady-state critical loads dataset.

Table UK-1. Sites calibrated using MAGIC.

Region	Location	Number of standing waters	Number of streams
Cairngorms & Galloway	Scotland[a]	97	0
Mourne Mountains	Northern Ireland	8	0
Lake District	North-west England	48[b]	0
South Pennines	northern England	62	0
Snowdonia	north Wales	34	27
Cambrian Mountains	south/central Wales	7	37
Totals		256	64

[a] Cairngorms in north-east Scotland and Galloway in south-west Scotland

[b] MAGIC run for 52 sites in this region, but 4 sites removed prior to data submission as their catchment areas <0.01 km^2

Input data

As far as possible, the input data used for dynamic modelling correspond to the data used to apply the FAB critical load model to the same freshwater sites included in the 2004 data submission to the CCE. These data include measured water chemistry, estimated soil nitrogen sinks, nitrogen and sulphur sinks to lake sediments, and forest nitrogen and base cation uptakes. Additional soils data required for MAGIC (cation exchange capacity, exchangeable base cations, depth, bulk density, pH, C and N pools) were obtained from the best available data for each region; for Scotland and Northern Ireland, representative data were extracted from soil databases held by the Macaulay Institute, while for the English and Welsh sites, data were obtained from a targeted survey of representative acid-sensitive soils undertaken by CEH Bangor and the Macaulay Institute during 2003 and 2004 (Evans et al., 2004). Catchment-weighted mean values of all soil parameters were calculated based on best available soils and land-use maps for each region.

Deposition scaling sequences (hindcast and forecast) were derived from EMEP data for the grid cells covering each region. Present-day SO_4 and chloride deposition were estimated from measured present-day catchment output fluxes, assuming conservative transport of both anions through the catchment according to the method described by Jenkins et al. (1997). Marine base cation deposition was estimated from chloride deposition assuming sea-salt ratios. National estimates of reduced and oxidised nitrogen deposition data for 1998-2000 at 5km resolution were obtained from CEH Edinburgh (Smith et al., 2000). Rainfall data were obtained from 1 km interpolated annual 1961-90 rainfall, supplied by CEH Wallingford. Runoff data were calculated from these rainfall data based on estimates of the percentage evapotranspiration under moorland (10%) and forest (20%) according to Jenkins et al. (1997). Forested sites were modelled using a simplified sequence, based on a regional average planting date, and with constant uptake and deposition enhancement thereafter to avoid anomalies in target loads otherwise generated due to rotation period.

Nitrogen dynamics were modelled for all sites, based on the relationship between soil N immobilisation and C:N ratio included within the MAGIC and VSD models (Cosby et al., 2001; Posch et al., 2003). Default values of $Cnrat_{RANGE}$, the difference between the C:N ratios at which 100% of deposited N is retained ($CNrat_{UP}$) and at which retention falls to zero ($CNrat_{LO}$), were defined for four vegetation types (heathland, grassland, conifer and broadleaf forest) from an analysis of C:N ratio versus N leaching data for a range of UK sites (Rowe et al., in prep.)

Model calibration and application

MAGIC was calibrated to present-day surface water base cation concentrations, soil exchangeable base cation fractions, soil pH, surface water inorganic N leaching, and soil C:N ratio. Parameters optimised were initial exchangeable base cation fractions, base cation weathering rates, soil water dissolved organic carbon concentration, initial soil C:N ratio and $CNrat_{UP}$. Ten calibrations were undertaken for each site, and the mean parameter set for all successful calibrations (i.e., those in which all target variables were simulated within acceptable ranges) was used as the basis for model forecasts and target loads calculations.

Model forecasts were undertaken based on currently agreed emissions reductions, with an implementation year of 2010 ('Gothenburg' scenario) and for a further reduction to EMEP background deposition levels by 2020; the latter indicates the maximum recovery that could be achieved. In each case UK deposition data were applied in the model, but scaled according to the deposition scaling sequences derived from the EMEP data. Target Load Functions (TLFs) were calculated for all sites according to the requirements of the call for data, with target years of 2030, 2050 and 2100. Critical ANC was consistent with values used in the FAB application for the 2004 data submission, i.e., in most cases equal to 20 $\mu eq\ l^{-1}$, with a small number of naturally acid sites having a critical value of 0 $\mu eq\ l^{-1}$. The number of sites for which TLFs could be calculated by region and year are summarised in Table UK-2 below.

Table UK-2. Summary of the number of freshwater sites for which TLFs could be calculated by region and year.

Region	Number of sites by region with TLF for year:		
	2030	2050	2100
Cairngorms & Galloway	14	16	17
Mourne Mountains	5	5	6
Lake District	8	8	12
South Pennines	7	12	13
Snowdonia	12	15	19
Cambrian Mountains	12	14	15
Totals	58	70	82

The UK will continue to apply MAGIC to the remainder of the freshwater sites for which FAB steady-state critical loads were submitted in 2004. In addition, data are being collated to enable dynamic models to be applied to selected regions of sensitive terrestrial habitats.

References

Cosby BJ, Ferrier RC, Jenkins A, Wright RF (2001) Modelling the effects of acid deposition – Fifteen years of MAGIC: Refinements, adjustments and inclusion of nitrogen dynamics. Hydrology and Earth System Sciences 5: 499-517

Evans CD, Jenkins A, Helliwell RC, Ferrier RC, Collins R (2001) Freshwater acidification and recovery in the United Kingdom, Centre for Ecology and Hydrology, Wallingford (ISBN 1 903741 01 7). 80 pp

Evans CD, Helliwell RC, Coull MC, Langan S, Hall J (2004) Results of a survey of UK soils to provide input data for national-scale dynamic modelling. Report to the Department of the Environment, Food and Rural Affairs under Contract No. CPEA 19, Centre for Ecology and Hydrology, Bangor

Hall J, Ullyett J, Heywood L, Broughton R, Fawehinmi J (2004) UK National Focal Centre report. In: J-P Hettelingh, M Posch, J Slootweg (eds): Critical loads and dynamic modelling results: CCE Progress Report 2004. RIVM Report 259101014, Bilthoven, The Netherlands, pp114-127

Hall J, Ullyett J, Heywood L, Broughton R & 12 UK experts (2004) Update to: The Status of UK Critical Loads – Critical Loads Methods, Data and Maps. February 2004. Report to Defra (Contract EPG 1/3/185). http://critloads.ceh.ac.uk

Jenkins A, Renshaw M, Helliwell RC, Sefton CEM, Ferrier RC, Swingewood P (1997) Modelling surface water acidification in the UK. IH Report No. 131. (ISBN 0 948540 79 6), Institute of Hydrology, Wallingford

Posch M, Hettelingh J-P, Slootweg J (eds) (2003) Manual for Dynamic Modelling of Soil Response to Atmospheric Deposition. RIVM Report 259101012, Bilthoven, The Netherlands

Smith RI, Fowler D, Sutton MA, Flechard C, Coyle M (2000) Regional estimation of pollutant gas dry deposition in the UK: model description, sensitivity analyses and outputs. Atmospheric Environment 34: 3757-3777

Appendix A. Instructions for the Call for Data

This Appendix is a reprint of the instructions as it was sent to the national focal centres with the call for data.

Instructions for Submitting Critical Loads and Dynamic Modelling Data

Coordination Center for Effects (CCE), Bilthoven, November 2004

1. Introduction

This document contains the instructions for the submission of data to the CCE on critical loads of acidity and eutrophication as well as dynamic modelling output.

Your submission should contain the following key outputs:

(1) Updated critical loads; and input variables to allow consistency checks and inter-country comparisons (Table 1; and Table 4 for surface waters)

(2) Target load functions for target years 2030, 2050 and 2100; and a damage or recovery delay time (Table 2)

(3) Values of chemical variables (e.g. Al concentration) in 1990, 2010 and in the target years for two different scenarios (Table 3)

(4) A document describing the sources and methods used to produce the data.

Please note:

- The deadline for the submissions is **28 February 2005**.
- The preferred file format of the data is an Access database file (mdb), but also files with formats of DBase, Excel, or comma separated ASCII files are accepted. The easiest way to comply with the requested format is to use an Access database that is made available by the CCE.
- Please email your submission to jaap.slootweg@rivm.nl . The data can be attached to the email, but large data files can also be uploaded using ftp to ftp://ftp.mnp.rivm.nl/cce/incoming/. If you have used ftp, please inform J. Slootweg with an email.
- Target load functions are asked for the **target years 2030, 2050 and 2100**[4], all with the **implementation year 2020**[1], in which deposition reductions after the **protocol year 2010** are fully implemented (see last section for details).
- Historic depositions of nitrogen and sulphur up to the Gothenburg protocol, and depositions originating from natural sources (background) are available from the CCE upon request.
- All information is also available on our website under ***News***: www.rivm.nl/cce

[4] The Working Group on Strategies and Review at its 36th session (Geneva, 13-16 September 2004) confirmed the choice of the implementation and target years. However, it noted that the target year 2100 should be used for scientific purposes only.

2. Most important changes since the last call for data:

- The implementation year has changed from 2015 to **2020**[1].
- The target load functions are **NOT** to be minimised with the critical load function.
- The values of output variables that are related to criteria for acidification are requested. for 5 years, using (1) deposition values following the Gothenburg protocol in 2010 keeping them constant for years thereafter (this scenario is abbreviated **Go** in the remainder of these Instructions) and (2) a deposition scenario based on EMEP MSC-W background values (**Bg)** as of the implementation year (see Table 3).
- The structure of Table 2 has been simplified, now containing a single row for each site.
- The status variables used as indicators for dynamic modelling are more clearly defined.
- New VSD features, e.g. calibration also for Gaines-Thomas exchange and arbitrary exponent *expAl*.
- The computation of Damage Delay Times (DDT) and Recovery Delay Times (RDT)
- The software provided by the CCE now enables you to perform consistency checks on your critical load database. Therefore it is important to use 'null' (i.e. 'nothing') to indicate missing or no value, and ***not***, e.g., '-1' or '-999' or '0'.

3. Data structure

The data structure is summarized in Tables 1 to 4 described below.

The easiest way to assemble and submit data is to use either of the two template **Access** databases that are provided by the CCE**,** one for VSD users (**VSD05NS.mdb**) and the second for NFCs that use other software/models (**call05NS.mdb**).

Both VSD05NS.mdb and call05NS.mdb contain 3 Tables, '*inputs*', '*targetloads*' and '*scenvars*', resp., with the attributes listed and described in Tables 1-3 of these Instructions respectively. VSD05NS.mdb is the ACCESS version of the VSD model, tailored for this call. After activation it automatically fills Tables 2 and 3. The file call05NS.mdb cannot automatically fill Tables 2 and 3, since results depend on the dynamic model(s) used by the NFC. It also includes Table 4 for the convenience of surface water modellers.

Finally, both VSD05NS.mdb and call05NS.mdb include software which allows you to perform consistency checks on your data. These checks can be carried out (see operating details provided on the CCE site or when receiving VSD05NS.mdb) and will generate screen messages.

The database call05NS.mdb and a more detailed description on how to make use of its features can be downloaded from our website www.rivm.nl/cce under 'News'.

Upon request of an NFC the CCE will provide the Access file VSD05NS.mdb including the deposition pathways 'Go' and 'Bg' for EMEP50-grid cells covering the requesting country. Scenario 'Go' includes grid average, semi-natural vegetation and forest specific deposition values; and the default for VSD will be set to forest specific deposition (if you wish to use VSD also for semi-natural vegetation, you will have to replace the deposition).

The CCE recommends using deposition files generated by the CCE in collaboration with EMEP MSC-W. However, these deposition files have to be requested from the CCE, if you do not use VSD (in which case they are contained in VSD05NS.mdb).

Every ecosystem within an EMEP50-grid cell for which critical loads are provided is represented in the Table 1 by one line (record), and every record has 47 entries, holding site information on critical loads, and input data for

CLs and dynamic modelling[5]. Records for which no dynamic modelling results are calculated should contain the value '–1' in the column 'DMstatus'. The target load functions themselves are to be submitted according to the structure given in Table 2. Finally, Table 3 contains the values of 7 chemical variables for 5 years obtained by running the dynamic model with the 2010 (Gothenburg) depositions kept constant afterwards ('Go') or reduced to depositions from natural sources only ('Bg'). Entries for Tables 1–4 are described in more detail below.

3.1 Data structure of critical loads and input data:

Table 1. Attributes of the table 'inputs' (47 columns; for surface waters see Table 4).

Variable	**Explanation**	Note
SiteID	Identifier for the site	1)
Lon	Longitude (decimal degrees)	2)
Lat	Latitude (decimal degrees)	2)
I50	EMEP50 horizontal coordinate	3)
J50	EMEP50 vertical coordinate	3)
EcoArea	Area of the ecosystem within the EMEP grid cell (km^2)	4)
CLmaxS	Maximum critical load of sulphur (eq ha^{-1} a^{-1})	
CLminN	Minimum critical load of nitrogen (eq ha^{-1} a^{-1})	
CLmaxN	Maximum critical load of nitrogen (eq ha^{-1} a^{-1})	
CLnutN	Critical load of nutrient nitrogen (eq ha^{-1} a^{-1})	
nANCcrit	The quantity $-ANC_{le(crit)}$ (eq ha^{-1} a^{-1})	5)
Nleacc	Acceptable nitrogen leaching (eq ha^{-1} a^{-1})	
crittype	Chemical criterion used: 1: molar [Al]:[Bc]; 2: [Al](eq/m^3); 3: base sat.(-); 4: pH; 5: [ANC](eq/m^3); 6: molar[Bc]:[H]; 7: molar [Bc]:[Al]; 0: empirical; –1: other	
critvalue	Critical value for the chemical criterion (given in *crittype*)	
thick	Thickness (root zone!) of the soil (m)	
bulkdens	Average bulk density of the soil (g cm^{-3})	
Cadep	Total deposition of calcium (eq ha^{-1} a^{-1})	6)
Mgdep	Total deposition of magnesium (eq ha^{-1} a^{-1})	6)
Kdep	Total deposition of potassium (eq ha^{-1} a^{-1})	6)
Nadep	Total deposition of sodium (eq ha^{-1} a^{-1})	6)
Cldep	Total deposition of chloride (eq ha^{-1} a^{-1})	6)
Cawe	Weathering of calcium (eq ha^{-1} a^{-1})	6)
Mgwe	Weathering of magnesium (eq ha^{-1} a^{-1})	6)
Kwe	Weathering of potassium (eq ha^{-1} a^{-1})	6)
Nawe	Weathering of sodium (eq ha^{-1} a^{-1})	6)
Caupt	Net growth uptake of calcium (eq ha^{-1} a^{-1})	6) 7)
Mgupt	Net growth uptake of magnesium (eq ha^{-1} a^{-1})	6) 7)
Kupt	Net growth uptake of potassium (eq ha^{-1} a^{-1})	6) 7)
Qle	Amount of water percolating through the root zone (mm a^{-1})	6)
lgKAlox	Equilibrium constant for the Al-H relationship (log_{10}) (The variable formerly known as Kgibb)	8)
expAl	Exponent for the Al-H relationship (=3 for gibbsite equilibrium)	8)
pCO2fac	Partial CO_2-pressure in soil solution as multiple of the atmospheric CO_2	6)

[5] NFCs who wish to make more detailed analyses of individual sites can use the "VSDStudio" software, developed in collaboration with Alterra and available on the CCE website.

	pressure (-)	
cOrgacids	Total concentration of organic acids (m*DOC) (eq m^{-3})	6)
Nimacc	Acceptable nitrogen immobilised in the soil (eq ha^{-1} a^{-1})	9)
Nupt	Net growth uptake of nitrogen (eq ha^{-1} a^{-1})	6)7)
Fde	Denitrification fraction (0<=fde<1) (-)	6)10)
Nde	Amount of nitrogen denitrified (eq ha^{-1} a^{-1})	6)10)
CEC	Cation exchange capacity (meq kg^{-1})	DM)
Bsat	Base saturation (-)	DM)
yearbsat	Year in which the base saturation was determined	DM)
lgKAlBc	Exchange constant for Al vs Bc (log_{10})	DM)
lgKHBc	Exchange constant for H vs Bc (log_{10})	DM)
Cpool	Amount of carbon in the topsoil (g m^{-2})	DM)
CNrat	C/N ratio in the topsoil (g/g)	DM)
yearCN	Year in which the CNrat and Cpool were determined	DM)
DMstatus	–1: no dynamic modelling for this site 0: non-violation of criterion & non-exceedance at present 1: Target Load information is given in Table 2	
EUNIScode	EUNIS code, max. 4 characters	11)

Notes on Table 1 (see last column):

1) Use integer values only (4-bytes)!
2) The geographical coordinates of the site or a reference point of the polygon (sub-grid) of the receptor under consideration (in decimal degrees, i.e. 48.5 for 48°30', etc.)
3) Indices (2-byte integers) of the 50km x 50km EMEP-grid cell in which the receptor is located. It is the grid with North Pole at (8,110) as described in the 2003 CCE Status Report, Appendix A, p.127.
4) Please remove spurious records with an ecosystem area smaller than 0.01 km^2.
5) The **negative** Acidity Neutralising Capacity, equal to $Al_{le(crit)} + H_{le(crit)} - HCO_{3,le(crit)}$ [$–OrgAcids_{le(crit)}$].
6) Values used in the critical load calculations.
7) These are net uptakes equal to the annual average amount removed from the site by harvesting.
8) From the equation $[Al]=KAl_{ox}\cdot[H]^{expAl}$ (with [Al] and [H] in mol/L). For help with unit conversions see Appendix C of the 2003 CCE Status Report.
9) In general this will *not* be the amount immobilised at present! If data permit calculate Nimacc as $N_i+N_{fire}+N_{eros}+N_{vol}–N_{fix}$ (see Mapping Manual at www.icpmapping.org).
10) These two are mutually exclusive, i.e. one of them has to be null!
11) You can find all the information on EUNIS codes at http://eunis.eea.eu.int/eunis/index.jsp

DM) These variables are used for dynamic modelling only.

3.2 Data structure for Target Load Functions and Delay Times:

Table 2 is automatically filled by VSD05NS.mdb for ecosystem sites for which in Table 1 the attribute 'DMstatus' is equal to 1, i.e. for which target loads exist.

A Target Load Function (TLF) in a target year consist of **4 nodes** (combinations of N and S depositions) of which the first is the (N,S) combination in year *y* (*y*=2030, 2050, 2100) with zero N deposition, i.e. (0,depS1_*y*) and the last for zero S deposition, i.e. (depN4_*y*,0). More than four nodes cannot be accepted. If the TLF consists of 3

nodes only, i.e. (0, depS1_*y*), (depN2_*y*, depS2_*y*) and (depN3_*y*,0), then (0,0) should be inserted for (depN4_*y*,depS4_*y*).

The Recovery Delay Time (RDT) and Damage Delay Time (DDT) is the year after 2010 and before 2100, generated with the deposition scenario **Go**. If recovery takes place before 2010 the RDT attribute should be set to 0; and if recovery occurs after 2100 then the RDT attribute should be 9999. Analogously, 0 and 9999 should be used when DDT is before 2010 or after 2100, respectively. Please note that it is not possible that for a single site both DDT and RDT exist simultaneously. However, it is possible that a site does not have any delay time. The concept of Recovery Delay Time (RDT) and Damage Delay Time (DDT) are further explained in a final section of this document and described in more detail in the CCE Dynamic Modelling Manual or Chapter 6 of the Mapping Manual.

Table 2. Attributes of the table 'targetloads' (30 columns).

Variable	**Explanation**
SiteID	Identifier for the site (relates to Table 1)
Status_2030	0: Non-exceedance in 2010 & no reduction required in target year 1: TL function present 2: Target load not feasible
Status_2050	
Status_2100	
RDT	Recovery Delay Time (a year)
DDT	Damage Delay Time (a year)
depN1_2030	N-value of first node of TLF for 2030 (should be 0!) (in eq ha^{-1} yr^{-1})
depS1_2030	S-value of first node of TLF for 2030
depN2_2030	N-value of second node of TLF for 2030
depS2_2030	S-value of second node of TLF for 2030
…	...
depN4_2100	N-value of the last node of the targetload for 2100
depS**4**_2100	S-value of the last node of the targetload for 2100 **(should be 0!)**

3.3 Data structure for scenario output:

In order to see the changes over time of the chemical status of ecosystems the following seven variables for year *a* (*a*=1990, 2010) and deposition scenario *dep* (*dep*=Go2030, Go2050, Go2100, Bg2030, Bg2050, Bg2100) are requested (concentrations are from the soil solution or, when aquatic systems are modelled, in surface water) for **all** ecosystems:

1. $[Al^{3+}]$ [eq m^{-3}] (Al_*a*; Al_*dep*)
2. [Ca+Mg+K] [eq m^{-3}] (Bc_*a*; Bc_*dep*)
3. pH (pH_*a*; pH_*dep*)
4. ANC concentration [eq m^{-3}] (ANC_*a ;* ANC_*dep*)
5. base saturation [-] (bsat_*a*; bsat_*dep*)
6. C:N ratio [g g^{-1}] (CNrat_*a* ; CNrat_*dep*)
7. Nitrogen (= $[NO_3]$ + $[NH_4]$) concentration in [eq m^{-3}] (cN_*a*; cN_*dep*)

These variables are independent of the scenario in 1990 and 2010, while for the years thereafter a distinction is required between the **Go** or **Bg** deposition scenario.

The extremes of the changes of variable values over time are assumed to be captured by the **Go** scenario (highest future depositions without emission reductions beyond what is already agreed in the Gothenburg protocol) and the **Bg** scenario (lowest possible depositions caused by non-anthropogenic emissions only). The **Bg** deposition scenario starts in 2020, and in the period 2010 and 2020 depositions are linearly interpolated between **Go** and **Bg.**

Table 3. Attributes of the table 'scenvars' (57 columns).

Variable	*Explanation*
SiteID	Identifier for the site (relate to Table 1)
Al_1990	Aluminium concentration in 1990
Al_2010	Aluminium concentration in 2010
Bc_1990	Base cation concentration in 1990
…	…
cN_2010	Nitrogen concentration in 2010
Al_Go2030	Aluminium concentration in 2030 under the **Go** scenario
Al_Go2050	Aluminium concentration in 2050 under the **Go** scenario
Al_Go2100	Aluminium concentration in 2100 under the **Go** scenario
…	…
cN_Go2100	Nitrogen concentration in 2100 under the **Go** scenario
Al_Bg2030	Aluminium concentration in 2030 under the **Bg** scenario
…	…
cN_Bg2050	Nitrogen concentration in 2050 under the **Bg** scenario
cN_Bg2100	Nitrogen concentration in 2100 under the **Bg** scenario

3.4 Aquatic ecosystems:

For aquatic ecosystems Table 1 should be replaced by Table 4 below; Tables 2 and 3 remain unchanged.

Table 4. Attributes of the table 'h2oinputs'.

Variable	**Explanation**
SiteID	Identifier for the site
Lon	Longitude (decimal degrees)
Lat	Latitude (decimal degrees)
I50	EMEP50 horizontal coordinate
J50	EMEP50 vertical coordinate
EcoArea	Area of the ecosystem(whole catchment) within the EMEPgrid (km^2)
CLmaxS	Maximum critical load of sulphur (eq ha^{-1} a^{-1})
CLminN	Minimum critical load of nitrogen (eq ha^{-1} a^{-1})
CLmaxN	Maximum critical load of nitrogen (eq ha^{-1} a^{-1})
CLnutN	Critical load of nutrient nitrogen (eq ha^{-1} a^{-1})
crittype	Criterion used: 6: [ANC](eq/m^3); 0: other
critvalue	Value of the criterion used
SoilYear	Year for soil measurements
ExCa	Exchangeable pool of calcium in given year (%)
ExMg	Exchangeable pool of magnesium in given year (%)
ExNa	Exchangeable pool of sodium in given year (%)
ExK	Exchangeable pool of potassium in given year (%)
thick	Thickness of the soil (m)
Porosity	Soil pore fraction (%)
bulkdens	Bulk density of the soil (g cm^{-3})
Nimacc	Acceptable amount of nitrogen immobilised in the soil (eq ha^{-1} a^{-1})
CEC	Cation exchange capacity (meq kg^{-1})

HlfSat	Half saturation of SO4 ads isotherm (μeq L^{-1})
Emx	Maximum SO4 ads capacity (meq kg^{-1})
Nitrif	Nitrification in the catchment (meq m^{-2} a^{-1})
Denitrf	Denitrification rate in catchment (meq m^{-2} a^{-1})
Cpool	Amount of carbon in the topsoil in the given yearCN(g m^{-2})
Npool	Amount of nitrogen in the topsoil in the given yearCN(g m^{-2})
CNRange	The C/N ratio range where N accumulation occurs
CNUpper	The upper limit of C/N ratio where N accumulation occurs
CaUpt	Net growth uptake of calcium (meq m^{-2} a^{-1})
MgUpt	Net growth uptake of magnesium (meq m^{-2} a^{-1})
KUpt	Net growth uptake of potassium (meq m^{-2} a^{-1})
NaUpt	Net growth uptake of sodium (meq m^{-2} a^{-1})
SO4Upt	Net growth uptake of sulphate (meq m^{-2} a^{-1})
NH4Upt	Net growth uptake of ammonia (meq m^{-2} a^{-1})
DepYear	Year for deposition measurements
Cadep	Total deposition of calcium (eq ha^{-1} a^{-1})
Mgdep	Total deposition of magnesium (eq ha^{-1} a^{-1})
Kdep	Total deposition of potassium (eq ha^{-1} a^{-1})
Nadep	Total deposition of sodium (eq ha^{-1} a^{-1})
Cldep	Total deposition of chloride (eq ha^{-1} a^{-1})
NH4dep	Total deposition of ammonia (eq ha^{-1} a^{-1})
NO3dep	Total deposition of nitrate (eq ha^{-1} a^{-1})
LakeYear	Year for lake measurements
Calake	Measured concentration of calcium in lake(μmol L^{-1})
Mglake	Measured concentration of magnesium in lake(μmol L^{-1})
Nalake	Measured concentration of sodium in lake(μmol L^{-1})
Klake	Measured concentration of potassium in lake(μmol L^{-1})
NH4lake	Measured concentration of ammonia in lake(μmol L^{-1})
SO4lake	Measured concentration of sulphate in lake(μmol L^{-1})
Cllake	Measured concentration of chloride in lake(μmol L^{-1})
NO3lake	Measured concentration of nitrate in lake(μmol L^{-1})
RelArea	The area of the lake relative to the catchment (%)
RelForArea	The area of the forest relative to the catchment (%)
RetTime	Retention time in the lake (a)
Qs	Annual runoff flux (m a^{-1})
expAl	Exponent for the Al-H relationship ()
pCO2	Partial CO_2-pressure in the lake in relation to the atmospheric CO_2 pressure (%atm)
DOC	DOC concentration in the lake (μmol L^{-1})
Nitriflake	Nitrification in the lake (%)
Cased	Sedimentation velocity of calcium in the lake (m a^{-1})
Mgsed	Sedimentation velocity of magnesium in the lake (m a^{-1})
Nased	Sedimentation velocity of sodium in the lake (m a^{-1})
Ksed	Sedimentation velocity of potassium in the lake (m a^{-1})
NH4sed	Sedimentation velocity of ammonia in the lake (m a^{-1})
SO4sed	Sedimentation velocity of sulphate in the lake (m a^{-1})
Clsed	Sedimentation velocity of chloride in the lake (m a^{-1})
NO3sed	Sedimentation velocity of nitrate in the lake (m a^{-1})
UptNH4lake	Uptake of ammonia in the lake (in % of measured value)
UptNO3lake	Uptake of Nitrate in the lake (in % of measured value)
DMstatus	–1: no TL is calculated 0: non-violation of criterion & non-exceedance at present 1: Target load information is given in Table 2
EUNIScode	EUNIS code (C1=standing waters; C2=running waters)

4. Documentation:

Please provide the CCE with documentation to substantiate and justify sources and methods applied in response to the call for data. It is strongly recommended to apply agreed methods as described in the Mapping Manual (www.icpmapping.org) and explicitly list and describe the deviations from the Manual.

You are requested to structure the contents of your documentation following the outline applied in the CCE progress report 2004. However, please do not apply 2-column or other layout features. The RIVM reporting requirements are currently best served with a plain single-column WORD layout.

Target Loads and Delay Times

The simplest and most straightforward use of a dynamic model is so-called *scenario analysis*. After the input data files, including (historical) deposition sequences, for a site are assembled and poorly known parameters are calibrated against observations, the model can be used to analyse the consequences of different future deposition (and land use) scenarios by comparing how selected soil chemical parameters develop over time.

Scenario analysis (in the context of dynamic modelling) is the computation of a future value of a chemical parameter for a chosen/given deposition trend as driving force, i.e., the future deposition is determined first, and then the (chemical) consequences for the soil/water are evaluated. This process could be repeated until an acceptable deposition reduction is achieved; however, this can be a lengthy trial and error process. To speed up this process, a so-called ***target load*** could be determined by back-calculating a suitable deposition path from a prescribed future value of a chemical variable, i.e. a target load is the deposition (path) which ensures that a prescribed chemical criterion (e.g., the Al/Bc ratio) is met in a given year. If it exists at all, there exists an infinite variety of deposition paths, i.e. target loads. To bring order into this multitude and to make results comparable, a target load is a deposition path characterised by three numbers (years): (i) the protocol year, (ii) the implementation year, and (iii) the target year (see Fig.1).

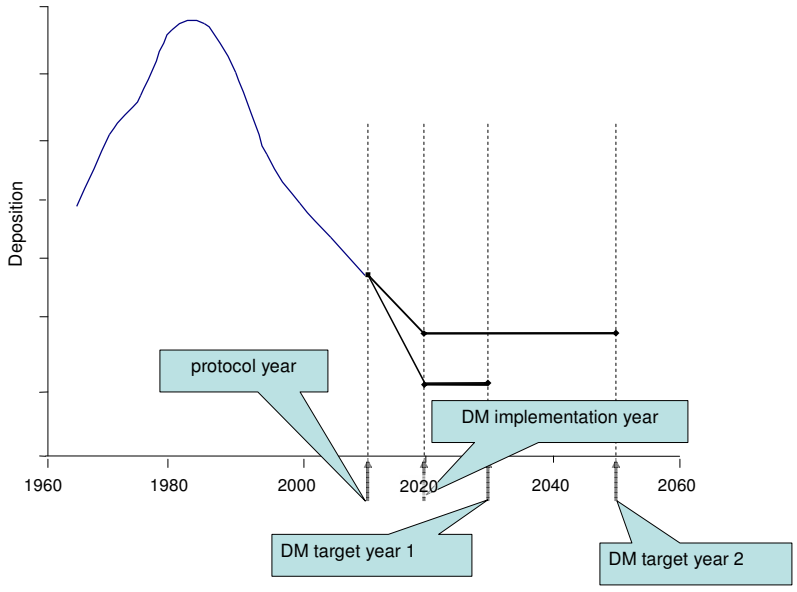


*Figure 1: Schematic representation of deposition paths leading to target loads by dynamic modelling (DM), characterised by three key years. (i) The year up to which the (historic) deposition is fixed (**protocol year**); (ii) the year in which the emission reductions leading to a target load are implemented (**DM implementation year**); and (iii) the years in which the chemical criterion is to be achieved (**DM target years**).*

The ***protocol year*** for dynamic modelling is the year up to which the deposition path is assumed to be known and cannot be changed. This can be the present year or a year in the (near) future, for which emission reductions are already agreed. An example is the year 2010, for which the Gothenburg Protocol, the EU NEC Directive and other (national) legislation is (soon expected to be) in place.

The ***implementation year*** for dynamic modelling is the year in which all reduction measures to reach the final deposition (the target load) are assumed to be implemented. Between the protocol year and the implementation year deposition are assumed to change linearly (see Fig.1). To avoid confusion with the term 'implementation year' as used by integrated assessment modellers, we (occasionally) prefix it with 'DM' for 'dynamic modelling'.

Finally, the ***target year*** for dynamic modelling is the year in which the chemical criterion (e.g., the Al/Bc ratio) is met (for the first time). Again, 'DM' is prefixed to emphasise the use of the term in dynamic modelling.

In summary, the above three special years and the accompanying prescriptions define a unique deposition path that is (also) referred to as target load.

In the Dynamic Modelling Manual and in Chapter 6 of the Mapping Manual it was argued and illustrated that ***a target load is the deposition for which a pre-defined chemical or biological status is reached in the target year and maintained (or improved) thereafter.*** This implies, *inter alia*, that a target load has always to be smaller (or equal) to the corresponding critical load. In addition, unnecessary calculations can be avoided by observing the following steps for calculating target loads: If at present the critical load is not exceeded and the (chemical) criterion is not violated, the site is 'safe' and no target load needs to be calculated (DMstatus=0 in Table 1). Otherwise the steps outlined in Fig.2 should be followed:

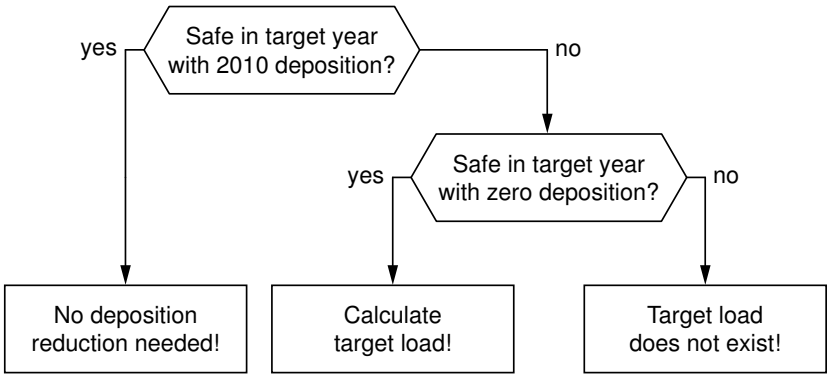


Figure 2: Decision tree for determining whether a target load has to be calculated. Note that 'Safe' means that there is non-exceedance of the critical load and non-violation of the criterion.

The above steps are automatically carried out in the VSD implementations in Access and the VSDStudio software.

So far, only a single pollutant has been considered. In the case of acidification, however, the deposition of both N and S contribute to the problem. Thus, pairs of N and S deposition have to be determined which result in the desired chemical status in the target year. And all pairs define the so-called ***target load function*** (TLF) in the (N_{dep},S_{dep}) plane, in the same way as critical loads define the critical load function. Of course, different TLFs are obtained for different target years, approaching the critical load function (CLF) when the target year moves towards infinity. Obviously, only a finite number of such pairs can be computed, and in most cases a small number will suffice. In this call for data, only 4-node TLFs are accepted by the CCE.

Examples of 4-node TLFs (for different target years) are shown in Fig.3. Due to the finite buffers in the soil, such as time-dependent immobilisation, a TLF can intersect with the CLF for certain values of the depositions (see Fig.3). To ensure that the chemical criterion is also met *after* the target year, the minimum of the TLF and the CLF has to be determined, but these computations will be carried out at the CCE.

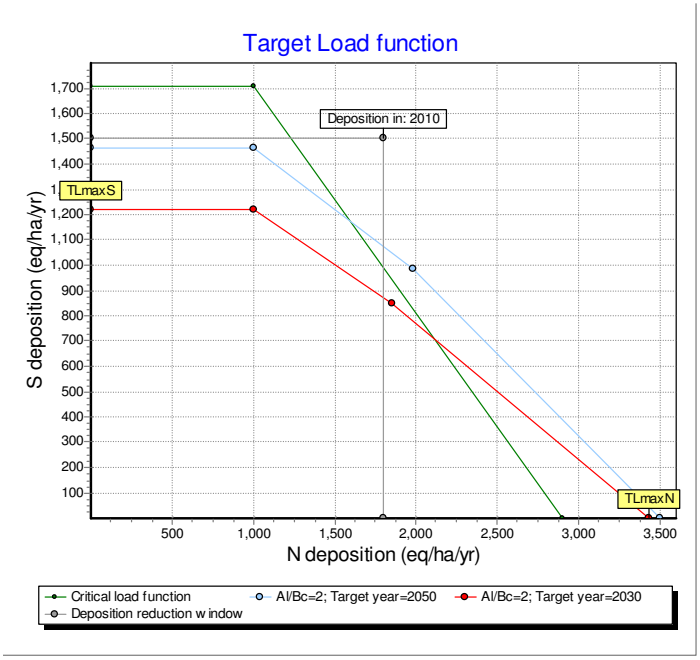


Figure 3: Examples of a 4-node target load functions for different target years (VSD-Studio output). Also shown is the corresponding critical load function (top line). The computations to determine the minimum of the TLF and the CLF will be carried out at the CCE.

Damage and Recovery Delay Times

It is often assumed that when attaining non-exceedance, i.e. when reducing deposition to (or below) critical loads, the risk of 'harmful effects' is immediately removed, i.e. the chemical criterion (e.g. the Al/Bc-ratio) that links the critical load to the effect(s), immediately attains a non-critical ('safe') value. But the reaction of soils, especially their solid phase, to changes in deposition is delayed by (finite) buffers (such as the cation exchange capacity). These buffer mechanisms can delay the attainment of a critical chemical parameter, and it might take decades or even centuries, before a desired state is reached. Only with a dynamic model can the times by computed that are involved in attaining a certain chemical state in response to given deposition scenarios. The time between the first exceedance of the critical load and the first violation of the criterion is called the Damage Delay Time (DDT), whereas the time between achieving non-exceedance and obtaining non-violation of the criterion is called Recovery Delay Time (RDT).

In this call for data the CCE asks (in Table 2) for the computation of damage and recovery delay times – or rather the year in which damage or recovery occurs – for the special case of constant S and N deposition after the protocol year (2010), i.e. for the case in which no further deposition reductions are carried out beyond the Gothenburg protocol.

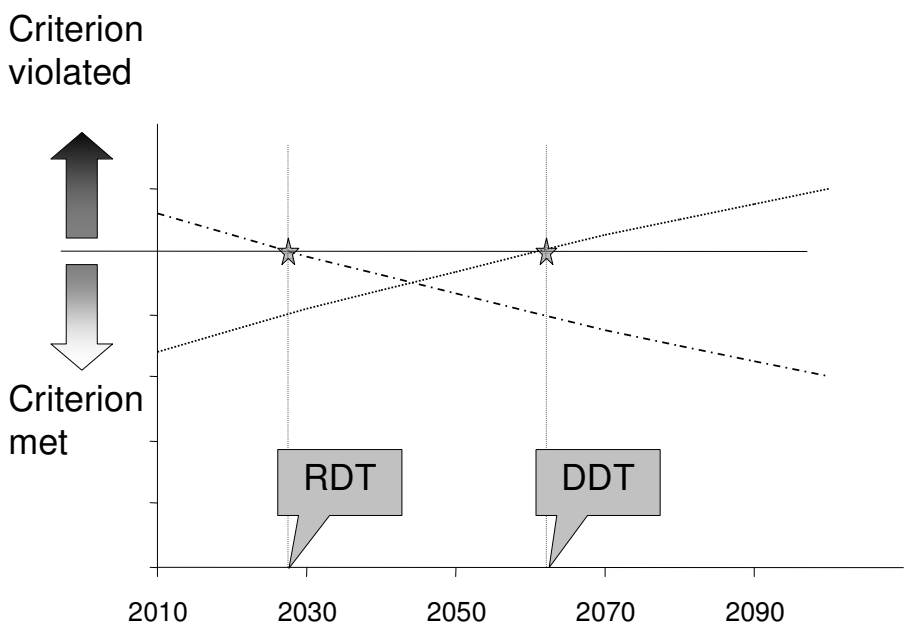


Figure 4: 'Typical' developments of a soil chemical variable (e.g. Al/Bc-ratio) in comparison to its criterion. The dashed-dotted line shows the development in case the deposition is below the critical load, whereas the dotted line shows the development for depositions exceeding critical loads. The year, in which the criterion is met [violated] for the first time, defines the Recovery Delay Time (RDT) [the Recovery Delay Time (RDT)] of the system. Note that for a criterion for which high values are 'good', the labels 'RDT' and 'DDT' have to be interchanged.

Note that:

(a) a ***damage delay*** exists only if there is exceedance of critical loads in the specified year (in this call 2010) , but non-violation of the chemical criterion; and

(b) ***recovery*** can only occur if there is non-exceedance of critical loads in the specified year, but the criterion is still violated.

In the other two possible cases – (c) exceedance and violation of the criterion, and (d) non-exceedance and non-violation – the system is 'damaged' or 'safe', respectively.